Synthesis and Characterization of New Ionic Liquids from 1, 10-Phenanthroline and 4, 4'-Bipyridine

Atakilt Abebe

A Thesis Submitted to

Chemistry Department

Presented in Fulfillments of the Requirements for the Degree of Doctor of Philosophy (Inorganic Chemistry)

Addis Ababa University

Addis Ababa, Ethiopia

June 2012

Addis Ababa University

School of Graduate Studies

This is to certify that the thesis prepared by Atakilt Abebe entitled: "**Synthesis and Characterization of New Ionic Liquids from 1, 10-Phenanthroline and 4, 4'-Bipyridine"** and submitted in fulfillment of the requirement for the degree of Doctor of Philosophy (Inorganic Chemistry) complies with the regulations of the university and meets the accepted standards with respect to originality and quality.

Signed by the examining committee:

Examiner---------- Signature---------- Date----------

Examiner---------- Signature---------- Date----------

Advisor ---------- Signature---------- Date----------

Advisor ---------- Signature---------- Date----------

_____

Chair of Department or Graduate Program Coordinator

Abstract

Synthesis and Characterizations of New Ionic Liquids from 1, 10-Phenanthroline and 4, 4'-Bipyridine

Atakilt Abebe

June 2012

New ionic liquids (ILs) from 1,10-Phenanthroline and 4, 4'- Bipyridine have been synthesized. The synthetic procedure is based on the typical alkylation plus anion methathesis steps common to commonly used ionic liquids. Optimization of the reaction conditions allows the successful monoalkylation of both 1, 10-Phenanthroline and 4, 4'-Bipyridine which is key for the low melting points observed. All new ionic liquids have been fully characterized using NMR, MS and CHN microanalysis. The phase behavior and decomposition temperatures of these ILs have been investigated using DSC and TGA. The ionic liquids were also analyzed using X-ray photoelectron spectroscopy (XPS). The binding energy data obtained in this research may find future use as a standard list of binding energies for 1, 10-Phenanthrolinium and 4, 4'-Bipyridinium based ionic liquids and other related compounds.

The solvent ability of these new ionic liquids was tested. Nanoparticle stabilizers such as 1, 10-Phenanthroline and its metal complexes were dissolved at high concentrations in 1, 10- Phenanthrolinium based ionic liquids and metal salts have shown very high solubilities in 4, 4'-Bipyridinium based ionic liquids. These dissolving abilities make the new ionic liquids very promising for applications such as catalysis, nanoparticle synthesis, electrodeposition or metal extraction.

Acknowledgments

Firstly, I am indebted to the help and support of my two supervisors, Dr. Yonas Chebude and Dr. Ignacio V. Garcia. Their wisdom and encouragement was a constant source of motivation throughout my research. Dr. Yonas, who putting strong faith recruited and allowed me to be a primary role player in realizing his dream, contribution of new ionic liquids from totally new moieties, to the scientific community in general and to the industrialists in particular. His qualities as a supervisor is also manifested in creating convenient research ground to his maximum potential. His latter quality is justified in his collaborations with abroad institutions such as School of Chemistry, University of Nottingham which greatly helped me in producing ample data on my research problem. Dr. Ignacio V. Garcia is credited for the accelerated fruition of this project because of his continuous follow up of the research.

Dr. Peter Licence is a corner stone in this research. In addition to his academic advice and supervision, Pete allowed me to use his well equipped laboratory at the School of Chemistry, University of Nottingham without any reservation. I must also mention Prof. Wondimagegn Mammo who was at my side whenever I needed academic and technical assistance. The presence of Prof. Isabel Diaz in the department was an inspiration for my work. The graceful encouragements I received from Prof. Negussie Reta and Prof. V. J. T. Raju fueled the fruition of this project.

It would be remiss of me to not mention the help of the technical staff in the School of Chemistry, University of Nottingham. I would like to particularly acknowledge the contributions of Ms Emily F. Smith, for unreserved assistance in running XP Spectrometer and Mr. Coxhill Graham, for his generous help in Mass Spectroscopy.

I must also thank Addis Ababa University, School of Graduate Studies for funding and Chemistry Department for creating conducive research environment. I want to extend my gratitude to School of Chemistry, University of Nottingham, for funding and Bahir Dar University for paying my subsistence for all these years.

Last but not least, I would like to thank my family, especially my wife Zufan Asgedom and my children, Bereket and Firezer, my father Ato Abebe Alemu as well.

Table of Contents

Table of Figures

List of Schemes

List of Tables

Abbreviations

ILs	-	Ionic Liquids
$[emim]^+$	-	1-ethyl-3-methylimidazolium cation
$[C_nmim]^+$	-	1-alkyl-3-methylimidazolium cation
$[C_nPhen]X$	-	[N-Alkyl-1, 10-Phenanthrolinium] Anion
$[C_nBipyr]X$	-	[N-Alkyl-4, 4-Bipyridinium] Anion
$[NTf_2]^-$	-	Bis(trifluoromethylsulfonyl)amide
$[OTf]^-$	-	Triflate, $(CF_3SO_3)^-$
$[TFA]^-$	-	Trifluoracetate, $(CF_3CO_2)^-$
XPS	-	X-ray Photoelectron Spectroscopy
FWHM	-	Full Width at Half Maximum
eV	-	Electron Volts
Tc	-	Crystallization temperature
Tm	-	Melting temperature
Tg	-	Glass transition temperature

CHAPTER ONE

1. INTRODUCTION

1.1 The Role of Solvents in Chemistry

Many chemical processes usually take place in solutions. Hence, the role of solvents in chemistry is vital. In principle, any liquid may be employed as a solvent. However, polar organic solvents have been extensively used for both synthetic chemistry and extraction technologies and have largely superseded water, which was widely employed historically. Organic solvents play a key role in industry. They provide a reaction media that allows the homogenization of the reaction mixtures, speed up reactions through improved mixing and contribute to safety by acting as a heat sink for exothermic reactions. Many of the chemical processes use volatile organic compounds (VOCs) as solvents because of their ease of removal by evaporation at the end of the process allowing the easy isolation of products. However, the ever increasing awareness of the detrimental health and environmental effects of some organic solvents has given chemists the impetus to search for better technologies [1, 2].

From an ecological and safety point of view, a chemical process that involves no solvent is the ideal situation. In fact many reactions are known that may be carried out without solvents. Nevertheless, most chemical reactions are largely dominated by processes taking place in solutions. Nowadays, there is an increased interest in using environmentally benign liquids as solvents for chemical reactions including water [3, 4],

perfluorinated hydrocarbons and supercritical fluids, in particular $ScCO_2$ [4,5], aqueous biphasic systems, and ionic liquids (ILs)[6].

1.2 Ionic Liquids (ILs)

Ionic Liquids (ILs) are low temperature melting salts (below 100 ^{0}C) [7]. In particular, the salts that are liquid at room temperature are called room temperature ionic liquids or RTILs [8-10]. In the current understanding, ILs contain large, organic cations (Figure 1.1) such as quaternary ammonium cations, heterocyclic aromatic compounds such as 1, 3-dialkylimidazolium, pyrrolidinium cations [11, 12], derivatives of natural products over which the monocharge is delocalized [13, 14], with a variety of anions (Figure1. 2). Slight modifications on either the cations or the anions or on both are useful tools to fine-tuning the properties of the resulting IL for desired 'solvent' properties. Clearly, the large quantity of possible combinations among the cations and anions results in a large number of different ILs having a wide range of physical and chemical properties.

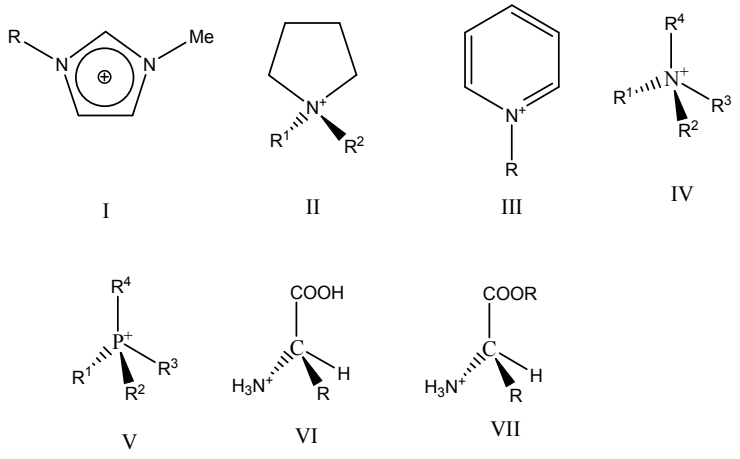

Figure 1. 1: Important cations:

I: 1-alkyl-3-methylimidazolium ions ($[C_nmim]^+$, C_n stands for n-alky residues C_nH_{n+1}); II: 1,1-dialkylpyrrolidium, III: pyridinium, IV: tetraalkylammonium, V: tetraalkylphosphonium, VI: α-amino acid cation, AA^+, VII: α-amino acid ester, AAE^+

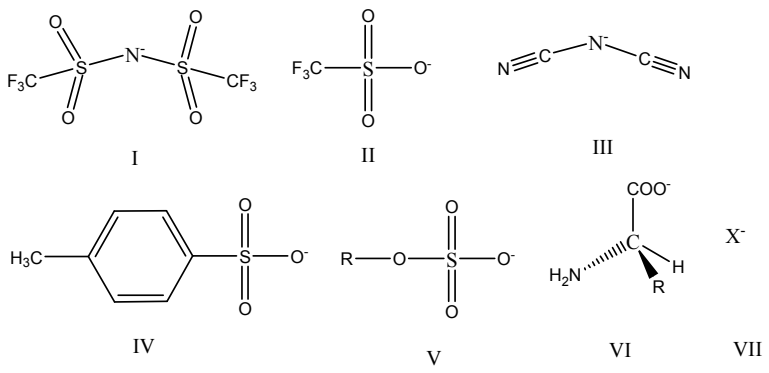

Figure 1. 2: Important anions:

I: Bis(trifluoromethylsulfonyl) amide, $[N\ Tf_2]^-$, II: Trifluotomethanesulfonate, $[OTf]^-$, III: dicyanamide, $[N(CN)_2]^-$, IV: tosylate, $[OTs]^{--}$, V: Alkylsulfates, $C_nOSO_3^-$, VI: α-amino acid anion, AA^-, VII: Halides (Cl^-, Br^- and I^-)

1.2.1 History of Ionic Liquids

The first report of room temperature molten salt, ethylammonium nitrate, $[EtNH_3]^+[NO_3]^-$ (m. p. 12^0C) goes back to 1914 [19, 20], but subsequently, it was not recognized that chemistry in such solvents could become a field of study. Organic chloroaluminates, namely alkylpyridinium (Rpy^+) chloroaluminate based ambient temperature ionic liquids first mentioned in 1951[21] and studied in detail from the 1970s onwards, are now considered to be the first generation of ionic liquids. However, it was the discovery of 1-ethyl-3-methylimidazolium, ($etmim^+$) based chloroaluminate ionic liquids in 1982 that afforded the impetus for a dramatic increase of activities in the area [22]. The latter class of compounds called the first generation ILs, exhibits a wider liquidus range and an electrochemical window of > 4.0V and has therefore become of great interest from both an electrochemical and synthetic point of view. A considerable drawback of these ambient ionic liquids is the need to protect rigorously the ionic liquids from moisture and other oxide impurities. Use of ambient temperature ionic liquids has therefore thus far been limited to a narrow range of organic substrates, typically those that react desirably

with Lewis acids such as *Friedel-Crafts* substrates. In 1992, *Wilkes and Zaworotko* reported the preparation of second generation ionic liquids with alternative 'neutral' weakly coordinating anions such as tetrafluoroborate, $[BF_4]^-$, and hexafluorophosphate, $[PF_6]^-$, which allowed a much wider range of applications for ionic liquids such as the development of a new work-up methods, including the separation of water-soluble by products by simple extraction [22]. Since then it became increasingly clear that many ion combinations form air and water stable ionic liquids and they became increasingly popular in academia and industry. More recently, chemists have been moving away from $[PF_6]^-$ and $[BF_4]^-$ (since they are highly toxic and hydrolyze) towards new anions such as bis(trifluoromethanesulfonyl)amide, $[(CF_3SO_2)_2)N]^-$, trifluoromethanesulfonate, $[CF_3SO_3]^-$, or even away from halogenated compounds completely towards anions such as dicyanamide, $[N(CN)_2]^-$, tosylate,$[H_3C\text{-}C_6H_4\text{-}SO_3]^-$, and alkyl sulfates, $[C_n\text{-}OSO_3]^-$[6]. Since 2000, the concept of "task-specific ionic liquids"(TSIL) was introduced to describe ILs, which have functional groups designed to impart to them specific properties or reactivity.

1.2.2 Properties of Ionic Liquids

The diversified characteristics of ionic liquids include that they are highly polar and non-coordinating in which a number of organic and inorganic solutes may be dissolved. This may be due to favorable solvating properties which depend mainly on polarity and hydrogen bonding ability. Composed solely of ions ILs are electrically conductive, which is an attractive feature in electrochemistry (electrolytes for batteries, fuel cells etc.) [23]. ILs also have a wide liquidus ranges: some ILs do not decompose below 300^0C and have melting points as low as -96^0C [24]. Thus the usable liquid range is suitable for

conventional synthetic chemistry and low temperature extractions. In addition to the stability of transient species that are often extended in the ionic environment, the low temperature reactions in these systems avoid dissociation, disproportionation, and degradation reactions which are encountered at higher temperature [25].

Due to their distinctive properties, ionic liquids are attracting increasing attention in many fields such as synthesis and polymerization [26], catalysis with increased rates [27], biocatalysis [20], analytical chemistry, nanotechnology [21], and combined reaction/separation processes ,where the reagents and products differ in IL solubility [22]. Liquid/liquid extractions offer excellent opportunities to reduce the reliance on VOCs in many industries.

Melting points of ILs

The solid-liquid phase transition of some of the current ILs has been examined by DSC [23]. In simple salts, interactions are controlled by long-range *Coulomb* forces between the net charges of the ions. In the case of ILs, however, the single charge loaded over the large component molecules results in low charge density. This softens the possible long range *Columbic* interactions between cations and anions and generates highly directional interactions of shorter range. The asymmetric nature of both the cations and anions as well as the free rotation possibility of the side chains hinders crystal packing resulting in low lattice energy. These two conditions are very important in lowering the melting points of ILs. The interaction potential depends on the distance of the ions and a set of angles for their mutual orientation, which again is influenced by electrostatic inductive and van der Waals (dispersive/repulsive) interactions [11, 15-18].

Some studies suggest that as the alkyl length increases, inter-chain hydrophobic packing takes a prominent role and the formation of bilayer-type structures result in an increase in melting points of $[C_nmim]^+$ with n > 8 [32].

Ngo *et al*. have studied the melting point trends of a series of common dialkylimidazolium based ILs. The result showed that the melting points decrease with the larger more asymmetrical substituted cations [31]. ILs containing highly fluorinated anions such as $[ONf]^-$, were reported to melt closer to room temperature. Smaller and more symmetrical cations result in higher melting points than ILs composed of unsymmetrical or larger cations [22]. Increased branching of side chains on the cations results in higher melting points [31].

Low Vapour pressure

The components of ionic liquids (ions) are attracted to each other by high Columbic forces. As a result, they release no vapor above the liquid surface. Consequently, many ILs exhibit very low vapour pressures [11, 35]. Their non-volatile nature minimizes their atmospheric contamination and makes them potentially none hazardous during their transportation, handling and use. More importantly for this research, their low vapour pressures allow the analysis of ILs under high vacuum pressures, with techniques such as XPS.

Thermal decomposition temperatures

ILs exhibit in general good thermal stability. The onsets of thermal decomposition temperatures are similar for the different cations. However, it decreases with the increase in anion hydrophilicity [36]. As a result, halide anions dramatically reduce the thermal

stability with the onset of decomposition. Relative anions stabilities have been suggested as PF_6^- >Tf_2N^-~BF_4^- > halides. Increasing the cation size from $[C_4mim]^+$ to $[C_8mim]^+$ doesn't appear to have a large effect[24].

Conductivity and Electrochemistry of ILs

ILs can be considered as unique class of compounds as they combined ion conduction and solvent properties. Although dependent up on the choice of working conditions, ILs are electrochemically very stable which is usually expressed as electrochemical window [37, 38]. Consequently, applications of ILs as components for batteries [39], electrochemical double-layer capacitors [40], dye-sensitized solar cells [41], fuel cells [42], and electrochemical sensors [43] are abundant. With regard to electrodeposition or electroplating of active metals involving ILs, what is very important is the solubility of the metal salt in the IL and that the cathodic limit is negative enough for deposition of the metal at the cathode.

Solvent Characteristics of ILs

The tremendous compositional possibilities in between the components of ILs allow solvent properties to be tailored to specific applications. Consequently ILs have been used as non-aqueous alternatives to organic solvents [44]. Depending on the anion and alkyl group of the imidazolium cation, the ILs can solubilise carbonyl compounds, alcohols, alkyl halides, supercritical CO_2 ($scCO_2$) [23, 45, 46]. Grafting coordinating moieties on the cation or anion of the IL (by derivatisation), transition metal complexes can also be dissolved [47-50]. More recently, ILs have been used as solvents for lignocellulosic biomass processing with the aim of developing alternatives for

lignocellulosic pretreatment [51, 52]. This can be attributed to their high polarity and tunable hydrogen bonding ability [53]. Using ILs as media of reactions has found to be more efficient compared with molecular solvents. This is because these solvents are ionic and highly structured which can give its own chemistry [54]. Moreover they are believed to act catalysts as and co-catalysts themselves in addition to their solvent role [53]. Catalytic reactions involving ILs as media of reactions are also found to be more efficient than their conventional counterparts. This is because ILs are viscous enough to limit diffusion of the nanoparticle catalysts and thus promote formation of larger particles and limit their growth. Consequently, the catalytically active surface area remains intact for longer period of time [54]. With time, however, it is found that agglomeration leads to a loss of activity, indicating that IL stabilization alone does have limitations. Adding other materials to ILs can combine different type of stabilization effect leading to more nanoparticle stabilization. The commonly used organic stabilizers include 1, 10-Phenanthrline. However, these stabilizers generally have low solubility in the common ILs [54].

1.3 Synthesis of Ionic Liquids

The simplest way to make ionic liquids is to neutralize Brønsted base with Brønsted acids. The first IL (ethylammonium nitrate) was made this way [19, 20, 33].

However, most ionic liquids are synthesized by quaternization of heterocyclic molecules with Lewis basic characteristics using alkyl halides. This is achieved by refluxing using appropriate solvents as media of reactions [33, 57]. The desired anion combination is obtained by metathesis (ion exchange) using the salt of the anion of interest. Moreover, a

very efficient, solvent free route of preparation of ionic liquids using microwaves is possible [57].

1.4 Characterization of Ionic Liquids

The synthesis and purity of ILs are investigated using the routine techniques such as NMR, thermal analysis, and CHN microanalysis. Moreover, X-ray photoelectron spectroscopy (XPS) is now accepted as a reliable method of characterization of ionic liquids [55]. This is because ILs are non volatile and chemically stable compounds. The basic purpose of characterizing ionic liquids using XPS is to confirm the purity and extraction of the binding energies of the component atoms that again illustrate the electronic environment of each atom of every element in the compound. However, to date only a small number of non-imidazolium based ionic liquids have been investigated using XPS [55, 56]. This fact opens an opportunity to investigate new ILs using XPS and present binding energy data of new moieties for the scientific community in general.

1.5 Objective

Known since the beginning of the 21st century, ILs based on 1-N-alkyl-3-methylimidazolium cation ionic liquids have attracted significant and growing interests, which have intrinsically useful properties, such as thermal stability, high ionic conductivity, negligible vapour pressure and a large electrochemical window. Depending on the anion and alkyl group of the imidazolium cation, they have been used for variety of applications. In certain applications such as catalysis, electrolytes in batteries, photovoltaic devices, and electrodeposition of metals, good mass transfer is needed [58, 59]. However, as the viscosity of most ionic liquids is much higher than most molecular solvents, the mass transport in ionic liquids is rather poor [60]. Moreover, the mass

transport is limited even further by the poor solubility of simple metal salts [61-64]. The limited solubility is due to the poor coordinating power of the anions such as $[BF_4]^-$, $[PF_6]^-$, or bis(trifluoromethylsulfonyl)amide, ($[NTf_2]^-$). To increase the solubility, functionalized ionic liquids can be used. This fact necessitates functionalizing either the cation or the anion or both by moieties such as nitrile and thiourea groups, which in turn can coordinate to the metal ion [65]. Another way to increase the solubility of metal ions in ionic liquids is to design ionic liquids with a metal complex as part of their composition [59, 66]. However, this strategy to increase the solubility of metals requires further amount of synthetic work and render the final application more laborious, expensive and less environmental friendly. Other activities that stimulate the solubility of metal salts in ionic liquids are incorporation of water or other coordinating organic solvents like methanol with the ionic liquid and then removing the solvent [61]. In catalytic reactions the stabilization of nanoparticle catalysts and retention of catalytic activity is crucial. The agglomeration of the nanoparticle catalysts diminishes their catalytic efficiency, which is usually slowed down by less mass transfer in ionic liquids due to their viscosity. With time, however, agglomeration takes place and the catalytic efficiency of the catalyst is lost. This is because agglomeration reduces the catalytically active surface area of the catalyst. To alleviate this problem attempts using organic stabilizers such as 1, 10-Phenanthroline are mixed with reaction mixture along with the catalysts which generally has low solubility in ionic liquids reported yet [54].

The above mentioned limitations of the common ILs highlights the need of discovering new ionic liquids exhibiting new properties. This can be achieved by using new charge carriers with different styles of interactions with solutes and substrates. Ionic liquids

based on 1, 10-Phenanthroline and 4, 4-Bipyridine are expected to improve the solubility of certain complexes and metal salts in the ionic liquid media. The structures of the starting materials include π-electrons for π-π interaction in 1, 10-Phenanthroline and coordinating ability through its unalkylated nitrogen in 4, 4-Bipyridine.

The synthesis of ionic liquids based on 1, 10-Phenanthrolinium cation may provide a solvent that is able to dissolve organic nanoparticle stabilizers such as 1, 10-Phenanthroline [54]. 1, 10-Phenanthroline is the parent molecule of an important class of chelating agents that form coordination compounds with various metal ions. The corresponding metal complexes have great potential for a variety of applications because of their high charge transfer mobility, strong absorption in the ultraviolet spectral region, bright red light emission and good electro- and photo-active properties. Due to its superb ability to coordinate many metal ions, 1, 10- Phenanthroline and its derivatives have been extensively used in many processes involving metal complexes as ligands for catalysis or as stabilizing agents for nanoparticle syntheses [54, 67-73]. These catalysts have been found to successfully catalyze a range of reactions such as decarboxilative biaryl synthesis from aromatic carboxylates and aryl triflates [74-77]. However, these classes of compounds are not soluble in any of the common ionic liquids. This fact impeded them from getting a place in the chemistry of ionic liquids. These catalysts should exhibit high solubilities and stabilities in the 1, 10-Phenanthrolinium cation based ILs, rendering the combination a very promising catalytic system.

4, 4-bipyridinium cations containing an unalkylated and not sterically hindered nitrogen have the potential to coordinate to metal ions. This will allow the dissolution of metal ions in this type of ionic liquids and consequently applications such as electrochemistry

and metal extraction could find in this media a very successful approach. Since the basicity of the unalkylated nitrogen is weakened interesting electronic property will arise that may find applications as a medium for electrodeposition of metals in this IL.

References

1. J. O. Metzger, *Chemosphere,* 2001, 43, 83-87.
2. M. Lancaster, *Green Chemistry, An Introductory Text*, ISBN 0-85404-620-8, RS. C 2002, pp. 130-165.
3. P. Wasserscheid, T. Welton, *Ionic Liquids in Synthesis*, 2nd ed, WILEY-VCH, Weinheim, 2007.
4. H. Olivier-Bourbigoy, L. Magna, *Journal of Molecular Catalysis A: Chemical*, 2002, **182,** 419-437.
5. S. G. Kazarian, B. J. Briscoe and T. Welton, *Chem Commun*., 2000, 2047-2048.
6. J. G. Huddleston, H. D. Willauer, R. P. Swatloski, A. E. Visser, R. D. Rogers, *Chem. Commun*., 1998, 1765-1766.
7. B. Coasne, L. Viau, A. Vioux, *J. Phys. Chem. Lett*. 2011, **2**, 1150–1154.
8. H. L. Chum, V. R. Koch, L. L. Miller, R. A. Osteryoung, *J. Am. Chem. Soc*.,1975, **97**, 3264-3265.
9. J. Robinson, R. A. Osteryoung, *J. Am. Chem. Soc.,*1979, **101**, 323-327.
10. J. S. Wilkes, J. A. Levisky, R. A. Wilson, C. L. Hussey, *Inorg. Chem*.,1982, **21**, 1263.
11. H. Weingärtner, *Angew. Chem. Int. Ed*. 2007, **46**, 2-19.
12. D. R. MacFarlane, P. Meakin, J. Sun, N. Amini and M. Forsyth, *J. Phys. Chem*. B, 1999, **103**, 4164.
13. J. H. Davis, K. J. Forrester and T. J. Merrigan, *Tetrahedron Lett*., 1998, **39**, 8955.

14. J. L. Thomas, J. Howarth, K. Hanton and D. McGuirk, *Tetrahedron Lett*., 2000, **41**, 413.

15. C. Wakai, A. oleinkova, M. Ott, H. Weingärtner, *J. Phys. Chem*. B, 2005, **109**, 17028.

16. H. Weingärtner, *Angew. Chem. Int. Ed., 2008*, **47**, 654-670.

17. H. Weingärtner, A. Knocks, W. Schrader, U. Kaatze, *J. Phys. Chem. A*, 2001, **105**, 8646-8650.

18. C. Daguenet, P. J. Dyson, I. Krossling, A. Oleinkova, J. Slattery, C. Wakai, H. Weingärtner, *J. Phys. Chem. B*, 2006, **220**, 12682-12688.

19. T. Welton, *Chem. Rev*. 1999, **99**, 2071-2083.

20. R. T. Carlin, H. Wilkins, *J. Chem. Soc*., 1929, 1291-1298.

21. F. H. Hurley, T. P. Weir, *J. Electrochem. Soc*., 1951, 98, 207.

22. J. S. Wilkes, M. J. Zaworotko, *Chem. Commun*., 1992, 965-967.

23. J. S. Wilkes, J. A. Levisky, R. A. Wilson, C. L. Hussey, *Inorg. Chem*.,1982, **21**, 1263.

24. A. E. Visser, R. P. Swatloski, R. D. Rogers, *Green Chem.*, 2000,**1**, 1-4.

25. A. A. Fannin, Jr., D. A. Floreani, L. A. King, J. S. Landers, B. J. Piersma, D. J. Stech, R. L. Vaughn, J. S. Wilks, J. L. Williams, *J. Phys. Chem*., 1984, **88**, 2614.

26. A. J. Carmichael, D. M. Haddleton, S. A. F. Bon, K. R. Seddon, *Chem. Commun.*, 2000, 1237.

27. V. Conte, E. Elakkari, B. Floris, V. Mirruzo, P. Tagliatesta, *Chem. Commun*., 2005, 1587-1588.

28. H. Schoefer, N. Kaftzik, P. Wasserscheid, U. Kragls, *Chem. Commun*., 2001, 425-426.

29. B. Yu, F. Zhou, G. Lui, Y. Liang, W. T. S. Huck, W. Liu, *Chem. Commun*., 2006, 2356.

30. J. G. Huddleston, H. D. Willauer, R. P. Swatloski, A. E. Visser, R, D. Rogers, *Chem. Commun*., 1998, 1765.

31. J. G. Huddleston, A. E. Vissor, W. M. Richert, H. D. Wellauer, G. A, Broker, R. D. Rogers, *Green Chem.*, 2001, **3**, 156-164.

32. A. E. Visser, R. P. Swatloski, R. D. Rogers, *Green Chem.*, 2000,**1**, 1-4.

33. P. Bonhote, A. P. Dias, N. Papageogiou, K. Kalyanasundaram, M. Gratzel, *Inorg. Chem*., 1996, 35, 1168-1178.

34. A. S. Larson, J. D. Holbrey, F. S. Tham, C. A. Reed, *J. Am. Chem. Soc*., 2000, 122, 7264-7272.

35. J. Asikkala, *Application of Ionic Liquids and Microwave Activation in Selected Organic Reactions*, Academic dissertation, ISBN-978-951-42-8719-0, OULU University press, 2008.

36. A. B. McEwen, H. L. Ngo, K. LeCompte, J. L Goldman, *J. Electrochem. Soc*., 1999, **146**, 1687-1895.

37. A. M. O'Mahony, D. S. Silvester, L. Aldous, C. Hardacre, R. G. Compton, *Journal of Chemical and Engineering Data*, 2008, **53**, 2884.

38. M. Diaw, A. Chagnes , B. Carr´e , P. Willmann , D. Lemordant *, Journal of Power Sources*, 2005, **146**, 682–684.

39. G. Feng, J. S. Zhang, R. Qiao, *J. Phys. Chem. C,* 2009**, 113***,* 4549–4559.

40. Y. Cao, J. Zhang, Y. Bai, R. Li, S. M. Zakeeruddin, M. Graetzel, P. Wang, *J. Phys. Chem. C,* 2008**, 112***,* 13775–13781.

41. H. Deligöz, M. Yılmazoeglu, *Journal of Power Sources,* 2011*,* **196**, 3496–3502.

42. B. Penga, J. Zhub, X. Liua, Y. Qina, *Sens. Actuators B*, 2008, **133**, 308–314.

43. M . Moniruzzaman, K. Nakashima, N. Kamiya, M. Goto, *Biochem Eng J*, 2010, **48**, 295 314.

44. P. B. Hitchcock, K. R. Seddon, T. Welton, *J. Chem. Soc. Dalton Trans*. 1993, 2639 -2643.

45. P. A. Z. Suarez, J. E. L.Dullius, S. Einloft, R. F. de Souza, J. Dupont, *Polyhedron*, 1996, **15**, 1217 - 1219.

46. A. E. Visser, R.P. Swattloski, W. M. Reichert, R. Mayton, S. Sheff, A.Wierzbicki, J. H. Davis, R. D. Rogers, *Chem. Commun*., 2001, 135-136.

47. R. A. Brown, P. Pollet, E. McKoon, C. A. Eckert, C. L. Liotta, P. G. Jessop, *J. Am. Chem. Soc.* 2001, **123**, 1254 - 1255

48. M . F. Sellin, P. B.Webb, D. J. Cole-Hamilton, *Chem. Commun*. 2001, 781 - 782.

49. A. G. Fadeev, M. M. Meagher, *Chem. Commun*. 2001, 295 - 296.

50. A. Brandt, JP. Hallett, DJ. Leak, RJ. Murphy, T. Welton, *Green Chem*., 2010, **12,** 672–679.

51. AP. Dadi, S. Varanasi, CA. Schall, *Biotechnol Bioeng,* 2006, **95**, 904–910.

52. T-AD. Nguyen, K-R. Kim, SJ. Han, HY. Cho, JW. Kim, SM. Park, JC. Park, SJ. Sim, *Bioresour Technol*, 2010, **101,** 7432–7438.

53. T. Welton, *Coordination Chemistry Reviews*, 2004, **248**, 2459-2477.

54. V. I. Parvulescu, C. Hardacre, *Chem. Rev*., 2007, **107**, 2615-2665.

55. K. R. J. Lovelock, I. J. Villar-Garcia, F. Maier, H. P. Steinruck,, P. Licence, *Chem. Rev.* 2010**, 110***,* 5158–5190

56. D. S. Silvester, T. L. Broder, L. Aldous, C. Hardacare, A. Crossley, R. G. Compton, *Analyst,* 2007, **132**, 196-198.

57. R. S. Varma, V. V. Namboodriri, *Chem. Commun*., 2001, 642-644.

58. J. Zhang, G. R. Martine, D. D. Desmarteau, *Chem. Commun*., 2003, 2334-2335.

59. N. R. Brooks, S. Schaltin, K. V. Hecke, L. V. Meervelt, K.Binnemans, J. Fransaer, *Chem. Eur. J.* 2011, 17, 5054 – 5059

60. N. Vanoanh, C. Houriez, B. Rousseau, *Phys. Chem.Chem.Phys*., 2010, **12**, 930-936.

61. C. Chiape, M. Malvaldi, B. Melai, S. Fantini, U. Bardi, S. Caporali, *Green. Chem*.,2010, **12**, 77-80.

62. L. C. Branco, J. N. Rosa, J. J. M. Ramos, C. A. M. Afonso, *Chem.-Eur. J*., 2002, **8**, 3671-3677.

63. F. Endres, S. Z. El Abedin A. Y. Saad, E. M. Moustefa, N. Borissenko, W. E. Price, G. G. Wallace, D. R MacFarlane, P. J. Newman, A. Bund, *Phys. Chem. Chem. Phys*., 2008, **10(16**), 2189-2199.

64. A. E. Visser, R. P. Swatloski, W. M. Reichert, S. T. Griffin, R. D.Rogers, *Ind. Eng. Chem. Res.*, 2000, **39**, 3596–3604.

65. A. E. Visser, R. P. Swatloski, W. M. Reichert, R. Rojers, *Environ. Sci. Technol*., 2002, **36**, 2523-2529.

66. I. J.B. Lin, C. S. Vasam, *J. Organomet. Chem.*, 2005, **690**, 3498.

67. F. M. Oireilly , J. M. Kelly, *New J. Chem*., 1998, 215-217.

68. S. Ramakrishnan, M. Palaniandavar, *J. Chem. Sci*., 2005, **117**, 179-186.

69. C. M. Thomas, T. R. Ward, *Chem. Soc. Rev*., 2005, **34**, 337–346.

70. J. D. Slinker, J. Rivnay, J. S. Moskowitz, J. B. Parker, S. Bernhard, H. D. Abruna, G. G.Malliaras, *J. Mater. Chem.,* 2007, **17**, 2976–2988.

71. G. Zassinovich, G. Mestroni, *Chem. Rev.* 1992**, 92***,* 1051-1009.

72. T.W. Ngan, C. C. Ko, N. Zhu, V. W. W. Yam, *Inorg. Chem.*, 2007, **46**, 1144–1152.

73. E. Schoffers, *Eur. J. Org. Chem.* **2003**, 1145-1152.

74. R. Kothandaraman , V. Nallathambi, K. Artyushkova , S. C. Barton, *Applied Catalysis B: Environmental*, 2009, **92**, 209–216.

75. M. Zhang, W. Zhang, T.Xiao, J. F. Xiang, X. Hao, W. H. Sun, *Journal of Molecular Catalysis A: Chemical*, 2010, **320**, 92-96.

76. V. Viossat, P. Lemoine, E. Dayan, N. H. Dung, B. Viossat, *Polyhedron*, 2003, **22**, 1461-1470.

77. W. R. Pitner, P. Krisch, K. Kawata, H. Shinohara, 2010. *Applications of Ionic Liquids in Electrolytic Systems,* pp 191-201. In: P. Wasserscheid and A. Stark (eds]. Handbook of Green Chemistry, Volume 6: Ionic Liquids. Wiley-VCH.

CHAPTER TWO

2. EXPERIMENTAL

2.1 Chemicals

1, 10-Phenanthroline monohydrate, 4, 4'-Bipyridine, all alkyl halides and Lithium bis[(trifluoromethane)sulfonyl]amide were obtained from Alfa Aesar. Hexafluorophosphoric acid and all the solvents used were obtained from Sigma – Aldrich and used as received.

2.2 Instruments

^{1}H NMR and ^{13}C NMR spectra were recorded on a 400 MHz Bruker 400 Ultra-Shield NMR with operating frequencies 270 MHz (^{1}H) and 68 MHz (^{13}C). Chemical shifts (δ) are reported in parts per million (ppm) with reference to residual traces in the commercial deuterated solvent, dimethyl sulfoxide $(CD_3)_2SO$ (δ_H 2.54, (δ_C 40.45) at ambient temperature. Coupling constants (*J*) are given in Hz.

The mass spectra were acquired on a Bruker Apex IV ICR-MS, equipped with an electron ionisation (EI) source, utilising external ionisation of the sample at 70 eV. The ion source was operated at a temperature of 130°C, although several samples required heating of the Direct Insertion Probe (DIP) in order to volatilise them. A typical maximum temperature of the DIP was 300°C. The mass range acquired was 50-1000, with free induction decay (FID) dataset size of 512K. Four spectra were averaged together prior to performing the Fourier Transform, in order to enhance signal-to-noise ratio.

Ion chromatography was performed to check for halide impurities in the ion exchanged salts. The instrument used is a Dionex ICS-3000, equipped with a Dionex AS20 (2x 250 mm) analytical column and a Dionex CG 20 guard column (2x 50 mm). The eluent was a mixture of Millipore Milli-Q 18 MΩ water, 100 mM NaOH aqueous solution and acetonitrile in a 60:15:25 volume ratios and the flow rate was 0.25 mL/min. The sample was prepared by pre-dissolving 2.5-5 mg of ionic liquid in 2 mL acetonitrile and adding 8 mL extra of Millipore Milli-Q 18 MΩ water. The measured retention times for the analytes investigated with this experimental set up are 10.9 minutes for the iodide, 32.2 minutes for the $[NTf_2]^-$ anion and 18.5 minutes for $[PF_6]^-$.

CHNS elemental analyses were performed with a Flash EA 1112 Elemental Analyser (Thermo Quest).

MALDI- TOF MS in reflectron mode were performed in a Bruker Ultraflex III. The matrix used was trans-2[3-(4-tert-Butylphenyl)-2-methyl-2-propenylidene] malononitrile, commonly referred to as DCTB. The sample solution and the DCTB in acetonitrile were mixed together to give about 10:1 excess of matrix. 0.5µl of this mixture was spotted onto a stainless steel target plate and allowed to evaporate to dryness before introduction into the mass spectrometer. The laser operates at a wavelength of 337 nm. Calibration of the data were performed in the FlexControl software.

Thermal data were determined by DSC (Q2000 V24.4 Build 116) and TGA (Q500 V20.10 Build 36). Samples were placed in a 40-µL sealed aluminum pan with a pinhole at the top of the pan. An empty aluminum pan was used as the reference. The samples inside the differential scanning calorimeter furnace were exposed to a flowing N_2 atmosphere. Measurements for melting, crystallization, and glass transition temperatures

were determined by cooling the samples from 200 °C to -20 °C, followed by heating from -20 °C to 200 °C, both at a rate of 10 °C/min.

The onset temperature (T_{onset}) is the intersection of the baseline weight after the drying step, and the tangent of the weight vs temperature curve as decomposition occurs.

The glass transition temperature (T_g) was determined to be the midpoint of a heat capacity change, whereas the melting and crystallization temperatures were determined at the respective peak maxima of the transition curve.

All XP spectra were recorded using a Kratos Axis Ultra spectrometer employing a focused, monochromated Al Kα source (hν = 1486.6 eV), hybrid (magnetic / electrostatic) optics, hemispherical analyzer and a multi-channel plate and delay line detector (DLD) with an X-ray incident angle of 0^0 (relative to surface normal). The information depth (ID) of these experiments may be defined as the depth, with in the sample, from which 95% of the measured signal will originate. ID is assumed to vary mainly with cos θ, where θ is the electron emission angle relative to the surface normal. ID = 7 – 9 nm and the data obtained may be considered as a representative of the bulk composition. X- ray gun power was set to 100 W. All spectra were recorded using an entrance aperture of 300 x 700 μm with pass energy of 80 eV for survey spectra and 20 eV for high-resolution spectra. The instrument sensitivity was 7.5 x 10^5 counts s^{-1} when measured the Ag $3d_{5/2}$ photoemission peak for a clean Ag sample recorded at a pass energy of 20 eV and 450 W emission power. Ag $3d_{5/2}$ full width at half maximum (FWHM) was 0.55 eV for the same instrument settings. Binding energy calibration was made using Au $4f_{7/2}$ (83.96 ev), Ag $3d_{5/2}$ (368.21 ev and Cu $2p_{3/2}$ (932.62 ev). The absolute error in the acquisition of binding energies is $\pm$0.1 eV, as quoted by the

instruments manufacturer (Kratos); consequently, any binding energy within 0.2 eV can be considered the same, within the experimental error.

2.3. Synthesis and Characterization of the New Ionic Liquids

The initial step in the synthesis of ionic liquids is the quaternization of an amine or phosphane, for example, to form the cation. Salts with different anions are obtained by anion exchange via metathesis reaction [1]. Products with melting points below 100 ^{0}C are obtained this way.

The quaternization of 1, 10-Phenanthroline is straightforward (Scheme 2.1) and was carried out using different alkyl halides which have different boiling points and reactivity following reported procedures [2]. Based on this the selection of best solvents, tuning of optimum reaction temperature and duration was carried out through logical trials as the reaction time and temperature are very dependent on the alkylating agent employed [3-6]. Even though it has two equally likely quaternizable nitrogen atoms, the first alkylations impedes the second due to steric hindrance [7]. As a result, a monocharged asymmetric salt can be obtained. This fact helps to get products with low melting points [8].

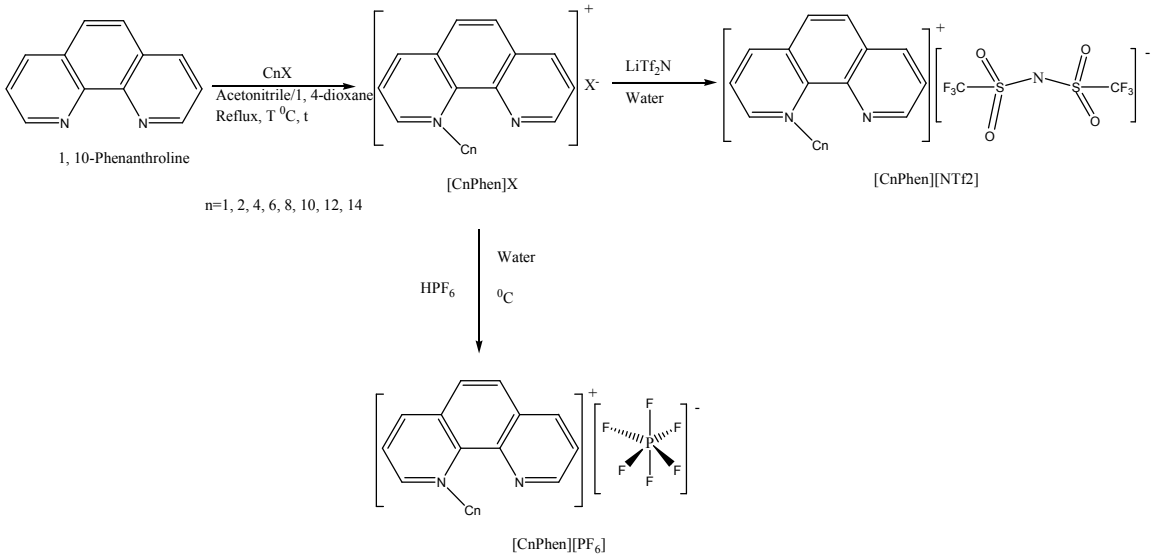

Scheme 2. 1: Synthesis of 1, 10-Phenanthrolinium Based Ionic Liquids

Unlike 1, 10-Phenanthroline, 4, 4-Bipyridine has two potentially equally likely quaternizable nitrogens that are not sterically hindered by the first alkylation. Therefore, it needs optimization to selectively quaternize only one of the nitrogens so as to get products with monocharge and less symmetric structure. Moreover, the monoalkylation creates an opportunity for the charge carrier to have coordinating site with metal ions. Otherwise, the alkylation of both nitrogens of 4, 4-Bipyridine results in products with two charges on each cation that produce strong Columbic force and higher melting point thereof. The monoalkylation was achieved by searching for a reaction medium in such a way that the first alkylation on one of the nitrogenes of 4, 4-Bipyridine results in a product that precipitates or forms a separate phase. 1, 4-dioxane was found to be the best solvent for this system of ionic liquids. Otherwise, the optimization of the reaction conditions were adopted from the synthesis of the 1, 10-Phenanthrolinium based ionic liquids system (Scheme 2.2).

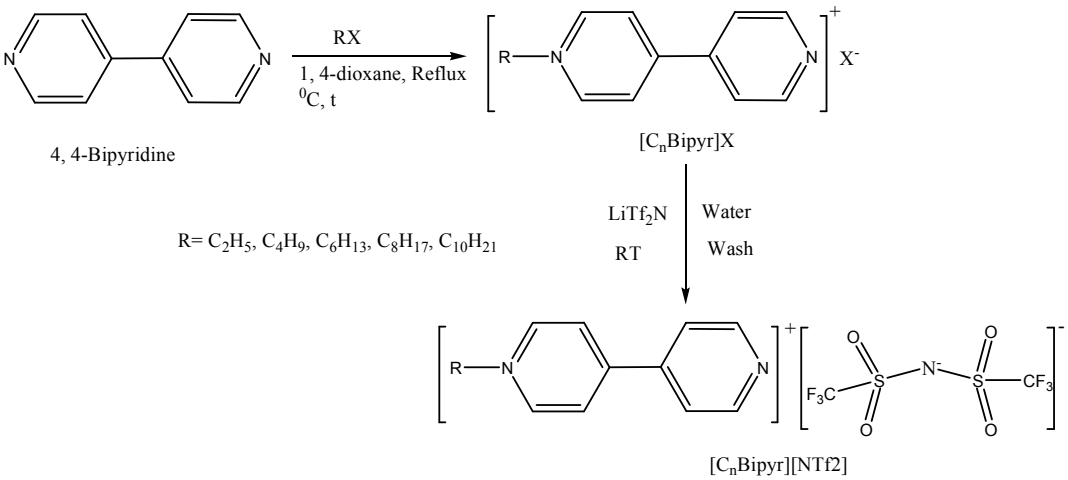

Scheme 2. 2: Synthesis of N-Alkyl-4, 4-Bipyridinium Based Ionic Liquids

2.3.1 Synthesis of N-Alkyl-1, 10-Phenanthrolinium Cation Based Ionic Liquids

2.3.1.1 Synthesis of N-Alkyl-1, 10-Phenanthrolinium Halide, [C_nPhen]X

1, 10-Phenanthroline was dried in an oven at 110 ^{0}C for 2 hrs. When CH_3I and C_2H_5I are used as alkylating agents, 20 g (0.11 mol) 1, 10-Phenanthroline was dissolved in dried acetonitrile in a 250 ml two necked round bottom flask fitted to a reflux condenser and covered with aluminum foil and guarded from moisture using $CaCl_2$. 0.12 mol alkyl halide was added drop wise to 1, 10-Phenanthroline while stirring. The mixture was stirred in an oil bath at 30-35 ^{0}C for 8 hrs. A yellow precipitate was obtained which was filtered thoroughly and washed with chloroform and dried and put in a dark vial. Involving alkyl bromides as alkylating agents the quantities of the reagents being the same as above, duration of the reaction time and the temperature were increased from 24 to 72 hrs and 40 to 80 ^{0}C, respectively, following the chain length. In all cases, gray precipitates were obtained. The precipitates were filtered and [C_4Phen]Br, [C_5Phen]Br

and [C_6Phen]Br were washed thoroughly with acetone while [C_8Phen]Br, [C_{10}Phen]Br, [C_{12}Phen]Br and [C_{14}Phen]Br were washed with 1, 4-Dioxane..

2.3.1.2 Synthesis of [C_nPhen][NTf_2]

The halide anions were exchanged with $[NTf_2]^-$ by dissolving 0.050 mol [C_nPh]X, X = Br^- , I^-; n = 1, 2, 4, 6, 8; in deionized water at room temperature to which 0.051 mol of $LiNTf_2$ dissolved in water was mixed gradually while stirring. White precipitates were obtained. The white powder was filtered, thoroughly washed with deionized water and dried. For n = 10, 12 and 14, the halide salt was dissolved in round-bottome flask at 70 ^{0}C to which slightly excess of equimolar amount solution of $LiNTf_2$ was added drop wise. A separate phase of a viscous liquid following the formation of white suspension was formed. The viscous liquid was decanted, washed thoroughly at 70 ^{0}C and dried in vacuo. The viscous mass solidified after several days.

2.3.1.3 Synthesis of [C_nPhen][PF_6]

0.01 mol of the halide salt was dissolved in deionized water in round bottom flask and cooled to 0 ^{0}C using ice bath. While stirring, solution of 0.011 mol of HPF_6 was added drop wise and a white precipitate was formed. The stirring was allowed to continue for 15 minutes and allowed to stand. The precipitate was decanted and dried in vacuo.

2.3.2 Synthesis of N-Alkyl-4, 4'-Bipyridinium Cation Based Ionic Liquids

2.3.2.1 Synthesis of [C_nBipyr]X

15 g (0.096 mol) of 4, 4-Bipyridine was dissolved in dry 1, 4 - dioxane in a two necked 250 ml round- bottom flask fitted to a condenser. Into this solution, 0.097 mol of 1-Bromoalkane ($C_nH_{n+1}Br$) was added drop wise at room temperature. The mixture was

allowed to stir for 72 hrs at 45-70 ^{0}C depending on the alkyl chain length. Grayish yellow solid precipitates were obtained. The products were characterized by ^{1}H and ^{13}C NMR and halide test and found to contain mixture of monoalkylated and dialkylated 4, 4-Bipyridinium bromide in which the dialkylated form was in very small proportion and is considered as an impurity. To this grayish yellow solid, chloroform (n = 4 & 6) and acetone (n = 8 &10) were added that dissolve the monoalkylated product,. The mixture was filtered and the supernatant was dried using rotary evaporator which resulted in a highly hygroscopic gray solid. Yield: (70-77%).

2.3.2.2 Synthesis of [C_nBipyr] [NTf_2]

0.072 mol of [C_nBipyr]Br was dissolved in deionized water in a 250 ml round-bottom flask. While stirring water solution 0.086 mol Li[$(CF_3SO_2)_2N$] was added drop wise which resulted in the formation of white suspension followed by yellowish droplets of separate phase viscous liquid. It was left to stand overnight. The droplets formed a completely separate phase from the water. The water was discarded and the product was washed three times in 50 ml of water each by stirring at 50 ^{0}C and dried in vacuo at 60 ^{0}C for 24 hrs. Finally nearly colorless [C_nBipyr][NTf_2] was collected. Yield: (80-87%).

2.3.3 Synthesis of N, N'-Dialkyl-4, 4'-Bipyridinium Cation Products

2.3.3.1 Synthesis of N, N'-Dialkyl-4, 4'-Bipyridinium Bromide, [$(Cn)_2$Bipyr] Br_2

10 g (0.064 mol) of 4, 4-Bipyridine was dissolved in dry acetonitrile in a two necked 250 ml round bottom flask fitted to a condenser. In to this solution, 0.0128 mol of 1-Bromoalkane ($C_nH_{n+1}Br$) was added drop wise.. The mixture was allowed to stir for 96 hrs at 45 ^{0}C when C_2H_5Br is the alkylating agent and 60-80 ^{0}C for C_4H_9Br, $C_6H_{13}Br$,

$C_8H_{17}Br$ and $C_{10}H_{21}Br$ depending on the alkyl chain length. Bright yellow solid precipitate was obtained. The product was filtered and washed repeatedly with acetonitrile (Scheme 2.3). Yield: (85-90%)

2.3.3.1 Synthesis of N, N'-Dialkyl-4, 4'-Bipyridinium [Bis(trifluormethylsulphonyl)amide], $[(Cn)_2Bipyr]\ [NTf_2]_2$

0.051 mol of $[(Cn)_2Bipyr]Br_2$ was dissolved in water in a 100 ml round-bottom flask. While stirring water solution of 0.113 mol of $Li[(CF_3SO_2)_2N]$ was added drop wise which resulted in the formation of white precipitates. The stirring was allowed to continue for 30 minutes and then left to stand overnight. The water was discarded and the powder was washed three times in water by stirring and was put in a desiccator. Then the powder was dried using vacuum line at 60 ^{0}C for 24 hrs (Scheme 2.3). (80-87%)

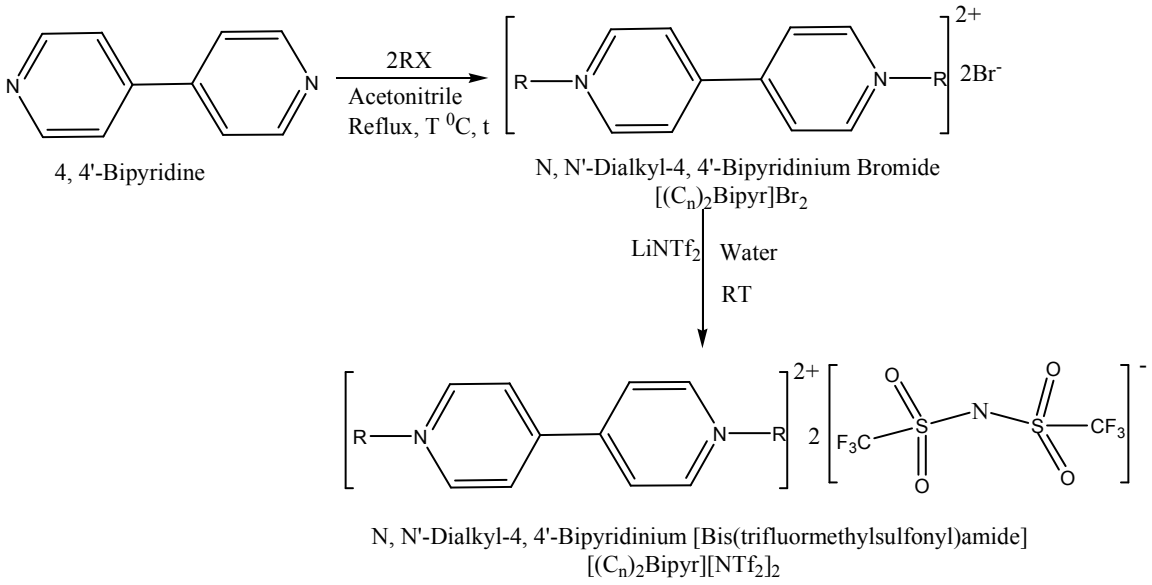

Scheme 2. 3: Synthesis of N, N'-Dialkyl-4, 4'-Bipyridinium based products

2.4 Results

2.4.1 Spectroscopic, CHN microanalysis and thermal properties of 1, 10-Phenanthroline based ILs

^{1}H, ^{13}C, ^{19}F and ^{31}P NMR

[C_1Phen]I: Yellow powder, yield: 87%

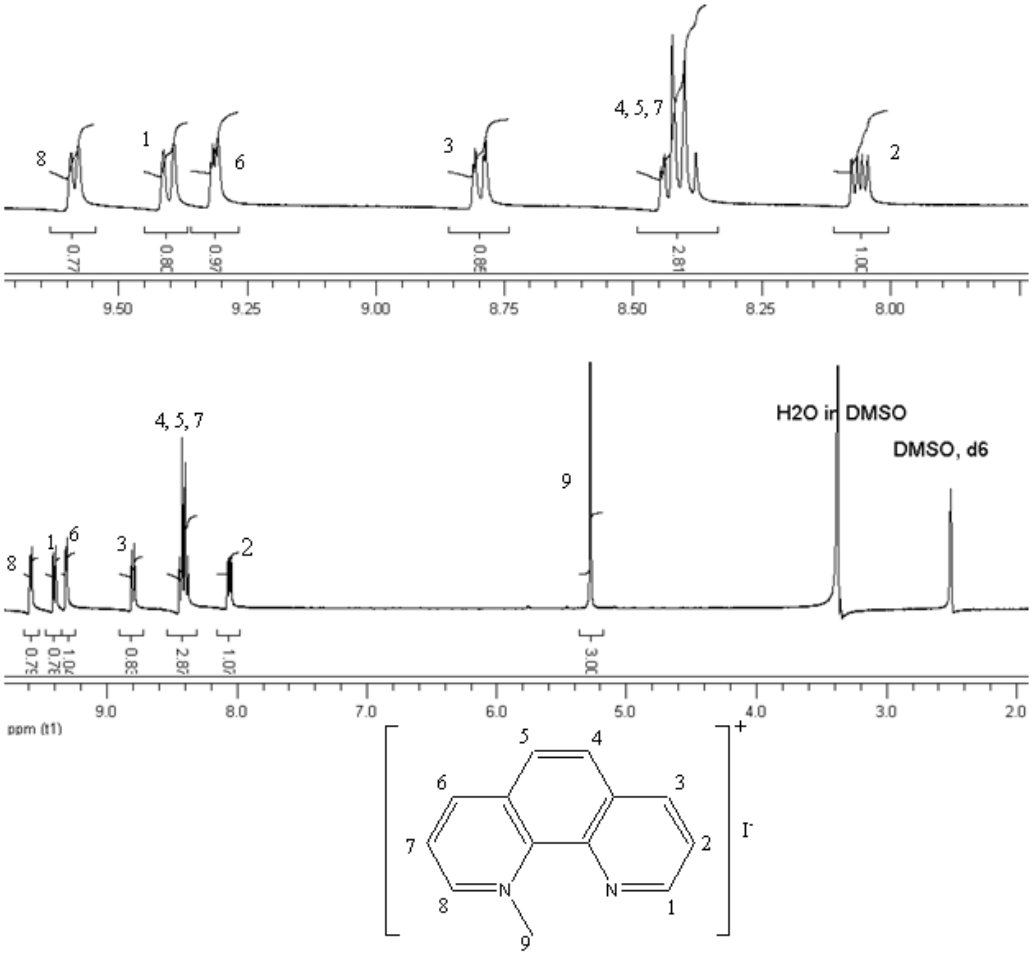

Figure 2. 1: ^{1}H NMR of [C_1Phen]I

^{1}H NMR (400 MHz, *DMSO, d_6*). δ ppm 5.28 (s, 3H), 8.06 (dd, J = 8.17, 4.26 Hz, 1H), 8.39 (d, J = 8.8 Hz, 1H),8.43(d, J =7.6Hz, 1H), 8.49(d, J =8.8Hz, 1H) 8.80 (dd, J = 8.20,

1.64 Hz, 1H), 9.31 (dd, *J* = 4.19, 1.68 Hz, 1H), 9.40 (d, *J* = 8.04 Hz, 1H), 9.58 (d, *J* = 5.68 Hz, 1H)

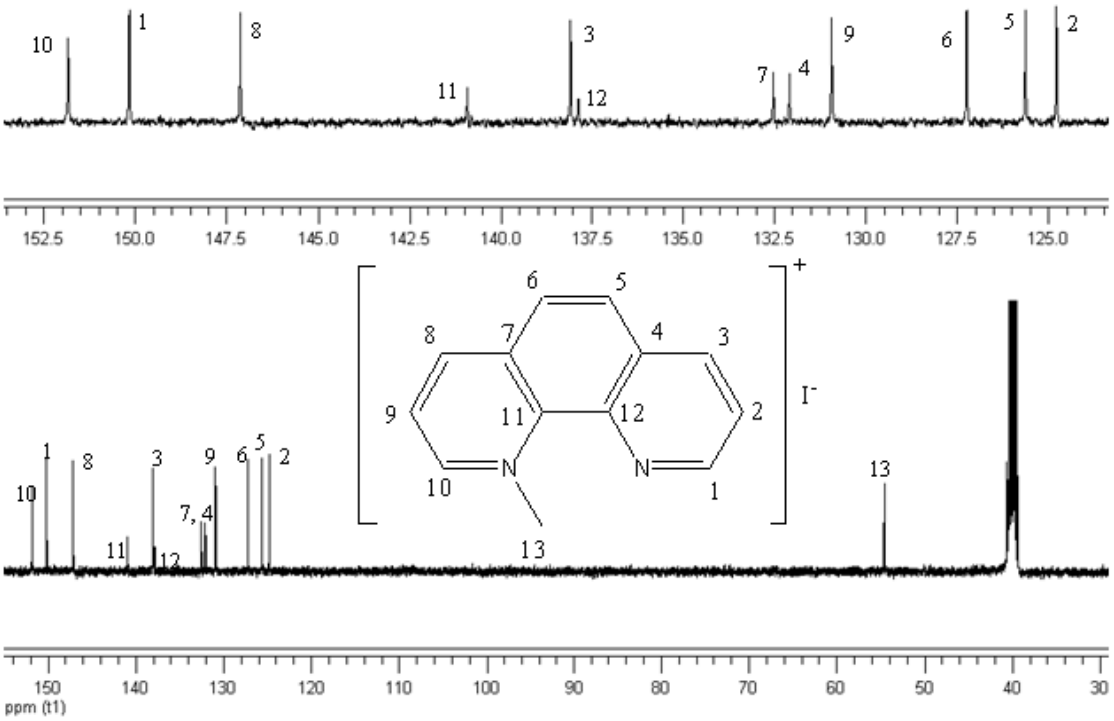

Figure 2. 2: ^{13}C NMR of $[C_1Phen]I$

^{13}C NMR (101 MHz, *DMSO, d_6*) δ ppm , 54.61 (s,1C), 124.79 (s,1C), 125.64 (s,1C), 127.24 (s,1C), 130.93 (s,1C), 132.09 (s,1C), 132.53 (s,1C), 137.86 (s,1C), 138.07 (s,1C), 140.93 (s,1C), 147.13 (s,1C), 150.17 (s,1C), 151.84 (s,1C)

ESI-MS: m/z =: 126.9040, I^+; m/z = 141.9276, CH_3I^+,; m/z = 180.0685, $Phen^+$,

[C_1Phen][NTf_2]: White powders, yield: 98%

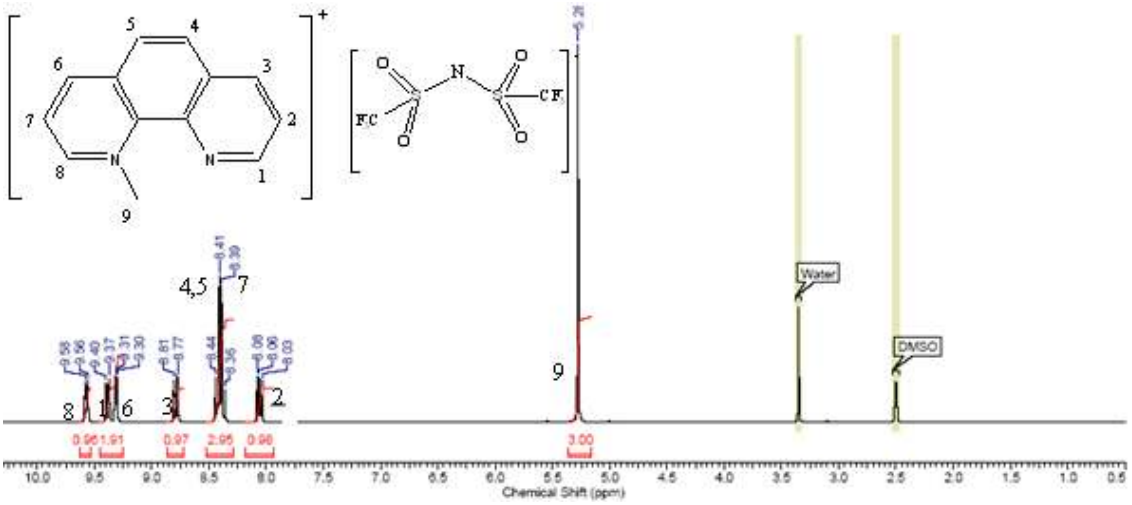

Figure 2. 3: ^{1}H NMR of [C_1Phen][NTf_2]

^{1}H NMR (400 MHz, *DMSO* d_6) δ ppm, 5.25 (s, 1H), 8.01 (dd, J = 8.18, 4.28 Hz, 1H), 8.32 (d, J = 8.81 Hz, 1H), 8.35 (d, J = 6.81 Hz, 1H), 8.37 (d, J = 0.92 Hz, 1H), 8.73 (dd, J = 8.20, 1.61 Hz, 1H), 9.28 (dd, J = 4.22, 1.70 Hz, 1H), 9.33 (d, J = 8.15 Hz, 1H), 9.49 (d, J = 5.89 Hz, 1H)

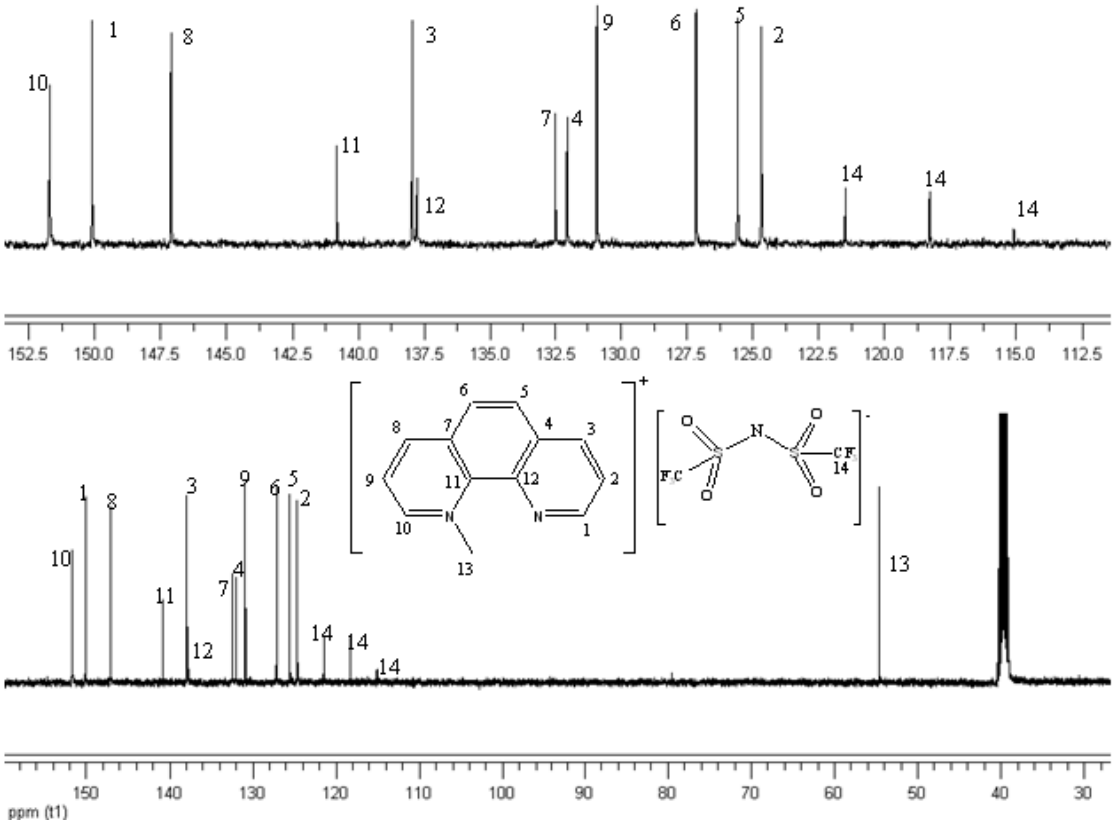

Figure 2. 4: ^{13}C NMR of $[C_1Phen][NTf_2]$

^{13}C NMR (101 MHz *DMSO, d_6)* δ ppm 54.60 (s,1C), 119.85 (q, *J* = 321.99, 322.00, 304.82Hz,1C), 124.67 (s,1C), 125.57 (s,1C), 127.15 (s,1C), 130.91 (s,1C), 132.04 (s,1C), 132.48 (s,1C), 137.79 (s,1C), 137.96 (s,1C), 140.82 (s,1C), 147.11 (s,1C), 150.10 (s,1C), 151.72 (s,1C)

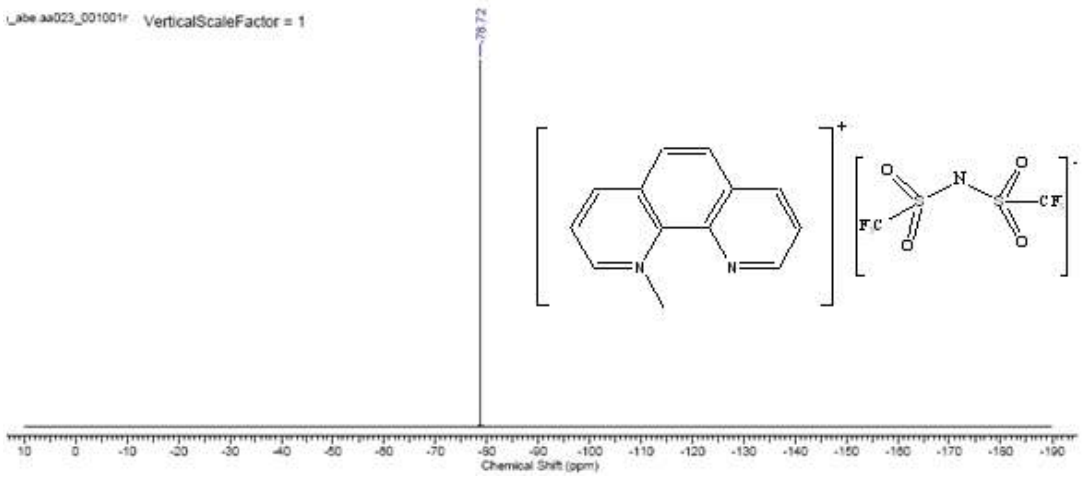

Figure 2. 5: ^{19}F NMR of $[C_1Phen][NTf_2]$

^{19}F NMR (376 MHz, DMSO-d_6) δ ppm -78.71 (s, 6 F)

ESI-MS:

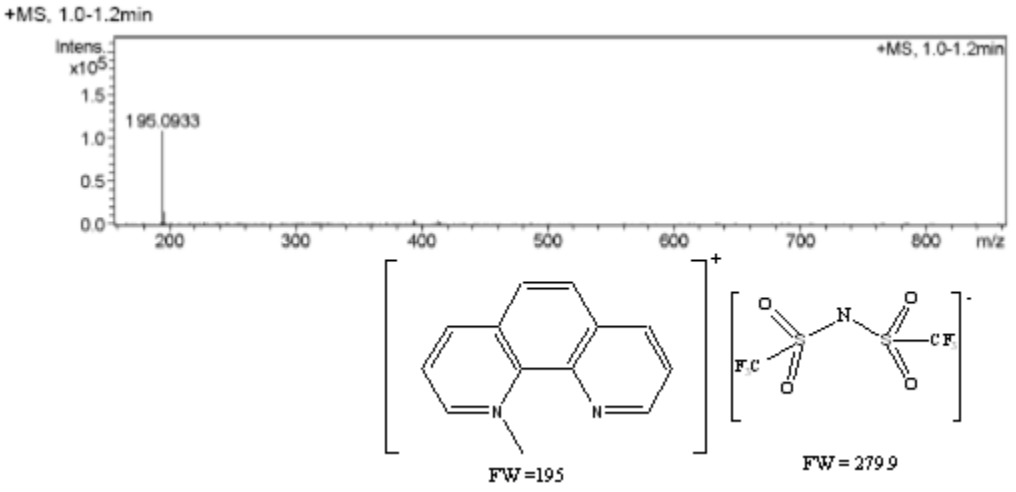

Figure 2. 6: ESI-MS of $[C_1Phen][NTf_2]$ with the positive formula method

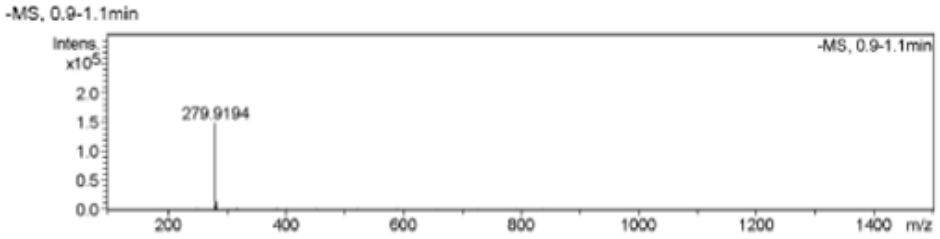

Figure 2. 7: ESI-MS of $[C_1Phen][NTf_2]$ with the negative formula method

m/z = 195.0918, $[C_1Phen]^+$; m/z = 670, $[C_1Phen][NTf_2][C_1Phen]$.

$[C_1Phen][PF_6]$

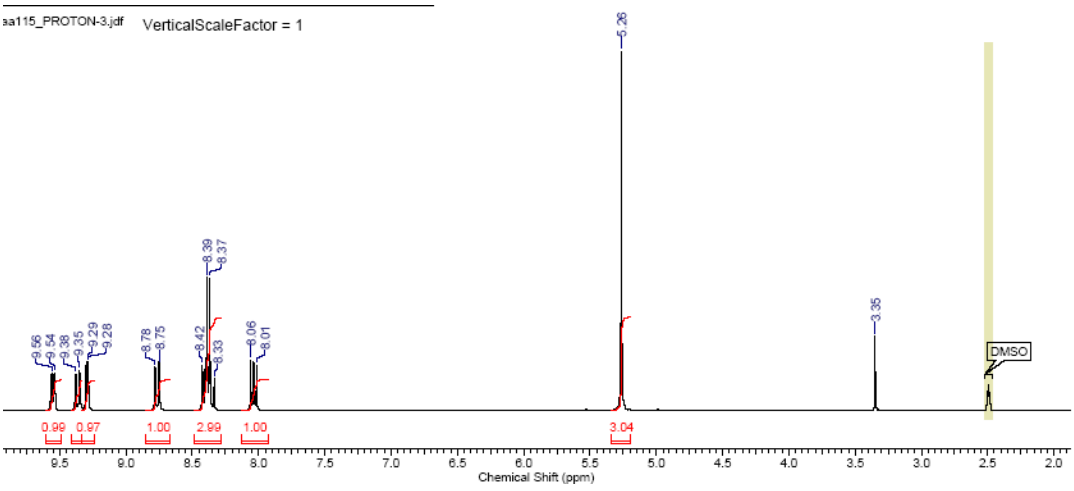

Figure 2. 8: ^1H NMR of $[C_1Phen][PF_6]$

^1H NMR (270 MHz, DMSO,d_6δ ppm 4.42 (s, 3 H) 7.19 (dd, *J* = 8.26, 4.27 Hz, 1 H) 7.41 - 7.66 (m, 3 H) 7.92 (dd, *J* = 8.26, 1.79 Hz, 1 H) 8.45 (dd, *J* = 4.27, 1.79 Hz, 1 H) 8.52 (dd, *J*=8.26, 1.10 Hz, 1 H) 8.65 - 8.76 (m, 1 H)

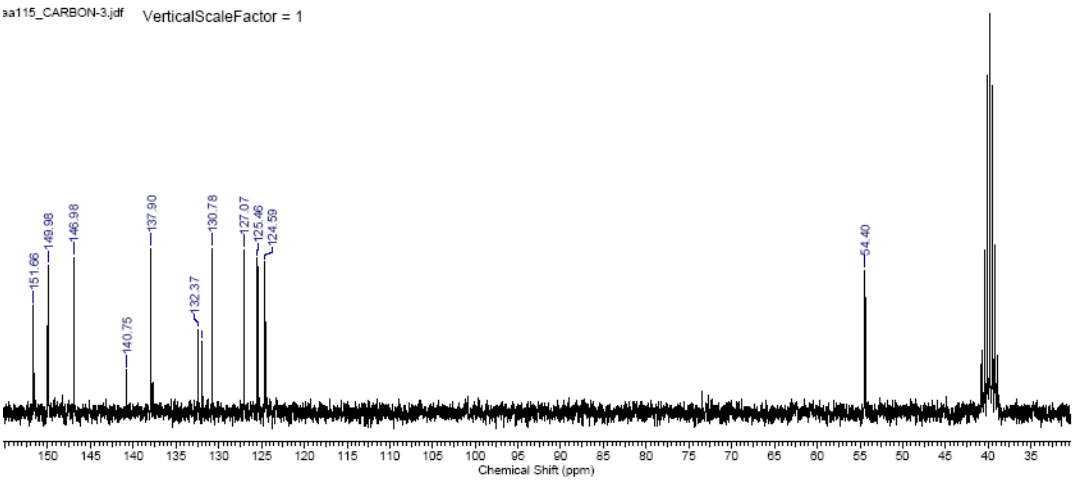

Figure 2. 9: ^{13}C NMR of [C_1Phen][PF_6]

^{13}C NMR(400MHz, DMSO,d_6) δ ppm, 54.40(s, 1C), 124.59(s, 1C), 125.46(s, 1C), 127.07(s, 1C), 130.78(s, 1C), 131.92(s, 1C), 132.37(s, 1C), 137.71(s, 1C), 137.90(s, 1C), 140.75(s, 1C), 146.98(s, 1C), 149.98(s, 1C), 151.66(s, 1C).

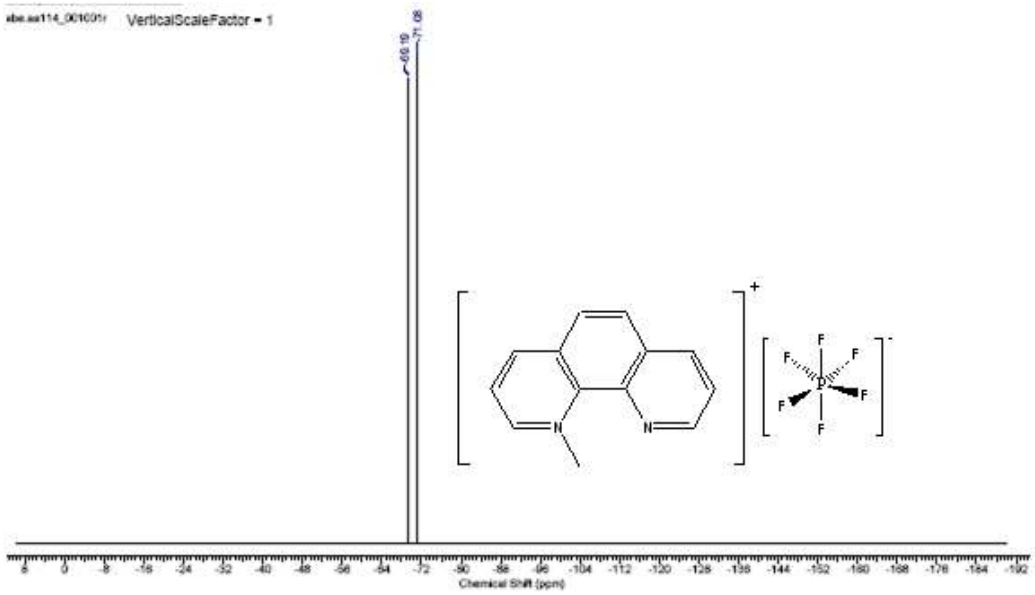

Figure 2. 10: ^{19}F NMR of [C_1Phen][PF_6]

^{19}F NMR (376 MHz, DMSO-d_6) TMS, δ ppm -70.14 (d, J = 1.00 Hz, 6 F)

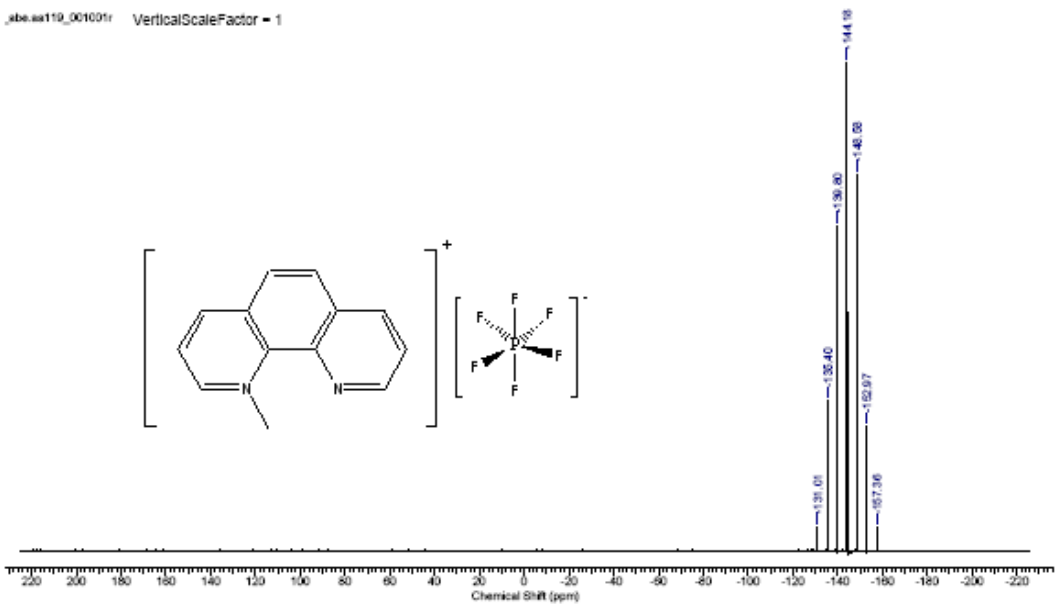

Figure 2. 11: ^{31}P NMR of [C_1Phen][PF_6]

^{31}P NMR (162 MHz, DMSO-d_6) δ ppm -161.84 - -125.40 (m, 1 P)

ESI-MS:

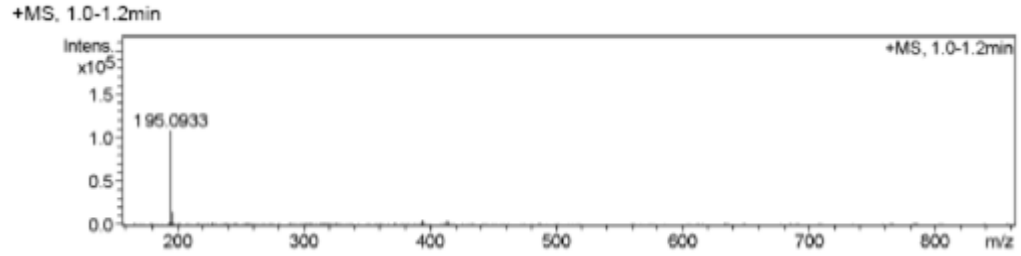

Figure 2. 12: ESI-MS of [C_1Phen][PF_6] with the positive formula method

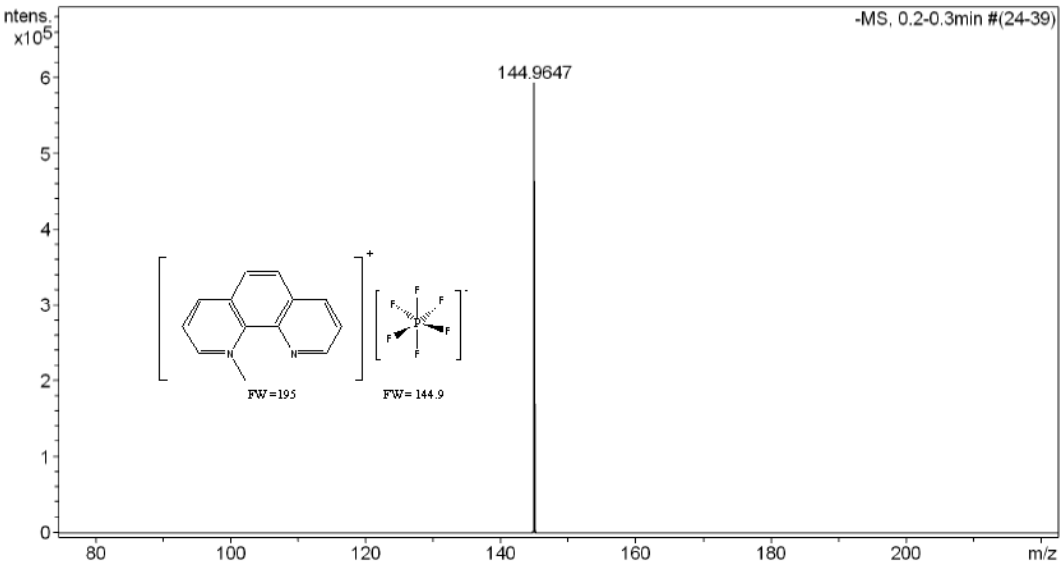

Figure 2. 13: ESI-MS of $[C_1Phen][PF_6]$ with the negative formula method.

m/z =195.0924, $[C_1Phen]^+$; m/e =144.9647, $[PF_6]^-$

$[C_2Phen]I$: Yellow powders, yield: 83%

^{1}H NMR (400 MHz, *D2O*) δ ppm 1.57 (t, *J* = 7.02, 7.02 Hz, 3H), 5.80 (q, *J* = 7.06, 6.94, 6.94 Hz, 2H), 7.73 (dd, *J* = 8.13, 4.14 Hz, 1H), 7.92 (d, *J* = 8.79 Hz, 1H), 7.99 (d, *J* = 8.71 Hz, 1H), 8.05 (dd, *J* = 8.06, 6.07 Hz, 1H), 8.36 (dd, *J* = 8.16, 1.63 Hz, 1H), 8.93 (dd, *J* = 8.11, 1.18 Hz, 1H), 9.05 (dd, *J* = 4.10, 1.58 Hz, 1H), 9.10 (d, *J* =*2.2*Hz, 1H)

^{13}C NMR (101 MHz, *D2O*) δ ppm 16.20 (s,1C), 60.11 (s,1C), 123.98 (s,1C), 125.00 (s,1C), 126.39 (s,1C), 130.65 (s,1C), 131.82-131.63 (m,1C), 137.51-137.30 (m,1C), 146.62 (s,1C), 149.35-149.24 (m,1C), 149.77 (s,1C)

ESI-MS: m/z = 126.9038, I^+; m/z = 127.9117, HI^+; m/z = 155.9430, $C_2H_5I^+$; m/z =180.068, $Phen^+$.

[C_2Phen]Br: White powders, yield: 78%

^{1}H NMR (400 MHz, , *DMSO, d_6*) δ ppm 1.71 (t, *J* = 6.98, 6.98 Hz, 3H), 5.96 (q, *J* = 7.00, 7.00, 7.00 Hz, 2H), 8.06 (dd, *J* = 8.17, 4.27 Hz, 1H), 8.39 (d, *J* = 8.81 Hz, 1H), 8.43 (d, *J* = 8.97 Hz, 1H), 8.45 (d, *J* = 8.07 Hz, 1H), 8.80 (dd, *J* = 8.22, 1.76 Hz, 1H), 9.32 (dd, *J* = 4.25, 1.79 Hz, 1H), 9.41 (dd, *J* = 8.23, 1.21 Hz, 1H), 9.67 (dd, *J* = 5.96, 1.28 Hz, 1H)

^{13}C NMR (101 MHz, *DMSO, d_6*) δ ppm 17.36 (s,1C), 59.81 (s,1C), 125.22 (s,1C), 125.82 (s,1C), 127.56 (s,1C), 130.97 (s,1C), 132.08 (s,1C), 132.98 (s,1C), 136.90-136.87 (m,1C), 138.36 (s,1C), 140.01-139.99 (m,1C), 147.42 (s,1C), 150.54 (s,1C), 151.25 (s,1C)

[C_2Phen][NTf_2]: White powders, yield: 94%

^{1}H NMR (400 MHz, *DMSO, d_6*)δ ppm 1.72 (t, *J* = 6.99, 6.99 Hz, 3H), 5.95 (q, *J* = 6.98, 6.98, 6.97 Hz, 2H), 8.05 (dd, *J* = 8.19, 4.27 Hz, 1H), 8.35 (d, *J* = 8.83 Hz, 1H), 8.38 (d, *J* = 5.51 Hz, 1H), 8.41 (d, *J* = 6.01 Hz, 1H), 8.77 (dd, *J* = 8.24, 1.76 Hz, 1H), 9.31 (dd, *J* = 4.27, 1.80 Hz, 1H), 9.35 (dd, *J* = 8.18, 1.20 Hz, 1H), 9.57 (dd, *J* = 5.95, 1.31 Hz, 1H)

^{13}C NMR (101 MHz, *DMSO, d_6*) δ ppm 17.28 (s,1C), 59.91 (s,1C), 119.88 (q, *J* = 645.72, 319.58 Hz,1C), 125.14 (s,1C), 125.80 (s,1C), 127.52 (s,1C), 131.00 (s,1C), 132.09 (s,1C), 132.99 (s,1C), 136.95 (s,1C), 138.32 (s,1C), 140.01 (s,1C), 147.40 (s,1C), 150.52 (s,1C), 151.11 (s,1C)

^{19}F NMR (376 MHz, DMSO-d_6) δ ppm -78.75 (s, 6 F)

ESI-MS: m/z = 209, $[C_2Phen]^+$; and m/e = 279.91, $[NTf_2]^-$

$[C_2Phen][PF_6]$

^{1}H NMR (270 MHz, DMSO-d_6) δ ppm 1.72 (t, *J* = 6.89 Hz, 3 H) 5.95 (q, *J* = 6.75 Hz, 2 H) 8.05 (dd, *J* = 8.06, 4.20 Hz, 1 H) 8.26 - 8.56 (m, 3 H) 8.77 (d, *J* = 7.44 Hz, 1 H) 9.18 - 9.49 (m, 2 H) 9.62 (d, *J*=5.37 Hz, 1 H)

^{13}C NMR (400 MHz, DMSO-d_6) δ ppm 16.85(s, 1C), 59.36(s, 1C), 124.73(s, 1C), 125.33(s, 1C), 127.08(s, 1C), 130.51(s, 1C), 131.62(s, 1C), 132.54(s, 1C), 136.47(s, 1C) 137.87(s, 1C), 139.55(s, 1C), 146.94(s, 1C), 150.04(s, 1C), 150.76(s, 1C).

^{19}F NMR (376 MHz, DMSO-d_6) δ ppm -70.12 (d, *J*=1.00 Hz, 6 F)

^{31}P NMR (162 MHz, DMSO-d_6) δ ppm -162.46 - -124.78 (m, 1 P)

$[C_4Phen]Br$: White powder, yield: 63%

^{1}H NMR (400 MHz, *CDCl3)* δ ppm 0.84 (t, *J* = 7.39, 7.39 Hz, 1H), 1.45 (sex, *J* = 7.60, 7.20, 7.60, 7.20 Hz, 2H), 1.93 (q, *J* = 7.60, 7.60, 7.60, 7.60 Hz, 2H), 6.04 (t, *J* = 7.60, 7.60 Hz, 2H), 7.83 (q, *J* = 4.00, 4.00, 4.40Hz, 1H), 8.18 (d, *J* = 8.78 Hz, 1H), 8.33 (t, *J* = 8.80, 8.80 Hz, 1H), 8.36 (t, *J* = 6.40, 8.00 Hz, 1H), 8.53 (dd, *J* = 8.19, 1.43 Hz, 1H), 9.07 (dd, *J* = 4.14, 1.71 Hz, 1H), 9.42 (d, *J* = 8.14 Hz, 1H), 10.17 (d, *J* = 5.92 Hz, 1H)

^{13}C NMR(101 MHz, CDCl3), δ ppm 13.66 (s,1C), 19.52 (s,1C), 33.76 (s,1C), 64.17 (s,1C), 125.00 (s,1C), 125.38 (s,1C), 127.39 (s,1C), 131.03 (s,1C), 132.01 (s,1C), 132.78

(s,1C), 136.41 (s,1C), 137.90 (s,1C), 139.72 (s,1C), 147.21 (s,1C), 149.72 (s,1C), 151.39 (s,1C)

[C_4Phen][NTf_2]: White powders, yield: 91%

^{1}H NMR (400 MHz, *DMSO, d_6*) δ ppm 1.00 (t, *J* = 7.40, 7.40 Hz, 3H), 1.55 (q, *J* = 7.20, 7.60, 7.20, 7.60, 7.20Hz, 2H), 2.04 (q, *J* = 7.60, 7.60, 7.20, 7.60 Hz, 2H), 5.91 (t, *J* = 8.80, 7.60 Hz, 2H), 8.06 (dd, *J* = 8.17, 4.27 Hz, 1H), 8.40 (d, *J* = 9.34 Hz, 1H), 8.38 (d, *J* = 11.69 Hz, 1H), 8.43 (s, 1H), 8.79 (d, *J* = 8.19 Hz, 1H), 9.31 (t, *J* = 1.60, 2.40Hz, 1H), 9.38 (d, *J* = 7.98 Hz, 1H), 9.59 (d, *J* = 5.86 Hz, 1H)

^{19}F NMR (376 MHz, DMSO-d_6) δ ppm -78.74 (s, 6 F)

ESI-MS: m/z = 237.1397, $[C_4Phen]^+$; m/e = 279.912, $[NTf_2]^-$

[C_6Phen][PF_6]

^{1}H NMR (270 MHz, DMSO-d_6) δ ppm 0.75 - 1.02 (m, 3 H) 1.20 - 1.46 (m, 4 H) 1.54 (quin, *J* = 7.09 Hz, 2 H) 2.06 (quin, *J* = 7.57 Hz, 2 H) 5.77 - 5.99 (m, 2 H) 8.07 (dd, *J* = 8.13, 4.27 Hz, 1 H) 8.30 - 8.56 (m, 3 H) 8.80 (dd, *J* = 8.26, 1.79 Hz, 1 H) 9.31 (dd, *J* = 4.27, 1.79 Hz, 1 H) 9.40 (dd, *J* = 8.19, 1.31 Hz, 1 H) 9.62 (dd, *J* = 5.92, 1.38 Hz, 1 H)

^{13}C NMR(400MHz, DMSO, d_6) δ ppm, 14.13(s, 1C), 22.25(s, 1C) 5.70(s, 1C), 31.01(s, 1C), 31.25(s, 1C), 63.74(s, 1C), 124.87(s, 1C), 125.67(s, 1C), 127.45(s, 1C), 130.85(s, 1C), 132.92(s, 1C), 136.76(s, 1C), 138.23(s, 1C), 139.91(s, 1C), 147.30(s, 1C), 150.24(s, 1C), 151.11(s, 1C).

^{31}P NMR (162 MHz, DMSO-d_6) δ ppm -164.31 - -121.07 (m, 1 P)

[C_8Phen]Br

^{1}H NMR (270 MHz, DMSO-d_6) δ ppm 0.68 - 0.93 (m, 3 H) 1.11 - 1.43 (m, 8 H) 1.43 - 1.61 (m, 2 H) 1.92 - 2.17 (m, 2 H) 5.77 - 6.01 (m, 2 H) 8.07 (dd, *J* = 8.26, 4.27 Hz, 1 H) 8.34 - 8.56 (m, 3 H) 8.82 (dd, *J* = 8.26, 1.79 Hz, 1 H) 9.28 (dd, *J* = 4.20, 1.86 Hz, 1 H) 9.46 (dd, *J* = 8.26, 1.38 Hz, 1 H) 9.76 (dd, *J* = 5.92, 1.38 Hz, 1 H)

^{13}C NMR (400MHz, DMSO, d_6), δ ppm 14.51(s, 1C)22.63(s, 1C), 26.28(s, 1C), 29.07(s, 1C), 29.12(s, 1C), 31.57(s, 1C), 31.71(s, 1C), 63.87(s, 1C), 125.20(s, 1C), 125.91(s, 1C), 127.70(s, 1C), 131.06(s, 1C), 132.19(s, 1C), 133.13(s, 1C), 136.89(s, 1C), 138.49(s, 1C), 140.11(s, 1C), 147.57(s, 1C), 150.46(s, 1C), 151.48(s, 1C).

[C_8Phen][NTf_2]: White powders, yield: 96%

^{1}H NMR (270 MHz, DMSO-d_6) δ ppm 0.74 - 0.93 (m, 3 H) 1.15 - 1.44 (m, 8 H) 1.51 (d, *J* = 7.30 Hz, 2 H) 2.04 (d, *J* = 7.30 Hz, 2 H) 5.80 - 5.97 (m, 2 H) 8.07 (dd, *J* = 8.26, 4.27 Hz, 1 H) 8.33 - 8.52 (m, 3 H) 8.80 (dd, *J* = 8.19, 1.86 Hz, 1 H) 9.30 (dd, *J* = 4.27, 1.79 Hz, 1 H) 9.39 (dd, *J* = 8.19, 1.31 Hz, 1 H) 9.61 (dd, *J* = 5.99, 1.45 Hz, 1 H)

^{13}C NMR (101 MHz, DMSO-d_6) δppm 14.24 (s,1C), 22.38 (s,1C), 26.03 (s,1C), 28.81(s,1C), 28.85 (s, 1C), 31.30 (s,1C), 31.46 (s,1C), 63.76 (s,1C), 124.88 (s,1C), 125.69 (s,1C), 127.47 (s,1C), 130.82 (s,1C), 131.98 (s,1C), 132.95 (s,1C), 136.79 (s,1C), 138.26 (s,1C), 139.95 (s,1C), 147.32 (s,1C), 150.24 (s,1C), 151.14 (s,1C)

^{19}F NMR (376 MHz, DMSO-d_6) δ ppm -78.72 (s, 6 F)

[C_{10}Phen]Br

^{1}H NMR (270 MHz, DMSO-d_6) δ ppm 0.71 - 0.99 (m, 3 H) 1.09 - 1.43 (m, 13 H) 1.50 (d, *J* = 6.89 Hz, 2 H) 2.03 (d, *J* = 6.75 Hz, 2 H) 5.79 - 6.01 (m, 2 H) 8.08 (dd, *J* = 8.13, 4.27 Hz, 1 H) 8.29 - 8.56 (m, 3 H) 8.75 - 8.90 (m, 1 H) 9.30 (d, *J* = 2.48 Hz, 1 H) 9.43 (d, *J* = 7.85 Hz, 1 H) 9.69 (d, *J* = 5.23 Hz, 1 H)

^{13}C NMR (270 MHz, DMSO-d_6), δppm, 13.93(s,1C), 22.06(s,1C), 25.68(s,1C), 28.52(s,1C), 28.66(s,1C), 28.85(s,1C), 30.97(s,1C), 31.24(s,1C), 63.36(s,1C), 124.59(s,1C), 125.34(s,1C), 127.15(s,1C), 130.52(s,1C), 131.65(s,1C), 132.60(s,1C), 136.40(s,1C), 137.94(s,1C), 139.60(s,1C), 147.00(s,1C), 149.90(s,1C), 150.87(s,1C).

[C_{10}Phen][NTf_2]

^{1}H NMR (270 MHz, DMSO-d_6) δ ppm 0.70 - 0.97 (m, 3 H) 1.09 - 1.45 (m, 12 H) 1.46 - 1.64 (m, 2 H) 1.92 - 2.18 (m, 2 H) 5.74 - 6.05 (m, 2 H) 8.07 (dd, *J* = 8.19, 4.20 Hz, 1 H) 8.29 - 8.53 (m, 3 H) 8.80 (dd, *J* = 8.19, 1.58 Hz, 1 H) 9.30 (dd, *J* = 4.20, 1.58 Hz, 1 H) 9.40 (d, *J* = 8.13 Hz, 1 H) 9.62 (d, *J* = 5.10 Hz, 1 H)

^{13}C NMR (270 MHz, DMSO-d_6) δ ppm, 14.52(s,1C), 22.67(s,1C), 26.31(s,1C), 29.13(s,1C), 29.27(s,1C), 29.46(s,1C), 31.60(s,1C), 31.86(s,1C), 127.19-112.97(m,1C), 125.17(s,1C), 125.96(s,1C), 127.75(s,1C), 131.16(s,1C), 132.27(s,1C), 133.24(s,1C), 137.07(s,1C), 138.57(s,1C), 140.23(s,1C), 147.62(s,1C), 150.51(s,1C), 151.43(s,1C).

^{19}F NMR (376 MHz, DMSO-d_6) δ ppm -78.73 (s, 6 F)

ESI-MS: m/z = 321.2323, $[C_{10}Phen]^+$ and m/e = 279.9165, $[NTf_2]$.

$[C_{12}Phen]Br$

^{1}H NMR (270 MHz, DMSO-d_6) δ ppm 0.76 - 0.92 (m, 3 H) 1.09 - 1.43 (m, 16 H) 1.51 (d, *J* = 7.16 Hz, 2 H) 1.97 - 2.16 (m, 2 H) 5.80 - 5.97 (m, 2 H) 8.08 (dd, *J* = 8.26, 4.27 Hz, 1 H) 8.37 - 8.53 (m, 3 H) 8.83 (dd, *J* = 8.26, 1.79 Hz, 1 H) 9.30 (dd, *J* = 4.27, 1.79Hz, 1 H) 9.44 (dd, *J* = 8.19, 1.31 Hz, 1 H) 9.70 (dd, *J* = 5.99, 1.31 Hz, 1 H)

^{13}C NMR (270 MHz, DMSO-d_6) δ ppm 13.94(s,1C), 22.07(s,1C), 25.69(s,1C), 28.53(s,1C), 28.68(s,1C), 28.86(s,1C), 28.89(s,1C), 28.97(s,1C), 29.01(s,1C), 30.98(s,1C), 31.26(s,1C), 63.36(s,1C), 124.60(s,1C), 125.34(s,1C), 127.16(s,1C), 130.52(s,1C), 131.66(s,1C), 132.60(s,1C), 136.39(s,1C), 137.95(s,1C), 139.60(s,1C),147.00(s,1C), 149.89(s,1C), 150.88(s,1C).

$[C_{12}Phen][NTf_2]$

^{1}H NMR (270 MHz, ACETONE-d_6) δ ppm -0.08 - 0.13 (m, 3 H) 0.32 - 0.71 (m, 17 H) 0.71 - 0.90 (m, 2 H) 1.31 - 1.53 (m, 2 H) 5.21 - 5.42 (m, 2 H) 7.26 (dd, *J* = 8.26, 4.27 Hz, 1 H) 7.51 - 7.76 (m, 3 H) 7.99 (dd, *J* = 8.26, 1.79 Hz, 1 H) 8.49 - 8.70 (m, 2 H) 8.83 (dd, *J* = 5.99, 1.45 Hz, 1 H)

^{13}C NMR (270 MHz, DMSO-d_6) δ ppm14.7(s,1C), 23.66(s,1C), 27.38(s,1C), 30.25(s,1C), 30.40(s,1C), 30.56(s,1C), 30.61(s,1C), 30.68(s,1C), 30.71(s,1C), 31.06(s,1C),65.80(s,1C),125.92(s,1C), 126.79(s,1C), 128.45(s,1C), 132.30(s,1C),

133.58(s,1C), 134.61(s,1C), 139.26(s,1C), 141.52(s,1C), 144.45(s,1C), 148.58(s,1C), 151.36(s,1C),151.87(s,1C)

^{19}F NMR (376 MHz, Acetone) δ ppm -79.86 (br. s., 6 F)

ESI-MS: m/z = 349.2627, $[C_{12}Phen]^+$ and m/e =2 79.9167 $[NTf_2]^-$.

$[C_{14}Phen]Br$

^{1}H NMR (270 MHz, DMSO-d_6) δ ppm 0.73 - 0.90 (m, 3 H) 1.19 (s, 21 H) 1.43 - 1.60 (m, 2 H) 2.08 (s, 2 H) 5.88 (d, *J* = 7.71 Hz, 2 H) 8.07 (dd, *J* = 8.13, 4.27 Hz, 1 H) 8.36 - 8.54 (m, 3 H) 8.82 (dd, *J* = 8.13, 1.79 Hz, 1 H) 9.29 (dd, *J* = 4.27, 1.79 Hz, 1 H) 9.44 (dd, *J* = 8.19, 1.31 Hz, 1 H) 9.71 (dd, *J* = 5.92, 1.38 Hz, 1 H)

^{13}C NMR (270 MHz, DMSO-d_6) δ ppm 14.54(s,1C), 22.69(s,1C), 26.32(s,1C), 29.16(s,1C), 29.30(s,1C), 29.49(s,1C), 29.52(s,1C), 29.60(s,1C), 29.62(s,2C), 63.97(s,1C), 125.23(s,1C), 125.96(s,1C), 125.77(s,1C), 131.14(s,1C), 132.27(s,1C), 133.21(s,1C), 136.98(s,1C), 138.56(s,1C), 140.20(s,1C), 147.63(s,1C), 150.50(s,1C), 151.50(s,1C).

$[C_{14}Phen][NTf_2]$

^{1}H NMR (270 MHz, DMSO-d_6) δ ppm 0.82 (m, *J* = 6.20, 6.20 Hz, 2 H) 1.07 - 1.44 (m, 21 H) 1.52 (br. s., 2 H) 2.07 (d, *J* = 7.71 Hz, 2 H) 5.72 - 6.01 (m, 2 H) 7.89 - 8.15 (m, 1 H) 8.28 - 8.55 (m, 3 H) 8.69 - 8.90 (m, 1 H) 9.30 (dd, *J* = 4.06, 1.58 Hz, 1 H) 9.40 (d, *J* = 7.71 Hz, 1 H) 9.62 (d, *J* = 5.65 Hz, 1 H)

^{13}C NMR (270 MHz, DMSO-d_6) δ ppm14.50(s,1C), 22.67(s,1C), 26.32(s,1C), 29.13(s,1C), 29.29(s,1C), 29.46(s,1C), 29.50(s,1C), 29.61(b,3C), 31.61(s,1C), 31.88(s,1C), 64.05(s,1C), 127.19-112.96(m,1C), 125.18(s,1C), 125.95(s,1C), 127.75(s,1C), 131.16(s,1C), 132.28(s,1C), 133.24(s,1C), 137.06(s,1C), 138.54(s,1C), 140.32(s,1C), 147.62(s,1C), 150.50(s,1C), 151.43(s,1C).

ESI-MS: m/z = 377.2956 , $[C_{14}Phen]^+$; m/e = 279.92, $[N\ Tf_2]^-$.

CHN Microanalysis Results

	Percentage composition: Found(Calculated)		
Compound/Element	**C**	**H**	**N**
$[C_1Phen]I$	48.48(48.44)	3.39(3.42)	8.52(8.70)
$[C_1Phen][NTf_2]$	37.83(37.89)	2.25(2.32)	8.65(8.84)
$[C_1Phen][PF_6]$	45.90(45. 90)	3.22(3.26)	8.12(8.23)
$[C_2Phen]I$	49.85(50.00)	3.84(3.87)	8.30(8.33)
$[C_2Phen][NTf_2]$	38.42(39.26)	2.60(2.66)	8.22(8.59)
$[C_2Phen][PF_6]$	47.58(47.47)	3.62(3.70)	7.98(7.91)
$[C_4Phen]Br$	59.96(60.76)	5.47(5.38)	8.42(8.86)
$[C_4Phen][NTf_2]$	42.12(41.78)	3.24(3.31)	7.97(8.12)
$[C_6Phen][NTf_2]$	44.27(44.03)	3.80(3.88)	7.62(7.70)
$[C_8Phen]Br$	64.56(64.34	6.71(6.75	7.38(7.50
$[C_8Phen][NTf_2]$	46.32(46.07)	4.01(4.39)	7.14(7.33)
$[C_{10}Phen]Br$	65.76(65.83)	7.25(7.28)	6.96(6.98)
$[C_{10}Phen][NTf_2]$	47.88(47.91)	4.82(4.86)	7.01(6.98)
$[C_{12}Phen]Br$	67.33(67.12)	7.64(7.75)	6.43(6.52)
$[C_{12}Phen]\ [NTf_2]$	49.83(49.59)	5.21(5.28	6.56(6.67)
$[C_{14}Phen]Br$	68.55(68.26)	8.03(8.15)	6.24(6.12)
$[C_{14}Phen][NTf_2]$	51.48(51.13)	5.65(5.67)	6.35(6.39)

Table 2. 1: CHN microanalysis results of 1, 10-Phenanthrolinium based products

Thermal Properties of $[C_nPhen]X$

The actual thermo gram of $[C_1Phen]I$, $[C_1Phen][\ NTf_2]$, is presented here. This same result of the other products is presented in the annex. The onset temperature (T_{onset}) is the intersection of the baseline weight after the drying step, and the tangent of the weight vs temperature curve as decomposition occurs.

The glass transition, if any, was determined to be the midpoint of a heat capacity change, whereas the melting and crystallization temperatures were determined peak maximum of the transition curve.

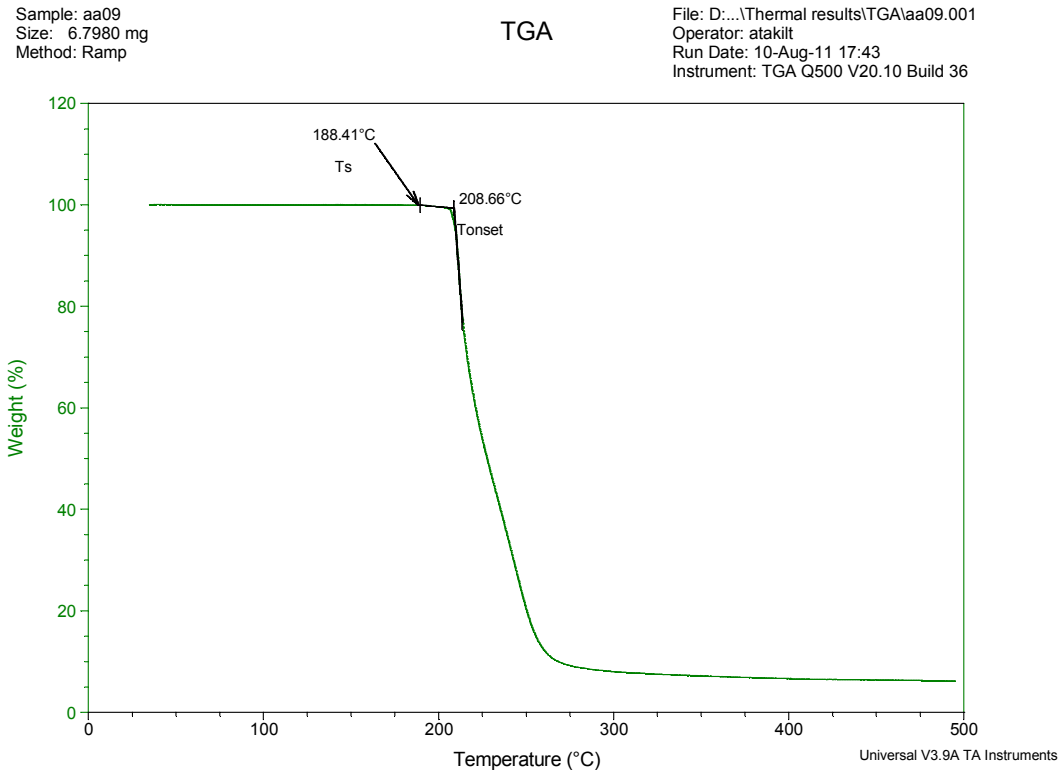

Figure 2. 14: TGA of $[C_1Phen]I$

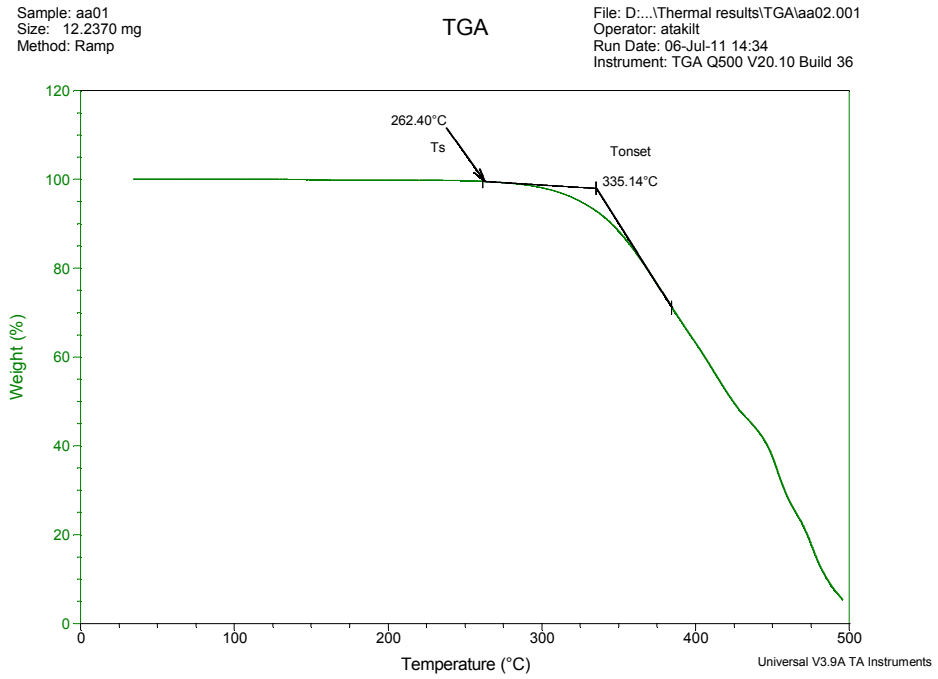

Figure 2. 15: TGA of [C_1Phen][NTf_2]

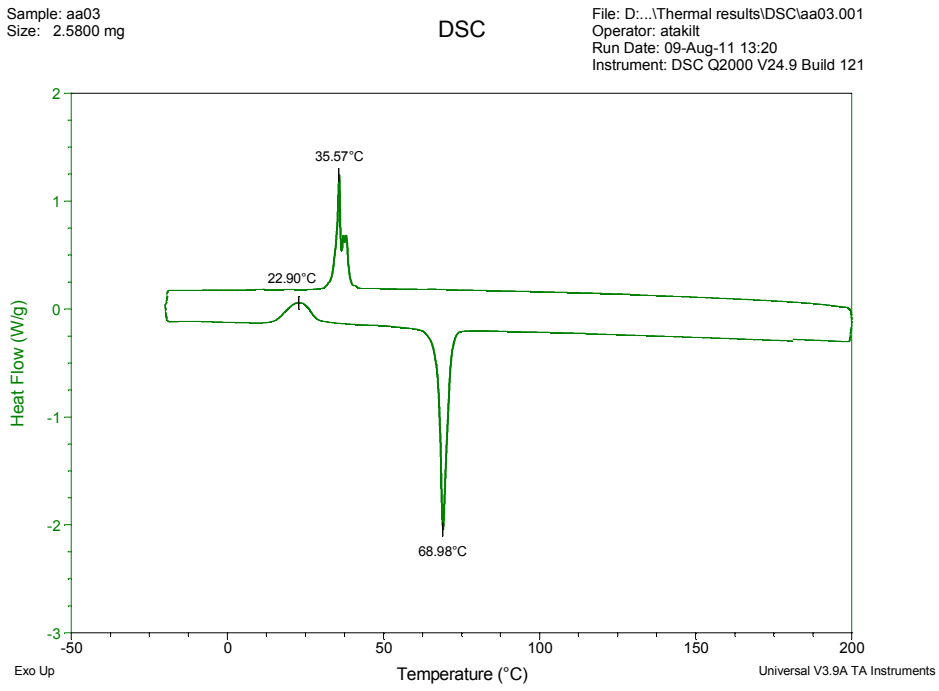

Figure 2. 16: DSC of [C_1Phen][NTf_2]

Compound	**Melting points, T_m, 0C**	**Glass transition temperature ,T_g,^{0}C**	**Crystallization temperature, T_c, ^{0}C**	**Start temperature, Ts, ^{0}C**	**Onset temperature,T_{onset}, ^{0}C**
[C_1Phen]I	205	-	-	201.12	207.07
[C_1Phen][NTf_2]	68.96	10.41	35.57	238.74	283.84
[C1Phen][PF_6]	111.21,140.30		106.20, 152.26	-	-
[C_2Phen]I	175	-	-	170	181.61
[C_2Phen][NTf_2]	65.53	-	15.39	275.93	296.65
[C_2Phen][PF_6]	166.96	-	156.40	-	-
[C_4Phen][NTf_2]	149.08	-	92.77	243.62	294.13
[C_6Phen][NTf_2]	90.80	-	69.80	250.9	377.35
[C_6Phen][PF_6]	-		-	214.72	265.63
[C_8Phen]Br			-	156.07	164.56
[C_8Phen][NTf_2]	67.13	-	20.61	229.17	308.70
[C_{10}Phen]Br			-	133.97	150.67
[C_{10}Phen][NTf_2]	50.50		0.80	264.81	294.45
[C_{12}Phen][NTf_2]	54.17	21.46	-		-
[C_{14}Phen][NTf_2]	48.77	-0.73	-11.28	244.41	290.31

Table 2. 2: T_m, T_g, T_C, T_s and T_{onset} of 1, 10-Phenathrolinium cation based compounds

2.4.2 Spectroscopic, CHN Microanalysis and Thermal Properties of 4, 4-Biyridine Based ILs

^{1}H, ^{13}C, ^{19}F and ^{31}P NMR

[C_2Bipyr][NTf_2]:White powder, yield: 88%

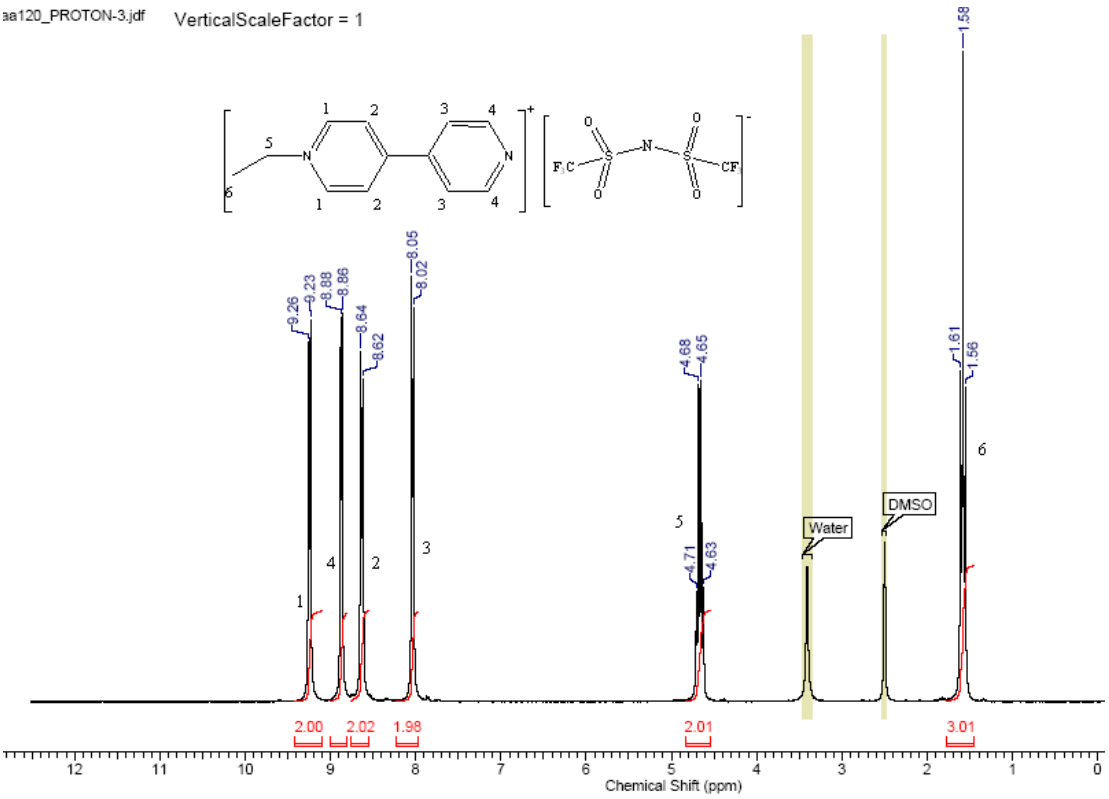

Figure 2. 17: ^{1}H NMR of [C_2Bipyr][NTf_2]

^{1}H NMR (270 MHz, DMSO-d_6) δ ppm 1.58 (t, *J*=7.30 Hz, 3 H) 4.67 (q, *J*=7.25 Hz, 2 H) 7.92 - 8.13 (m, 2 H) 8.63 (d, *J*=6.61 Hz, 2 H) 8.79 - 9.00 (m, 2 H) 9.24 (d, *J*=6.75 Hz, 2 H)

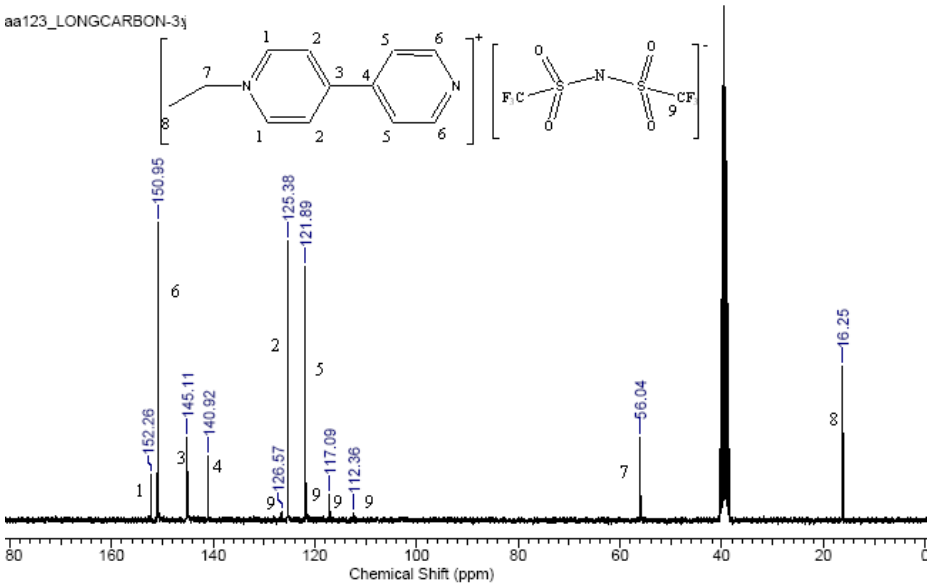

Figure 2. 18: ^{13}C NMR of [C_2Bipyr][NTf_2]

^{13}C NMR (68 MHz, DMSO-d_6) δ ppm 16.87 (s, 1 C) 56.65 (s, 1 C) 122.51 (s, 2 C) 126.00 (s, 2 C) 141.54 (s, 2 C) 145.73 (br. s., 1 C) 150.04 - 151.95 (s, 2 C) 152.88 (s, 1 C)

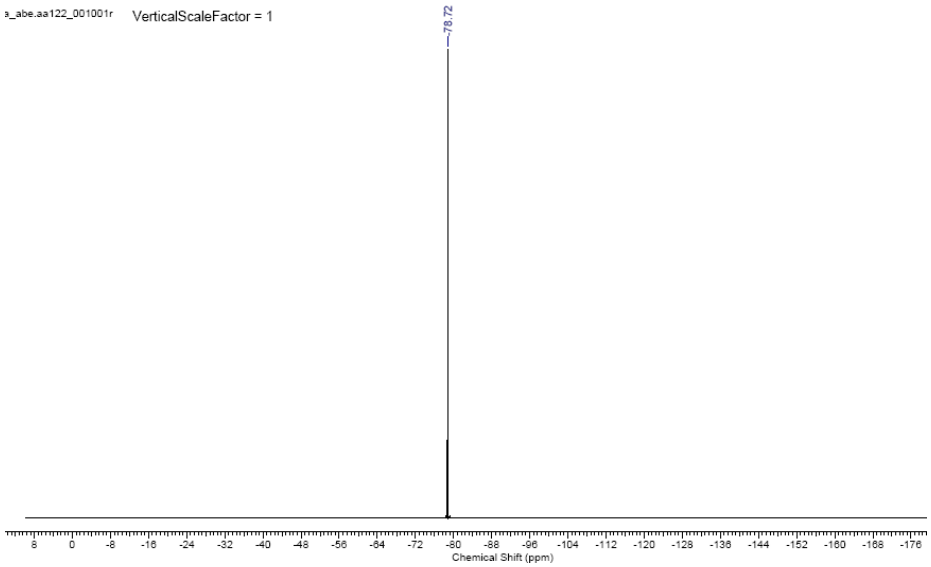

Figure 2. 19: ^{19}F NMR of [C_2Bipyr][NTf_2]

^{19}F NMR (376 MHz, DMSO-d_6) δ ppm -78.72 (s, 6 F)

ESI-MS

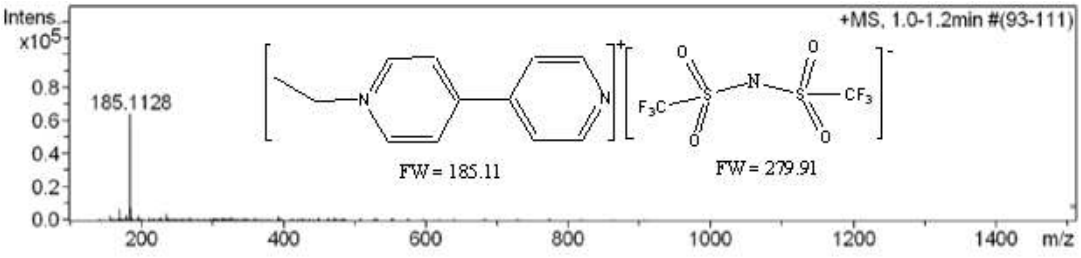

Figure 2. 20: ESI-MS of [C_2Bipyr][NTf_2] with the positive formula method

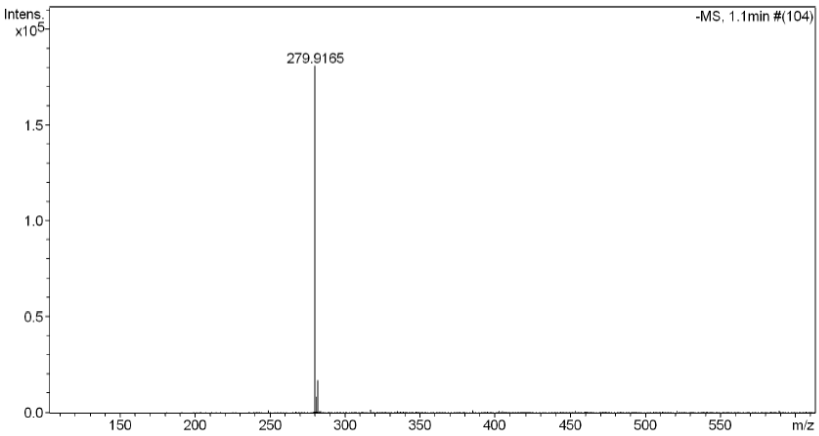

Figure 2. 21: ESI-MS of [C_2Bipyr][NTf_2] with the negative formula method

m/z = 185.1128, $[C_2Bipyr]^+$; m/e = 279.9165,$[NTf_2]^-$

[C_4Bipyr]Br: A gray powders, yield: 78%

^{1}H NMR (270 MHz, DMSO-d_6) δ ppm 0.93 (t, *J* =1.00 Hz, 3 H) 1.35 (sxt, *J* = 1.00 Hz, 2 H) 1.29 - 1.40 (m, 2 H) 1.95 (quin, *J* =7.47 Hz, 2 H) 4.68 (t, *J* = 7.44 Hz, 2 H) 8.07 (dd, *J* = 1.00 Hz, 2 H) 8.67 (d, *J* = 6.75 Hz, 2 H) 8.87 (dd, *J* = 1.00 Hz, 2 H) 9.31 (dd, *J* = 7.00 Hz, 2 H)

^{13}C NMR (68 MHz, DMSO-d_6) δ ppm 13.35 (s, 1 C) 18.77 (s, 1 C) 32.66 (s, 1 C) 60.08 (s, 1 C) 121.93 (s, 2 C) 125.39 (s, 2 C) 140.85 (s, 1 C) 145.31 (s, 2 C) 150.06 - 151.38 (s, 2 C) 152.19 (s, 1 C)

[C_4Bipyr][NTf_2]: Light yellow viscous liquid, yield: 87%.

^{1}H NMR (270 MHz, DMSO-d_6) δ ppm 0.79 - 1.06 (t, 3 H) 1.33 (d, *J* =7.57 Hz, 2 H) 1.95 (t, *J* = 7.44 Hz, 2 H) 4.64 (t, *J* = 7.44 Hz, 2 H) 7.94 - 8.12 (m, 2 H) 8.62 (d, *J* = 6.61 Hz, 2 H) 8.86 (d, *J* = 5.92 Hz, 2 H) 9.23 (d, *J* = 6.61 Hz, 2 H)

^{13}C NMR (68 MHz, DMSO-d_6) δ ppm 13.57 (s, 1 C) 19.10 (s, 1 C) 32.95 (s, 1 C) 60.54 (s, 1 C) 112.68-126.90(q, 1 C) 122.20 (s, 2 C) 125.73 (s, 2 C) 141.21 (s, 1 C) 145.60 (s, 2 C) 151.27 (s, 1 C) 152.67 (s, 1 C)

^{19}F NMR (376 MHz, DMSO-d_6) δ ppm -78.75 (s, 6 F)

ESI-MS: m/z = 213.1382, $[C_4Bipyr]^+$, m/e = 279.9171, $[N\ Tf_2]^-$

[C_6Bipyr]Br: Highly hygroscopic gray powders, yield: 73%

^{1}H NMR (270 MHz, DMSO-d_6) δ ppm 0.76 - 0.95 (m, 3 H) 1.29 (s, 6 H) 1.96 (d, *J* = 6.20 Hz, 2 H) 4.64 (t, *J* = 7.37 Hz, 2 H) 7.97 - 8.13 (m, 2 H) 8.65 (d, *J* = 6.89 Hz, 2 H) 8.78 - 8.92 (m, 2 H) 9.26 (d, *J* = 6.89 Hz, 2 H)

^{13}C NMR (68 MHz, DMSO-d_6) δ ppm 13.84 (s, 1 C) 21.86 (s, 1 C) 25.08 (s, 1 C) 30.62 (d, *J*=5.71 Hz, 1 C) 60.35 (s, 1 C) 121.92 (s, 2 C) 125.40 (s, 2 C) 140.86 (s, 1 C) 145.30 (s, 2 C) 150.98 (s, 2 C) 151.97 - 153.10 (m, 1 C)

[C_6Bipyr][NTf_2]: Light yellow viscous liquid, yield: 89%

^{1}H NMR (270 MHz, DMSO, d_6) δ ppm 0.73 - 0.98 (m, 3 H) 1.18 - 1.53 (m, 6 H) 1.93 - 2.17 (m, 2 H) 4.62 (t, *J* = 7.57 Hz, 2 H) 7.64 - 7.78 (m, 2 H) 8.32 (d, *J* = 6.89 Hz, 2 H) 8.80 - 8.85 (m, 2 H) 8.88 (d, *J* = 7.02 Hz, 2 H)

^{13}C NMR (68 MHz, DMSO) δ ppm 13.59 (s, 1 C) 21.02 - 23.13 (m, 1 C) 25.62 (s, 1 C) 30.95 (s, 1 C) 31.33 (s, 1 C) 62.26 (s, 1 C) 121.65 (s, 2 C) 126.26 (s, 2 C) 141.01 (s, 1 C) 144.83 (br. s., 2 C) 151.37 (s, 2 C) 154.71 (s, 1 C)

ESI-MS: m/z = 241.1700,[C_6Bipyr]$^+$;

[C_8Bipyr]Br: Highly hygroscopic gray solid, yield: 74%

^{1}H NMR (270 MHz, DMSO-d_6) δ ppm 0.84 (s, 3 H) 1.14 - 1.43 (m, 10 H) 1.84 - 2.03 (m, 2 H) 4.64 (s, 2 H) 7.98 - 8.15 (m, 2 H) 8.65 (d, *J* = 6.89 Hz, 2 H) 8.78 - 8.93 (m, 2 H) 9.27 (d, *J* = 7.02 Hz, 2 H)

^{13}C NMR (68 MHz, DMSO-d_6) δ ppm 13.92 (s, 1 C) 22.03 (s, 1 C) 24.92 - 26.04 (m, 1 C) 28.41 (d, *J*=5.19 Hz, 2 C) 30.69 (s, 1 C) 31.13 (s, 1 C) 60.33 (s, 1 C) 120.69 - 123.44 (m, 2 C) 125.38 (s, 2 C) 140.85 (s, 1 C) 145.30 (s, 2 C) 150.21 - 151.58 (m, 2 C) 152.26 - 153.98 (m, 1 C)

[C_8Bipyr][NTf_2]: Light yellow viscous liquid, yield: 88%

^{1}H NMR (270 MHz, DMSO-d_6) δ ppm 0.73 - 0.96 (m, 3 H) 1.13 - 1.44 (m, 10 H) 1.97 (d, *J* = 6.33 Hz, 2 H) 4.63 (t, *J* = 7.37 Hz, 2 H) 7.97 - 8.12 (m, 2 H) 8.62 (s, 1 H) 8.80 - 8.95 (m, 2 H) 9.23 (d, *J* = 6.89 Hz, 2 H)

^{13}C NMR (68 MHz, DMSO-d_6) δ ppm 13.89 (s, 1 C) 13.75 - 14.02 (m, 1 C) 22.04 (s, 1 C) 25.44 (s, 1 C) 28.41 (d, *J*=5.19 Hz, 2 C) 30.72 (s, 1 C) 31.14 (s, 1 C) 60.46 (s, 1 C) 112.38-126.59(q, 1C) 121.45 - 122.25 (m, 2 C) 125.41 (s, 2 C) 140.91 (s, 1 C) 145.28 (s, 2 C) 150.96 (s, 2 C) 152.31 (s, 1 C)

^{19}F NMR (376 MHz, DMSO-d_6) δ ppm -78.75 (s, 6 F)

ESI-MS: m/z = 279.9189, $[C_8Bipyr]^+$, m/e = 279.9189, $[NTf_2]^-$

[C_{10}Bipyr]Br: **Highly hygroscopic gray powders, yield: 74%**

^{1}H NMR (270 MHz, DMSO-d_6) δ ppm 0.75 - 0.92 (m, 3 H) 1.10 - 1.43 (m, 14 H) 1.95 (br. s., 2 H) 4.65 (t, *J* = 7.37 Hz, 2 H) 7.98 - 8.15 (m, 2 H) 8.66 (d, *J* = 6.89 Hz, 2 H) 8.80 - 8.95 (m, 2 H) 9.28 (d, *J* = 6.89 Hz, 2 H)

^{13}C NMR (68 MHz, DMSO-d_6) δ ppm 14.25 (s, 1 C) 22.38 (s, 1 C) 25.70 (s, 1 C) 28.70 (s, 1 C) 28.94 (s, 1 C) 29.08 (s, 1 C) 29.17 (s, 1 C) 30.90 - 31.15 (m, 1 C) 31.56 (s, 1 C) 60.63 (s, 1 C) 121.00 - 123.74 (m, 2 C) 125.68 (s, 1 C) 141.15 (s, 2 C) 145.61 (s, 1 C) 151.27 (s, 2 C) 152.50 (s, 1 C)

[C_{10}Bipyr][NTf_2]: Light yellow viscous liquid, yield: 82%

^{1}H NMR (270 MHz, DMSO-d_6) δ ppm 0.72 - 0.90 (m, 3 H) 1.09 - 1.43 (m, 14 H) 1.97 (br. s., 2 H) 4.65 (t, *J* = 7.37 Hz, 2 H) 7.95 - 8.07 (m, 2 H) 8.61 (s, 1 H) 8.77 - 8.95 (m, 2 H) 9.25 (d, *J* = 6.89 Hz, 2 H)

^{13}C NMR (68 MHz, DMSO-d_6) δ ppm 14.10 (s, 1 C) 22.39 (s, 1 C) 25.77 (s, 1 C) 28.73 (s, 1 C) 28.97 (s, 1 C) 29.10 (s, 1 C) 29.20 (s, 1 C)31.08 (s, 1 C) 31.60 (s, 1 C) 60.83 (s, 1

C)112.71-126.92(q, 2 C) 122.15 (s, 2 C) 125.70 (s, 2 C) 141.17 (s, 1 C) 145.60 (s, 2 C) 151.24 (s, 2 C) 152.71 (s, 1 C)

^{19}F NMR (376 MHz, DMSO-d_6) δ ppm -78.85 (s, 6 F)

ESI-MS: m/z = 297.2325, $[C_{10}Bipyr]^+$; m/e = 279.9163, $[NTf_2]^-$

CHN microanalysis results

	Percentage composition Found(Calculated)		
Compound/Element	**C**	**H**	**N**
$[C_2Bipyr][NTf_2]$	28.04(27.91)	2.26(2.34)	7.00(7.23)
$[C_4Bipyr][NTf_2]$	38.96(38.94)	3.45(3.47)	8.50(8.52)
$[C_6Bipyr][NTf_2]$	41.41(41.46)	4.03(4.06)	8.09(8.06)
$[C_8Bipyr][NTf_2]$	43.78(43.71)	4.56(4.59)	7.56(7.65)
$[C_{10}Bipyr][NTf_2]$	45.64(45.75)	5.02(5.06)	7.11(7.27)

Table 2. 3: CHN microanalysis results of 4, 4’ - Bipyridinium based products

Thermal Properties of $[C_nBipyr][NTf_2]$

The actual thermo gram of $[C_4Bipyr][NTf_2]$ is given here. The thermo gram of the other 4, 4’-Bipyridinium based compounds is found in the annex.

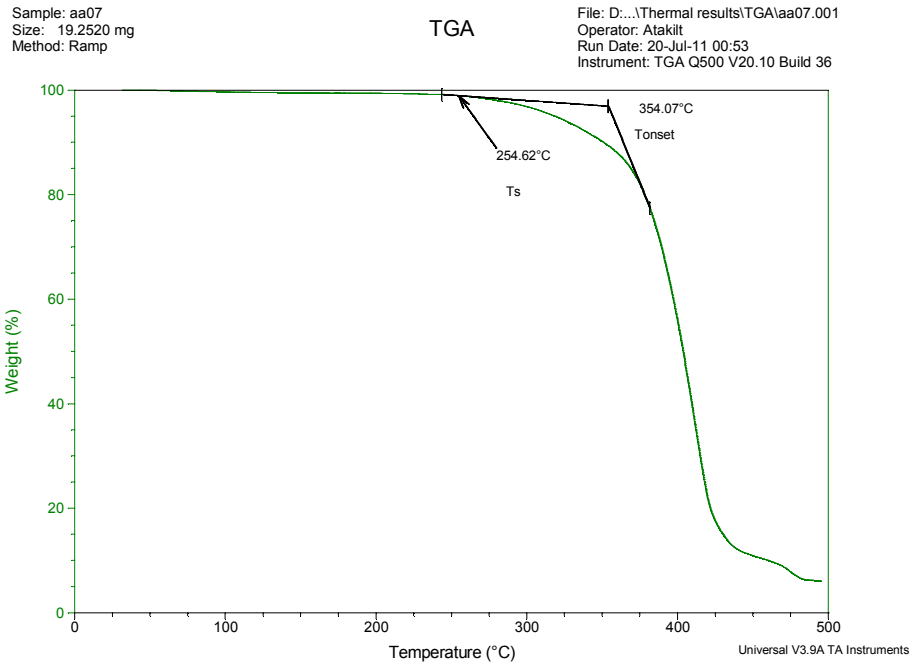

Figure 2. 22: Thermo gravimetric analysis (TGA) of $[C_4Bipyr][NTf_2$

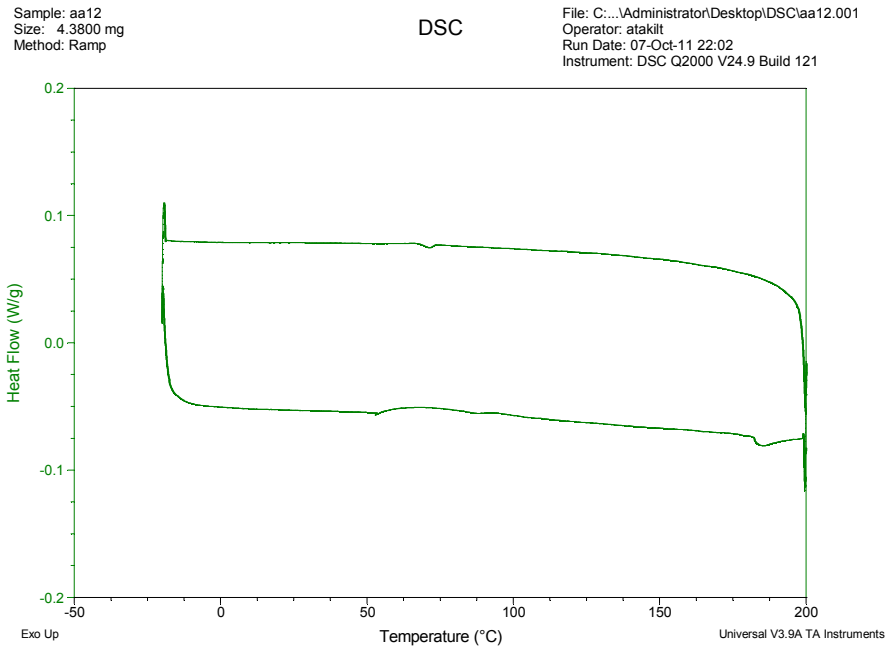

Figure 2. 23: Differential scanning calorimetry (DSC) thermogram of$[C_4Bipyr][NTf_2]$

Compound	Melting points, T_m, ^0C	Glass transition temperature, T_g, ^0C	Crystallization temperature, T_c, ^0C	Start temperature, T_s, ^0C	Onset temperature, T_{onset}, ^0C
$[C_2Bipyr][NTf_2]$	68.84	-	39.99	-	-
$[C_4Bipyr][NTf_2]$	<-20	-	-	254.62	354.07
$[C_6Bipyr][NTf_2]$	<-20	-	-	282.21	358.71
$[C_8Bipyr][NTf_2]$	<-20	-	-	244.5	355.57
$[C_{10}Bipyr][NTf_2]$	<-20	-41.36	-	251.74	352.97

Table 2. 4: T_m, T_g, T_C, T_s and T_{onset} of $[C_nBipyr][NTf_2]$

2.4.3 Spectroscopic, CHN Microanalysis and Thermal Properties of N, N'-Dialkyl - 4, 4- Biyridinium Based Products

^{1}H, ^{13}C, and ^{19}F

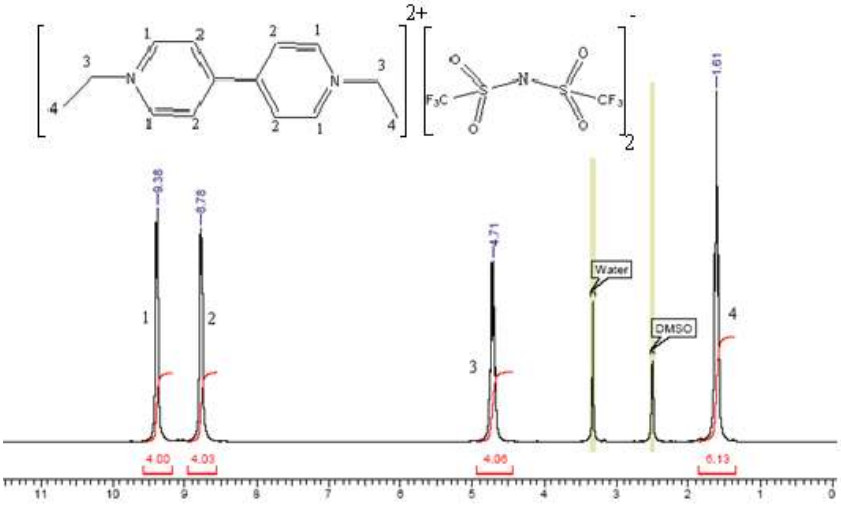

Figure 2. 24: ^{1}H NMR of $[(C_2)_2Bipyr][NTf_2]_2$

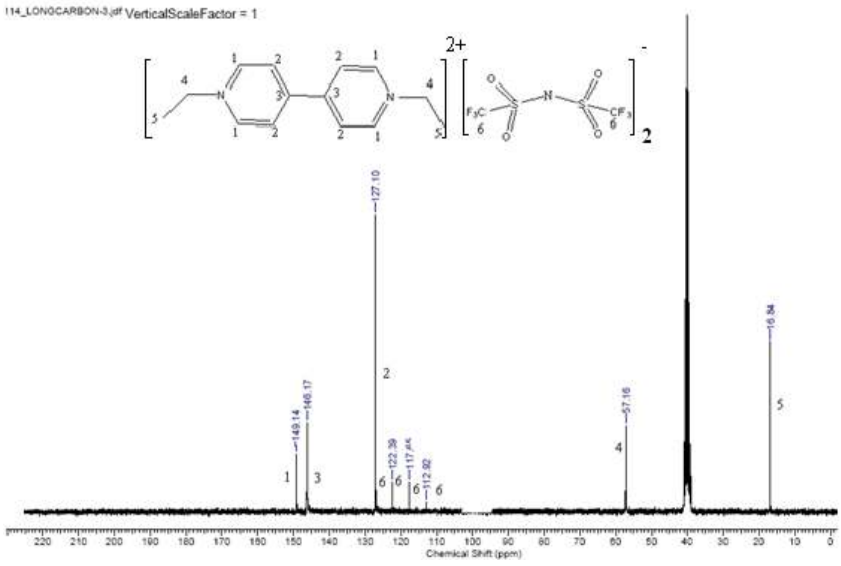

Figure 2. 25: ^{13}C NMR of $[(C_2)_2Bipyr]$ $[NTf_2]_2$

[$(C_4)_2$Bipyr] [$NTf_2]_2$

^{1}H NMR (270 MHz, DMSO-d_6) δ ppm 0.80 - 1.08 (t, 6 H) 1.21 - 1.48 (m, 4 H) 1.83 - 2.15 (m, 4 H) 4.69 (br. s., 4 H) 8.77 (br. s., 4 H) 9.37 (br. s., 4 H)

^{19}F NMR (376 MHz, DMSO-d_6) δ ppm -78.73 (s, 12 F)

[$(C_8)_2$Bipyr] [$NTf_2]_2$

^{1}H NMR (270 MHz, DMSO-d_6) δ ppm 0.70 - 0.97 (m, 6 H) 1.10 - 1.51 (m, 20 H) 1.97 (br. s., 4 H) 4.67 (br. s., 4 H) 8.77 (d, *J*=5.10 Hz, 4 H) 9.37 (d, *J*=5.37 Hz, 4 H)

^{13}C NMR (68 MHz, DMSO-d_6) δ ppm 14.49 (s, 2 C) 22.63 (s, 2 C) 26.03 (s, 2 C) 29.01 (d, *J*=6.23 Hz, 4 C) 31.35 (s, 2 C) 31.73 (s, 2 C) 61.57 (s, 2 C) 127.21-112.97(q, 4C)127.21 (s, 2 C) 146.34 (s, 2 C) 149.25 (s, 2 C).

^{19}F NMR (376 MHz, DMSO-d_6) δ ppm -78.75 (s, 12 F)

[$(C_{10})_2$Bipyr] [$NTf_2]_2$

^{1}H NMR (270 MHz, DMSO-d_6) δ ppm 0.76 - 0.94 (m, 6 H) 1.14 - 1.49 (m, 28 H) 1.88 - 2.11 (m, 4 H) 4.58 - 4.78 (m, 4 H) 8.78 (d, *J*=6.33 Hz, 4 H) 9.38 (d, *J*=6.47 Hz, 4 H)

^{13}C NMR (68 MHz, DMSO-d_6) δ ppm 14.24 (s, 2 C) 22.39 (s, 2 C) 25.73 (s, 2 C) 28.60 - 28.79 (m, 2 C) 28.87 - 29.02 (m, 2 C) 29.14 (d, *J*=4.67 Hz, 4 C) 31.04 (s, 2 C) 31.57 (s, 2 C) 61.26 (s, 2 C) 126.90-112.66 (q, 4) 126.90 (s, 2 C) 144.59 - 147.00 (m, 2 C) 148.92 (s, 2 C)

^{19}F NMR (376 MHz, DMSO-d_6) δ ppm -78.72 (s, 12 F)

Thermal Properties of $[(C_n)_2Bipyr]\ [NTf_2]_2$

The phase transition temperatures of [(Cn)2Bipyr]2[NTf2] obtained from DSC are indicated in Table 2.3

Compound/Transition temperature, ^0C	T_{c1}	T_{c2}	T_{m1}	T_{m2}
$[(C_2)_2Bipyr]\ [NTf_2]_2$	105.72	-	-	136.91
$[(C_4)_2Bipyr]\ [NTf_2]_2$	2.14	73.68	47.94	87.30
$[(C_8)_2Bipyr]\ [NTf_2]_2$	140.28	135.70	37.22	138.50
$[(C_{10})_2Bipyr]\ [NTf_2]_2$	12.65	170.41	35.43	172.87

Table 2. 5: The phase transition temperatures of $[(C_n)_2Bipyr]\ [NTf_2]_2$

2.5 Discussion

1, 10-Phenanthrolinium Based Products

The first step, the typical quaternization reaction, gives only a monoalkylated N-alkyl-1, 10-Phenanthrolinium halide as a product. The 1, 10- Phenanthroline molecule loses its symmetry after the alkylation of only one of its nitrogen atoms and this new characteristic feature helps in the identification of the new salt, as new peaks appear in both the ^1H and ^{13}C NMR spectra. The asymmetric nature of the cation also helps in lowering the melting point of the final product. It is also of paramount importance for the reduction of the melting point that no dialkylation occurs as salts composed of doubly charged cations normally exhibit higher melting points than those composed of single charged ones [9]. The dialkylation of 1, 10-Phenanthroline is known not to be possible due to the steric hindrance of the nonalkylated nitrogen atom after monoalkylation [10]. The 1, 10-

Phenanthroline molecules can be dialkylated only by using dihaloalkanes [11]. The synthesized N-alkyl-1, 10-Phenanthrolinium halide salts, $[C_nPhen]X$, have melting points of greater than 100 °C and they are therefore, not ionic liquids. Exchanging the halide anions via a metathesis reaction [12] by the [bis(trifluoromethyl)sulfonyl]amide anion, $[NTf_2]^-$, rendered most of the products, $[C_nPhen][\ NTf_2]$ (n = 1, 2, 8, 10, 12 & 14) to be ionic liquids.

The success in the exchange of the halides with [bis(trifluoromethylsulfonyl)]amide, $[NTf_2]^-$, as a counter anion is evident from the appearance of new carbon quartets. This was further confirmed from the appearance of a strong peak at around δ =-78.9 to -79.22 ppm which is a characteristic chemical shift for compounds containing CF_3 moieties in ^{19}F NMR. Similarly, the halide anion exchange with hexafluorophosphate anion,PF_6^-, is confirmed by doublets due to ^{19}F NMR and septet in ^{31}P NMR. In both cases, the absence of any other peak representing F and P reveals the purity of the products.

From the thermal data, it can clearly be seen that the behavior of the compounds is significantly influenced by the nature of the anion. The products with halide anions showed significantly higher melting points and lower thermal stabilities (decompose at lower temperatures) than products with highly fluorinated anions such as $[NTf_2]^-$. This indicates the basicity of the anion accelerates the decomposition [13]. The products with different side chain length but the same anion shows little difference in their onset temperature [14, 15]. This confirms that the side chain length of the cation has little impact on the thermal stability of the product.

$[C_1Phen][NTf_2]$ T_m= 68.96 ^{0}C, $[C_2Phen][NTf_2]$ T_m = 65.53 ^{0}C, $[C_8Phen][NTf_2]$ T_m = 67.13 ^{0}C, $[C_{10}Phen][NTf_2]$ T_m = 50.50 ^{0}C, $[C_{12}Phen][NTf_2]$ T_m = 54.17 ^{0}C and

$[C_{14}Phen][NTf_2]$ $T_m = 48.77\ ^0C$, full fill the requirement to be classified as Ionic Liquids [12]. It can also be observed that the liquidus range of the products categorized as ionic liquids is as high as 240 ^0C. It is also evident that, all the 1 10-Phenanthrolinium products with Tf_2N^- anion show sharp melting points. Certain of this class of products showed sharp crystallization temperatures which showed a decreasing trend as the alkyl chain length increases. This may be speculated to be the effect of the increase in the degree of freedom of rotation that diminishes the alignment of the alkyl chains. The melting point trend of the products is summarized in Figure 2.1.

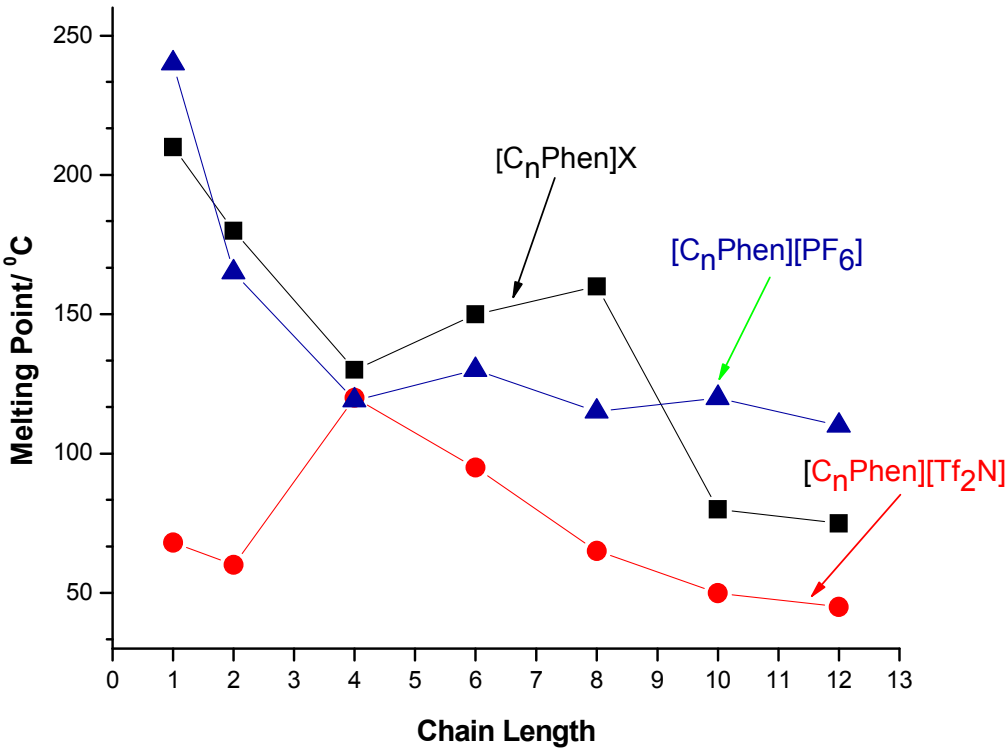

Figure 2. 26: Melting point trend of 1, 10-Phenanthrolinium based ILs

Figure 2.26 shows that, melting point generally decreases as the side chain length increases. This fact can be anticipated as the increase in the side chain length increases the degree of freedom of rotation of the side chain that diminishes the proximity of the side chains of the cations that again decreases the Van der Waals interaction.

The melting points of the products with Tf_2N^- anion are generally smaller than their counterparts with halides and PF_6^- anions. This also can be explained that the basicity of Tf_2N^- anion is far smaller than the halides and PF_6^- that strongly diminishes the columbic interaction between the anions and cations. Similar reasoning can be given why melting points of the products with PF_6- anions are smaller than the products with halide anions.

Specifically, the melting points of $[C_1Phen][NTf_2]$ and $[C_2Phen][NTf_2]$ are relatively smaller than $[C_3\text{-}C_6Phen][NTf_2]$ salts probably due the sizes of the anion and the former cations have comparable size match that may prevent the Van der Waals interaction between the side chains of the cations. However, as the side chain grows to C3-C6, the increase allows the possible Van der Waals interaction between side chains of the cations that increases the melting points of the products from $[C_3\text{-}C_6Phen][NTf_2]$. Interestingly, the melting points of the products from $[C_8Phen][NTf_2]$ comes down probably due to the increase in the degree of freedom of rotation of the side chains prevents them from approaching to each other consequently loses the possible Van der Waals interaction.

N-Alkyl-4, 4'-Bipyridinium Based Products

The synthesis of monoalkylted salts is evident from all ^1H and ^{13}C and ^{19}F NMR results. As a result of the mono alkylation the starting 4, 4'-Bipyridine lost its symetry and four proton peaks and six carbon peaks in the aromatic region have appeared in addition to

the alkyl peaks in their corresponding low field regions. For the dialkylated or noalkylated bipyridine only two proton and three carbon peaks would have appeared.

The success in the exchange of the halides with [bis(trifluoromethylsulfonyl)]amide, $(CF_3SO_2)_2N^-$, as a counter anion to acquire the desired property is evident from the appearance of new carbon quartets. This was further confirmed from the appearance of a strong peak at around σ = -78.9 to -79.22 ppm which is a characteristic chemical shift for compounds containing CF_3 moieties in ^{19}F NMR. The absence of any other peak reveals the purity of the products. In these products only one of the two nitrogen atoms of 4, 4'-Bipyridine is alkylated due to the optimization made in such a way that the monoalkylated product comes out of the solution so that it does not have a chance to undertake the second alkylation. Particularly, the solvent chosen as a medium of reaction, 1, 4-dioxane, was found to be the best solvent to get the intended type of product.

In addition to the evidence obtained from the integration area of the ^1H NMR and absence of any additional peaks other than the intended ones in all NMR data, the purity of the products is reliable and consistent as confirmed from CHN microanalysis data in which there is a very good agreement between the experimentally found and theoretically calculated values.

All products synthesized are salts and all of them with $[NTf_2]^-$ as counter anion are classified as ILs (melting points < 100 ^{0}C). The existence of these products as couples of cations and anions was strongly confirmed by using electro spray ionization mass spectrometry; ESI-MS. Using this technique, the cations and the anions of each compound were detected on their characteristic m/z and m/e values.

As can be seen from Table 2.2, only $[C_2Bipyr][NTf_2]$ shows true phase transition by having melting point T_m= 69.11 ^{0}C, crystallization temperature T_c = 40.05 ^{0}C. The other compounds with $[NTf_2]^-$ anion have no crystallization points, have melting points less than -20 ^{0}C and they are classified as room temperature ionic liquids, RTILs. Evident from their onset temperature, T_{onset}, alkyl side chain length has little effect on this properties [12, 13]. The liquidus range of these ILs, which have no melting or freezing points, is very large and is as high as 344.12 ^{0}C in the case of $[C_{10}Bipyr][NTf_2]$. This fact opens great opportunities for processes requiring low as well as high temperatures.

N, N'-Dialkyl - 4, 4- Biyridinium Based Products

As in the case of the other compounds, the synthesis of dialkylated 4, 4'-Bipyridinium based compounds is evident from NMR results. However, what is more interesting is the thermal behavior of this class of compounds. Table 2.3 shows that, except $[(C_2)_2Bipyr]$ $[NTf_2]_2$, the others show two crystallization and two melting points (Figure 2.1 and 2.2).

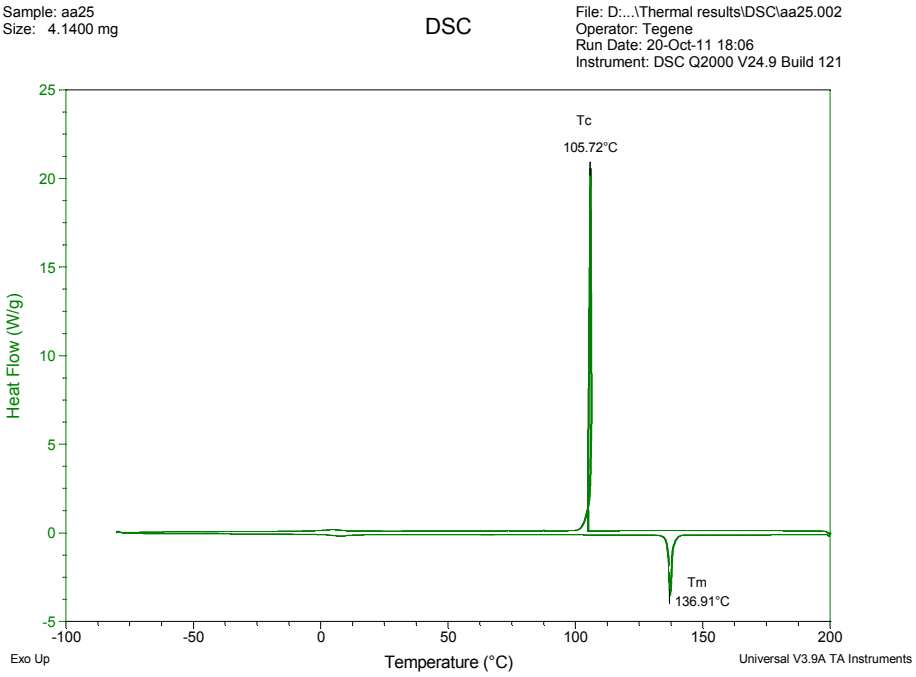

Figure 2. 27: Differential scanning calorimetry (DSC) thermogram of $[(C_2)_2Bipyr][N\ Tf_2]_2$

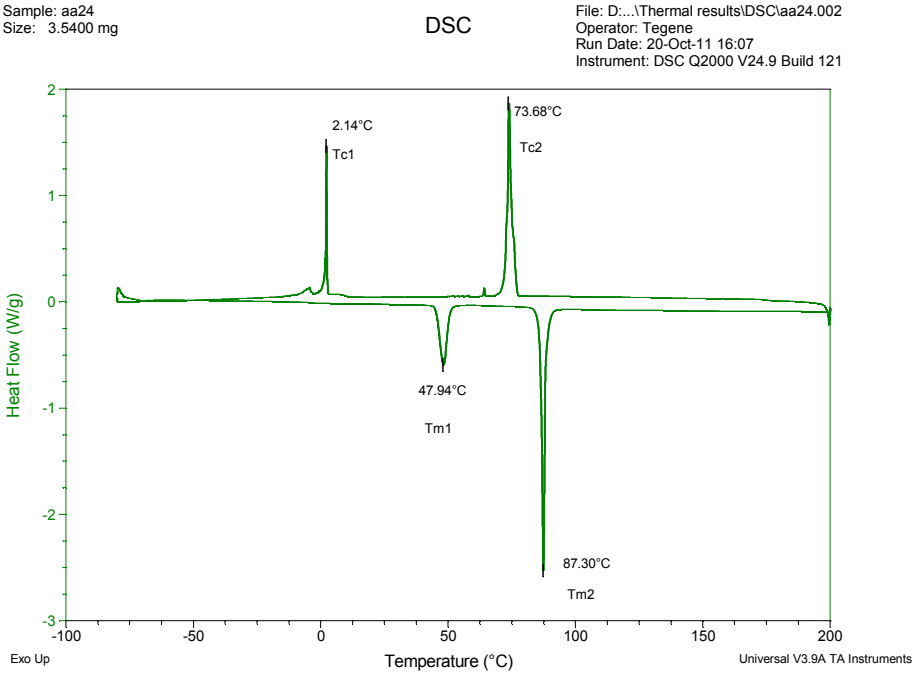

Figure 2. 28: Differential scanning calorimetry (DSC) thermogram of $[(C_4)_2Bipyr][N\ Tf_2]_2$

As the alkylating agent chain length increases, the structural flexibility of the cation increases. As a result of this the cation-anion interaction further weakens. Consequently; more than one modes of packing may result which is evidenced on the DSC thermogram of this class of compounds [16-18]. From this observation, because $[(C_2)_2Bipyr]\ [NTf_2]_2$ has just one crystallization temperature and one melting point temperature, it can be concluded that it has just one morphology. Moreover, because its melting point is > 100 ^0C, it is ruled out that it cannot be regarded as an ionic liquid. However, each of $[(C_4)_2Bipyr]\ [NTf_2]_2$, $[(C_8)_2Bipyr]\ [NTf_2]_2$ and $[(C_{10})_2Bipyr]\ [NTf_2]_2$ possess two phase transition points in both the cooling and heating curves. This indicates that these compounds have more than one morphology. Moreover, since $[(C_4)_2Bipyr]\ [NTf_2]_2$ has the highest phase transition temperature at 87.30 ^0C in the heating curve, it can be classified as an IL with polycharged cation. In contrast, $[(C_8)_2Bipyr]\ [NTf_2]_2$ and $[(C_{10})_2Bipyr]\ [NTf_2]_2$ showed phase transition temperatures at 138.50 ^0C and 172.87 ^0C in the heating curve, respectively. This fact makes them not to be ILs. The reason for this may be their longer chains have undertaken hydrophobic packing that contributed in stronger van der Waals interactions.

It should be noted that, because $[(C_2)_2Bipyr]\ [NTf_2]_2$, $[(C_4)_2Bipyr]\ [NTf_2]_2$, $[(C_8)_2Bipyr]\ [NTf_2]_2$ and $[(C_{10})_2Bipyr]\ [NTf_2]_2$ are doubly charged on the charge carrier moiety, they showed significantly larger melting points than their corresponding singly alkylated and monocharged counterparts.

Conclusions

The objective of this project (synthesis and characterizations) is met by succeeding in synthesizing pure ionic liquids from new moieties, 1, 10-Phenathroline and 4, 4'-Bipyridine. This was confirmed from the different characterization techniques. This can be an example in looking for new properties of ionic liquids from other starting materials with new properties and corresponding applications. Even though the liquid ranges of this class of salts is very large, acquisition of ionic liquids with melting points below 47 ^{0}C from 1, 10-Phenanthrolinum cation was found to be difficult. This may be due to the rigidity and the large number of component atoms in the charge carrier moiety which strongly contributes in the van der Waals interaction, as compared to the conventional ionic liquids. However, products obtained from 4, 4'-Bipyridinium cations resulted in RTILs with amazing liquidus range, with melting points < -20 ^{0}C. This may be due to the relatively non-rigidity and the less number of atoms in the positive charge carrier part in addition to the lifting of the symmetry due to the monoalkylation. The thermal properties of both classes of ionic liquids open new opportunity for those processes requiring large liquidus ranges.

As predicted, the dialkylated products of the 4, 4'-Bipyridine system showed significantly larger melting points than the monoalkylated counterparts. This is because of the development of two positive charges per charge carrier head that results in higher *Columbic* interactions between the cation and the anion.

References

1. P. Wasserschied, W. Kiem; *Angew. Chem. Int. Ed*.; 2000, **39**, 3772, -3789.
2. P. Bonhôte, A. P. Dias, N. Papageorgiou, K. Kalyanasundaram, M. Grätzel, *Inorg. Chem*., 1996, **35**, 1168–1178.
3. J. G. Huddleston, H. D. Willauer, R. P. Swatloski, A. E. Visser, R, D. Rogers, *Chem. Commun*., 1998, 1765.
4. J. Asikkala, *Application of Ionic liquids and microwave activation in selected organic reactions*, 2008, 17-20.
5. R. S. Varma and V. V. Namboodriri, *Chem. Commun*., 2001, 642-644.
6. J. Zhang, G. R. Martine and D. D. Desmarteau, *Chem. Commun*., 2003, 2334-2335.
7. A. R. Katritzky, A. J. Buolton, *Advances in heterocyclic chemistry*, **Vol. 22**, Academic press, INC., New York, 1978, ISBN 0-12-020622-6.
8. H. Ohno, *Electrochemical Aspects of Ionic Liquids*, **2nd ed**. Wiley, New Jersey, 2011, ISBN 978-0-470-64781-3.
9. J.D. Holbrey, R.D. Rogers, *Physicochemical properties of ionic liquids: melting points and phase diagrams*, in: P. Wasserscheid, T. Welton (Eds.), *Ionic liquids in synthesis*, Wiley-VCH, Weinheim, 2008, pp. 57–72.

10. L.A. Summers, *The Phenanthrolines*, in: A.R. Katritzky, A.J. Boulton (Eds.), *Advances in Heterocyclic Chemistry* Vol. 22, Elsevier, Gainesville, 1978, pp. 1–69.

11. J. G. Huddleston, A. E. vissor, W. M. Richert, H. D. Wellauer, G. A, Broker, R. D. Rogers, *Green Chemistry*, 2001, **3**, 156-164.

12. T. Cardinaels, K. Lava, K.Goossens, S.V. Eliseeva, K. Binnemans, *Langmuir,*2011, 2036–2043.

13. A. B. McEwen, H. L. Ngo, K. LeCompte, J. L Goldman, *J. Electrochem. Soc*., 1999, **146**, 1687-1895.

14. J. D. Holbrey, K. R. Seddon, *J. Chem. Soc., Dalton Trans*., 1999, 2133-2139.

15. F. S. Emily, I. J. V. Garcia, D. Briggs, P. Licence, *Chem. Commun*., 2005, 5633–5635.

16. A.V. Mudring, *Aust. J. Chem.* **2010**, *63*, 544–564

17. J. D. Holbrey, W. M. Reichert, M. Nieuwenhuyzen, K. R. Seddon, R. D. Rogers, *Chem. Commun.* **2003**, 1636. doi:10.1039/ B304543A

18. D. R. MacFarlane, J. Sun, J. Golding, P. Meakin, M. Forsyth, *Electrochim. Acta* **2000**, *45*, 1271.

CHAPTER THREE

3. X-ray Photoelectron Spectroscopy of 1, 10-Phenanthrolinium and 4, 4'-Bipyridinium Based Ionic Liquids

3.1 Introduction

X-ray photoelectron spectroscopy (XPS) is now accepted as a reliable method of characterization of ionic liquids [1]. This is because ILs are non volatile and chemically stable. However, it is only a small number of non-imidazolium based ionic liquids that have been investigated using XPS [1, 2]. The basic purpose of characterizing ionic liquids using XPS is confirmation of its purity as well as determination of the electronic environment of the component atoms. The commonly used laboratory lubricants and greases are the main sources of impurities in the form of their component elements, namely, silicon [4, 5], carbon and oxygen [6]. Following the purity (composition) investigation, the binding energies of the component atoms that again illustrate the information about their electronic environment of each atom of every element in the compound is extracted.

For ionic liquids, the most common, complex and often relevant element is carbon. Therefore, the development of a C 1s fitting model which deconstructs these different electronic environments into as small a number of components as possible is a critical goal in all XPS studies [1, 7]. Fitting models have been developed, particularly for XP spectra of the carbon region [1, 5, 7]. Adopting these fitting models has resulted in

successful charge correction of XP spectra giving accurate and reproducible binding energies for ionic liquids [7]. Fitting models for other than 1, 3-dialkyimidazolium based ionic liquids are required and need to be developed.

In this study, we investigate XP spectra of N-alkyl-1, 10-Phenanthrolinium and N-alkyl-4, 4'-Bipyridinium - based ionic liquids. The electronic environment of each element present in the compounds is discussed. Peak fitting models are developed for C 1s and N 1s regions of $[C_nPhen][NTf_2]$, n = 1, 2, 4, 6, 8and 10 as well as $[C_nBipyr][NTf_2]$, n = 4, 6 and 8. These models are believed to be valid for compounds containing 1, 10-Phenanthroline and 4, 4'-Bipyridine as a part, respectively. Table 3. 1 presents the structure of the compounds investigated using XPS.

Abbreviation	Structure	Name
$[C_1Phen]I$	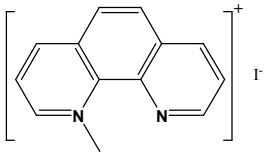	*N-Methyl-1, 10-Phenanthrolinium iodide*
$[C_1Phen][PF_6]$	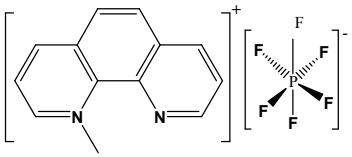	*N-Methyl-1, 10-Phenanthrolinium hexafluorophodphate*
$[C_1Phen][NTf_2]$	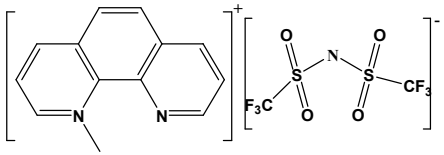	*N-Methyl-1,10-Phenanthrolinium bis[(trifluoromethyl)sulfonyl]amide*
$[C_2Phen][NTf_2]$	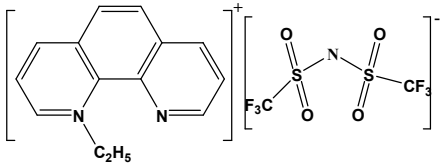	*N-ethyl-1,10-Phenanthrolinium bis bis[(trifluoromethyl)sulfonyl]amide*

$[C_4Phen][NTf_2]$	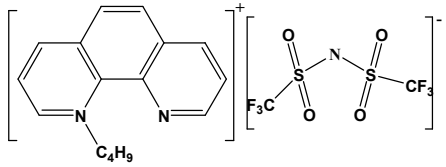	*N-butyl-1,10-Phenanthrolinium bis bis[(trifluoromethyl)sulfonyl]amide*
$[C_6Phen][NTf_2]$	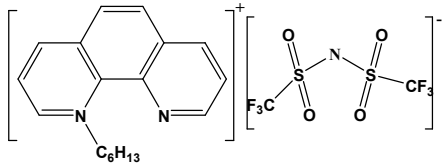	*N-hexyl-1,10-Phenanthrolinium bis bis[(trifluoromethyl)sulfonyl]amide*
$[C_6Phen][PF_6]$	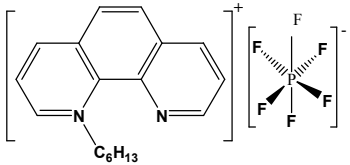	*N-hexyl-1,10-Phenanthrolinium hexafluorophosphate*
$[C_8Phen][NTf_2]$	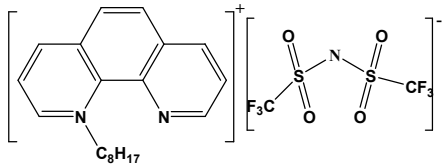	*N-octyl-1,10-Phenanthrolinium bis bis[(trifluoromethyl)sulfonyl]amide*

$[C_{10}Phen]\ [NTf_2]$	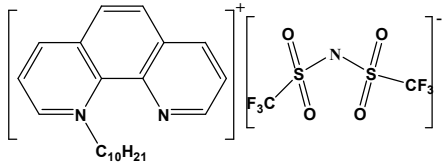	*N-decyl-1,10-Phenanthrolinium bis bis[(trifluoromethyl)sulfonyl]amide*
$[C_4Bipyr][NTf_2]$	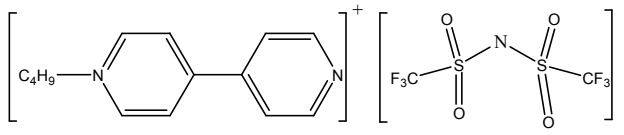	*N-butyl-4,4'-Bipyridinium bis[(trifluoromethyl)sulfonyl]amide*
$[C_6Bipyr][NTf_2]$	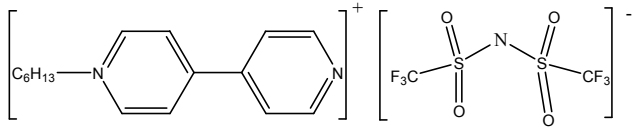	*N-hexyl-4,4'-Bipyridinium bis[(trifluoromethyl)sulfonyl]amide*
$[C_8Bipyr][NTf_2]$	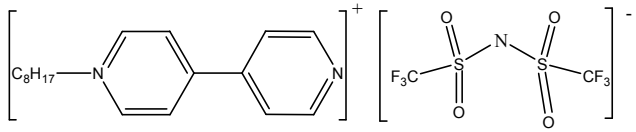	*N-octyl-4,4'-Bipyridinium bis[(trifluoromethyl)sulfonyl]amide*
$[C_{10}Bipyr][N\ Tf_2]$	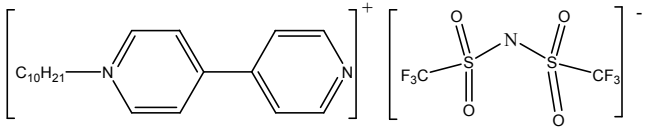	*N-decyl-4,4'-Bipyridinium bis[(trifluoromethyl)sulfonyl]amide*

Table 3.1: Structure of the compounds investigated using XPS

3.2 Experimental

Materials

All of the compounds were dried in vacuo before submission for XPS measurments. Ion chromatographic analysis of the products revealed that the residual ion concentrations $[Br]^-$ and $[I]^-$ were below accepted threshold concentrations, i. e., < 10 ppm. In all cases, no residual signals of halides or lithium were detected from XPS analysis.

XPS Data Collection

Samples were prepared by placing a small amount (≈ 20 mg) of the ionic liquid in to a depression on a stainless steel sample stub. The powder samples were cast into thin films (approx. thickness 0.5 – 1 mm), before rapid transfer to the preparative pumping chamber of the XPS instrument. Initial pumping to high vacuum pressure ($p \leq 1 \times 10^{-7}$ mbar) was carried out in the preparation to insure the complete removal of adsorbed volatiles including permanent gases, water vapor and other volatile impurities. The samples were then transferred to the main analytical vacuum chamber. The pressure in the main chamber remained $\leq 1 \times 10^{-8}$ mbar during XPS measurements of the samples.

3.3 Results and Discussion

3.3.1 N-alkyl-1, 10-Phenanthrolinium based products

Figure 3.1 shows the survey XP spectrum for $[C_8Phen][NTf_2]$,

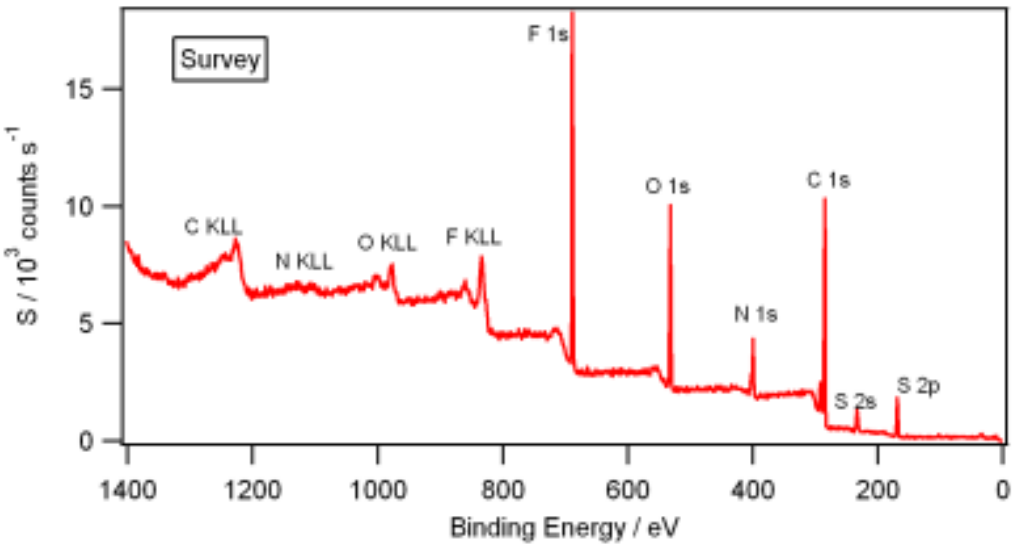

Figure 3. 1: Survey spectrum for $[C_8Phen][NTf_2]$

From Figure 3.1, it can be observed that all the expected elements are signaled by their envelopes on their respective position. It can also be seen that there is no evidence of either Li or halide contamination carried over from ion exchange processes. Experimental stoichiometries were within experimental error of nominal stoichiometries calculated from the empirical formula of the sample.

Binding energies

In order to obtain absolute binding energies for components within 1, 10-Phenanthrolinium based compounds, it is necessary to charge correct the XP spectra using an appropriate internal reference. To investigate whether such an internal reference exists for 1, 10-Phenanthrolinium-based compounds, all peaks in the XP spectra must be identified, and related to the chemical structure of the compounds, i. e., an appropriate multicomponent model must be applied in the deconstruction of the measured photoemission envelopes.

The electronic environment of carbon, the development of a fitting model

To establish a fitting model for our compounds, identification of the different electronic environments for C 1s and then assigning them is vital. For $[C_nPhen][NTf_2]$, where n =2, 4, 6, 8 and 10, (Figure 3.2) five components were used to fit the C 1s experimental spectrum. The peak at highest binding energy (≈ 293) is assigned to CF_3 group of the anion [24]. The other peaks at 285.7-286.9 eV and ≈ 285 eV are assigned for the carbon components within $[C_nPhen]^+$. Based on this the first of these four environments is carbons bonded to the alkylated nitrogen; $[C_nPhen]^+$ contains three such atoms labeled as (C^1). The second environment is the two carbon atoms bonded to the non-alkylated nitrogen labeled as (C^3), the third assignment goes to the other eight carbon atoms in the ring labeled as (C^4+C^5), and finally the alkyl environment labeled as (C_{Alkyl}) whose magnitude varies depending upon *n*. Regarding $[C_1Phen][NTf_2]$, the total number of contributions for C 1s is four as the alkyl chain not directly linked to nitrogen is missing.

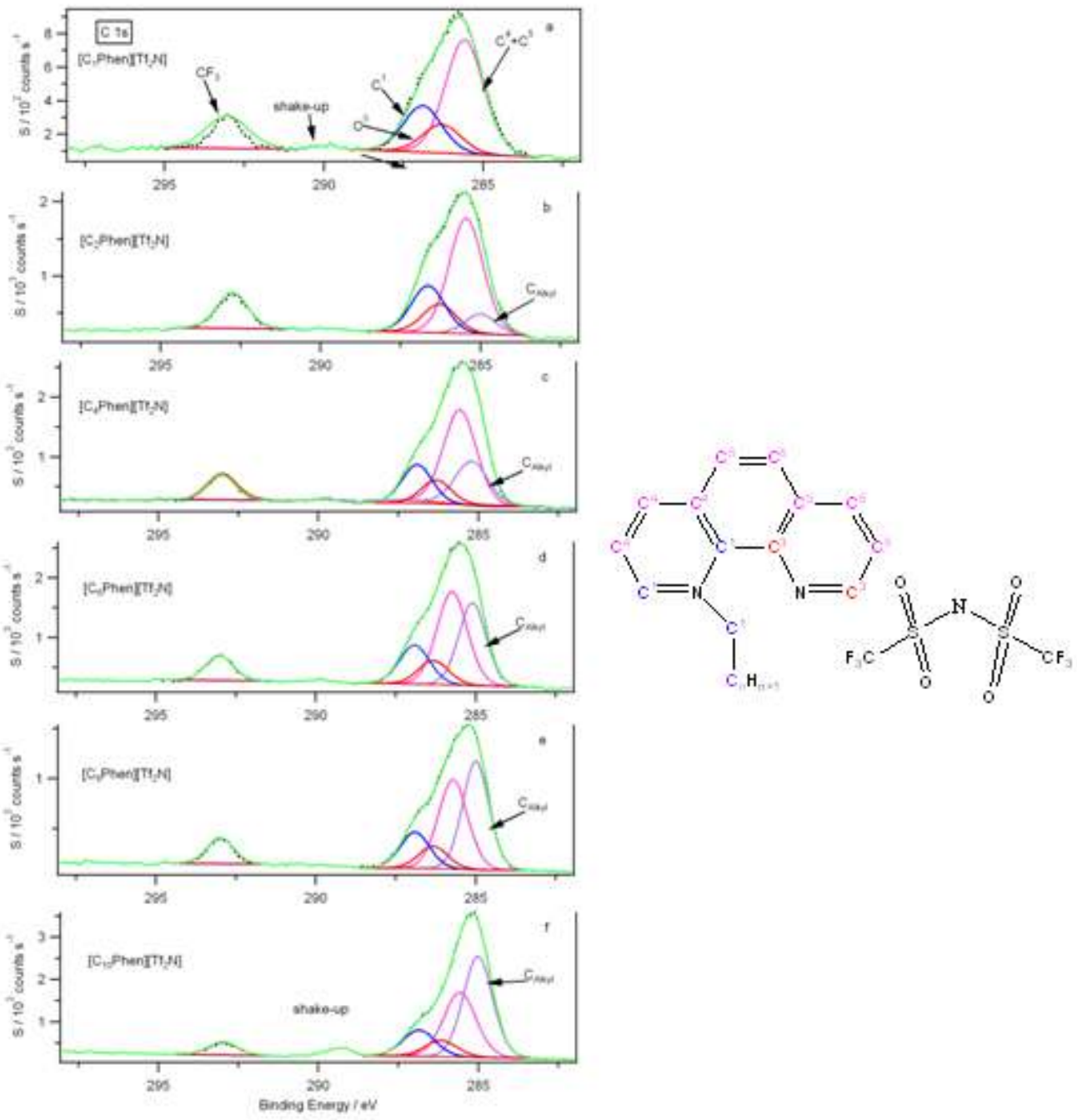

Figure 3. 2: C 1s XP spectra with component fittings for a(a) [C_1Phen][NTf_2],(b) [C_2Phen][NTf_2], (c) [C_4Phen][NTf_2], (d) [C_6Phen][NTf_2], (e) [C_8Phen][NTf_2], (f) [C_{10}Phen][NTf_2]

The constraints used to establish this model was started from [C_1Phen][NTf_2] in which there are 14 C atoms whose ratio is given by (CF_3 : C^1 : (C^3) : C^4+C^5) : (C_{Alkyl}). However, shake up satellite can be observed as broad features in the spectrum from about 289.12-

291.24 eV. (Figure 3.2). Such features are originated from delocalized ring system consequently; approximately 20% of the photoelectrons emanated from the ring system are lost to the satellite feature. Therefore, the C 1s peaks should be fitted considering this redistribution of the photoelectrons. In this regard the peak due to (C^1), (C^4+C^5) and (C^3) is reduced by 20%. As the peak area of aliphatic carbons is not affected by the shake-up phenomenon, the relative peak area ratios for the four cationic components would be 1: 2.6: 1.6: 6.4. While the Full Width at Half Maximum, FWHM, for C^1, (C^3) and (C^4+C^5) were set to be equal and set to be 1.1, from 0.9 to 0.95 was for CF_3. In general for all compounds studied here, similar procedures were followed and the fit shows an excellent agreement to the experimentally acquired signal.

For further confirmation, the fitting models of C 1s in the XP spectra are compared with [C_1Phen]I, [C_1Phen][PF_6] and[C_1Phen][NTf_2], as well as [C_6Phen][PF_6] [C_6Phen][NTf_2] (Figure 3.3). In this result it is revealed that peak due to CF_3 from $(CF_3SO_2)_2N$, is missing in the compounds containing I and PF_6 as counter anion. However, the other C 1s peaks are found in their respective position unchanged which indicates that the type of the anion does not have impact in their binding energies.

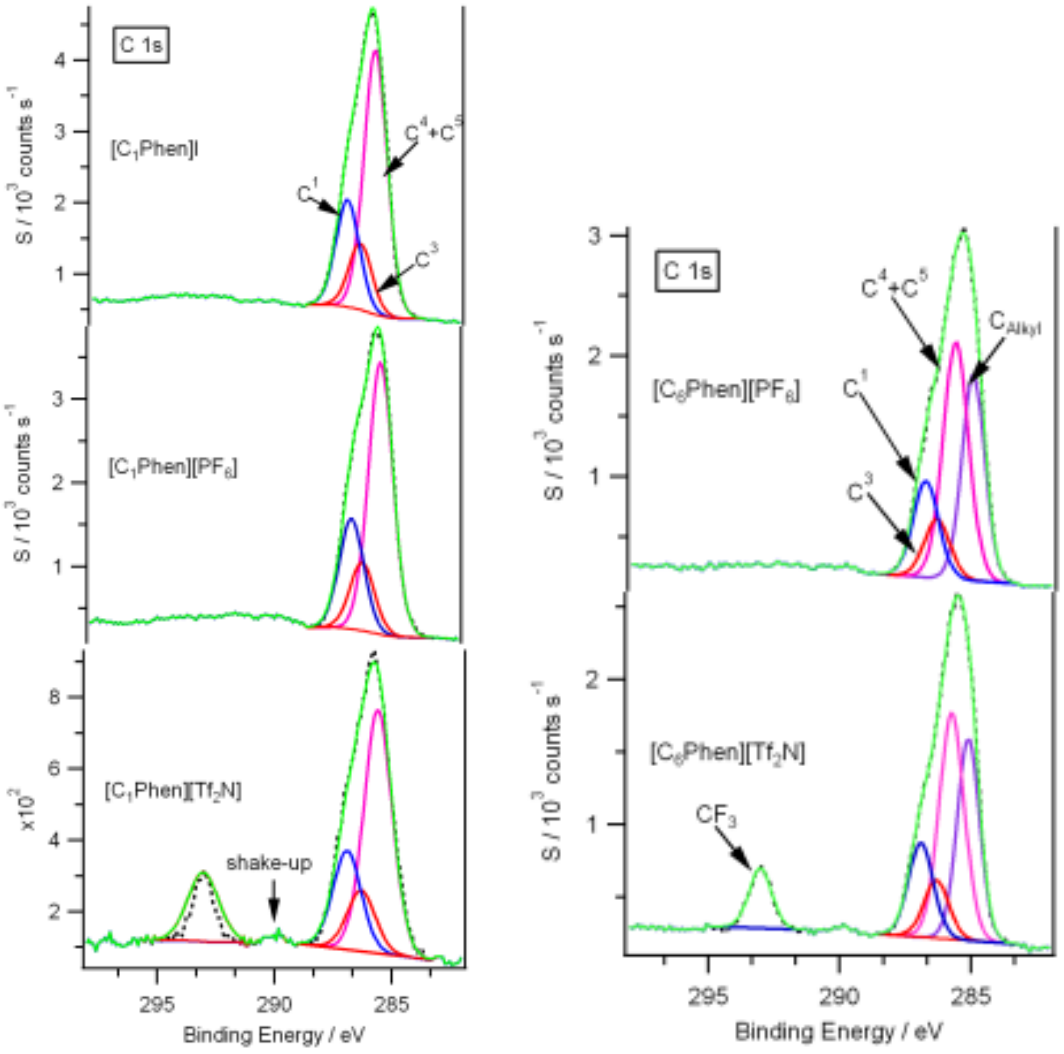

Figure 3. 3: Comparative fitting models of C 1s XP spectra of (a) $[C_1Phen]I$, $[C_1Phen][PF_6]$ and $[C_1Phen][NTf_2]$; (b) $[C_6Phen][PF_6]$ and $[C_6Phen][NTf_2]$

Electronic environment of nitrogen and other anion associated regions

The N 1s XP spectra for $[C_nPhen][\ NTf_2]$ contain three characteristic peaks (Figure 3.4). The peak at higher binding energy, 402.2 eV is assigned to the alkylated nitrogen of the cation, $N_{Cation,}$ while the peak at lower binding energy whose FWHM is nearly twice the

former represents enveloped two nitrogens, the unalkylated nitrogen, $N^{'}_{Cation}$, (399.52 ev), of the cation and that of the anion, $[NTf_2]^-$ (399.35 eV). This binding energy is comparable with that observed for a range of imidazolium based ionic liquids [5, 7, 11].

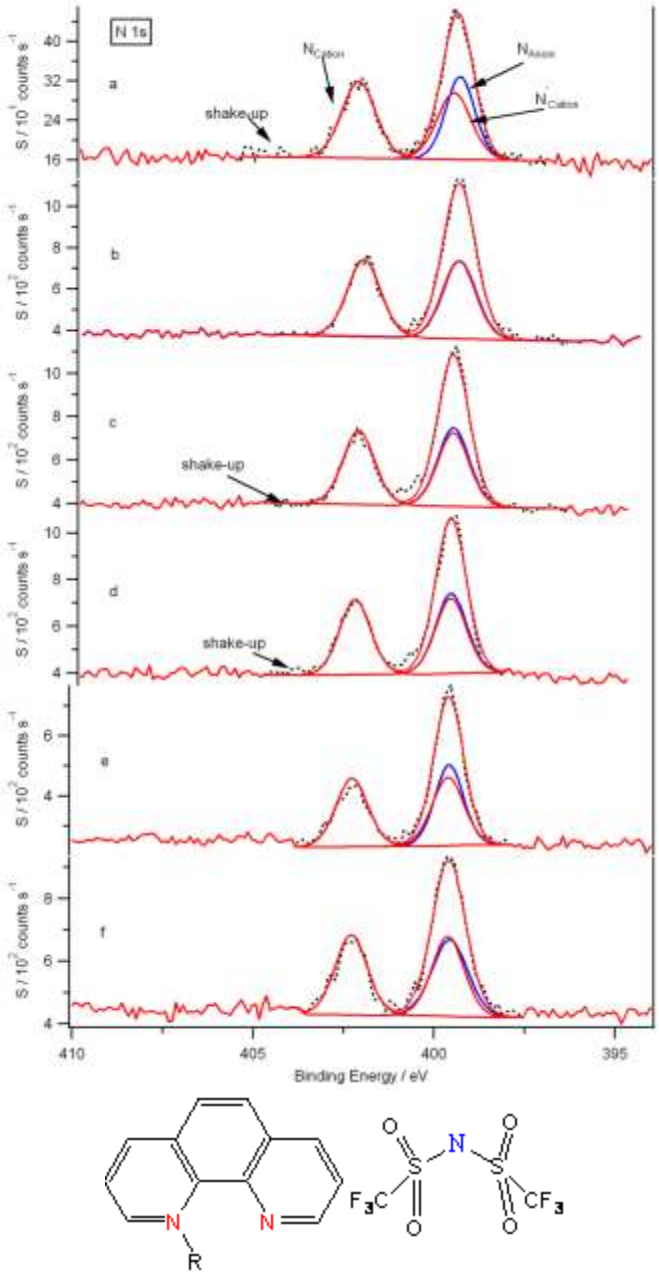

Figure 3. 4: N 1s XP spectra with component fittings for a (a) $[C_1Phen][NTf_2]$, (b) $[C_2Phen][NTf_2]$,(c) $[C_4Phen][NTf_2]$,(d) $[C_6Phen][NTf_2]$, (e) $[C_8Phen][NTf_2]$, (f) $[C_{10}Phen][NTf_2]$

Interestingly, the proportions of FWHM due to N 1s confirms the reliability of the above assignment when XP spectra fitting models due to N 1s of $[C_1Phen]I$, $[C_1Phen][PF_6]$ and $[C_1Phen][NTf_2]$ as well as $[C_6Phen][PF_6]$ and $[C_6Phen][NTf_2]$ are compared as indicated in Figure 3.5. In this comparison, compounds without $(CF_3SO_2)_2N$, show nearly equal FWHM of N 1s picks at the two binding energies as the C 1s contribution by C of CF_3 is missing.

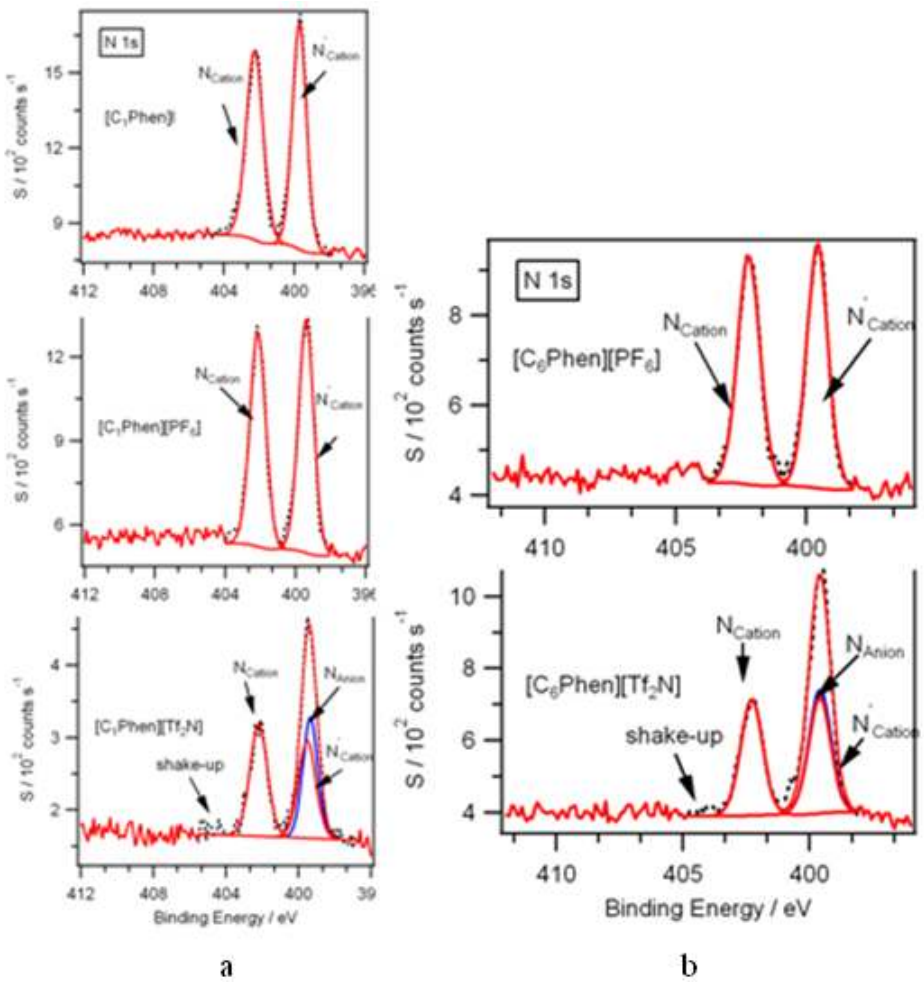

Figure 3. 5: Comparative N 1s fitting models of XP spectra of (a) $[C_1Phen]I$, $[C_1Phen][PF_6]$ and $[C_1Phen][NTf_2]$; (b) $[C_6Phen][PF_6]$ and $[C_6Phen][NTf_2]$

Fluorine, oxygen and sulfur of these compounds each show a single electronic environment [5, 7, 11]. This is because of the obvious reason that the six fluorine atoms

are chemically indistinguishable. This fact works the same for the four oxygen atoms and the two sulfur atoms. The doublet due to the region of sulfur does not signify the existence of two electronically different regions. This doublet peak is created because this element acquires two electronic states with respect to its 2p orbitals due to spin-orbit splitting into the S $2p_{1/2}$ and $2p_{3/2}$ levels with area ratio of 1:2 when bombarded and excited by the X-ray photons(Figure 3.6).

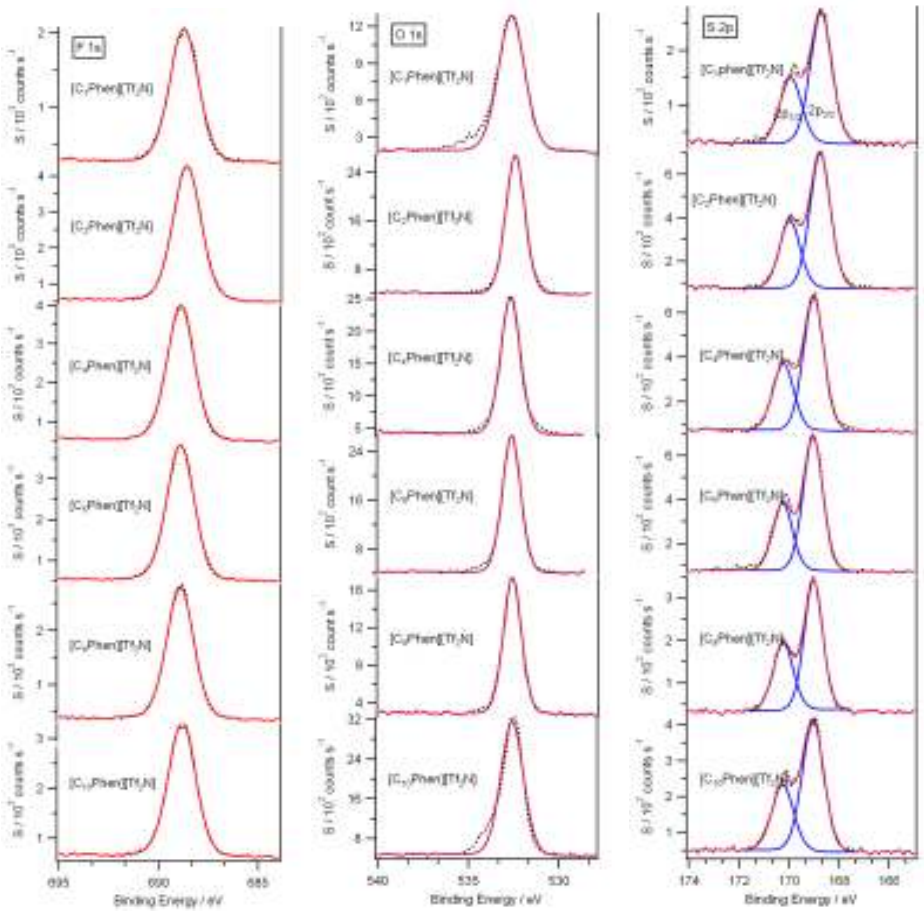

a **b** **c**

Figure 3. 6: (a) O 1s, (b) F 1s, (c) S 2p XP spectra for $[C_1Phen][NTf_2]$, $[C_2Phen][NTf_2]$, $[C_4Phen][NTf_2]$,$[C_6Phen][NTf_2]$, $[C_8Phen][NTf_2]$, and $[C_{10}Phen][NTf_2]$

Similarly, iodine and phosphorous of $[C_1Phen]I$, $[C_1Phen][PF_6]$ and $[C_6Phen][PF_6]$ also show single electronic environment in addition to the obvious position of the other elements. Like sulfur, however, these elements show doublets of different separations that depend up on their spin orbit splitting as can be seen in Figure 3.7. Here, it can be seen that the area ratio between the doublets of 3d, namely $3d_{3/2}$ and $3d_{5/2,}$ as well as the doublets of 4d, namely, $4d_{3/2}$ and $4d_{5/2}$, is 2:3.

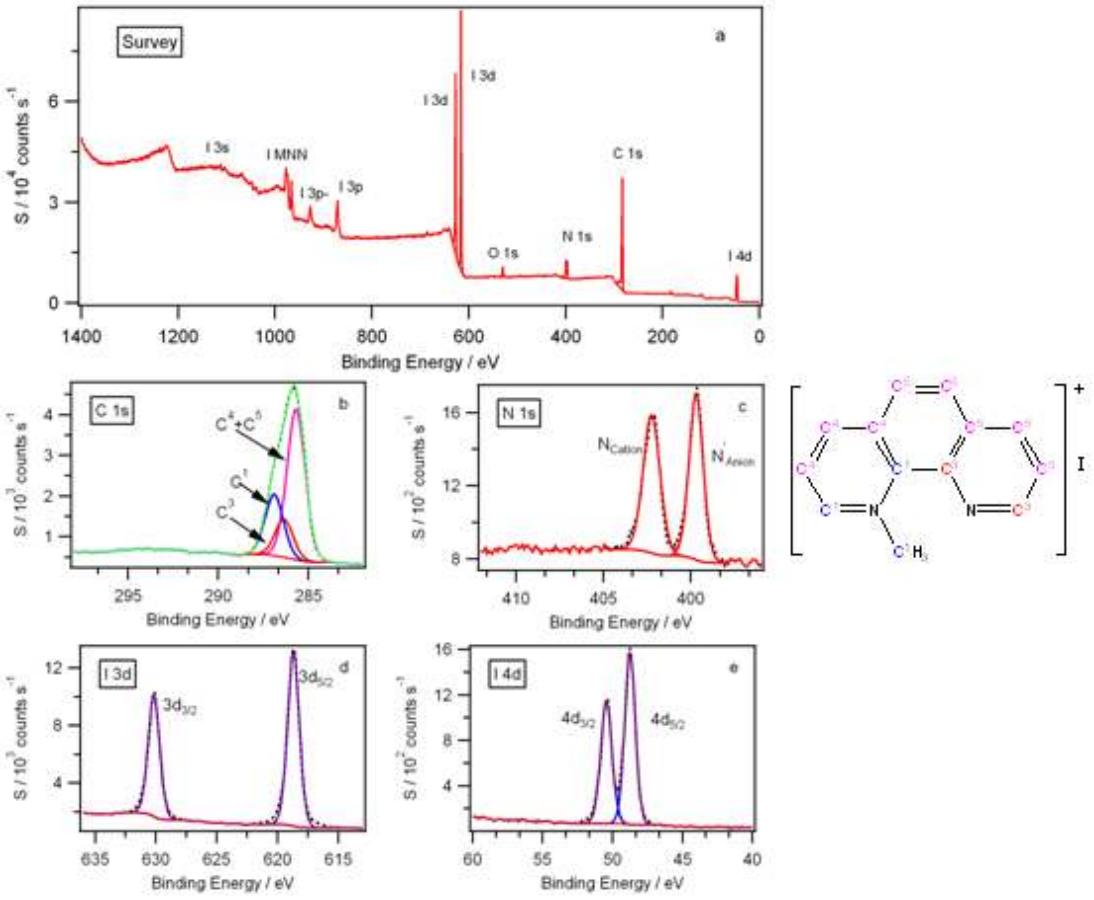

Figure 3. 7: XP spectra with component fittings of $[C_1Phen]I$ for: (a) survey, (b) C 1s, (c) N 1s, (d) I3d, (e) I4d.

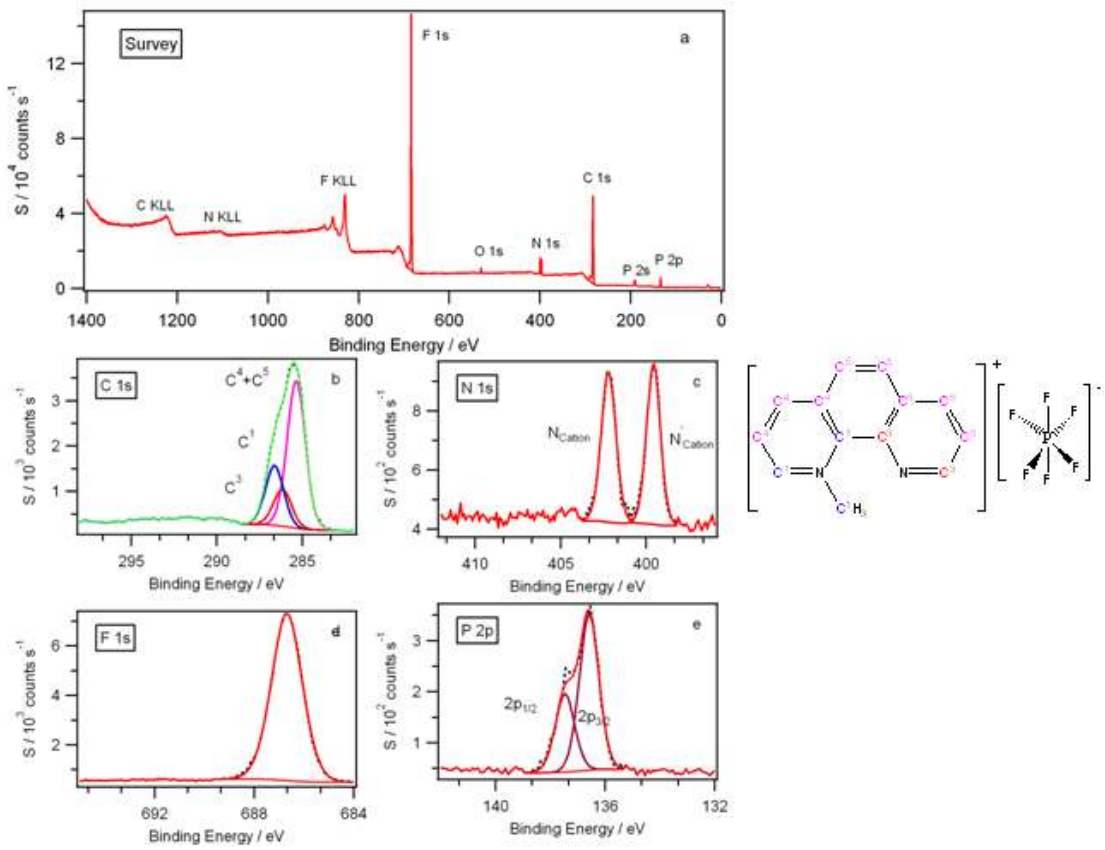

Figure 3. 8: XP spectra with component fittings of $[C_1Phen][PF_6]$ for: (a) survey, (b) C 1s, (c) N 1s, (d) F 1s, (e) P 2p.

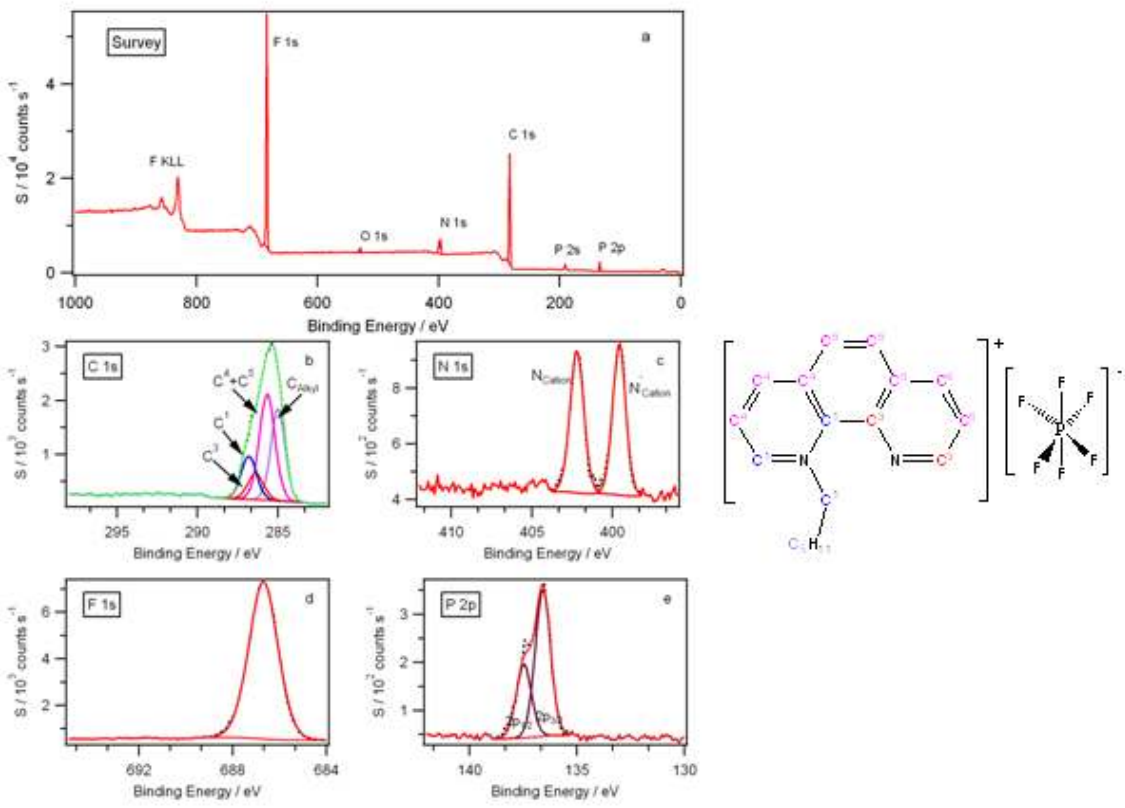

Figure 3. 9: XP spectra with component fittings of $[C_6Phen][PF_6]$ for: (a) survey, (b) C 1s, (c) N 1s, (d) F 1s, (e) P 2p.

The measurement of accurate binding energies

As stated earlier, charge compensation was not carried out consequently the recorded binding energies for these compounds cannot be considered as absolute values. This fact necessitates charge correction by setting the binding energy of aliphatic component of $[C_8Phen][NTf_2]$ to be 285.0 eV. Subsequently, all the other regions are shifted by the same amount as the $C_{Aliphatic}$ 1s component where the binding energy of the alkylated nitrogen, N_{Cation} 1s, shifts to 402.2 eV. Because the electronic environment of the cationic nitrogen is expected to be unaffected by the alkyl chain length, this latter value can then be used to charge correct all other $[C_nPhen][NTf_2]$ products. Figures 3.2-3.9 show the

charge corrected XP spectra of all the elements for these products. The binding energy of each element in the six compounds is summarized in the following tables.

It should be noted that the experimental errors associated with the measurement of binding energies in all the above spectra is of the order $\pm 0.1 eV$

Ionic Liquid	Binding Energy/eV										
Cation	C_{Alkyl}1s	$C_1$1s	$C_3$1s	C_{4+5}1s	$CF_3$1s	N'_{Cation}1s	N^+_{Cation}1s	N^-_{Anion}1s	O1s	F1s	S2p3/2
[C_1Phen]	-	286.9	286.3	285.6	293.0	399.6	402.2	399.4	532.5	688.9	168.9
[C_2Phen]	285.2	286.9	286.8	285.6	292.9	399.6	402.3	399.5	532.6	688.7	168.9
[C_4Phen]	285.2	286.9	286.4	285.6	292.9	399.6	402.2	399.5	532.7	688.8	168.9
[C_6Phen]	285.1	286.9	286.3	285.7	293.0	399.6	402.2	399.6	532.6	688.8	169.0
[C_8Phen]	285.0	286.9	286.3	285.7	292.9	399.6	402.2	399.6	532.7	688.8	169.0
[C_{10}Phen]	285.0	286.9	286.2	285.7	292.9	399.6	402.2	399.6	532.7	688.8	169.0

Table 3. 1: Binding energies in eV for all regions for [C_nPhen][NTf_2]

	Binding Energy/eV								
Compound	$C_{Alkyl}1s$	$C_1 1s$	$C_3 1s$	$C_{4+5}1s$	$N'_{Cation}1s$	$N^+_{Cation}1s$	F1s	$I3d_{5/2}$	$P2p_{3/2}$
$[C_1Phen]I$	-	286.9	286.3	285.6	399.6	402.2	-	618.7	-
$[C_1Phen][PF_6]$	-	286.9	286.2	285.5	399.5	402.2	688.8	-	136.4
$[C_6Phen][PF_6]$	285.0	286.9	286.3	285.6	399.6	402.2	688.9	-	136.0

Table 3. 2: Binding energies in eV for all regions for $[C_1Phen]I$, $[C_1Phen][PF_6]$, and $[C_6Phen][PF_6]$

3.3.2 XPS of N-alkyl-4, 4'-Bipyridinium Based Products

Figure 3.10 shows the survey XP spectrum for $[C_8Bipyr][NTf_2]$ from this class of ionic liquids.

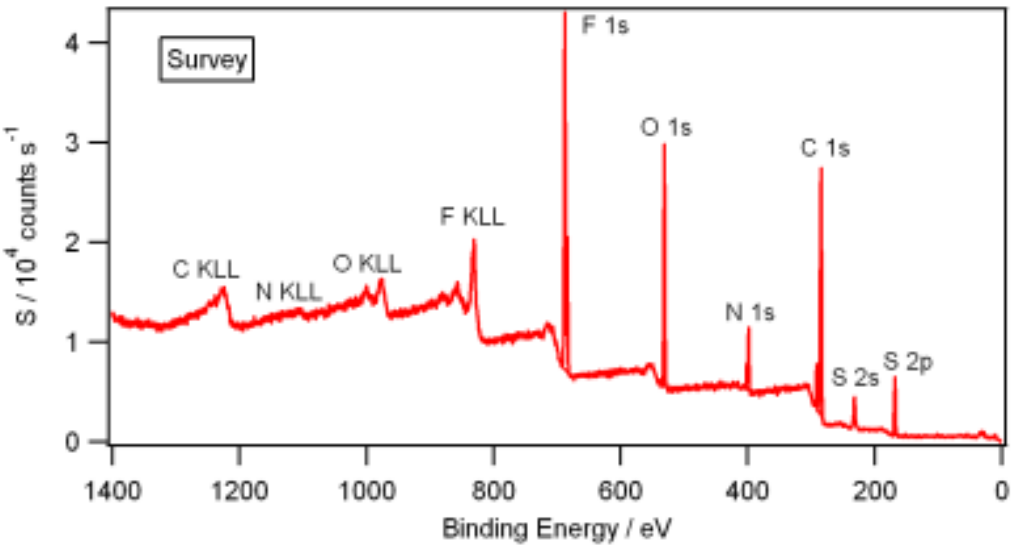

Figure 3. 10: Survey spectrum for $[C_8Bipyr][NTf_2]$

From Figure 3.10, it can be observed that all the expected elements are signaled by their envelopes on their respective position. It can also be seen that no evidence of either Li or halide contamination carried over from ion exchange processes. Experimental stoichiometries were within experimental error of nominal stoichiometries calculated from the empirical formula of the sample.

Binding energies

In order to obtain absolute binding energies for components within 4, 4'-Bipyridinium based compounds, it is necessary to charge correct the XP spectra using an appropriate internal reference. To investigate whether such an internal reference exists for 4, 4'-Bipyridinium based compounds, all peaks in the XP spectra must be identified, and

related to the chemical structure of the compounds, i. e. an appropriate multicomponent model must be applied in the deconstruction of the measured photoemission envelopes.

Peak fitting procedure for N-octyl-4, 4'-Bipyridinium-based [C_nBipyr][NTf_2] ILs

The high resolution C 1s spectra of N-alkyl-4, 4'-Bipyridinium-based ionic liquids can be fitted following our intuition which was mentored by previous reports based on imidazolium based ionic liquid [7, 11-13].

The electronic environment of carbon, the development of a fitting model

As indicated in figure 3.11, each type of carbon assigned with different numbers corresponding to distinctly different chemical environments. In addition to those present in the cation, the C in the CF_3 of the anion has its own chemical environment which introduce additional component.

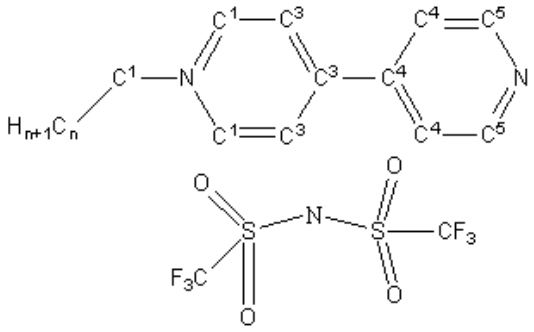

Figure 3. 11: N-Alkyl-4, 4'-Bipyridinium Bis(trfluormethylsulfony]amide and its C 1s assignment.

For [C_nBipyrir][Tf_2N], where n=4, 6 and 8; (Figure 3.12) five components were used to fit the C 1s experimental spectrum. The peak at highest binding energy (≈ 293 eV) is assigned to CF_3 group of the anion [10, 18]. The other values 285.7-286.9 eV and ≈ 285 eV assigned for the carbon components within $[C_nBipyr]^+$. Based on this the first of these

four environments is carbon bonded to the alkylated nitrogen; $[C_nBipyr]^+$ contains three such atoms labeled as (C^1). The second environment is the three carbon atoms indirectly bonded to the alkylated nitrogen and the two carbons linked to the non-alkylated nitrogen labeled as (C^3 + C^5), the third assignment goes to the three carbon atoms indirectly linked to the unalkylated nitrogen labeled as (C^4), and finally the alkyl environment labeled as C_{Alkyl} whose magnitude varies depending upon *n* (Figure 3.12).

The constraints used to establish this model was started from $[C_4Bipyr][NTf2]$ in which there are 16 C atoms whose ratio is given by CF_3 : (C^1) : (C^3+C^5) : (C^4) : (C_{Alkyl}) = 2 : 3 : 5 : 3 : 3. However, shake up satellite can be observed as broad features in the spectrum from about 289.12-291.24 eV (Figure 3.12). Such features originate from delocalized ring system. Consequently approximately 20% of the photoelectrons emanated from the ring system are lost to the satellite feature. Therefore, the C 1s peaks should be fitted considering this redistribution of the photoelectrons. In this regard the peak due to C 1s of (C^1), (C^3+C^5) and (C^4) is reduced by 20%. As the peak area of aliphatic carbons is not affected by the shakeup phenomenon, the relative peak area ratios for the four cationic components would be 2: 2.6: 4: 2.4: 3. While the Full Width at Half Maximum, FWHM, for (C^1) and (C^3+ C^5), (C^3) were set to be equal and set to be 1.11, from 0.9 to 0.95 was for CF_3. In general for all compounds studied here, similar procedures were followed and the fit shows an excellent agreement to the experimentally acquired signal. In the case of $[C_6Bipyr][NTf_2]$, $[C_8Bipyr][NTf_2]$ and $[C_{10}Bipyr][NTf_2]$ the ratio of the component contributors would be CF^3 : (C^1) : (C^3+C^5) : (C^4) : (C_{Alkyl}) =2: 2.6: 4: 2.4: 5 , 2: 2.6: 4: 2.4: 7 and 2 : 2.6 : 4 : 2.4 : 9, respectively.

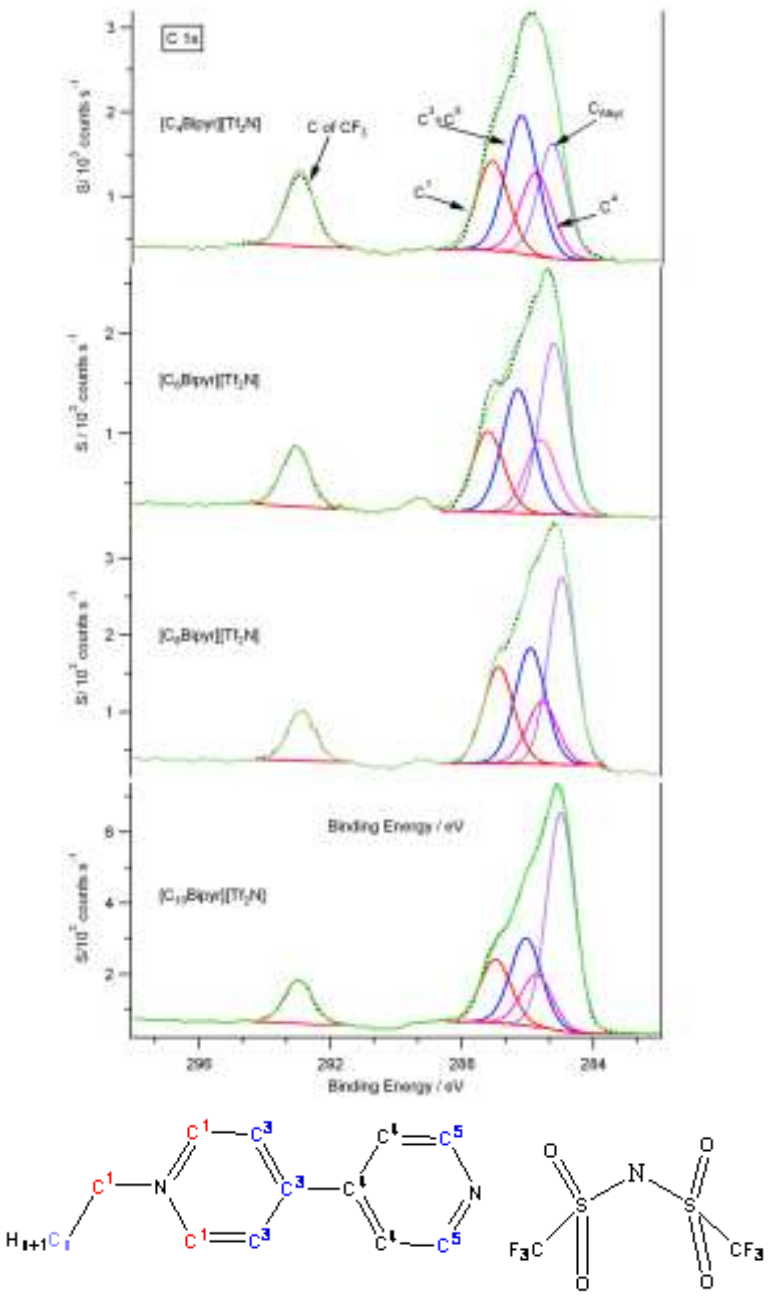

Figure 3. 12: C 1s XP spectra with component fittings for $[C_4Bipyr][_N NTf_2]$, $[C_6Bipyr][NTf_2]$, $[C_8Bipyr][NTf_2]$ and $[C_{10}Bipyr][NTf_2]$

Electronic environment of nitrogen and other anion associated regions

The N 1s XP spectra for $[C_nBipyr][NTf_2]$ contain three characteristic peaks(Figure 3.13). The peak at higher binding energy, 402.2 eV is assigned to the alkylated nitrogen of the cation, $N_{Cation,}$ while the peak at lower binding energy whose FWHM is nearly twice the former represents enveloped two nitrogenes, the unalkylated nitrogen, N'_{Cation}, (3.99.52 eV), of the cation and that of the anion, NTf_2^- (399.51 eV). This binding energy is comparable with that observed for a range of imidazolium [6, 7, 14] based ionic liquids.

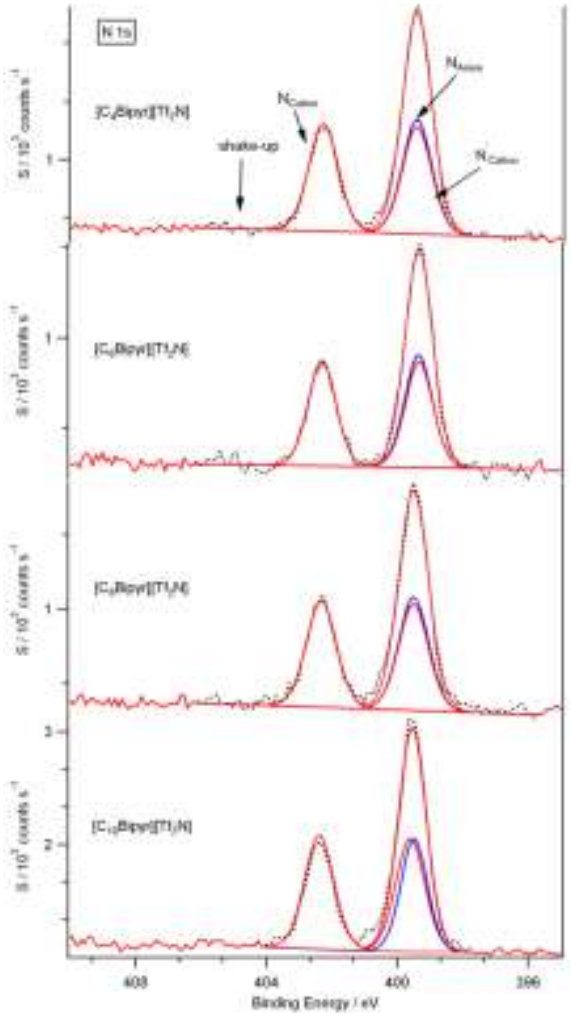

Figure 3. 13: N 1s XP spectra with component fittings for $[C_4Bipyr][NTf_2]$, $[C_6Bipyr][NTf_2]$ $[C_8Bipyr][NTf_2]$ and $[C_{10}Bipyr][NTf_2]$

Just like in the case of N-alkyl-1, 10-Phenanthrolinium, fluorine, oxygen and sulfur of these compounds each show a single electronic environment (Figure 3.14).

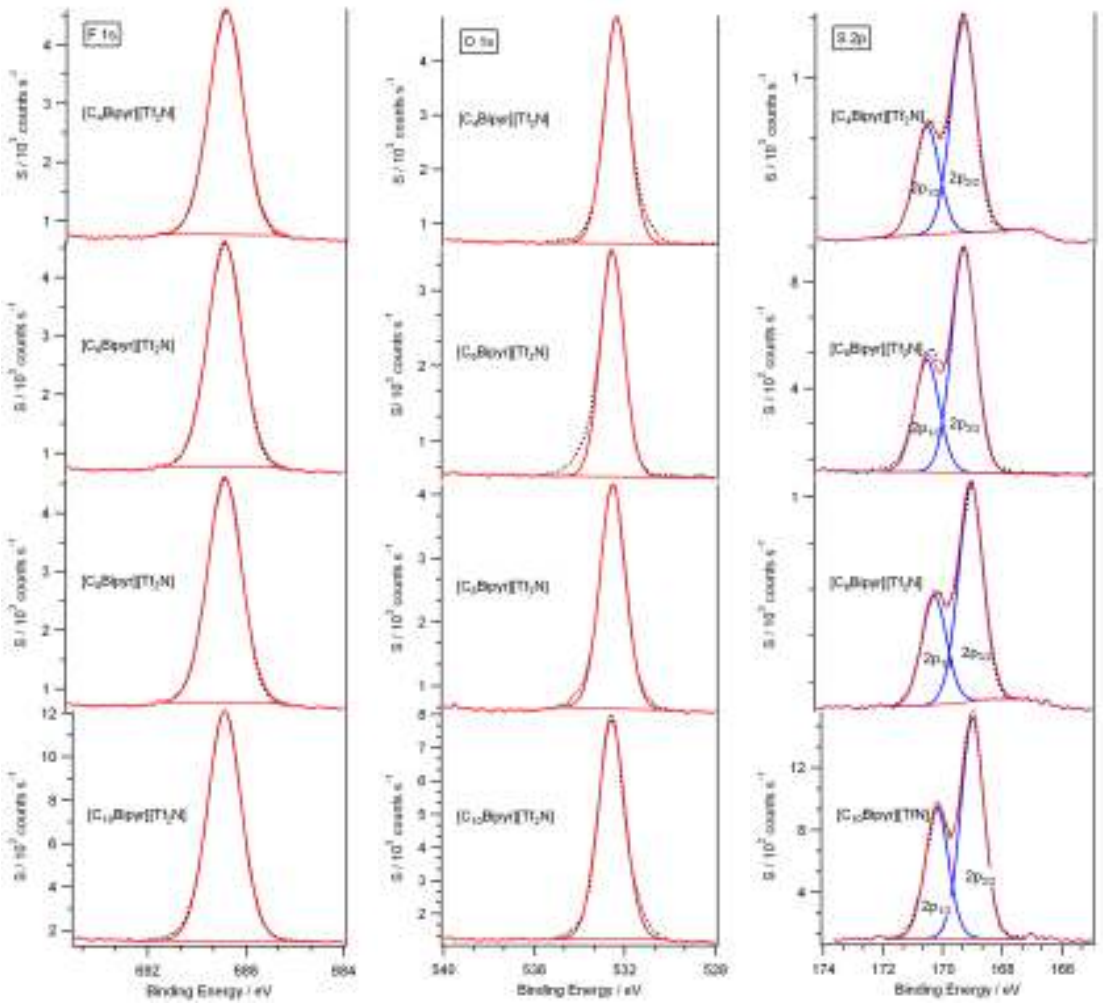

a **b** **c**

Figure 3. 14: (a) F 1s, (b) O 1s, (c) S 2p XP spectra for $[C_4Bipyr][NTf_2]$, $[C_6Bipyr][NTf_2]$, $[C_8Bipyr][NTf_2]$, and $[C_{10}Bipyr][NTf_2]$

It should be noted that the experimental errors associated with the measurement of binding energies in all the above spectra is of the order $\pm 0.1 ev$.

The measurement of accurate binding energies

As stated earlier, charge compensation was not carried out consequently the recorded binding energies for these compounds cannot be considered as absolute values. This fact necessitates charge correction by setting the binding energy of aliphatic component of $[C_8Bipyr][NTf_2]$ to be 285.0 eV. Subsequently, all the other regions are shifted by the same amount as the $C_{Aliphatic}$ 1s component where the binding energy of the alkylated nitrogen, N_{Cation} 1s, shifts to 402.2 eV. Because the electronic environment of the cationic nitrogen is expected to be unaffected by the alkyl chain length, this latter value can then be used to charge correct all other $[C_nBipyr][NTf_2]$ products. Figures 3-5 show the charge corrected C 1s and N 1s XP spectra for these products. The binding energy of each element in the six compounds is summarized in the following table.

onic Liquid	Binding Energy/eV										
Cation	C_{Alkyl}1s	C^{1} 1s	C^{3+5} 1s	C^{4} 1s	$CF_3$1s	N'_{Cation}1s	N^{+}_{Cation}1s	N^{-}_{Anion}1s	O1s	F1s	S2p3/2
[C_4Bipyr]	285.0	286.9	286.2	285.6	292.9	399.4	402.3	399.4	532.4	688.5	169.0
[C_6Bipyr]	285.1	286.9	286.3	285.6	292.9	399.6	402.3	399.5	532.6	688.7	168.9
[C_8Bipyr]	285.0	286.9	286.4	285.6	292.9	399.6	402.2	399.5	532.7	688.8	168.9
[C_{10}Bipyr]	285.0	286.9	286.4	285.6	292.9	399.6	402.2	399.5	532.7	688.8	168.9

Table 3. 3: Binding energies in eV for all regions for [C_nBipyr][NTf_2]

Conclusions

We have successfully measured XP spectra for ten 1, 10- Phenanthrolinium based ILs varying the anions and the chain length of the cation. Similarly, XP spectra of three 4, 4'-Bipyridinium based ionic liquids, varying only the aliphatic chain length of the cation keeping the anion constant was measured. The salts are of high purity, allowing conclusions to be drawn on the physicochemical properties of 1, 10-Phenanthrolinium and the 4, 4'-Bipyridinium based ionic liquids in particular and any compound containing 1, 10-Phenanthrolin and 4, 4'-Bipyridine in general. The electronic environments of all elements were identified. A robust fitting model for the C 1s and N 1s regions of 1, 10-Phenanthrolinium and 4, 4'-Bipyridinium -based ionic liquids was produced. The binding energy of the aliphatic carbon (C_{Alkyl} 1s) moiety was determined with high confidence. As reliable binding energies were obtained for C_{Alkyl} 1s, charge corrected binding energies (absolute binding energies) for all components could be obtained. Variation of *n* was shown to have little or no effect on the electronic interaction of the charge-bearing head groups of the ionic liquid. The binding energy data table presented in this report may find future use as a standard list of binding energies for1, 10-Phenanthrolinium and 4, 4'-Bipyridinium -based ionic liquids consequently it will be helpful in following up the property changes between these solvents and their solutes in future applications.

References

1. K. R. J. Lovelock, I. J. Villar-Garcia, F. Mair, H. P. Steinruck, P. Licence, *Chem. Rev*., 2010, **110**, 5158-5190.
2. D. S. Silvester, T. L. Broder, L. Aldous, C. Hardacre, A. Crossley, R. G. Compton, *Analyst,* 2007, **132**, 196-198.
3. Q. H. Zhang, S. M. Liu, Z. P. Li, J. Li, Z. J. Chen, R. F. Wang, L. J. Lu, Y. Q. Deng, *Chem.-Eur. J*., 2009, **15**, 765-778.
4. E. F. Smith, I. J. Villar Garcia, D. Briggs and P. Licence, Chem. Commun., 2005, 5633-5635.
5. K. R. J. Lovelock, C. Kolbeck, T. Cremer, N. paape, P. S. Schulz, P. Wasserscheid, F. Mair, H. P. Steinruck, *J. Phys. Chem. B*, 2009, 113, 2854-2864.
6. H. Hashimoto, A. Ohno, K. Nakajima, M. Suzuki, H. Tsuji, K. Kimura, *Surf. Sci.,* 2010, 604, 464-469.
7. I. J. Villar-Garcia, E. F. Smith, A. W. Taylor, F. L. Qui, K. R. J. Lovelock, R. G. Jones, P. Licence, *Phys. Chem. Chem. Phys.,*2011, **13**, 2797-2808.
8. A. Deyko, K. R. J. Lovelock, J. A. Corfield, A. W. Taylor, P. N. Gooden, I. J. Villar-Garcia, P. Licence, R. G. Jones, V. G. Krasovskiy, E. A. Chernikova and L. M. Kustov, *Phys. Chem. Chem. Phys*., 2009, 11, 8544-8555.
9. N. Papaiconomou, J. Salminen, J. M. Lee and J. M. Prausnitz, *J. Chem. Eng. Data*, 2007, 52, 833-840.
10. D. R. MacFarlane, P. Meakin, J. sun, N. Amini and M. Forsyth, *J. Phys. Chem. B*, 1999, **103**, 4164-4170.

11. E. F. Smith, F. J. M. Rutten, I. J. Villar-Garcia, D. Briggs, P. Licence, *Langmuir*, 2006, **22**, 9386-9392.

12. C. D. Wagner, L. E. Davis, M. V. Zeller, J. A. Taylor, R. H. Raymond, L. H. Gale, *Surf. Interface Anal.,* 1981, **3**, 211-225.

13. *Surface Analysis by Auger and X-ray Photoelectron Spectroscopy*, ed. D. Briggs and J. T. Grant, IM Publications, Manchester, 2003.

CHAPTER FOUR

4. Applications of the New Ionic Liquids

4.1 Introduction

ILs are tunable materials and consequently involved in significantly large varieties of applications. ILs have been applied as electrolytes for electrochemical devices and processes, solvents for organic and catalytic reactions, new materials, i.e. lubricants or heat transfer fluids and solvents for separation and extractions processes [1-3]. Unfortunately, the low solubility of 1, 10-Phenanthroline and its metal complexes in the common ionic liquids is hindering their use in homogeneous catalysis and many other areas [4-6]. Moreover, metal salts of the form $MCl_2 \cdot nH_2O$ are hardly soluble in the common ILs [7]. The dissolution of such salts is possible only by functionalizing the ionic liquids in a way they coordinate to the metal ion [8–10]. However, this strategy requires further amount of synthetic work and render the final application more laborious, expensive and less environmental friendly. In that respect, 1, 10- Phenanthrolinum and 4, 4'-Bipyridinium ionic liquids have been synthesized following the typical steps used for the synthesis of commonly used ionic liquids. The other objective of this project was to test the dissolving abilities of these ionic liquids for such as Nanoparticle stabilizers such as 1, 10-Phenanthroline [4] and its metal complexes and metal salts. To test if this objective were met, complexes as solute for $[C_nPhen][NTf_2]$ were synthesized from $NiCl_2 \cdot 6H_2O$, $CoCl_2 \cdot nH_2O$, $FeCl_3 \cdot nH_2O$, $PdCl_2$ and 1, 10-Phenanthroline following

reported procedures [11]. $NiCl_2$ and $Cu(NO_3)_2$ were used as solutes for $[C_4Bipyr][NTf_2]$ and $[(C_4)_2\ Bipyr][NTf_2]_2$

4.2 Dissolution of 1, 10-Phenanthroline and its Metal Complexes in $[C_1Phen][NTf_2]$

Experimental

Into each of five 25 ml round-bottom flasks, 2g $[C_1Phen][NTf_2]$ was heated up to 70 ^{0}C (melting temperature) in an oil bath. While stirring, 1, 10-Phenanthroline, $[Ni(Phen)_2Cl_2]\cdot 5H_2O$, $[Co(Phen)_2H_2OCl]Cl$, $[Fe(Phen)_2 2H_2O]\ Cl_2$, and $[Pd(Phen)Cl_2]$ was added gradually by observing whether the complex is being dissolved. The comparative solubility of these complexes in certain of the conventional ionic liquids, $[C_4mim][PF_6]$, $[C_4mim][NTf_2]$ and $[C_4mim][BF_4]$ were also tested by following exactly the same procedure as the above.

The solution of $[Ni(Phen)_2 2Cl]\cdot 5H_2O$ in $[C_1Phen][NTf_2]$ was also characterized using matrix assisted laser desorption spectroscopy, MALDI-MS.

Leaching Test

For the solution of $[Ni(Phen)_2 2Cl]\cdot 5H_2O$ in $[C_1Phen][NTf_2]$ leaching test, the abstraction of the metal ion from complexes by water from the ionic liquid was carried out. 0.5g of the solution was transferred into 25 ml round bottomed flask to which deionized water was filled and stirred at room temperature for 24 hrs. 5ml of the water phase was taken and diluted to 25 ml and the concentration of Ni^{2+} in the water phase was measured using atomic absorption spectroscopy.

Again, 0.5g of the solution was transferred to another 25 ml round bottomed flask which again was filled by deionized water and stirred at 70 ^{0}C in oil bath for 24 hrs. It was allowed to stand to cool. 5 ml of the water phase was taken and diluted to a 25 ml with deionized water and the concentration of Ni^{2+} in the water phase was tested using atomic absorption spectroscopy.

Results

1, 10-Phenanthroline and its complexes showed good solubility in $[C_1Phen][NTf_2]$. In contrast, these compounds are found totally insoluble in $[C_4mim][PF_6]$, $[C_4mim][NTf_2]$ and $[C_4mim][BF_4]$ at the same temperature. The result is summarized in Table 4.1.

Complex/IL	**$[C_1hen][NTf_2]$**	**$[C_4mim][PF_6]$**	**$[C_4mim][NTf_2]$**	**$[C_4mim][BF_4]$**
1, 10-Phenanthroline	>74.0mol%	Insoluble	Insoluble	Insoluble
$[Ni(Phen)_2Cl].5H_2O$	>12.6mol%	"	"	"
$[Co(Phen)_2H_2OCl]Cl$	>8.57mol%	"	"	"
$[Fe(Phen)_22H_2O]2Cl$	>8.34mol%	"	"	"

Table 4. 1: Table of comparative solubilities of 1, 10-Phenanthroline and its complexes in $[C_1phen][NTf_2]$ and $[C_4mim][PF_6]$, $[C_4mim][NTf_2]$ and $[C_4mim][BF_4]$

MALDI-MS of solution of $[Ni(Phen)_22Cl]\cdot5H_2O$ in $[C_1Phen][NTf_2]$ is presented in Figure 4.1.

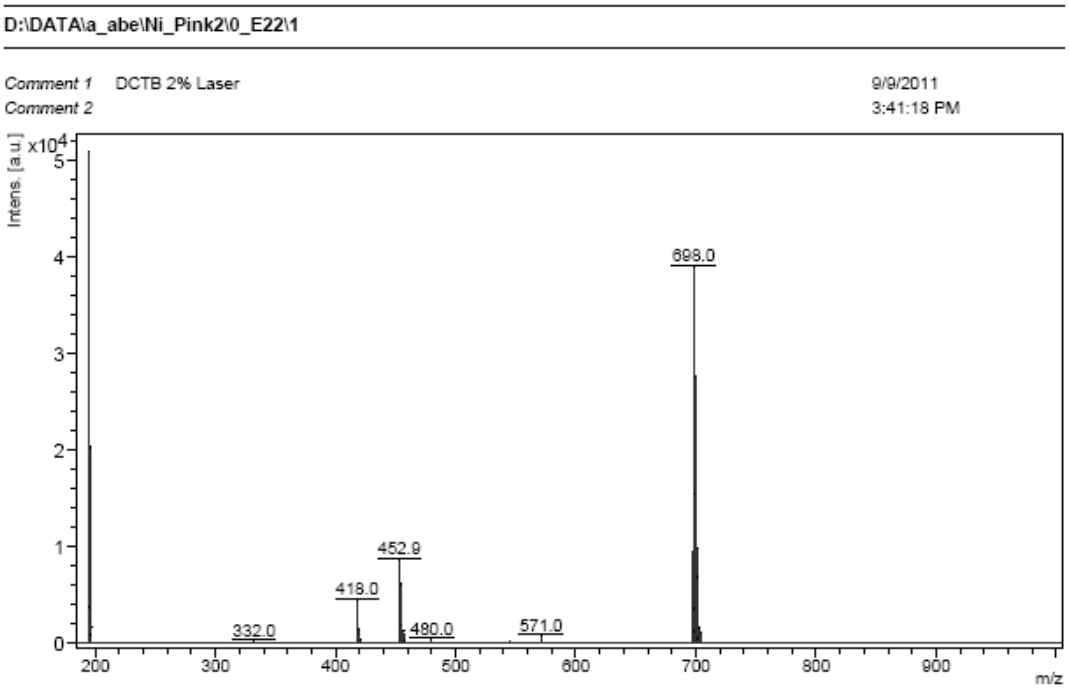

m/z	Rel. Intens.
194.848	100
195.208	7
195.546	2
195.857	40
196.093	0
196.209	1
196.863	3
332.039	0
417.954	9
418.959	2
419.952	3
420.956	0
452.940	17
453.948	3
454.939	12
455.945	2
456.941	2
457.948	0
479.976	0
571.043	1
697.987	76
698.681	2
698.998	30
699.291	1
700.003	54
700.697	1
701.014	19
701.311	0

Figure 4. 1: MALDI-MS of solution of $[Ni(Phen]_2 2Cl].5H_2O$ dissolved in $[C_1phen][NTf_2]$

The m/z assignment of fragments with their intensities in the MALDI-MS of solution of $[Ni(Phen]_2 2Cl].5H_2O$ dissolved in $[C_1phen][NTf_2]$ is given in Table 4.2.

This result is summarized in Table 4.2

Intensity	m/z	Suggested moiety	Theoretical m/z
100	194.848	$[C_1Phen]^+$	195.092
7	195.208		
2	195.546		
40	195.857		
1	196.209		
17	452.940	$[Ni(Phen)_2]Cl$	453.042
3	453.948		
12	454.939		
2	455.945		
2	456.941		
76	697.987	$[Ni(Phen)_2]$ [NTf2]	697.99
2	698.681		
30	698.998		
1	699.291		
54	700.003		
1	701.014		

Table 4. 2: Assigned values in MALDI-MS for $[Ni(Phen)_2]2Cl].5H_2O$ dissolved in $[C_1Phen][NTf_2]$

In Table 4.2, the m/z values around 195 are the ionic liquid finger prints.

4.3 Dissolution of $NiCl_2$ and $Cu(NO_3)_2$ in $[C_4Bipyr][NTf_2]$ and $[(C_4)_2Bipyr][NTf_2]_2$

Experimental

a) In to each of four 25 ml round bottomed flask fitted in oil bath 2g $[C_4Bipyr][NTf_2]$, $[C_4C_1Im][BF_4]$, $[C_4C_1Im][PF_6]$, and $[C_4C_1Im][NTf_2]$ were put. While stirring, $NiCl_2$ was added to each flask very gradually by observing whether the salt is being dissolved. To the flask the solute is found to be soluble, the addition

continued until the solution is changed to honey like viscosity when dissolution stops. Similar procedure was followed using $Cu(NO_3)_2$ as a solute instead of $NiCl_2$.

b) Two 25 ml round bottomed flask were fitted in an oil bath. In to each of the flasks 3g $[(C_4)_2$ Bipyr$][NTf_2]_2$was melted heating to 90- 100 ^{0}C. While stirring, $NiCl_2$ into one of the flasks and $Cu(NO_3)_2$ into the other were added.

The solution of $NiCl_2$ and $Cu(NO_3)_2$ in $[C_4Bipyr][NTf_2]$ was also characterized using matrix assisted laser desorption spectroscopy, MALDI-MS.

Leaching test was carried out stirring the solution of the metal salts in $[C_4Bipyr][NTf_2]$ using water at room temperature.

Results

The solubilities of the salts in each of the ionic liquids is indicated in Table 4.3.

IL	**$NiCl_2$**	**$Cu(NO_3)_2$**
$[C_4C_1Im][BF_4]$	< 0.05 mol %	< 0.05 mol %
$[C_4C_1Im][PF_6]$	< 0.05 mol %	< 0.05 mol %
$[C_4C_1Im][NTf_2]$	< 0.05 mol %	< 0.05 mol %
$[C_4Bipyr][NTf_2]$	> 37.73 mol %	> 20.86 mol %
$[(C_4)_2$ Bipyr$][NTf_2]_2$	< 0.05 mol %	< 0.05 mol %

Table 4. 3: Solubilities of $NiCl_2$ and $Cu(NO_3)_2$ in $[C_4C_1Im][BF_4]$, $C_4C_1Im][PF_6]$, $[C_4C_1Im][NTf_2]$, $[C_4Bipyr][NTf_2]$ and $[(C_4)_2$ Bipyr$][NTf_2]_2$

The MALDI- MS of solution of $NiCl_2$ in $[C_4Bip][NTf_2]$ is shown in Figure 4.2.

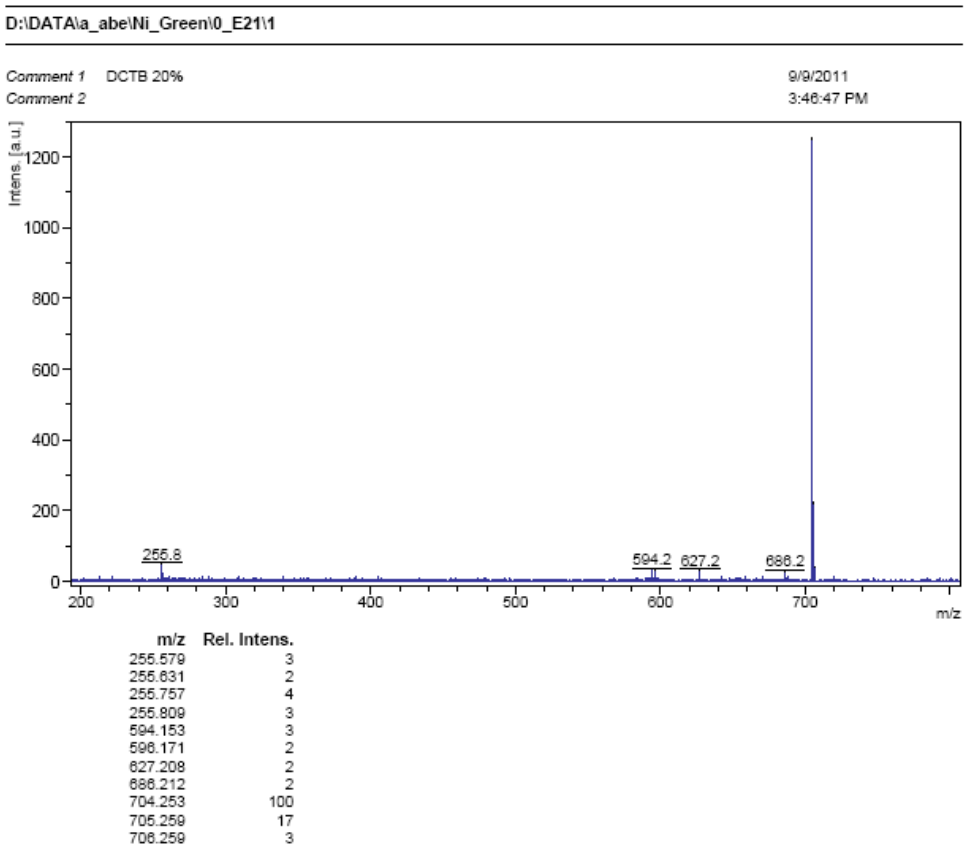

Figure 4. 2: MALDI-MS of $NiCl_2$ solution in $[C_4Bipyr][NTf_2]$

The MALDI-MS spectra are summarized in Table 4.4.

Intensity	**m/z**	**Suggested moiety**	**Theoretical m/z**
100	704.253	$[C_4Bipyr][NTf_2][C_4Bip]$- 2H lost	704.18
3	706.259	[Bipyr]Ni$[C_4Bip][NTf_2]$	706.196
17	705.259	$[C_4Bipyr][NTf_2][C_4Bip]$- 1H lost	705.192
3	594.153	$[C_4Bipyr]_4Ni][NTf_2]$- $3H^+$ & 1H lost	594.197
4	255.757	$[[C_4Bipyr]_2Ni][NTf_2]$-1H added	255.718

Table 4. 4: Summary of assigned value of MALDI-MS spectrum result of solution of $NiCl_2$ in $[C_4Bipyr][NTf_2]$

From the leaching test of solutions of $NiCl_2$ and $Cu(NO_3)_2$ in $[C_4Bipyr][NTf_2]$, the aqueous phase became colored leaving the ionic liquid in a separate phase.

Discussion

It is evident from table 4.1 that the solvent capacity of $[C_1Phen][NTf_2]$ on 1, 10-Phenanthroline and its metal complexes is very high. Especially, the capacity to solubilize a metal complex is exceptionally high because three commonly used ionic liquids based on the imidazolium cation, 1-butyl-3-methylimidazolium bis(trifluoromethylsulfonyl)amide, $[C_1C_4Im][NTf_2]$, tetrafluoroborate, $[C_1C_4Im][BF_4]$, and hexafluorophosphate, $[C_1C_4Im][PF_6]$, were unable to solubilize even small amounts of the tested complexes. The reasons for this enhanced solubility may be explained by the fact that 1, 10-Phenanthroline and the 1, 10-Phenanthrolinium based ionic liquid are totally miscible, whereas the other tested ionic liquids failed to solubilize the 1, 10-Phenanthroline molecule. It is then suggested that the complex is solubilized in the ionic liquid media due to the interaction of the 1, 10-Phenanthroline ligand with the N-methyl-1, 10-Phenanthrolinium cations ("like dissolves like") and not due to the coordination of the ionic liquid with the metal complex. Any new coordination should involve the participation of the non-alkylated nitrogen atom in the cation and this can be ruled out by two observations which suggest that the nonalkylated nitrogen atom is not available for coordination. Firstly, the commented non-reactivity of the N-alkyl-1, 10-Phenanthrolinium cation towards alkylation and secondly, the fact that the chloride salts ($NiCl_2{\cdot}6H_2O$, $FeCl_3{\cdot}6H_2O$ and $CoCl_2{\cdot}6H_2O$), used as the precursors for the synthesis of the $[M(Phen)_2(OH_2)_2]Cl_2$ complexes, with M = Ni, Fe and Co, were found to be insoluble in $[C_1Phen][NTf_2]$ at the reaction conditions required for the synthesis of the metal complexes. The high solubility of 1, 10-Phenanthroline metal complexes facilitates the application of the full range of 1, 10-Phenanthroline based applications in the ionic liquid

media. One of the main uses of 1, 10-Phenanthroline metal complexes is as catalysts [12-15]. An important factor for the application of a solvent–catalyst combination in homogeneous catalyst is the ability of the reaction media to immobilize the catalyst.

The excellent solvation ability of $[C_1Phen][NTf_2]$ towards 1, 10-Phenanthroline and 1, 10-Phenanthroline based metal complexes opens a path for the successful application of 1, 10-Phenanthroline based chemistry in the ionic liquid media. It is expected that applications such as catalysis and nanoparticle synthesis, which have been hindered by the poor solvation abilities towards metallic complexes of commonly used ionic liquids, should find in this media a more successful result. In particular, the successful immobilization of the metal complexes in the ionic liquid media, confirmed by leaching tests, offers a very promising potential for the application of these ionic liquids in homogeneous catalysis. The ionic liquid phase could be used to immobilize the catalyst while another solvent, such as water, could be used to extract the products from the reaction.

MALDI-MS of $[Ni(Phen]_22Cl].5H_2O$ dissolved in $[C_1Phen][NTf_2]$ revealed the complex resides in the ionic liquid dissolved. In this spectrum it is possible to see that $[Ni(Phen)_2]$ is found clustered with $[NTf_2]$ as $[Ni(Phen)_2]$ $[NTf_2]$ as in Figure 4.2a

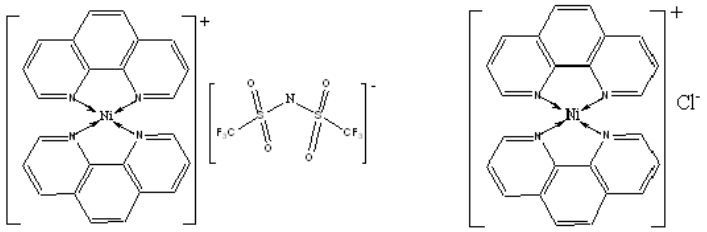

a b

Figure 4. 3: The forms of existence of $[Ni(Phen)_22Cl].5H_2O$ in $[C_1Phen][NTf_2]$

m/z = 698 strongly confirms the complex is dissolved in our ionic liquid. The complex preferred to exist in square planar geometry when dissolved in the ionic liquid. Moreover, the value m/z = 452.94, in the lower portion of the spectrum are representatives of [Ni(Phen)$_2$] clustered with one Cl^- as [Ni(Phen)$_2$]Cl as in Figure 4.2b. This explains the possible interaction of the complex with the solvent to be through π-π interaction. In addition to the electronic advantage by π-π interaction, the acquisition of this geometry by the solute complex is driven by thermodynamic reason in the development of positive entropy [16, 17]. During dissolution, the complex is changed from octahedral to square planar. Consequently, each mole of the complex add two more moles of particles that decreases the Gibbs free energy.

The complexes are highly soluble in water and the ionic liquid is hydrophobic. However, the leaching test on the N-Alkyl-1, 10-Phenanthrolinium cation based system reveals that the complexes strongly prefer to exist in the IL rather than going to water. This phenomenon supports the above speculation that the solubility of the complexes in the ionic liquid takes place via π-π interaction. This achievement is a good opportunity in developing biphasic processes such as separation and supported ionic liquid phase (SILP) catalysis using this novel IL with recyclability [18]. SILP is a system of catalysis in which usually expensive catalysts are dissolved (homogenized) in ILs and this solution is dispersed as thin physisorbed film on the large internal surface area of a porous solid material without the catalyst being covalently linked to the solvent so that its catalytic activity and selectivity is retained intact. Since the thickness of the ionic liquid is within the nanometer range, diffusion problems are minimized by the extremely small diffusion distances [19]. Excellent IL utilization is achieved; that is, the same catalytic performance

can be achieved with a much smaller total amount compared to liquid-liquid biphasic system [20]. The resulting catalyst behaves similar to those found under homogeneous reaction conditions due to the solvation of the metal complex by the ILs with the reaction taking place in thin liquid film in the one hand and heterogeneous systems in that the reactions take place in biphasic process [18-20]. This catalysis method is, therefore, one that combined the advantages of both homogeneous and heterogeneous catalysis together that makes it advanced and more efficient than either of the two. Important features of biphasic systems using ILs as compared to other aqueous-organic biphasic catalysis are their much better dissolving ability of most organic substrates and their compatibility to certain ligands which readily decomposes in water. The need to employ SILP concept emerged from the desire to overcome certain drawbacks of the biphasic ionic liquid systems which are the relatively high amounts of expensive IL that are required and its intrinsically high viscosity, which leads to slow mass transport between the two liquid phases.

Because 1, 10-Phenanthroline is the precursor of $[C_1Phen][NTf_2]$, the possibility of dissolution of the former in the latter was nearly certain. The success in the dissolving ability of 1, 10-Phenanthroline as speculated at the start of this project is also believed to open a new gate of improvement in certain catalytic reaction processes by the enhancement of the catalytic efficiency of certain catalysts by prevention of the agglomeration of the catalyst so as to retain its catalytically active surface area as large as possible. This is achieved by using coordinating molecules such as 1, 10-Phenanthroline without affecting the catalytic behavior and specialty of the catalyst [4]. In this regard, one of the objectives of this project was met.

From Table 4.4, it is evident that $NiCl_2$ and $Cu(NO_3)_2$ are highly soluble in $[C_4Bipyr][NTf_2]$ far more than the common ionic liquids used here for comparison and the dialkylated form, $[(C_4)_2$ Bipyr] $[NTf_2]_2$. The reason for this could be the availability of a Lewis basic nitrogen in the cation of $[C_4Bipyr][NTf_2]$. Since the free nitrogen coordinates with the metal ions of the salts, the dissolution takes place easily [21-25]. However, such coordinating component does not exist either in the cation or the anions of common ionic liquids or in $[(C_4)_2$ Bipyr] $[NTf_2]_2$that impedes the solubility of the salts.

From MALDI-MS (Figure 4.2) m/z = 594.153 could be assigned for $[C_4Bipyr]_4Ni][NTf_2]$ losing $3H^+$ & 1H. This is a strong support for the argument that $NiCl_2$ has been dissolved in $[C_4Bipyr][NTf_2]$.

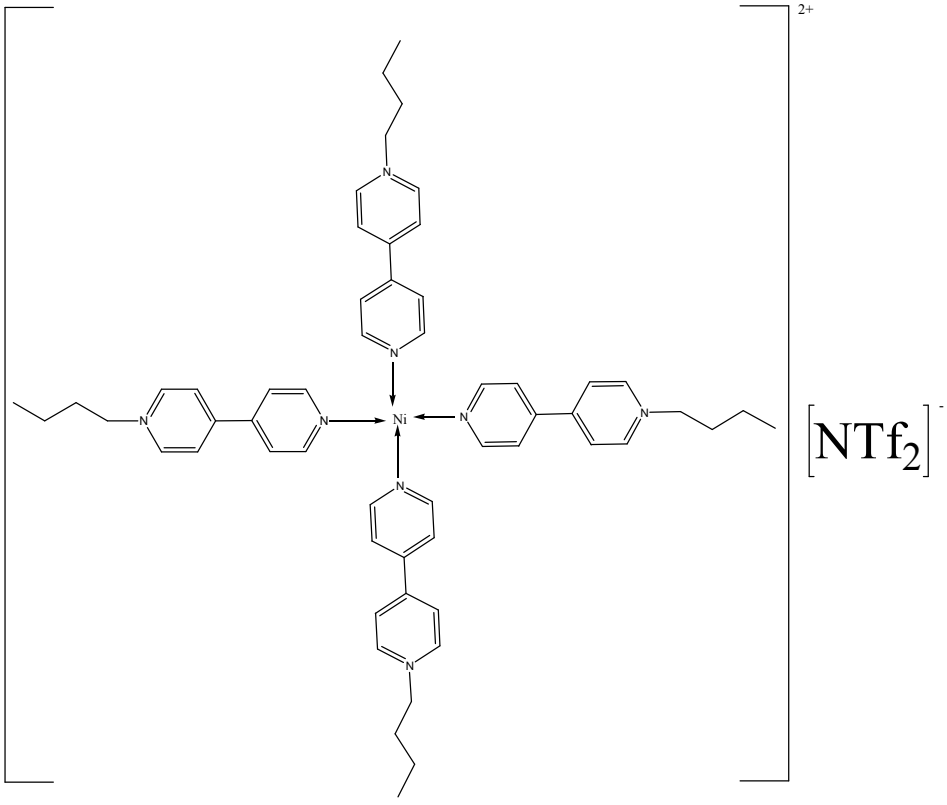

Figure 4. 4: The structure of the complex of Ni^{2+} with cation of the ionic liquid

Regarding the leaching test, when the metal salt solution in $[C_4Bipyr][NTf_2]$ is added to water the salt is found to go completely to the latter solvent leaving the ionic liquid in a separate phase. This was evident from the appearance of the characteristic color of the salts in the aqueous phase. Because the metal centre is already rich in positive charge, the approach of neutral molecules like water, take the advantage to take away the metal ions from the positively charged cation of the IL. This property, we believe, is a good opportunity in applications such as electrochemistry and catalytic reactions. Since lose (weak) coordination of the ionic liquid with the metal ions of the salt gives opportunity to be reduced very easily. Similarly, this same phenomenon is crucial property in catalysis in that it avoids lose of activity and selectivity of the catalyst [26-28].

Conclusion

In conclusion, we have succeeded in synthesizing new ionic liquids that can solubilize molecules like 1, 10-Phenanthroline and its complexes as well as metal salts and demonstrated that high concentrations can be obtained by directly dissolving the complexes or the salt. Concerning the N-alkyl-1, 10-Phenanthrolinium based system we anticipated that it is due to the existence of similar moieties in the ionic liquid and the complexes as well as π-π interaction. Because of these two factors, the complexes strongly preferred to exist in the ionic liquid when extraction with water is attempted which opened a new gate for biphasic processes such as liquid-liquid separation and SILP with recyclability.

Regarding the N-alkyl-4, 4'-Bipyridinium system, the existence of the Lewis basic nitrogen on the cation make them capable of coordinating to the metal ions of metal salts so that easy dissolution of metal salts is possible. This argument is supported by the

unability of the common imidazolium based ILs and dialkylated N, N'-Dibutyl-4, 4'-Bipyridinium Bis(trifluoromethylsulphonyl)amide to dissolve the same metal salt solutes.

References

1. C . J. Adams, M. J. Earle, K. R. Seddon, *Green Chem*. 2000, 2, 21 – 23.
2. J . G. Huddleston, A. E. Visser, W. M. Reichert, H. D. Willauer, G. A. Broker, R. D. Rogers, *Green Chem*. 2001, **3**, 156 – 164.
3. P. Hapiot, C. Lagrost, *Chem. Rev.* 2008, **108**, 2238-2264.
4. V. I. Pârvulescu, C. Hardacre; *Chem. Rev*. 2007**, 107**, 2615-2665.
5. J.D. Holbrey, I. Lopez-Martin, G. Rothenberg, K.R. Seddon, G. Silvero, X. Zheng, *Green Chem*., 2008, **10**, 87–92.
6. H. Ohno, *Physical properties of ionic liquids for electrochemical applications*, in: F. Endres, D. MacFarlane, A. Abbott (Eds.), *Electrodeposition from Ionic Liquids*, Wiley- VCH Weinheim, 2008, pp. 47–83.
7. A. E. Visser, R. P. Swatloski, W. M. Reichert, R. Mayton, S. Sheff, A. Wierzbicki, J. H. Davis, R. D. Rogers, *Chem. Commun*. 2001,135 – 136.
8. Z.F. Fei, T.J. Geldbach, D.B. Zhao, P.J. Dyson, *Chem. Eur. J.,* 2006, **12**, 2123–2130.
9. J.H. Davis, *Chem. Lett*., 2004, **33**, 1072–1077.
10. S.G. Lee, *Chem. Commun*., 2006, 1049–1063.
11. S. Arounaguiri, D. Easwaramoorthy, A. Ashokkumar, A. Dattagupta,, B Gmmaiya; *Chem. Sci.*, 2000, **112**, 1–17
12. E. Schoffers, , *Eur. J. Org. Chem*. 2003, 1145–1152.
13. S.A. Prikhod'ko, N.Y. Adonin, V.N. Parmon, *Tetrahedron Lett*., 2010, **51,** 2265–2268.
14. F. Shi, J.J. Peng, Y.Q. Deng, *J. Catal*., 2003, **219**, 372–375.

15. F. Shi, Y.D. He, D.M. Li, Y.B. Ma, Q.H. Zhang, Y.Q. Deng, *J. Mol. Catal. A-Chem*., 2006, **244**, 64–67.

16. I. Krossing, J. M. Slattery, C. Daguenet, P. J. Dyson, A. Oleinikova and H. Weingartner, *J. Am. Chem. Soc.*, 2006, **128**, 13427-13434.

17. I. Krossing, J. M. Slattery, C. Daguenet, P. J. Dyson, A. Oleinikova and H. Weingärtner, *J. Am. Chem. Soc.*, 2007, **129**, 11296-11296.

18. M. Jakuttis, A. Schonweiz, S. Werner, R. Franke, K. D. Wiese, M. Haumann, P. Wasserscheid; Angew. *Chem. Int. Ed*. 2011, **50**, 4492 –4495.

19. P. Goodrich, C. Hardacre, C. Paun, A. Ribeiro, S. Kennedy, M. J. V. LourenÅo, H. Manyar, C. A. Nieto de Castro, M. Besnea, V. I. P_rvulescuc; *Adv. Synth. Catal*. 2011, **353**, 995 – 1004

20. E. Öchsnera, M. J. Schneider, C. Meyera, M. Haumann, P. Wasserscheid, *Applied Catalysis A: General*, 2011, **399**, 35-41.

21. C. Chiape, M. Malvaldi, B. Melai, S. Fantini, U. Bardi, S. Caporali, *Green. Chem*.,2010, **12**, 77-80.

22. L. C. Branco, J. N. Rosa, J. J. M. Ramos, C. A. M. Afonso, *Chem.-Eur. J*., 2002, **8**, 3671-3677.

23. F. Endres, S. Z. El Abedin A. Y. Saad, E. M. Moustefa, N. Borissenko, W. E. Price, G. G. Wallace, D. R MacFarlane, P. J. Newman, A. Bund, *Phys. Chem. Chem. Phys*., 2008, **10**(16), 2189-2199.

24. A. E. Visser, R. P. Swatloski, W. M. Reichert, S. T. Griffin, R. D.Rogers, *Ind. Eng. Chem. Res.*, 2000, **39**, 3596–3604.

25. A. E. Visser, R. P. Swatloski, W. M. Reichert, R. Rojers, *Environ. Sci. Technol*., 2002, **36**, 2523-2529.

26. M. Jakuttis, A. Schonweiz, S. Werner, R. Franke, K.D. Wiese, M. Haumann, P. Wasserscheid; *Angew. Chem. Int. Ed*. 2011, 50, 4492 –4495

27. P. Goodrich, C. Hardacre, C. Paun, A. Ribeiro, S. Kennedy, M. J. V. LourenÅo, H. Manyar, C. A. Nieto de Castro, M. Besnea, V. I. P_rvulescu; *Adv. Synth. Catal*. 2011, **353**, 995 – 1004

28. E. Öchsnera, M. J. Schneidera, C. Meyer, M. Haumann, P. Wasserscheid, *Applied Catalysis A: General*, 2011, **399**, 35-41.

Appendices

Appendix 1

A1 NMR spectra for Chapter 2

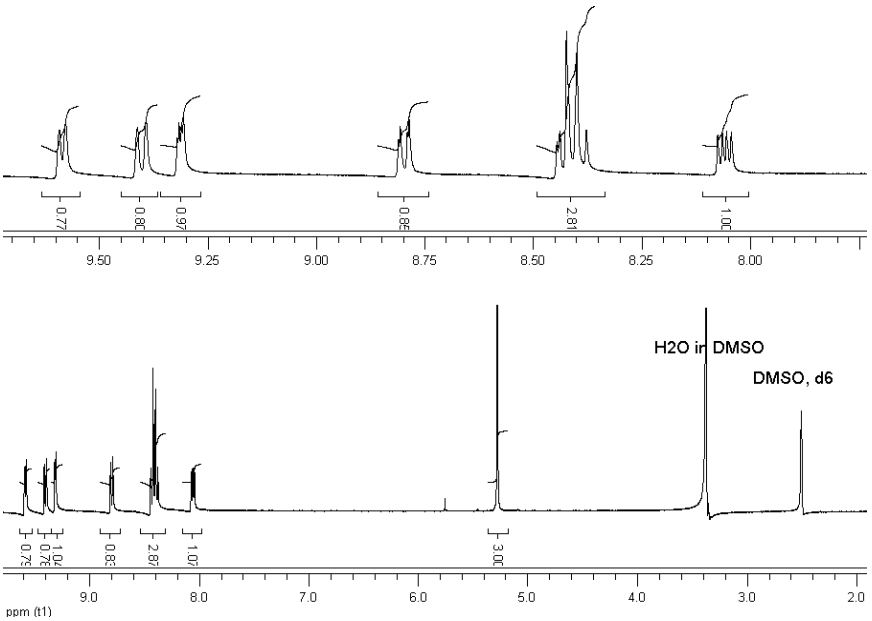

^{1}H NMR of [C_1Phen]I

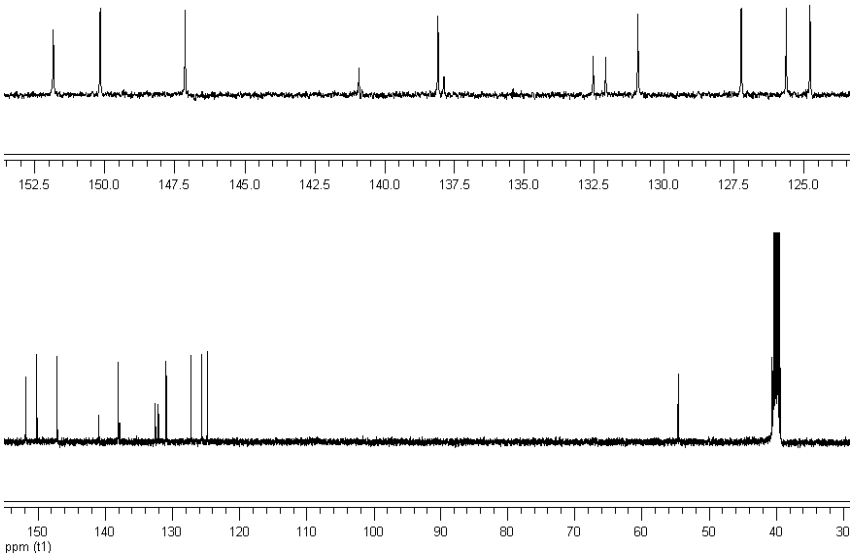

^{13}C NMR of [C_1Phen]I

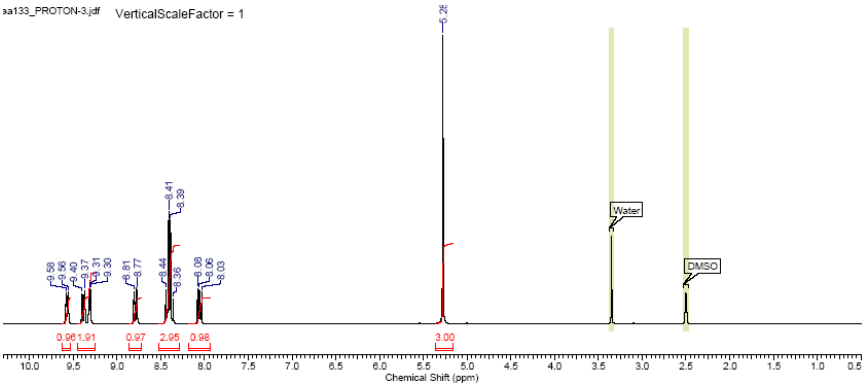

^{1}H NMR of [C_1Phen][NTf_2]

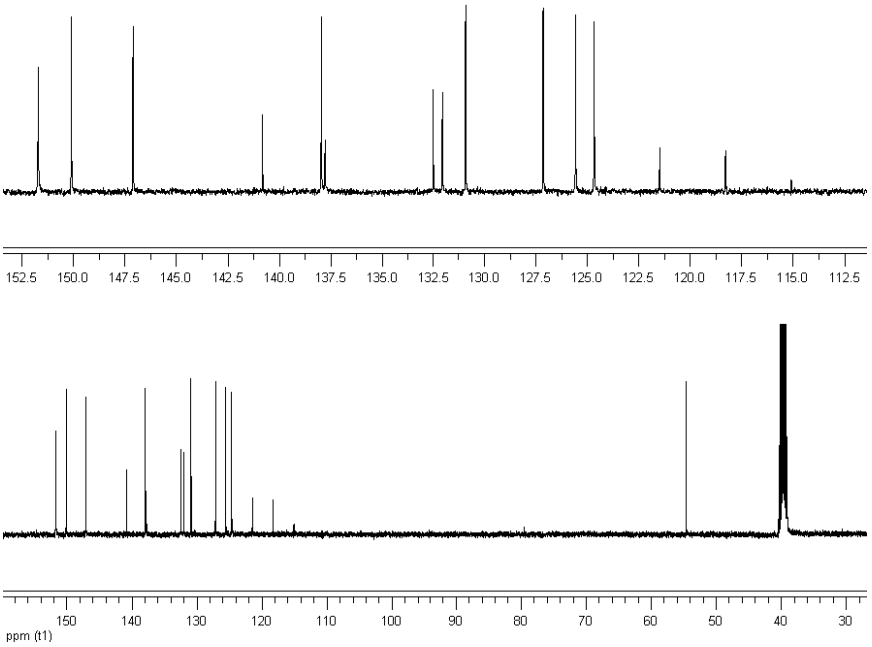

^{13}C NMR of [C_1Phen][NTf_2]

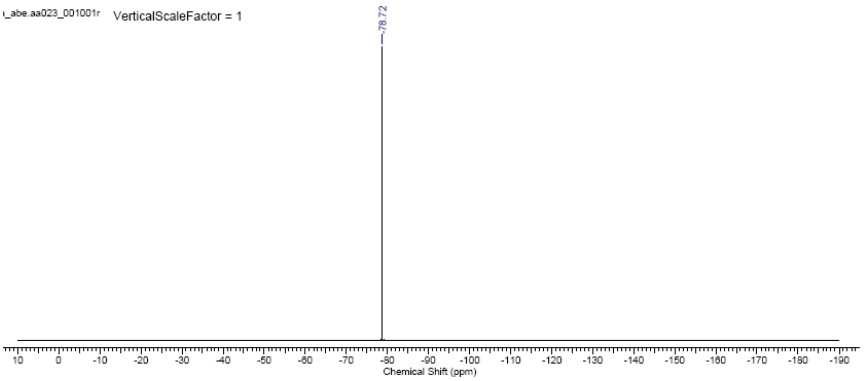

^{19}F NMR of $[C_1Phen]$ $[NTf_2]$

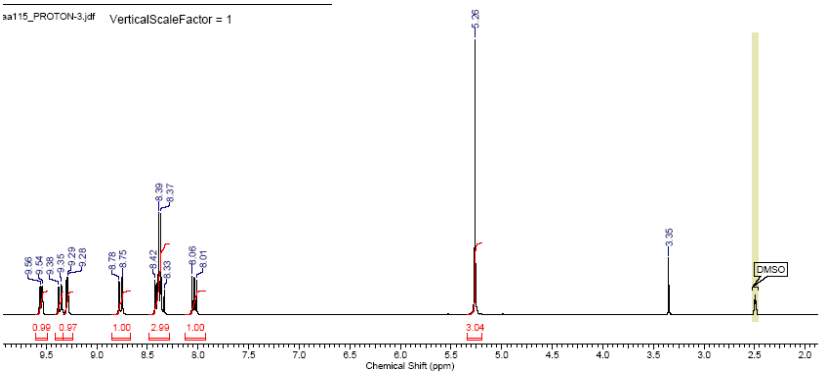

^{1}H NMR of $[C_1Phen][PF_6]$

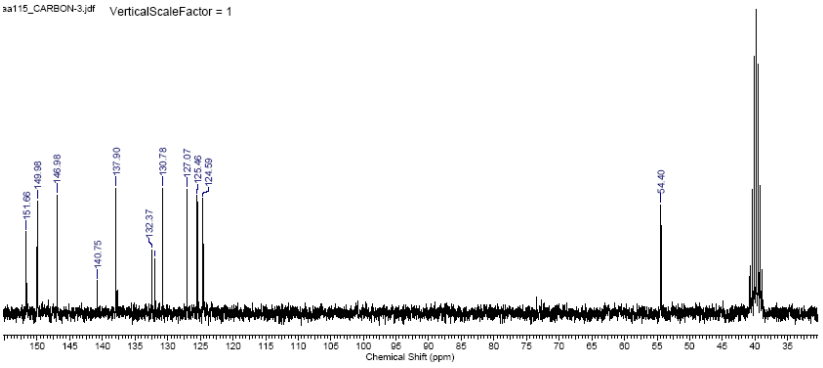

^{13}C NMR of $[C_1Phen][PF_6]$

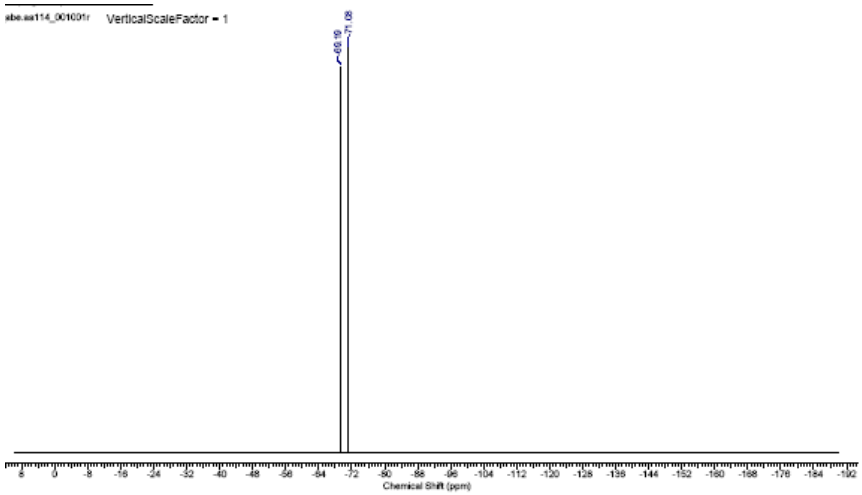

^{19}F NMR of $[C_1Phen][PF_6]$

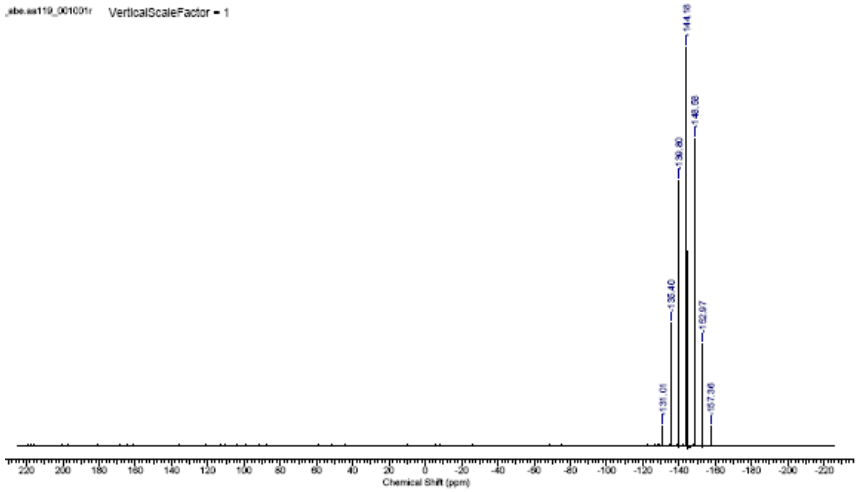

^{31}P NMR of $[C_1Phen][PF_6]$

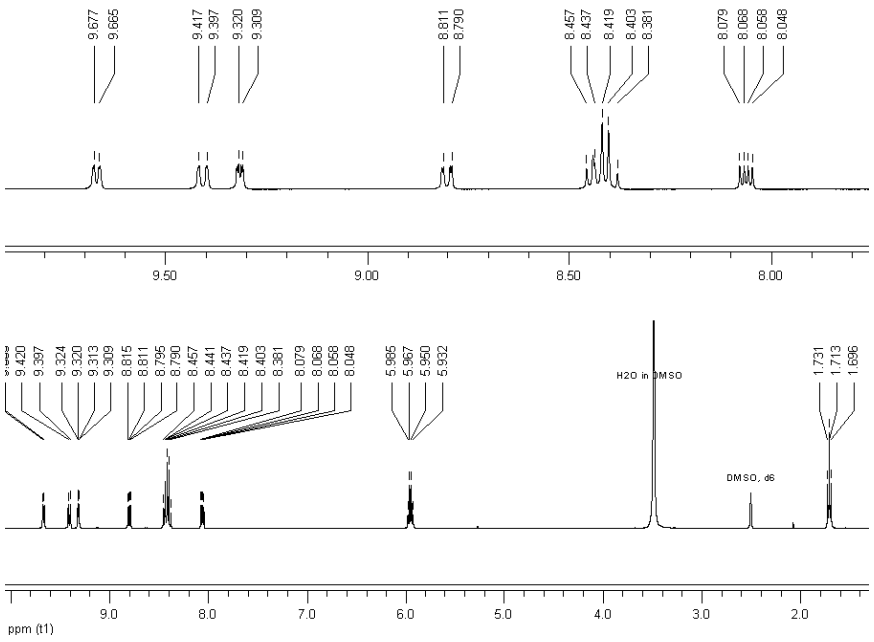

^{1}H NMR of [C_2Phen]I

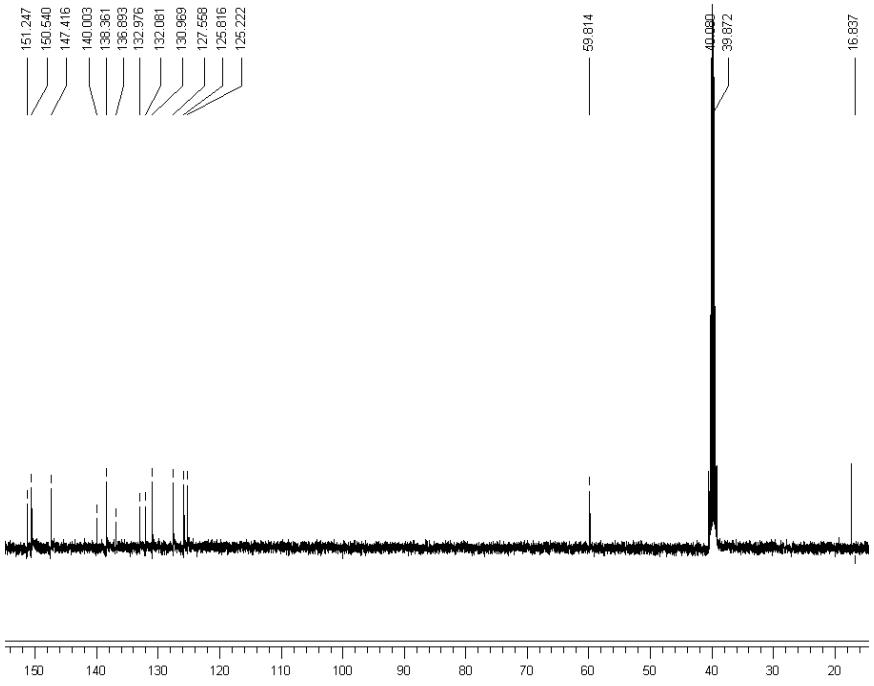

^{13}C NMR of [C_2Phen]I

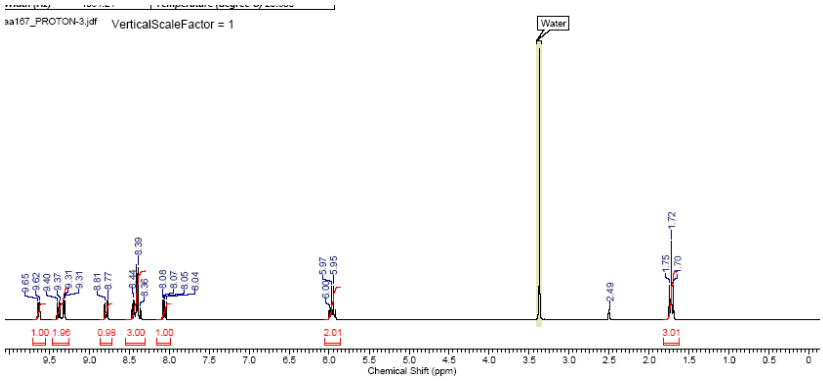

^{1}H NMR of [C_2Phen][NTf_2]

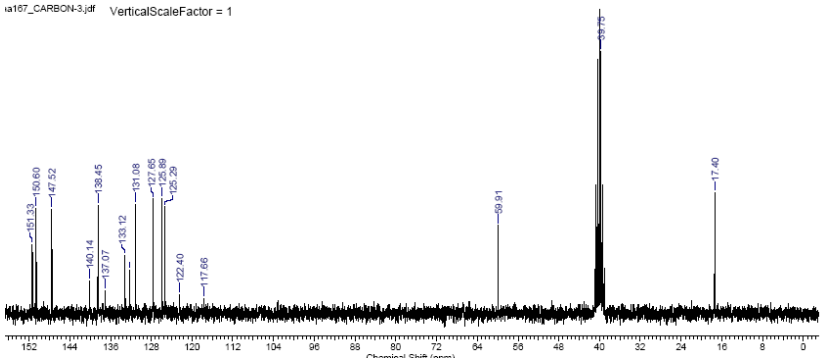

^{13}C NMR of [C_2Phen][NTf_2]

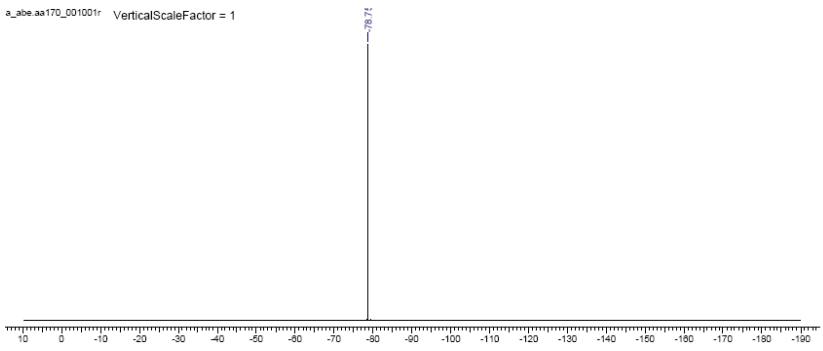

^{19}F NMR of [C_2Phen][NTf_2]

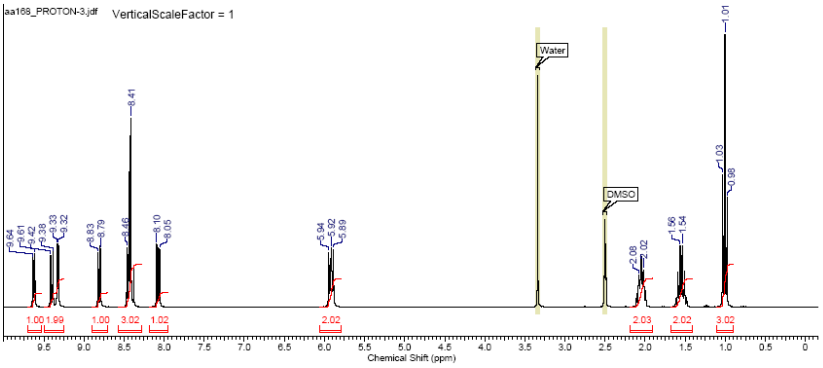

^{1}H NMR of [C_4Phen][NTf_2]

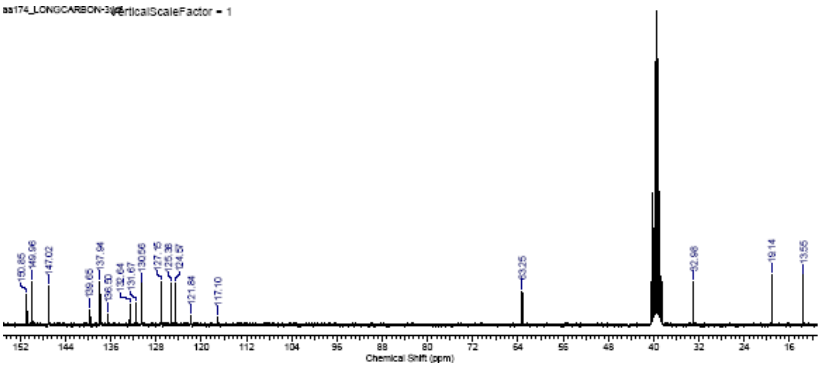

^{13}C NMR of [C_4Phen][NTf_2]

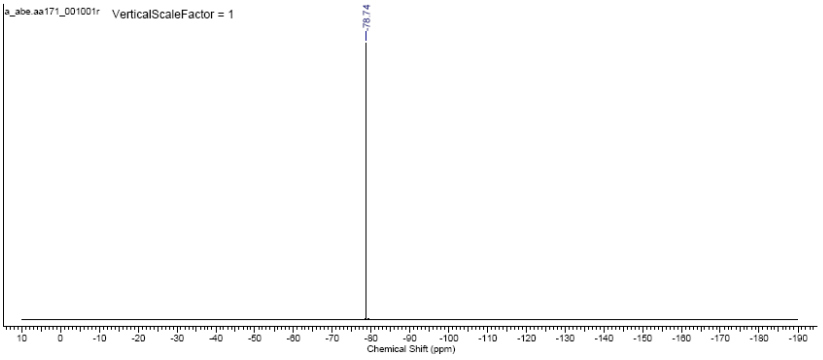

^{19}F NMR of [C_4Phen][NTf_2]

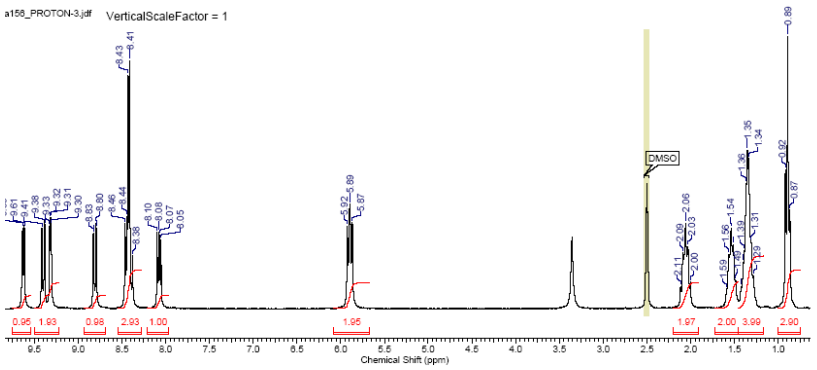

^{1}H NMR of [C_6Phen][NTf_2]

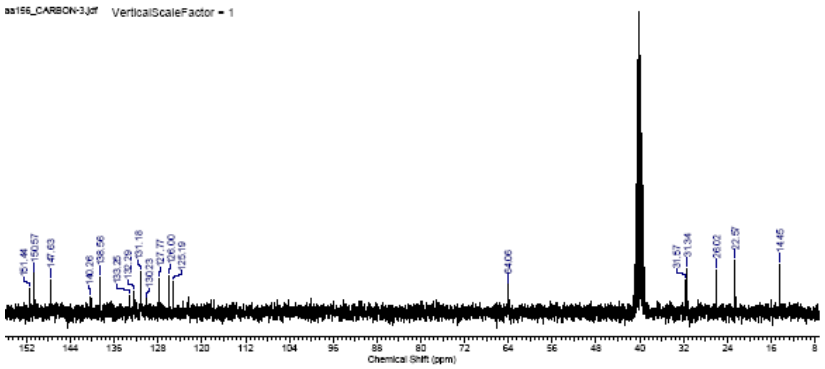

^{13}C NMR of [C_6phen][NTf_2]

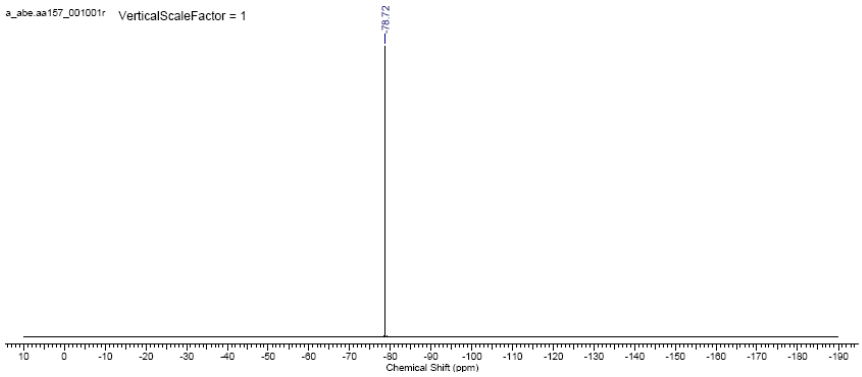

^{19}F NMR of [C_6Phen][NTf_2]

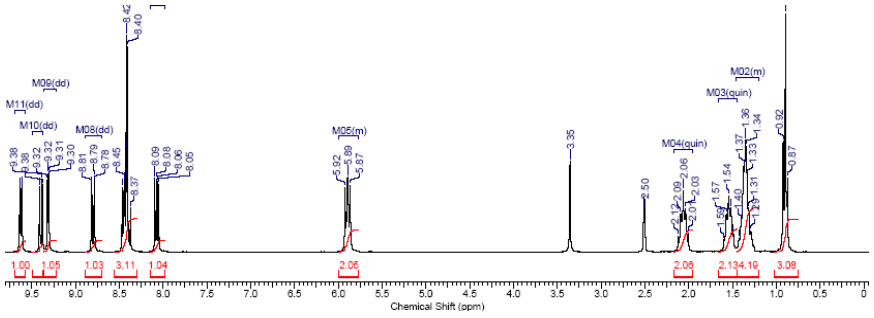

^{1}H NMR of [C_6Phen][PF_6]

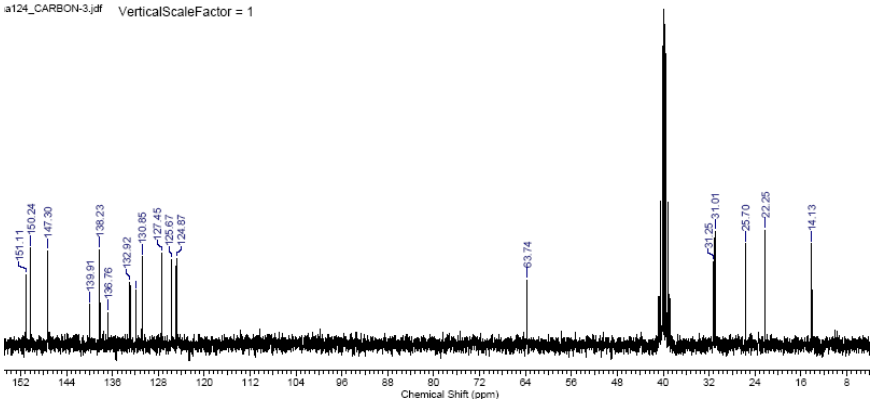

^{13}C NMR of [C_6Phen][PF_6]

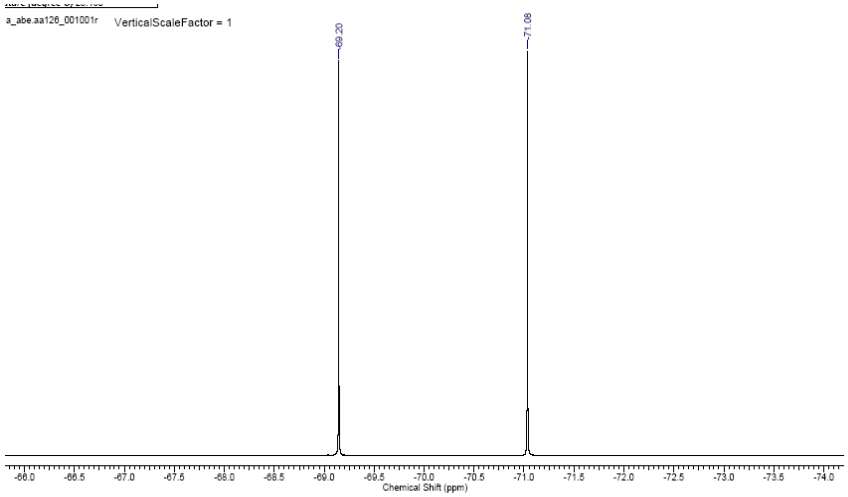

^{19}F NMR of [C_6Phen][PF_6]

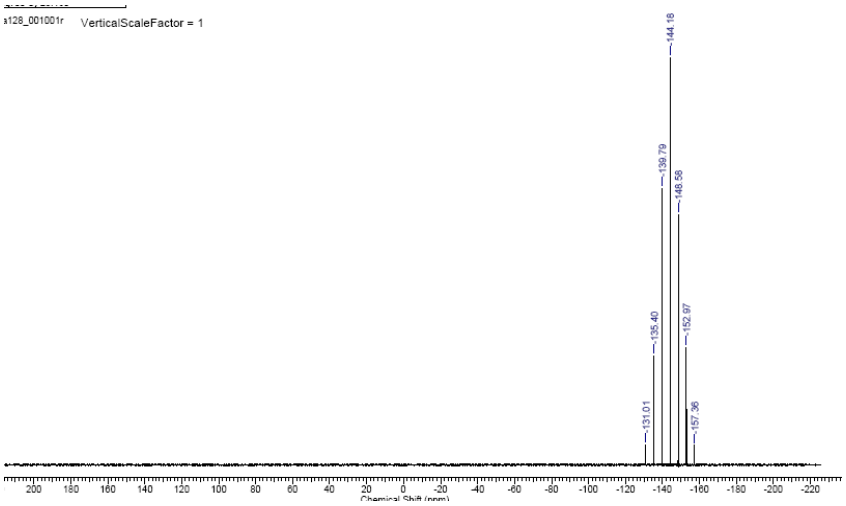

^{31}P NMR of $[C_6Phen][PF_6]$

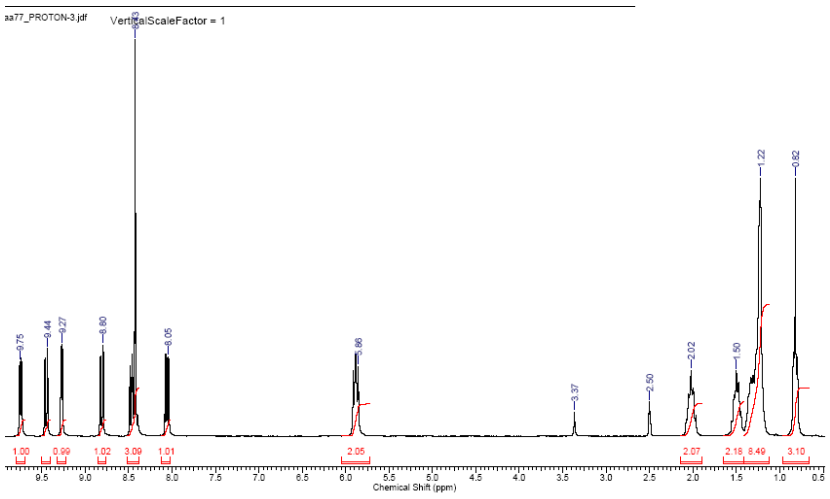

^{1}H NMR of $[C_8Phen]Br$

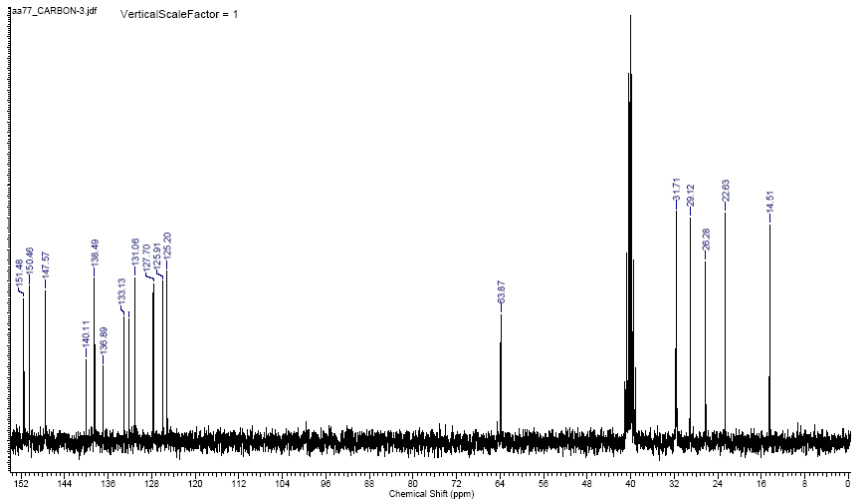

^{13}C NMR of $[C_8Phen]Br$

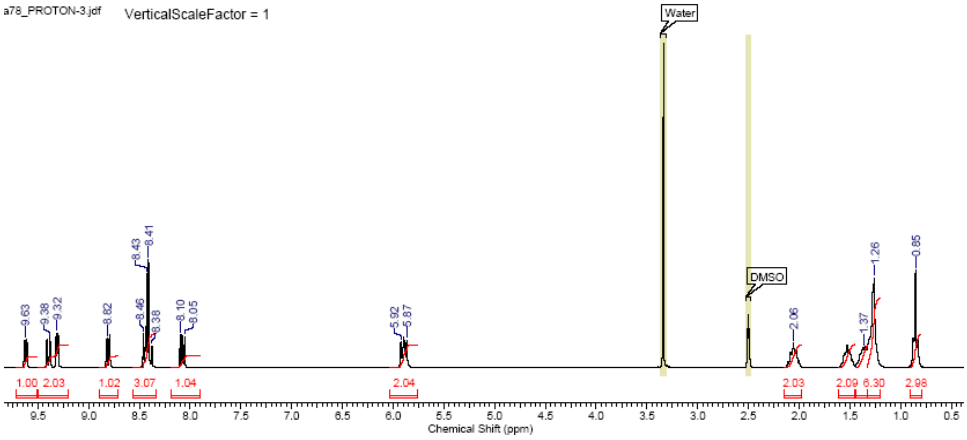

^{1}H NMR of $[C_8Phen][NTf_2]$

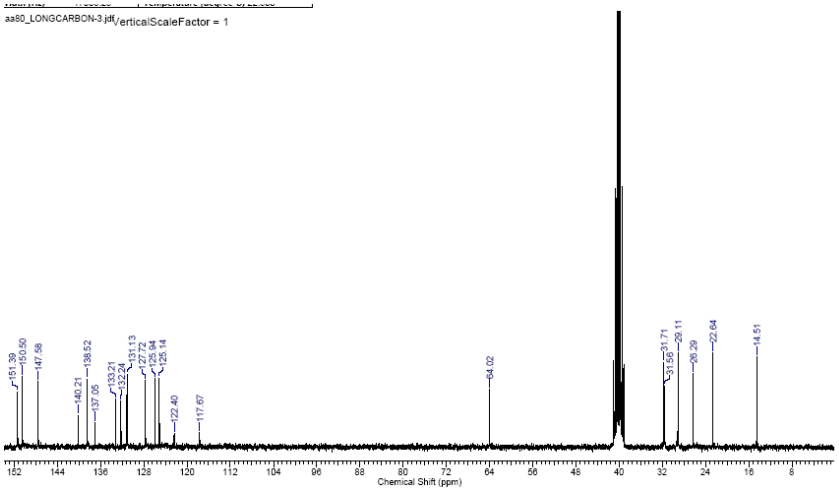

^{13}C NMR of [C_8Phen][NTf_2]

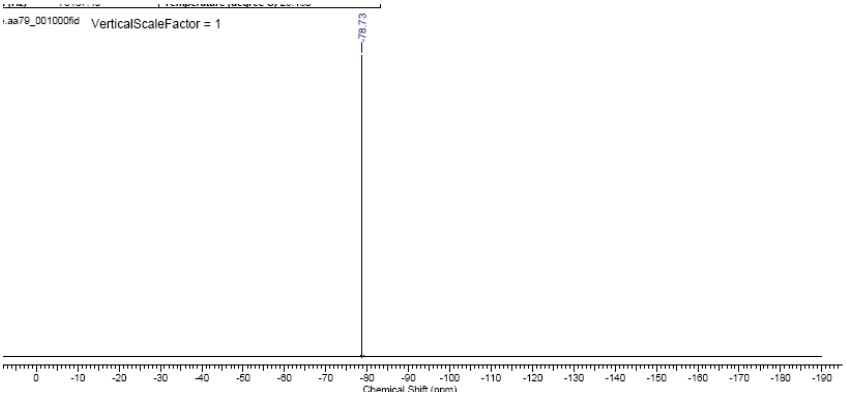

^{19}F NMR of [C_8Phen][NTf_2]

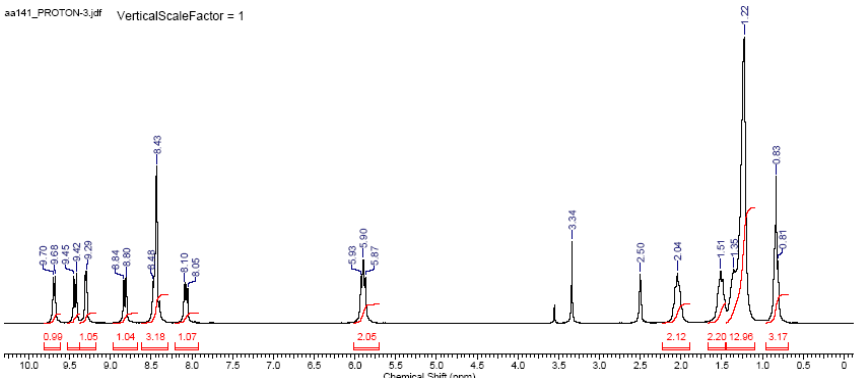

^{1}H NMR of [C_{10}Phen]Br

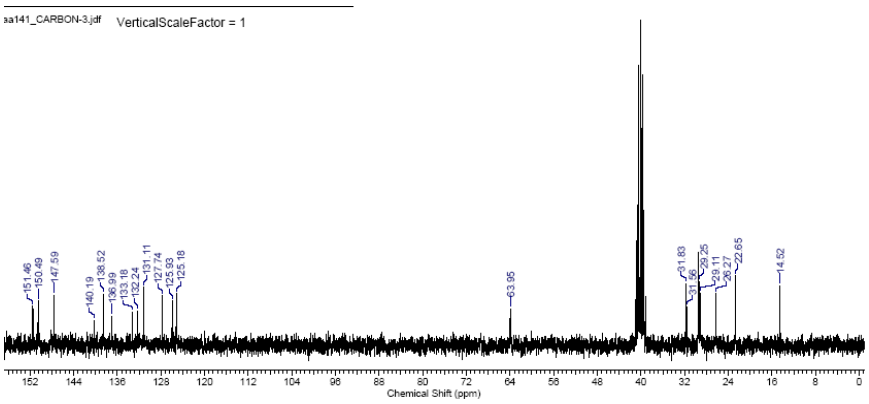

^{13}C NMR of $[C_{10}Phen]Br$

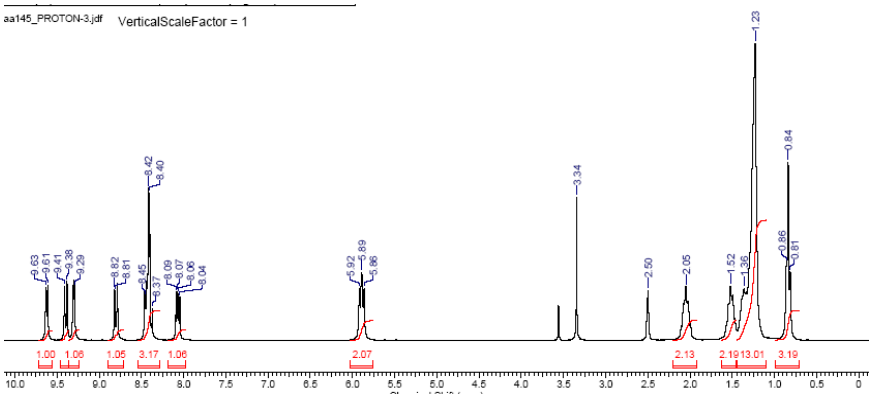

^{1}H NMR of $[C_{10}Phen][NTf_2]$

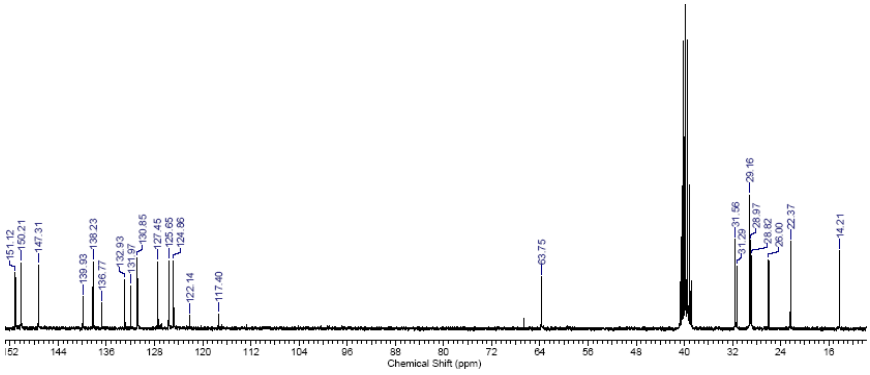

^{13}C NMR of $[C_{10}Phen][NTf_2]$

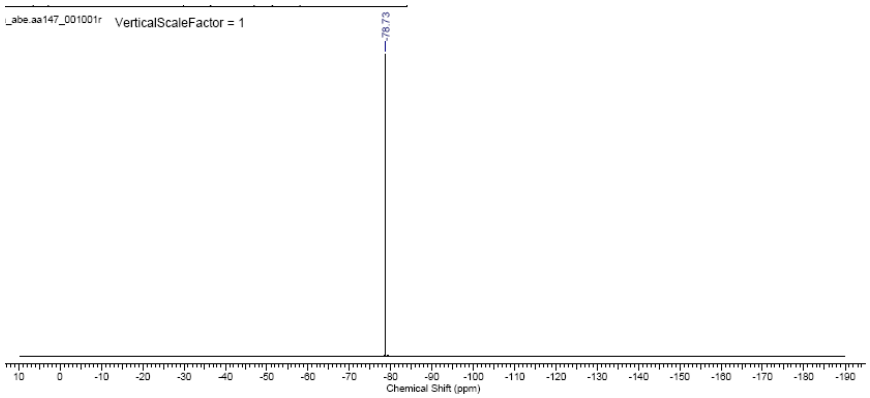

^{19}F NMR of $[C_{10}Phen][NTf_2]$

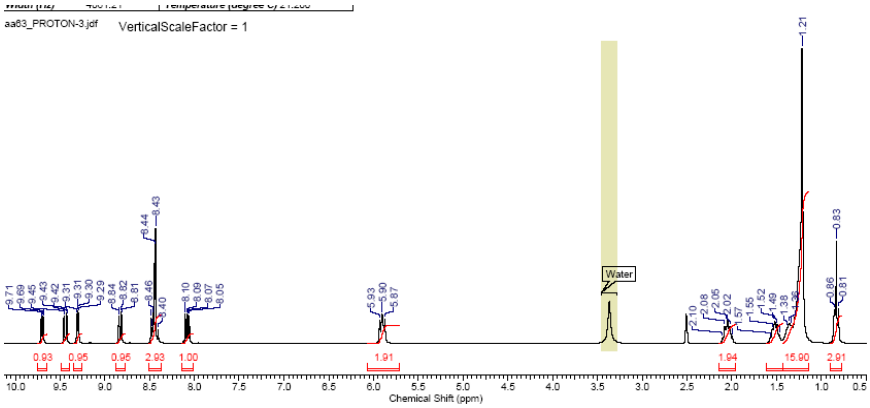

^{1}H NMR of $[C_{12}Phen]Br$

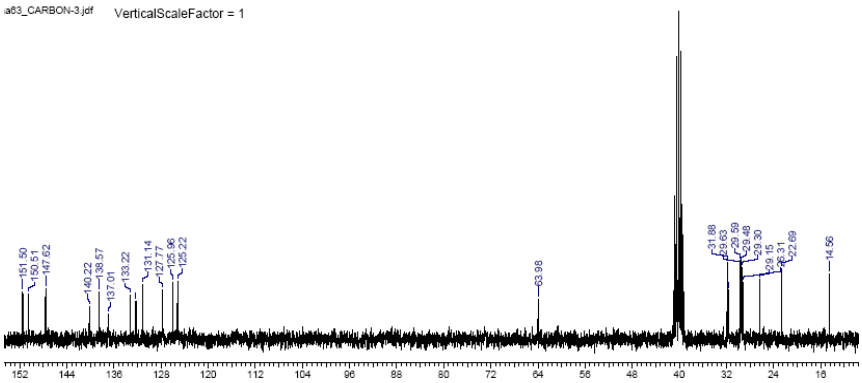

^{13}C NMR of $[C_{12}Phen]Br$

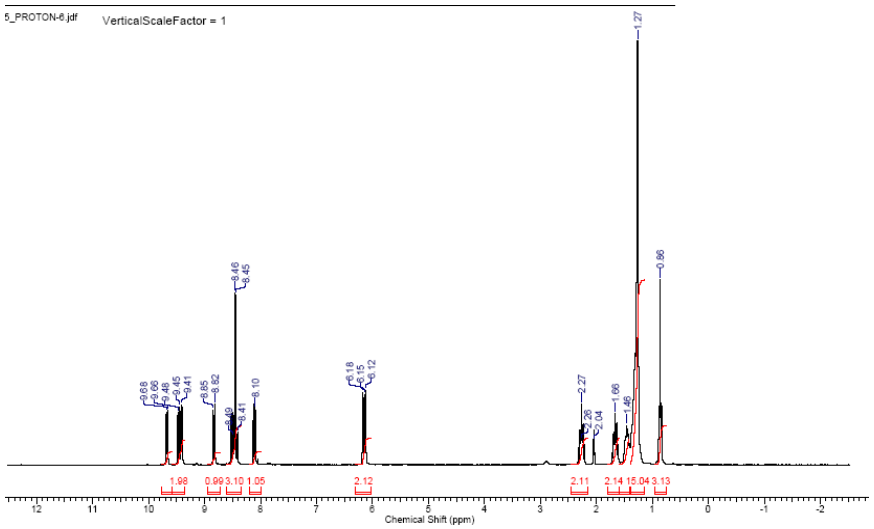

^{1}H NMR of [C_{12}Phen][NTf_2]

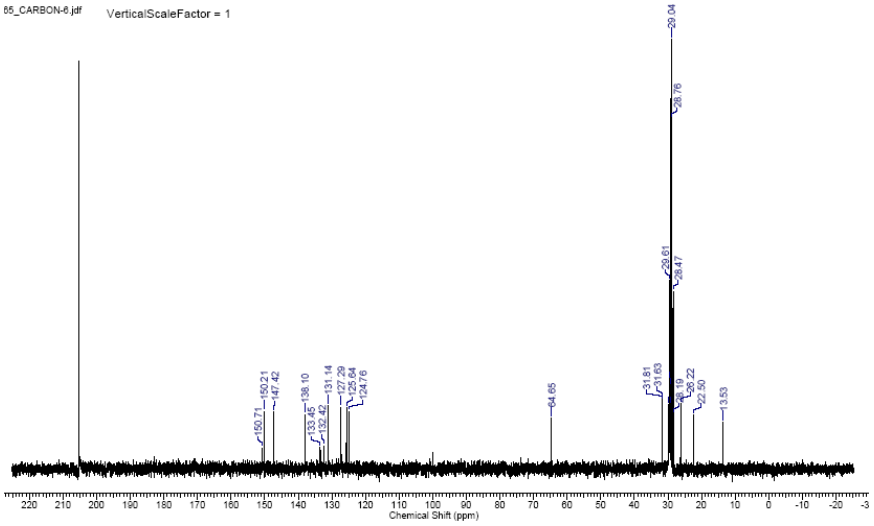

^{13}C NMR of [C_{12}Phen][NTf_2]

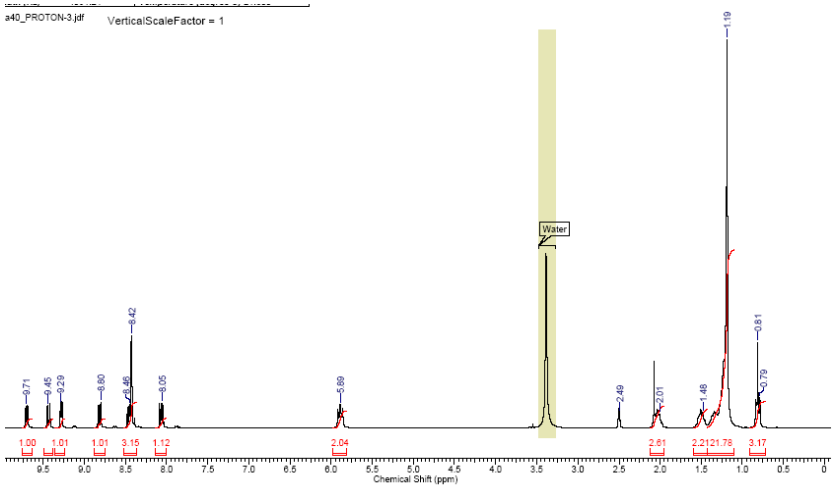

^{1}H NMR of [C_{14}Phen][NTf_2]

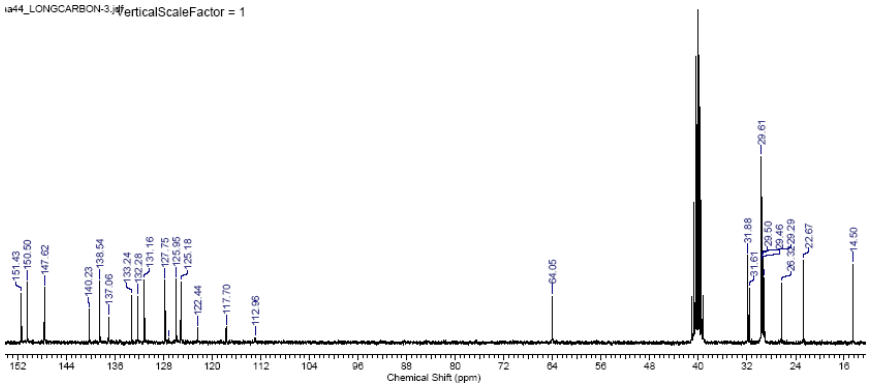

^{13}C NMR of [C_{14}Phen][NTf_2]

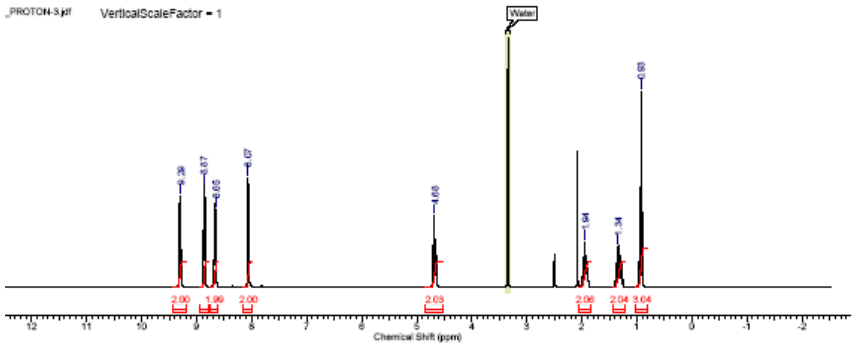

^{1}H NMR of [C_4Bipyr]Br

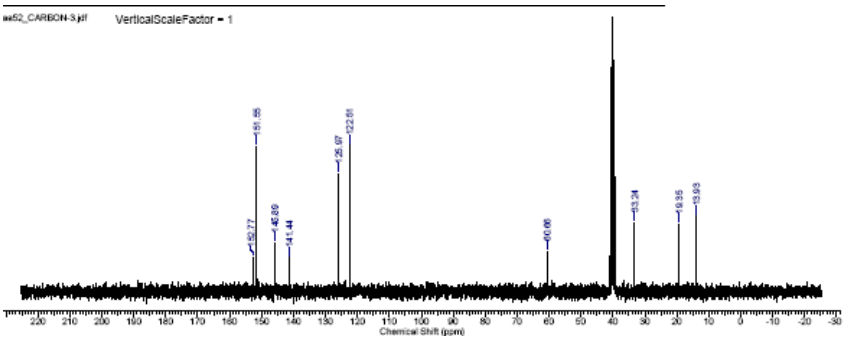

^{13}C NMR of [C_4Bipyr]Br

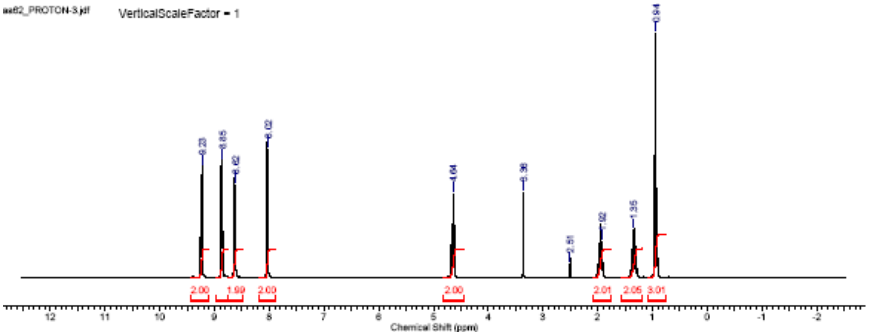

^{1}H NMR of [C_4Bipyr][NTf_2]

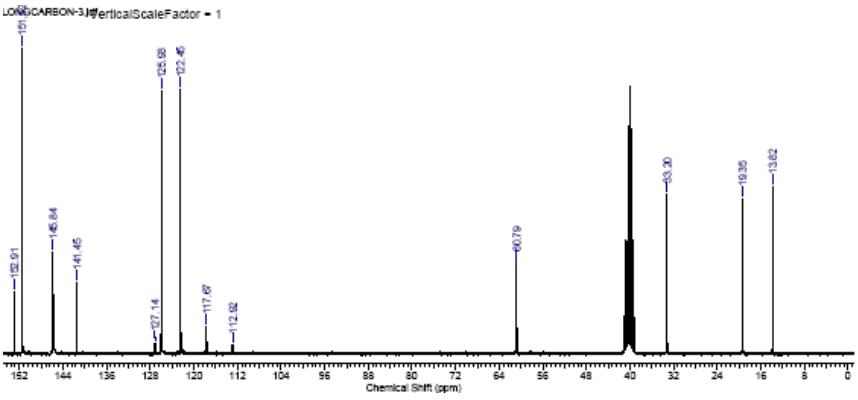

^{13}C NMR of [C_4Bipyr][NTf_2]

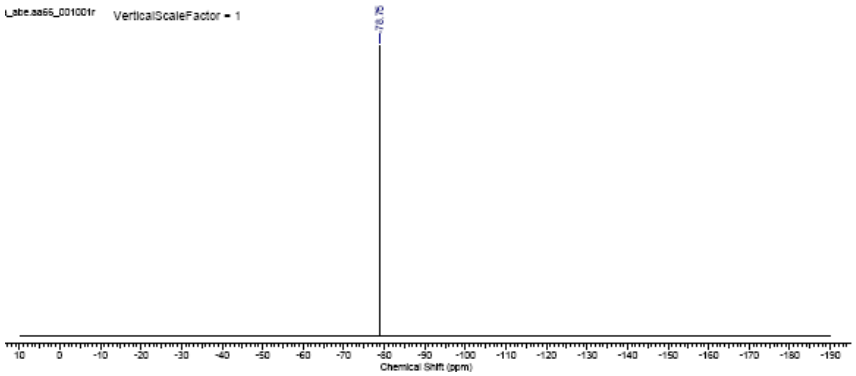

^{19}F NMR of $[C_4Bipyr][NTf_2]$

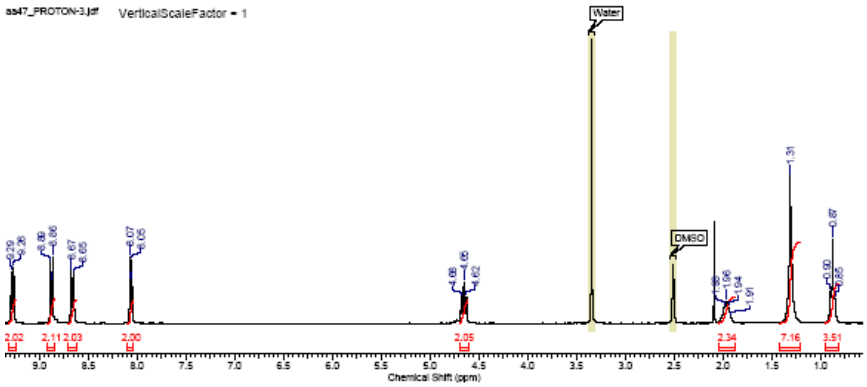

^{1}H NMR of $[C_6Bipyr]Br$

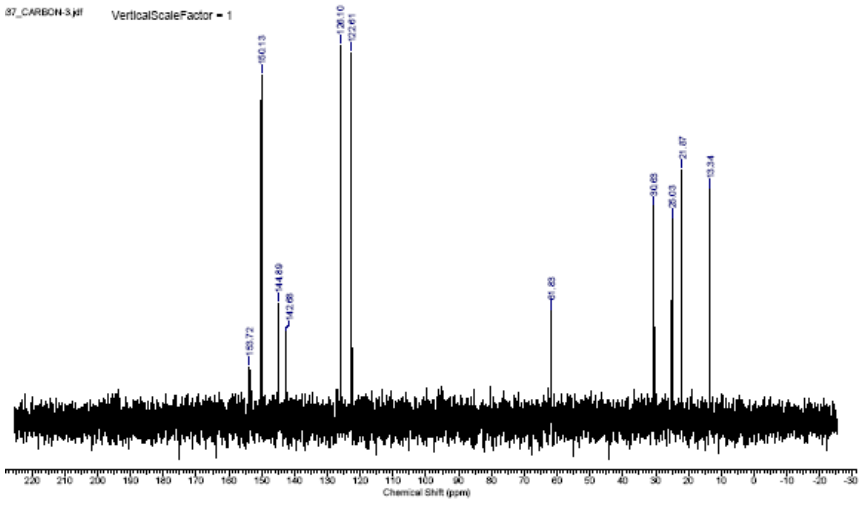

^{13}C NMR of $[C_6Bipyr]Br$

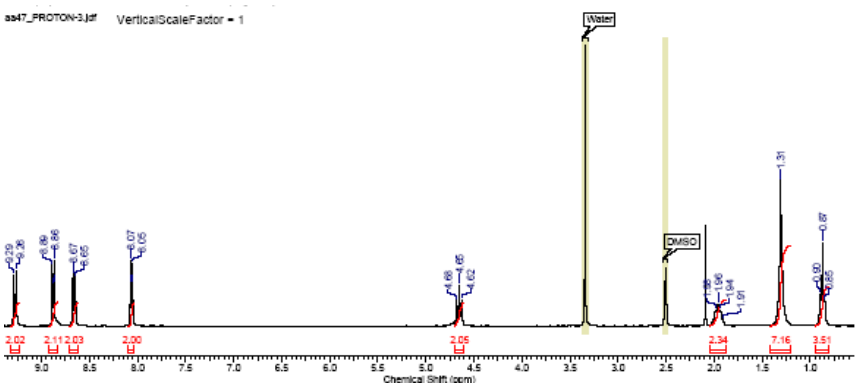

^{1}H NMR of [C_6Bipyr][NTf_2]

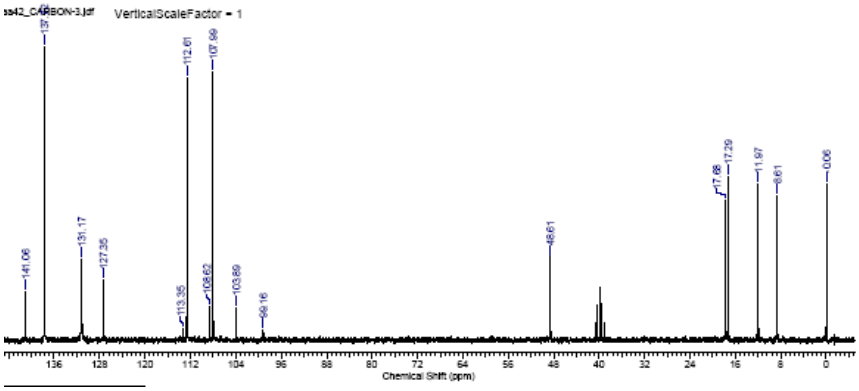

^{13}C NMR of [C_6Bipyr][NTf_2]

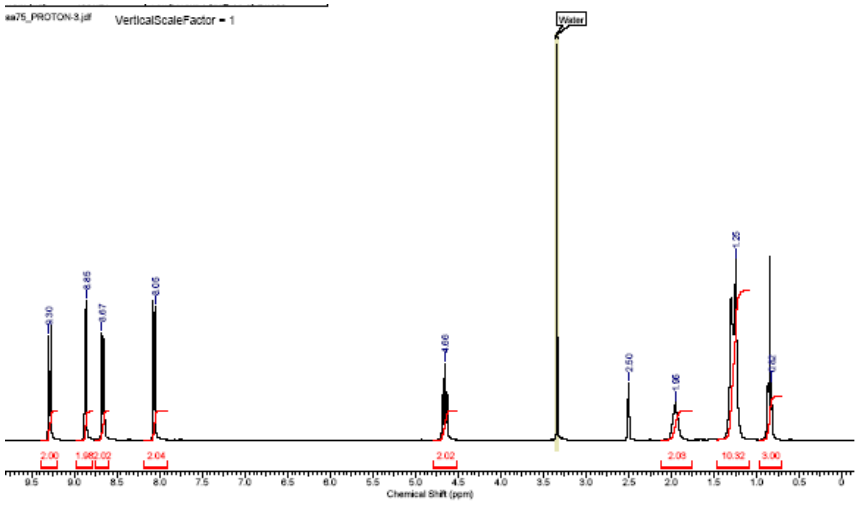

^{1}H NMR of [C_8Bipyr]Br

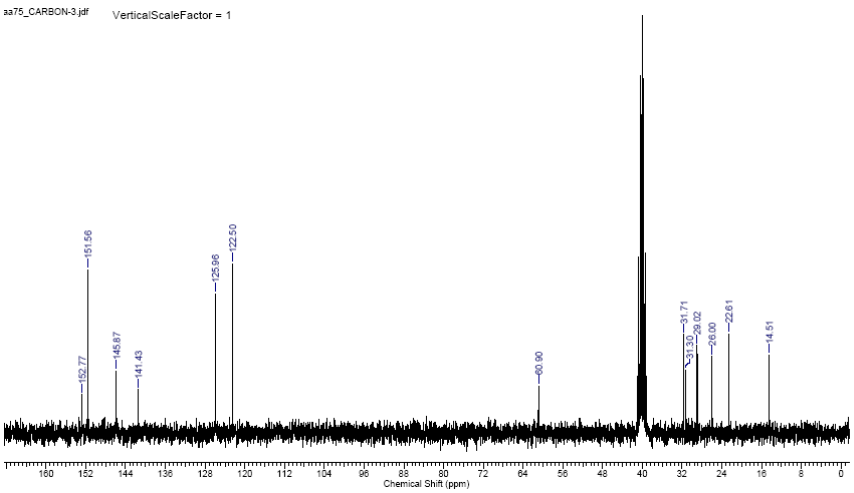

^{13}C NMR of [C_8Bipyr]Br

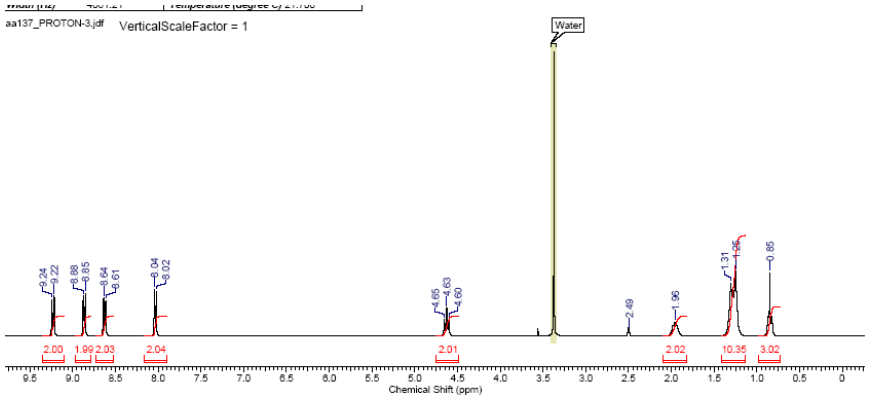

^{1}H NMR of [C_8Bipyr][NTf_2]

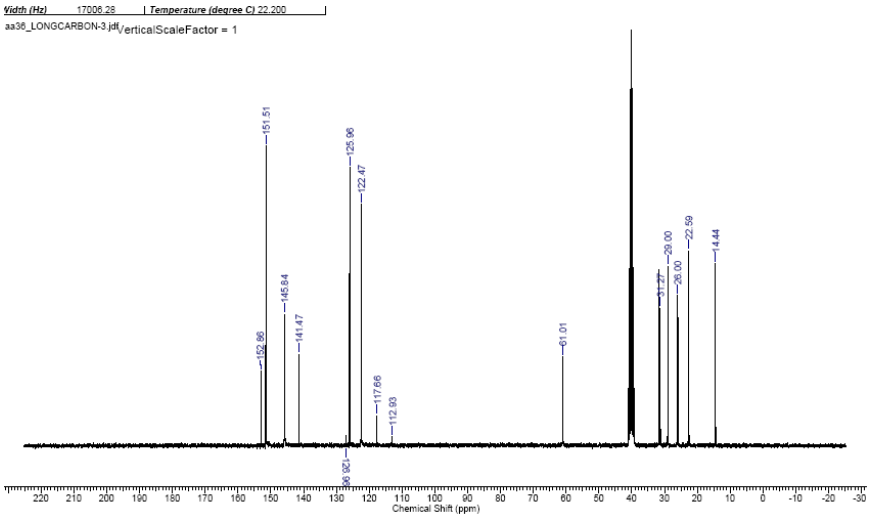

^{13}C NMR of $[C_8Bipyr][NTf_2]$

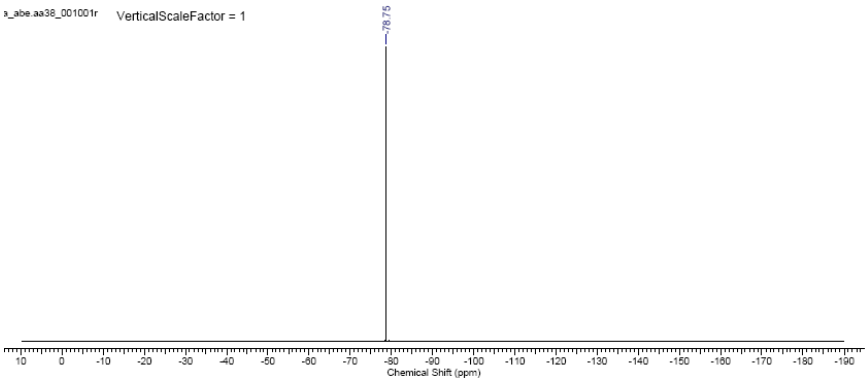

^{19}F NMR of $[C_8Bipyr][NTf_2]$

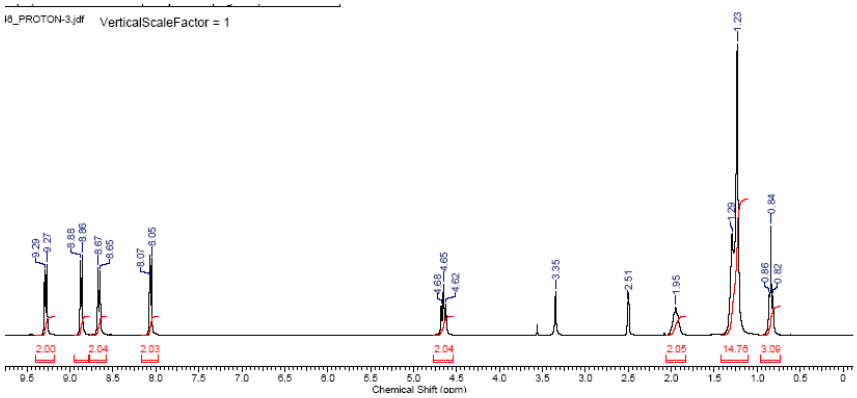

^{1}H NMR of $[C_{10}Bipyr]Br$

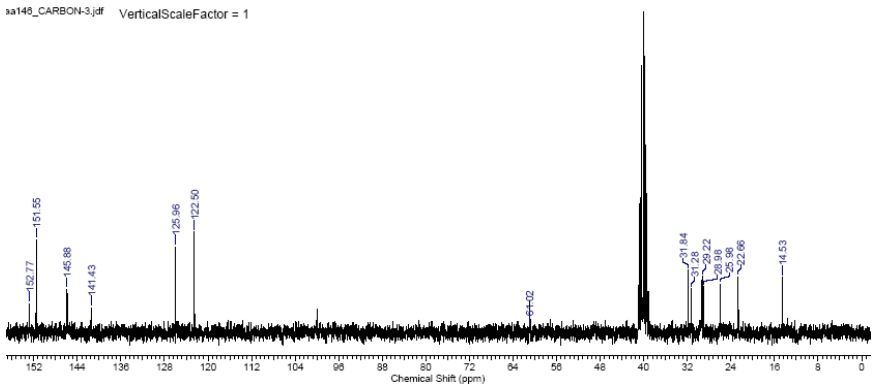

^{13}C NMR of [C_{10}Bipyr]Br

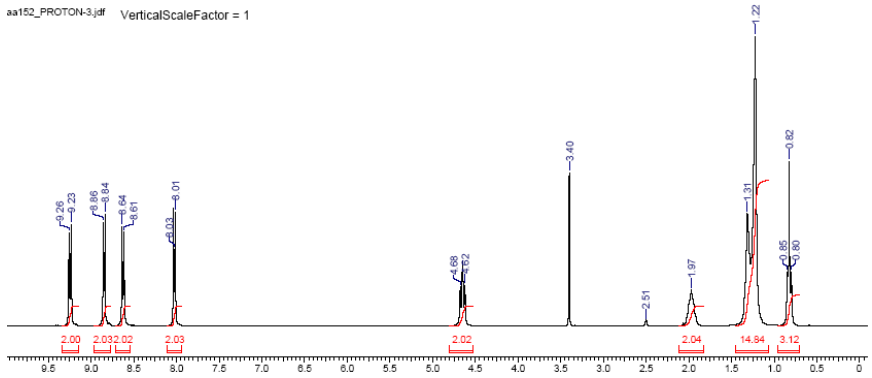

^{13}C NMR of [C_{10}Bipyr][NTf_2]

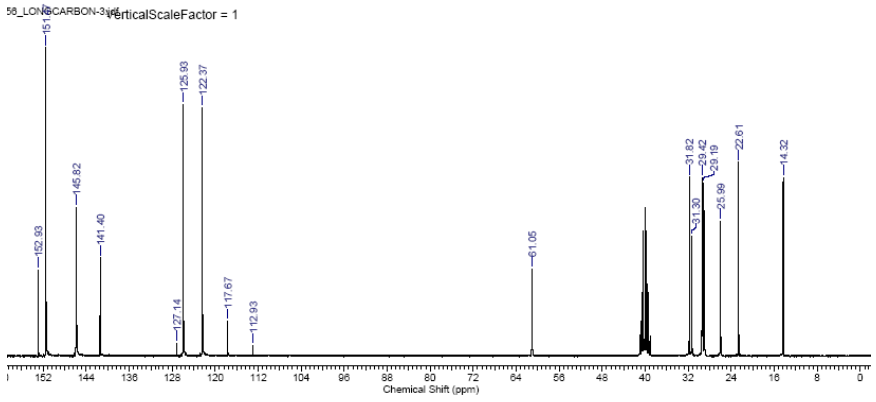

^{13}C NMR of [C_{10}Bipyr][NTf_2]

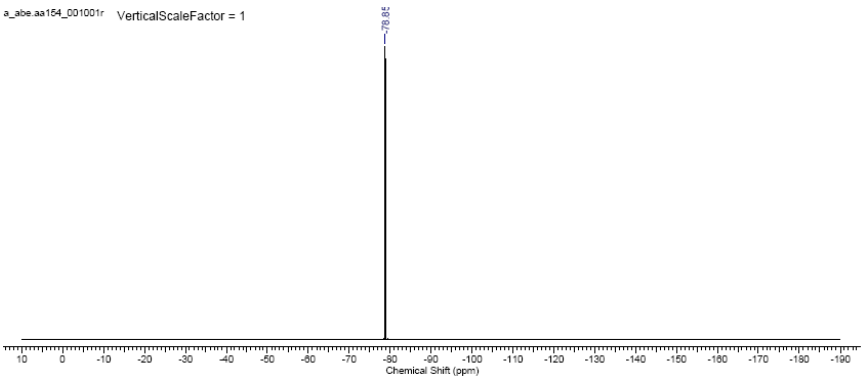

^{19}F NMR of [C_{10}Bipyr][NTf_2]

Appendix 2

A2. ESI-MS spectra for Chapter 2

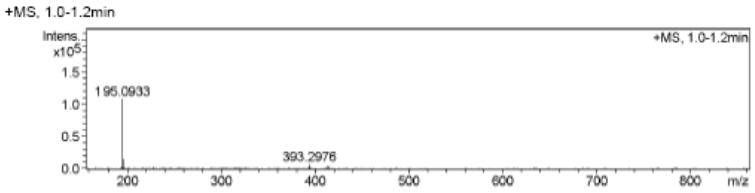

ESI-MS of [C_1Phen][NTf_2] of the positive formula method

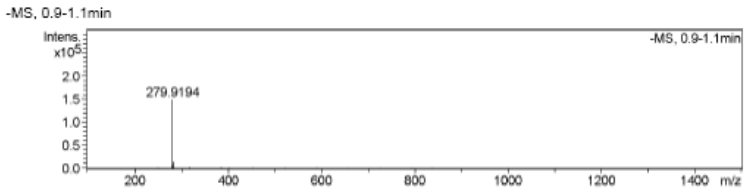

ESI-MS of [C_1Phen][NTf_2] of the negative formula method

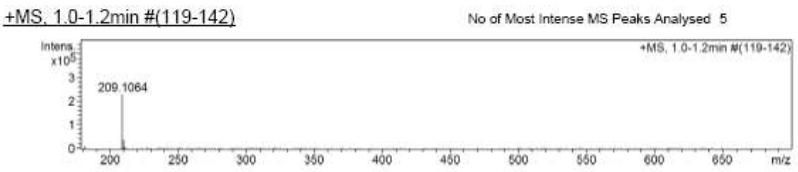

ESI-MS of $[C_2Phen][NTf_2]$ of the positive formula methode

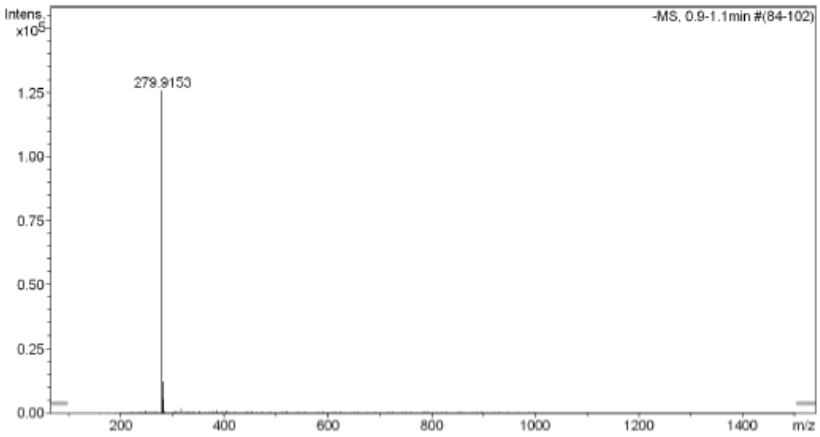

ESI-MS of $[C_2Phen][NTf_2]$ of the negative formula methode

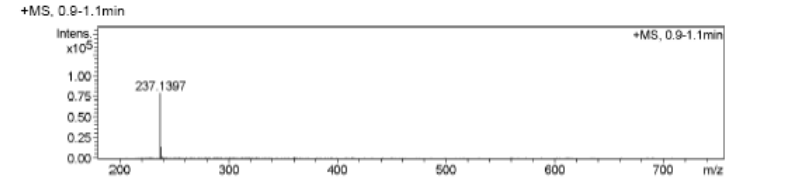

ESI-MS of $[C_4Phen][NTf_2]$ of positive formula methode

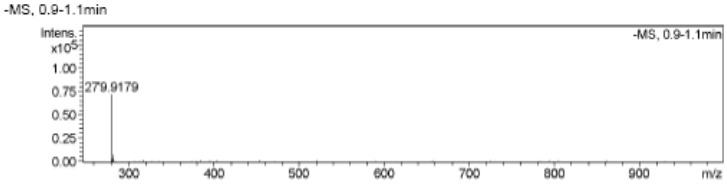

ESI-MS of $[C_4Phen][NTf_2]$ of the negative formula methode

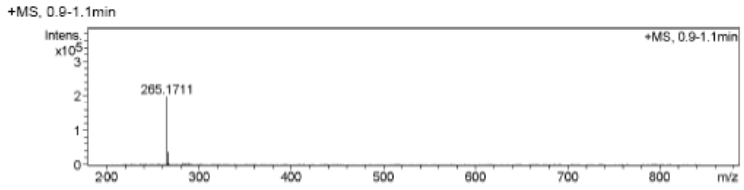

ESI-MS of $[C_6Phen][NTf_2]$ of the positive formula methode

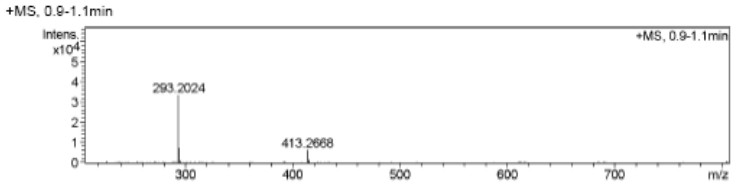

ESI-MS of $[C_8Phen][NTf_2]$ of the positive formula methode

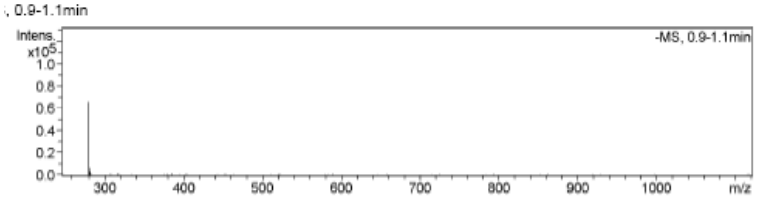

ESI-MS of $[C_8Phen][NTf_2]$ of the negative formula methode

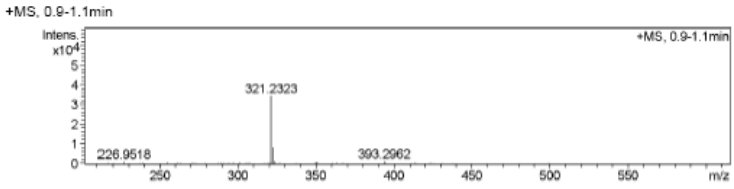

ESI-MS of $[C_{10}Phen][NTf_2]$ of the positive formula methode

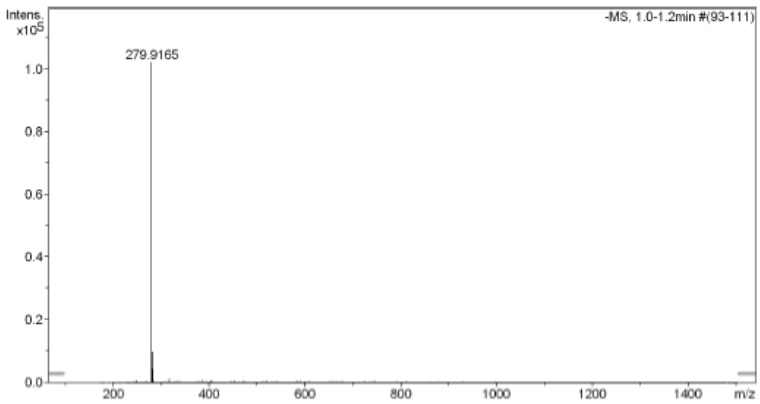

ESI-MS of $[C_{10}Phen][NTf_2]$ of the negative formula methode

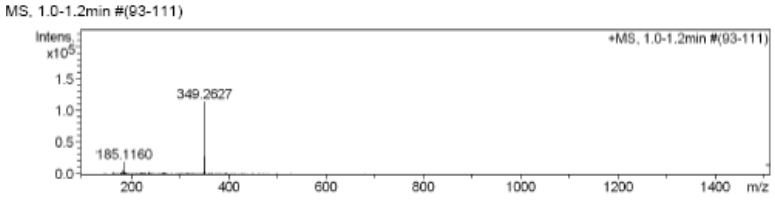

ESI-MS of $[C_{12}Phen][NTf_2]$ of the positive formula methode

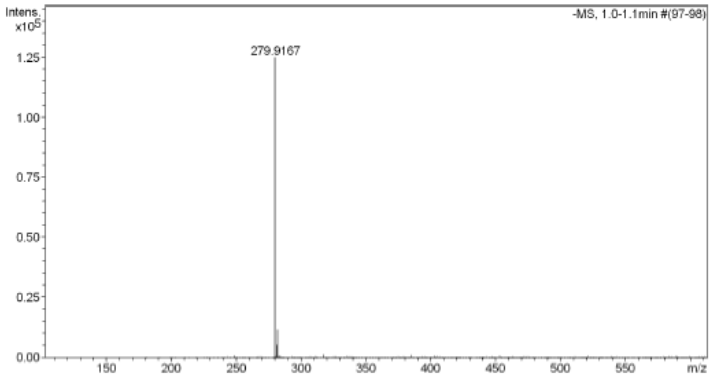

ESI-MS of $[C_{12}Phen][NTf_2]$ of the negative formula methode

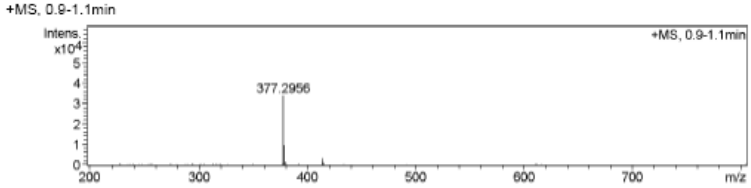

ESI-MS of $[C_{14}Phen][NTf_2]$ of the positive formula methode

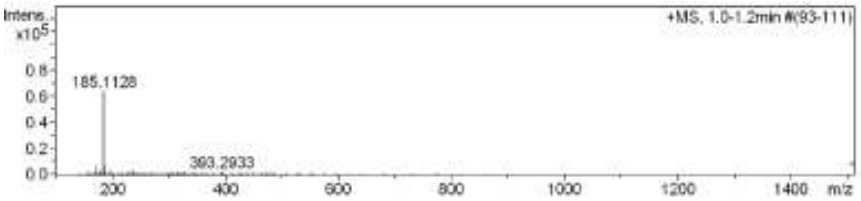

ESI-MS of $[C_2Bipyr][NTf_2]$ with the positive formula method

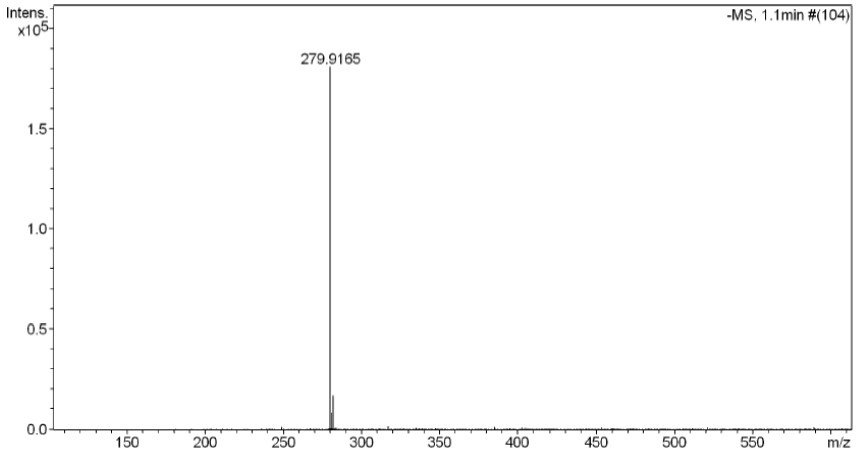

ESI-MS of $[C_2Bipyr][NTf_2]$ with the negative formula method

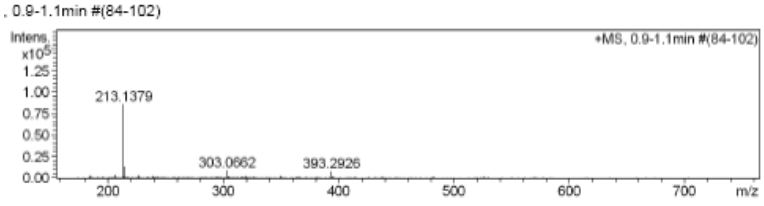

ESI-MS of $[C_4Bipyr][NTf_2]$ of the positive formula method

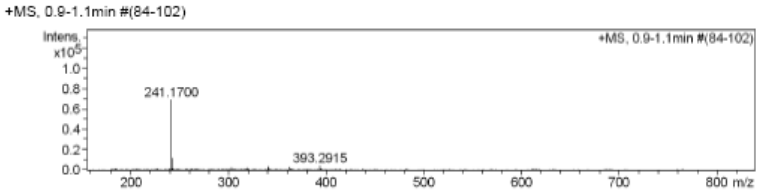

ESI-MS of [C_6Bipyr][NTf2] of the positive formula method

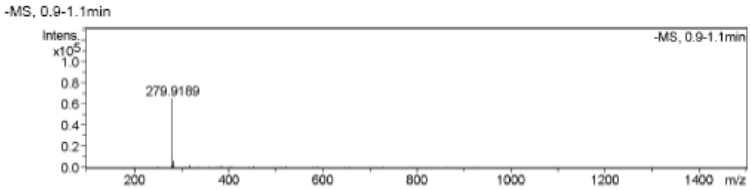

ESI-MS of [C_8Bipyr][NTf_2] of the positive formula method

Appendix 3

A3. Thermal data

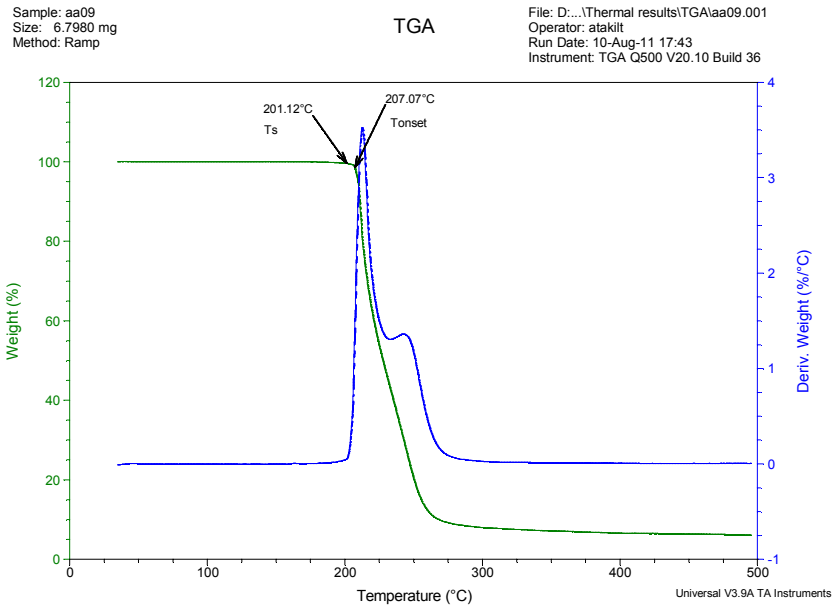

Characteristic decomposition curve of [C_1Phen]I, determined by TGA, indicating the start and onset temperatures.

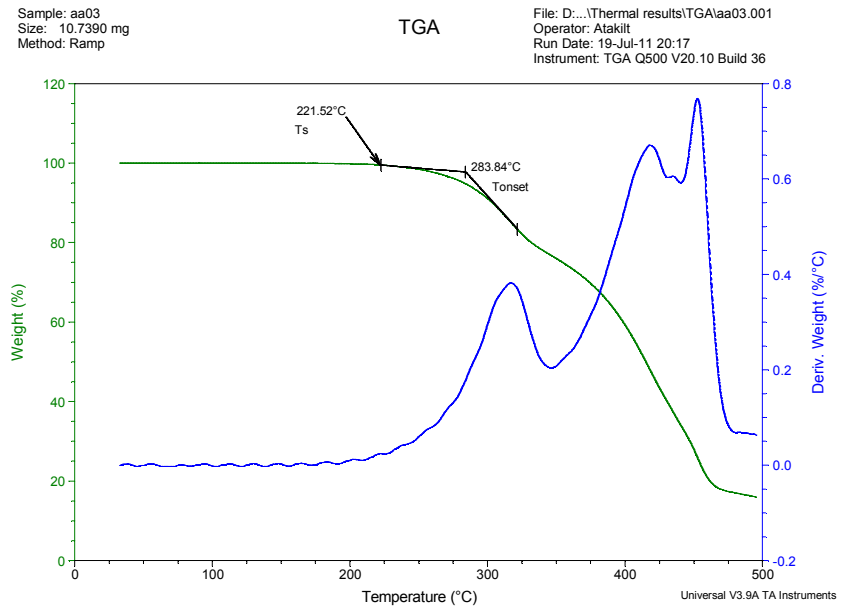

Characteristic decomposition curve of $[C_1Phen][NTf_2]$, determined by TGA, indicating the start and onset temperatures.

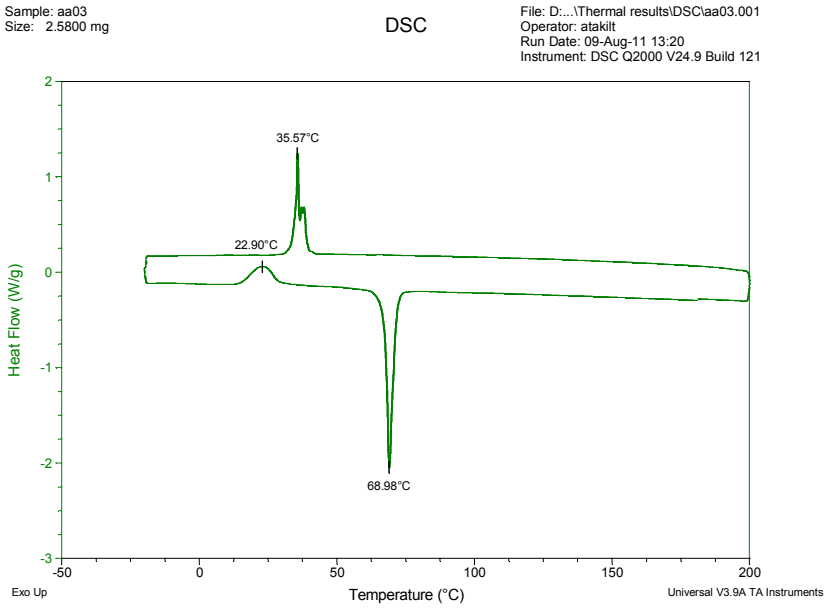

Characteristic phase transition of $[C_1Phen][NTf_2]$, determined by DSC, indicating the melting and crystallization temperatures.

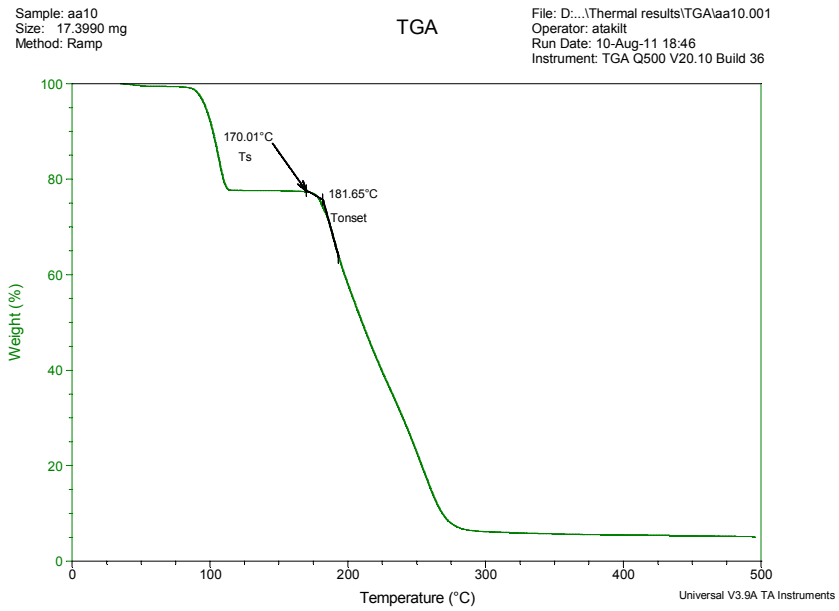

Characteristic decomposition curve of $[C_2Phen]I$, determined by TGA, indicating the start and onset temperatures.

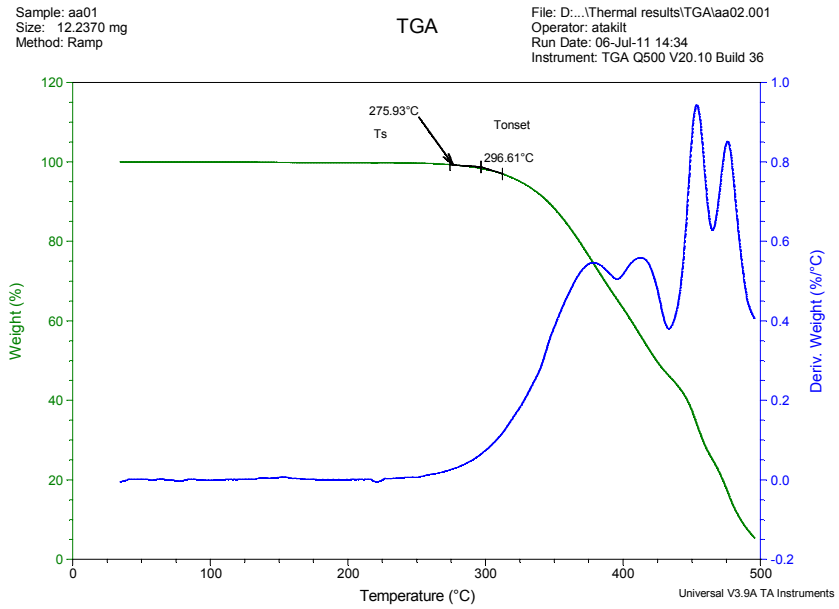

Characteristic decomposition curve of $[C_2Phen][NTf_2]$, determined by TGA, indicating the start and onset temperatures.

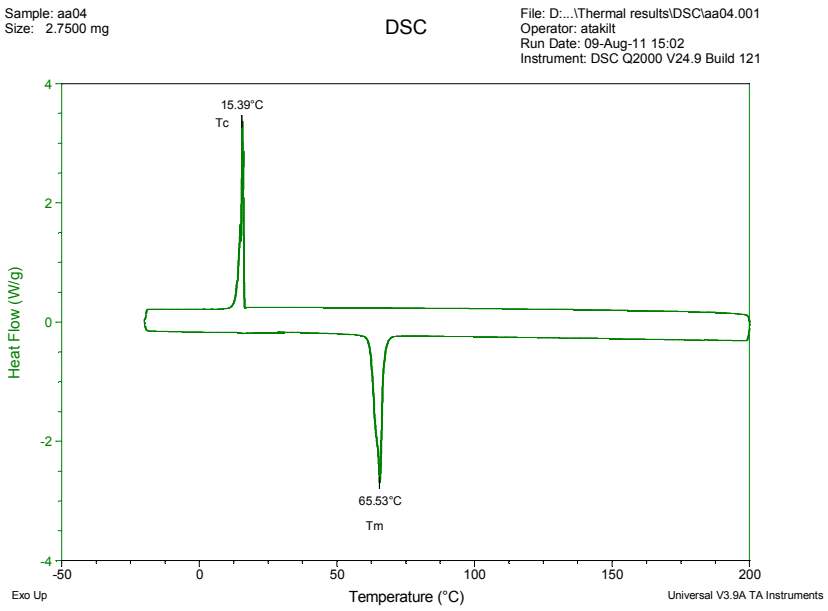

Characteristic phase transition of $[C_2Phen][NTf_2]$, determined by DSC, indicating the melting and crystallization temperatures.

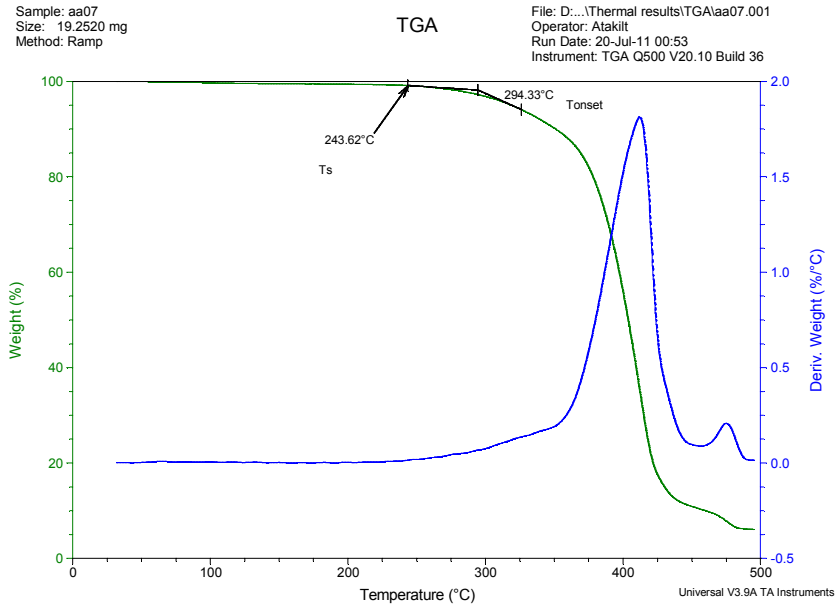

Characteristic decomposition curve of $[C_4Phen][NTf_2]$, determined by TGA, indicating the start and onset temperatures.

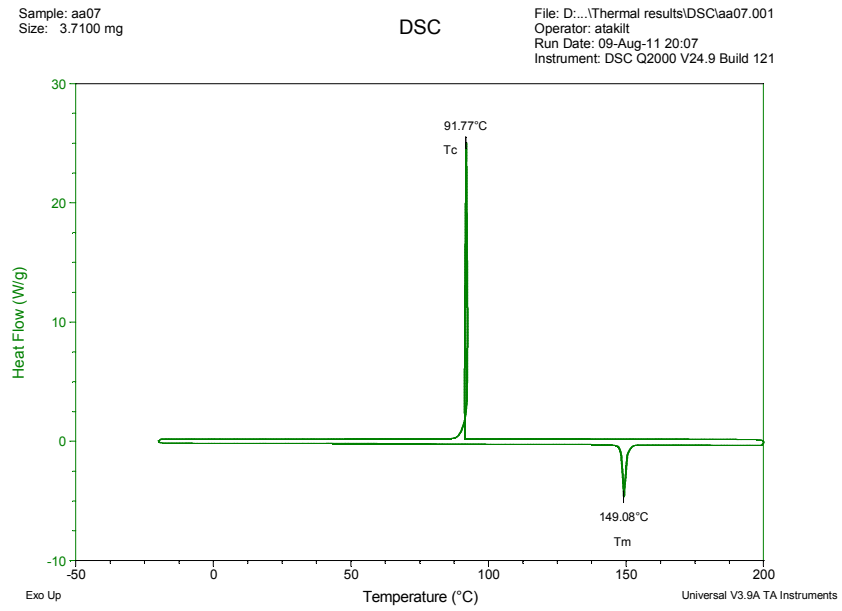

Characteristic phase transition of $[C_4Phen][NTf_2]$, determined by DSC, indicating the melting and crystallization temperatures.

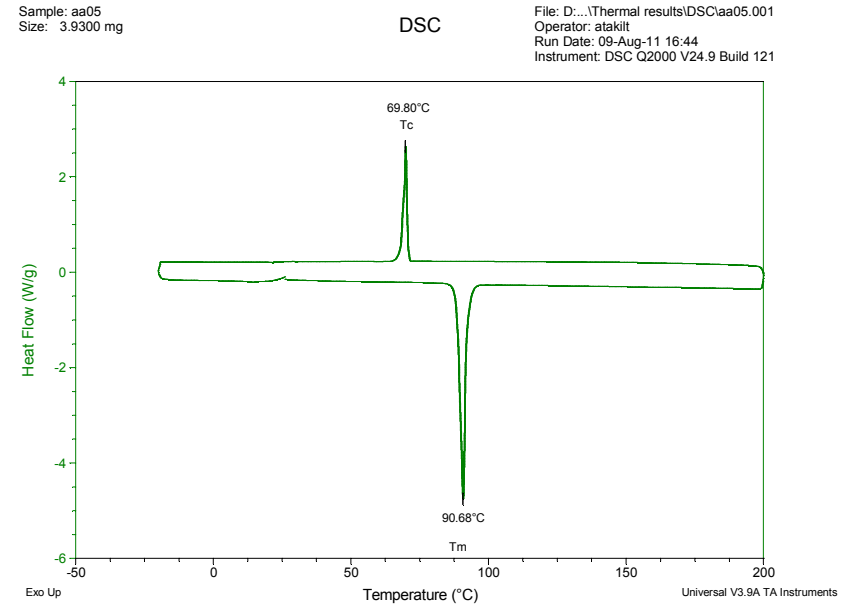

Characteristic phase transition of $[C_6Phen][NTf_2]$, determined by DSC, indicating the melting and crystallization temperatures.

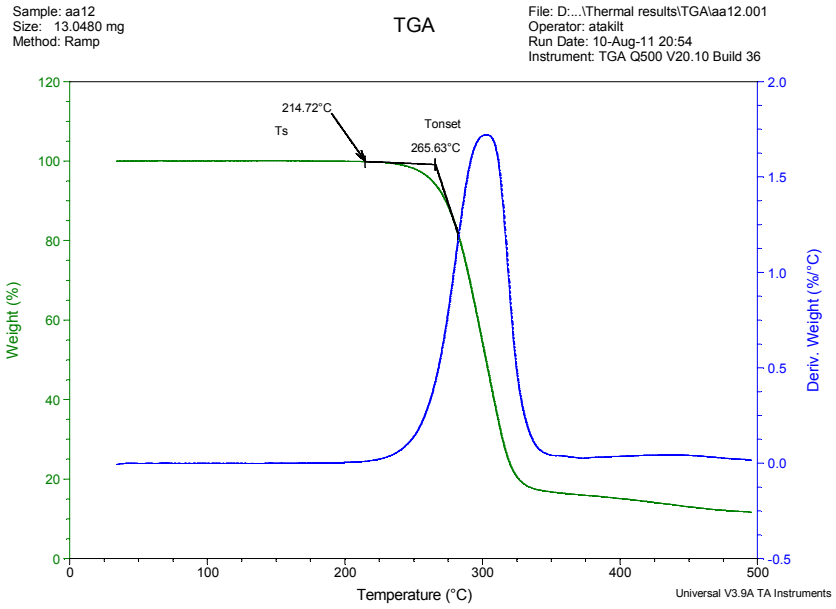

Characteristic decomposition curve of $[C_6Phen][PF_6]I$, determined by TGA, indicating the start and onset temperatures.

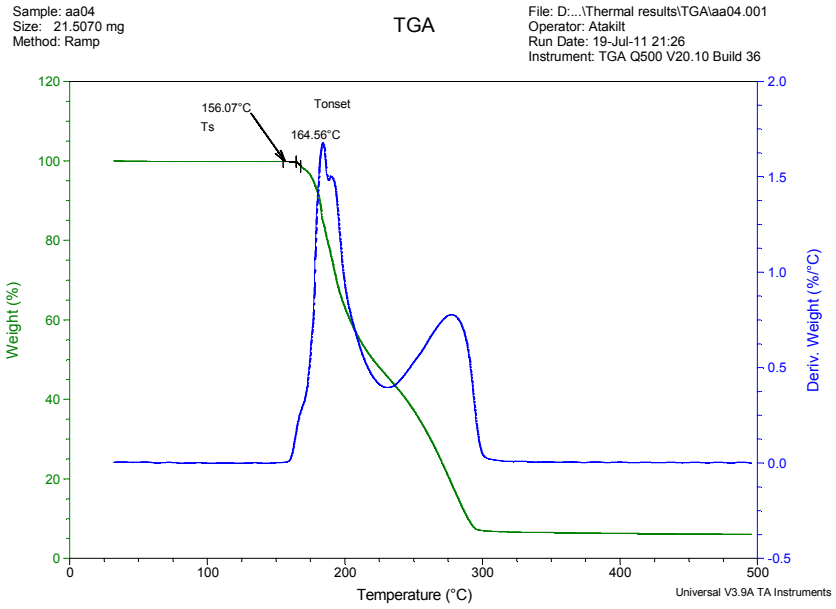

Characteristic decomposition curve of$[C_8Phen]Br$, determined by TGA, indicating the start and onset temperatures.

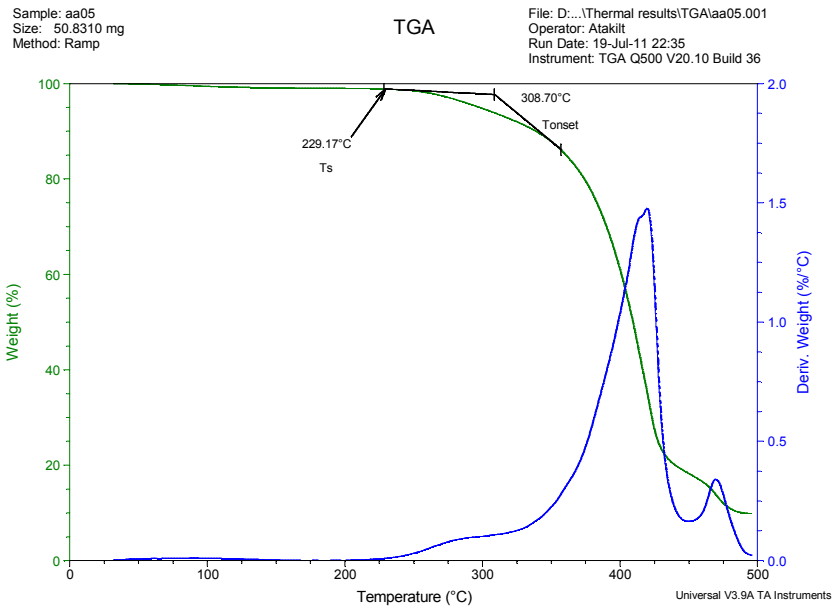

Characteristic decomposition curve of $[C_8Phen][NTf_2]$, determined by TGA, indicating the start and onset temperatures.

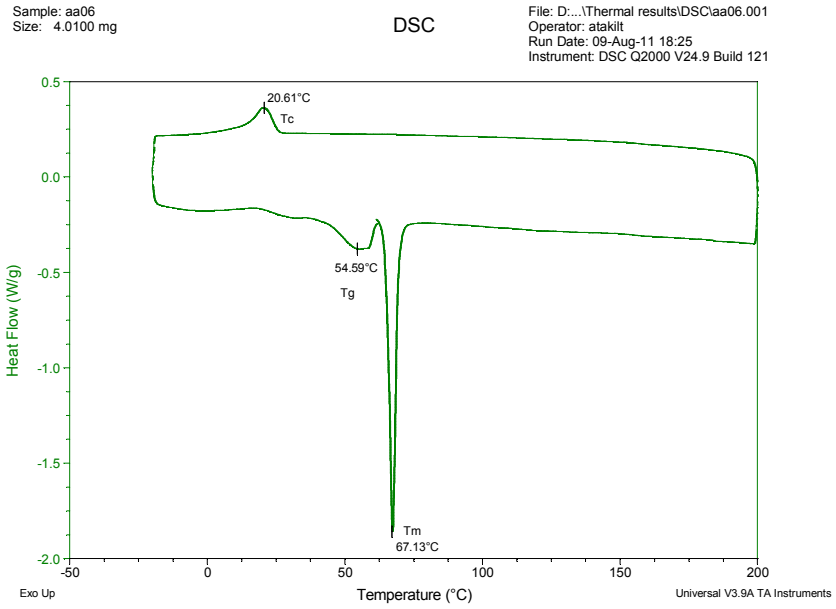

Characteristic phase transition of $[C_8Phen][NTf_2]$, determined by DSC, indicating the melting and crystallization temperatures.

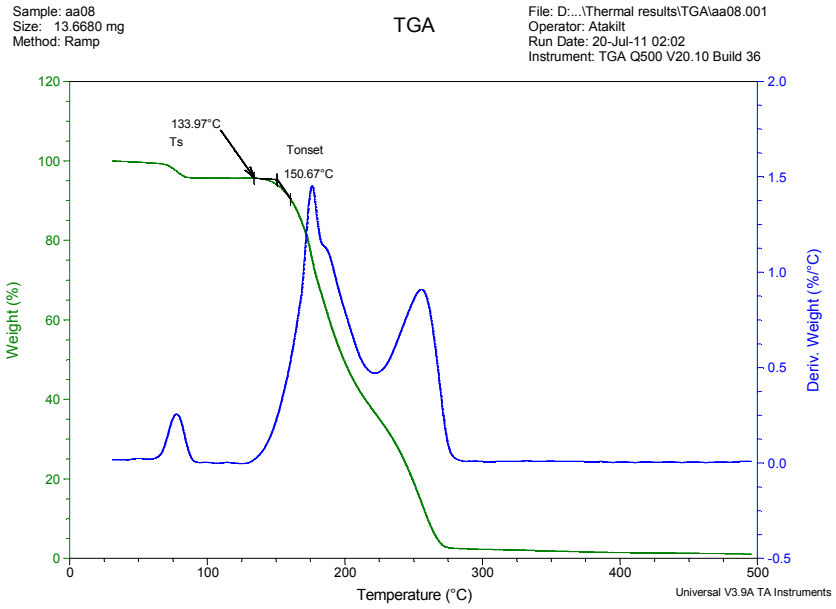

Characteristic decomposition curve of $[C_{10}Phen]Br$, determined by TGA, indicating the start and onset temperatures.

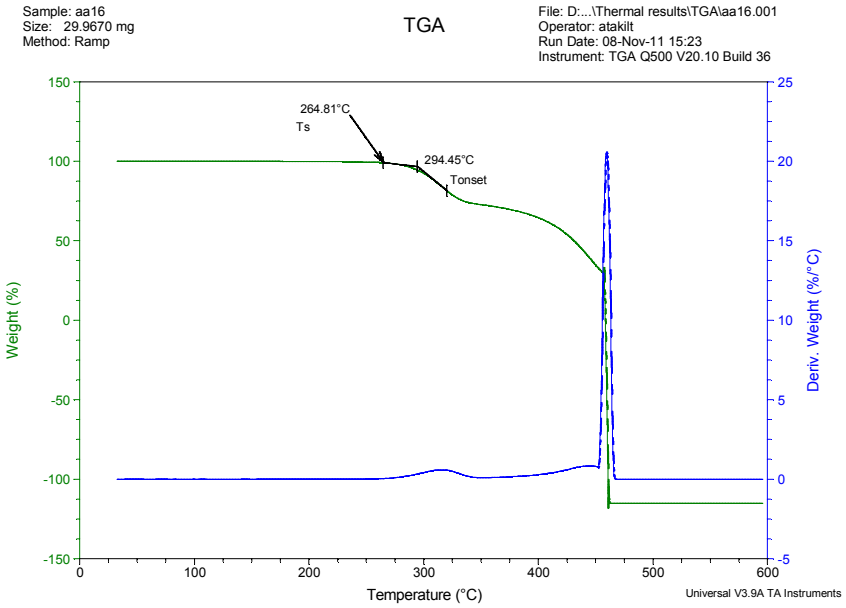

Characteristic decomposition curve of $[C_{10}Phen][NTf_2]$, determined by TGA, indicating the start and onset temperatures.

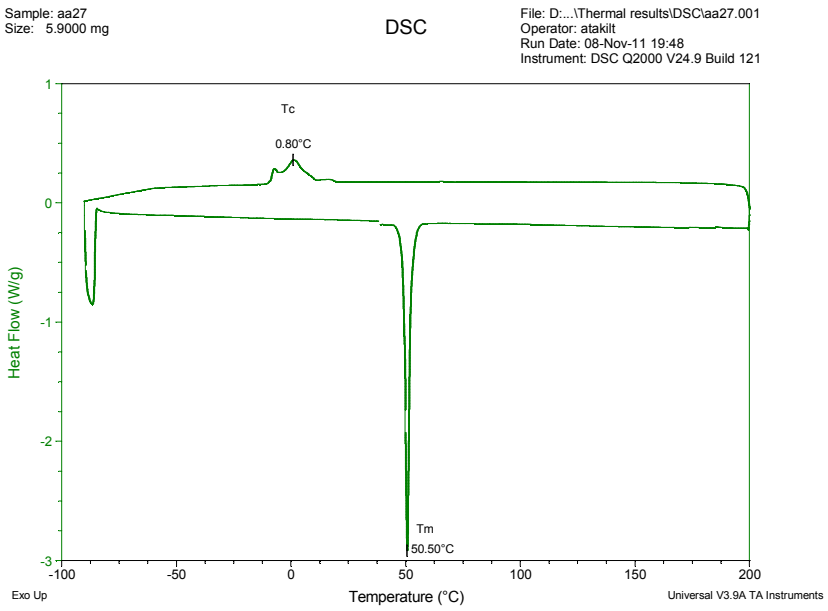

Characteristic phase transition of $[C_{10}Phen][NTf_2]$, determined by DSC, indicating the melting and crystallization temperatures.

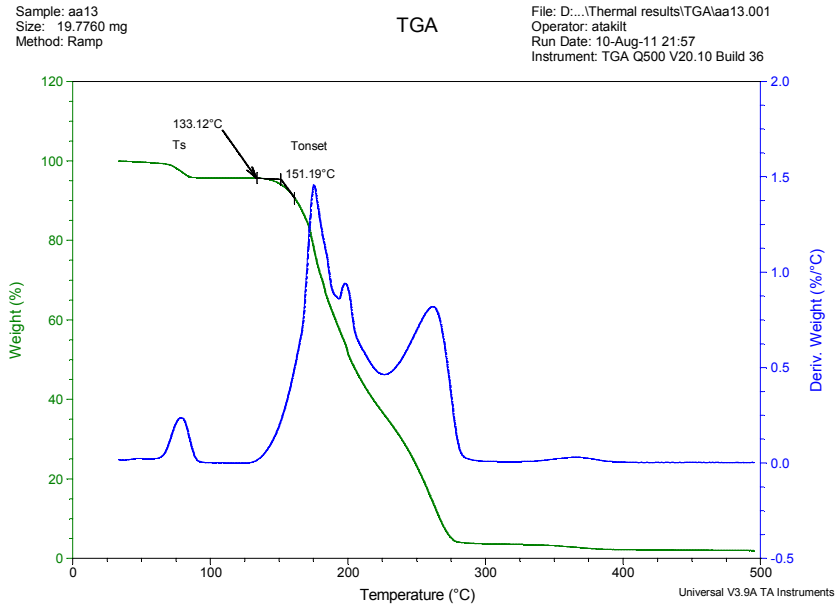

Characteristic decomposition curve of $[C_{12}Phen]Br$, determined by TGA, indicating the start and onset temperatures.

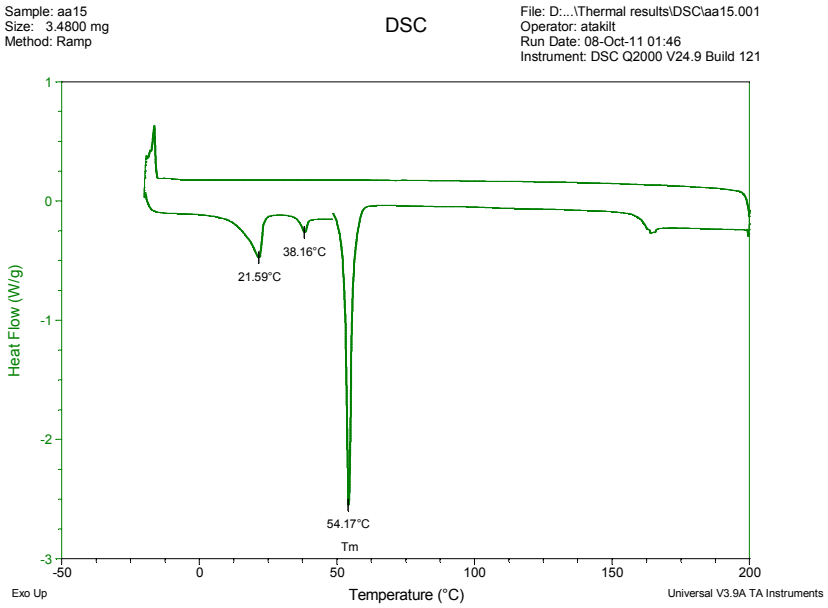

Characteristic phase transition of $[C_{12}Phen][NTf_2]$, determined by DSC.

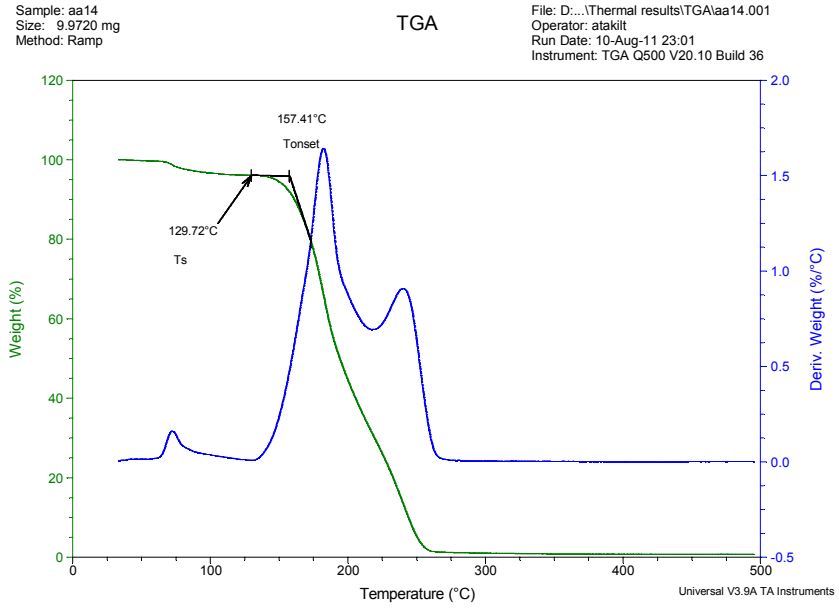

Characteristic decomposition curve of $[C_{14}Phen]Br$, determined by TGA, indicating the start and onset temperatures.

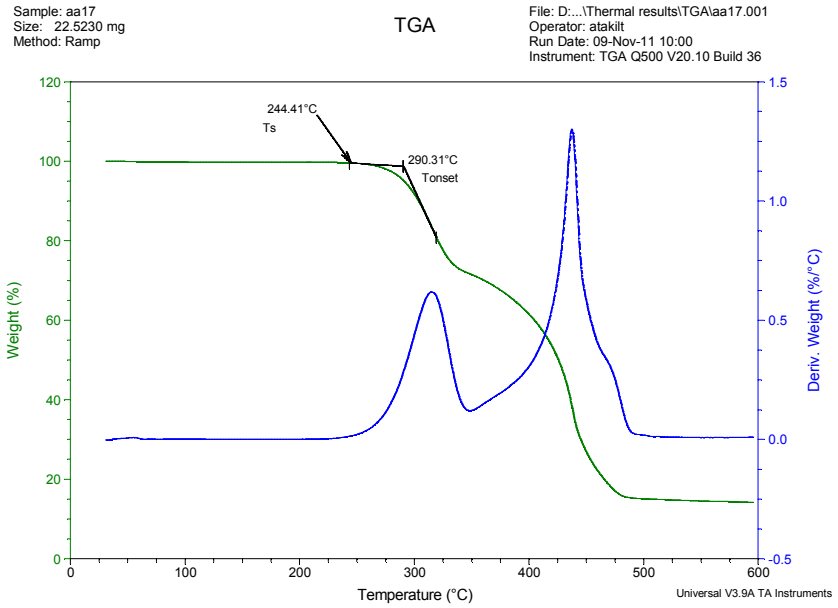

Characteristic decomposition curve of $[C_{14}Phen][NTf_2]$, determined by TGA, indicating the start and onset temperatures.

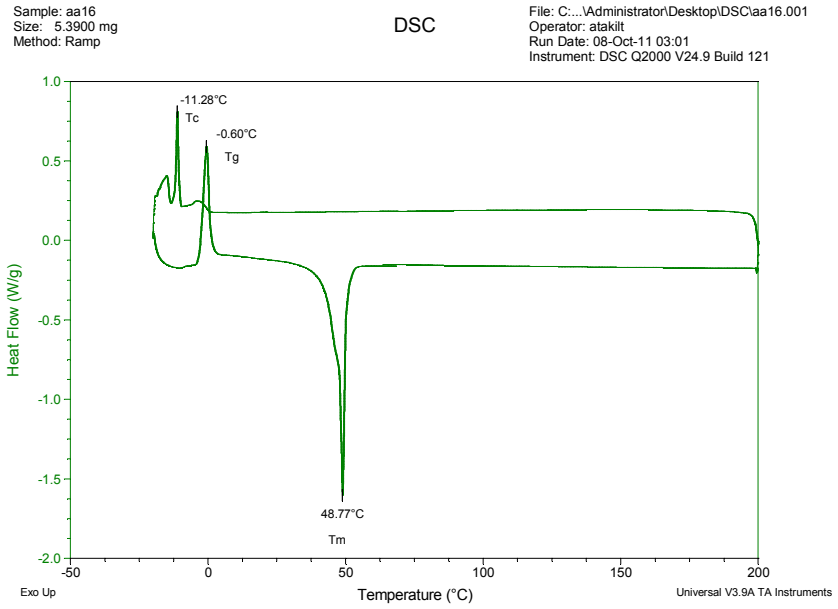

Characteristic phase transition of $[C_{14}Phen][NTf_2]$, determined by DSC, indicating the melting and crystallization temperatures.

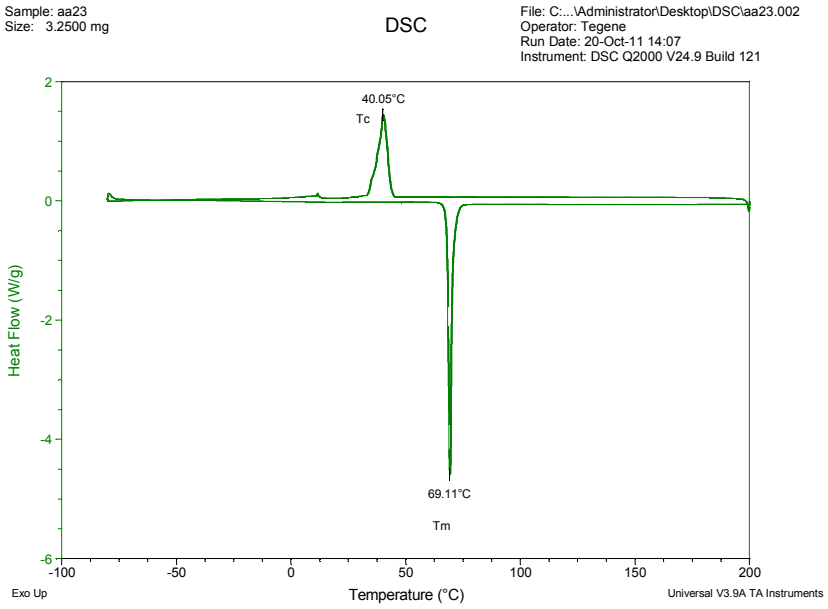

Characteristic phase transition of $[C_2Bipyr][NTf_2]$, determined by DSC, indicating the melting and crystallization temperatures.

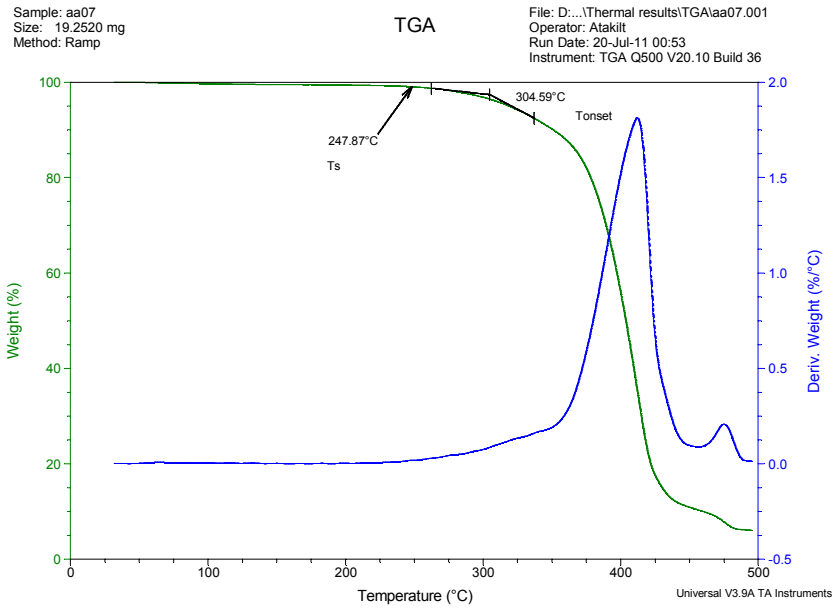

Characteristic decomposition curve of $[C_4Bipyr][NTf_2]$, determined by TGA, indicating the start and onset temperatures.

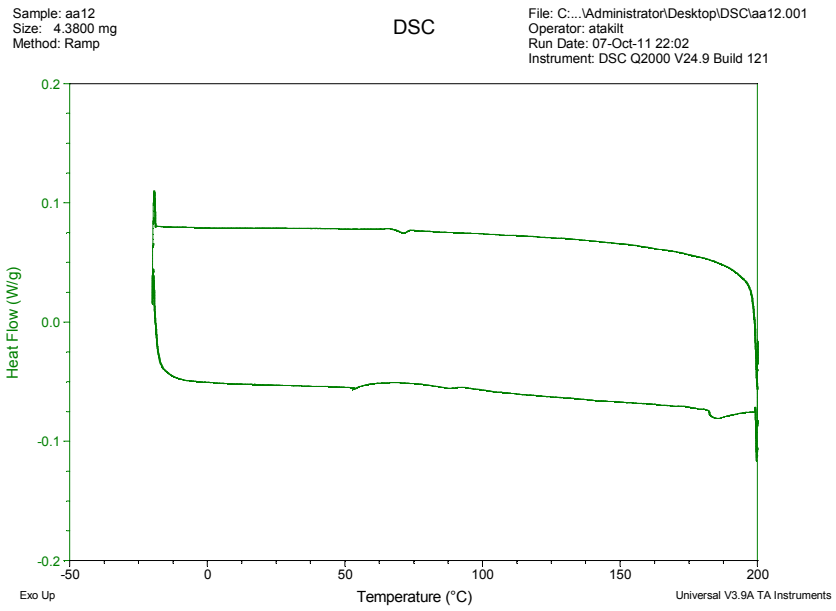

DSC of $[C_4Bipyr][NTf_2]$

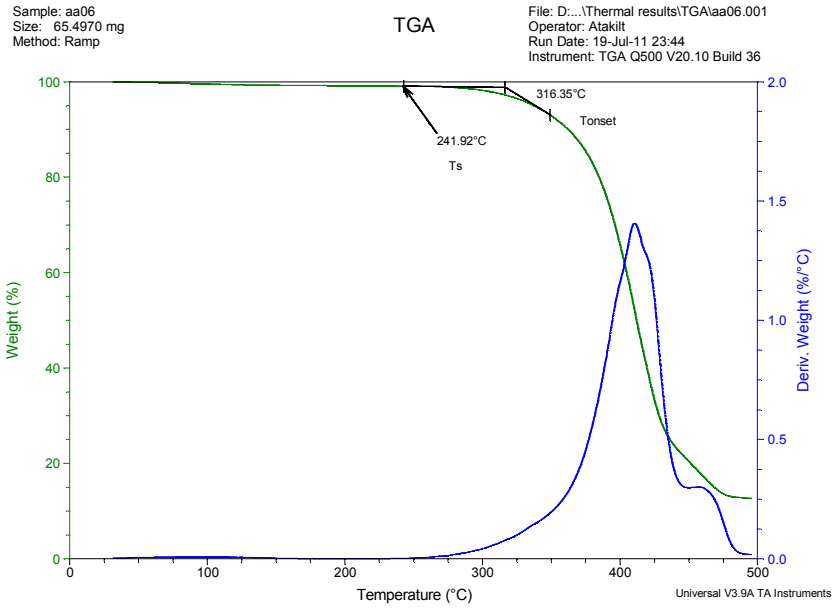

Characteristic decomposition curve of $[C_6Bipyr][NTf_2]$, determined by TGA, indicating the start and onset temperatures.

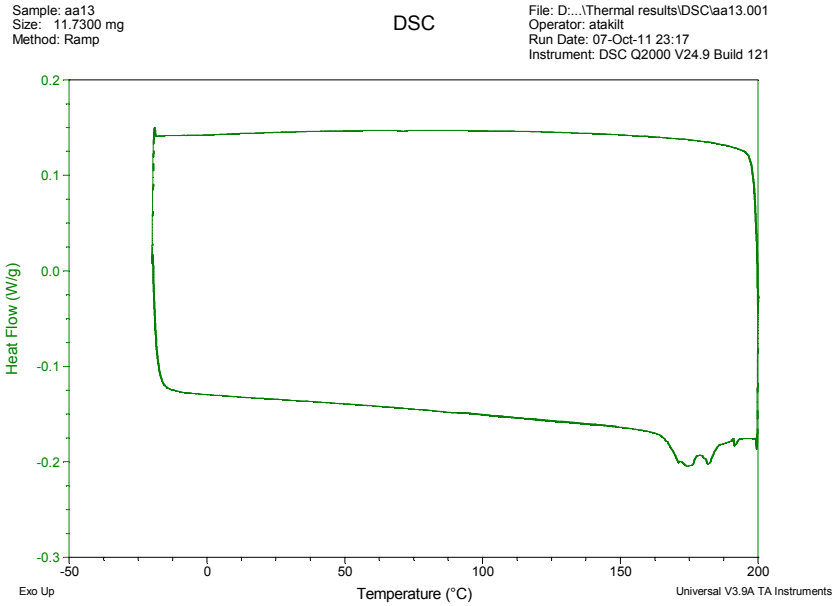

DSC of $[C_6Bipyr][NTf_2]$

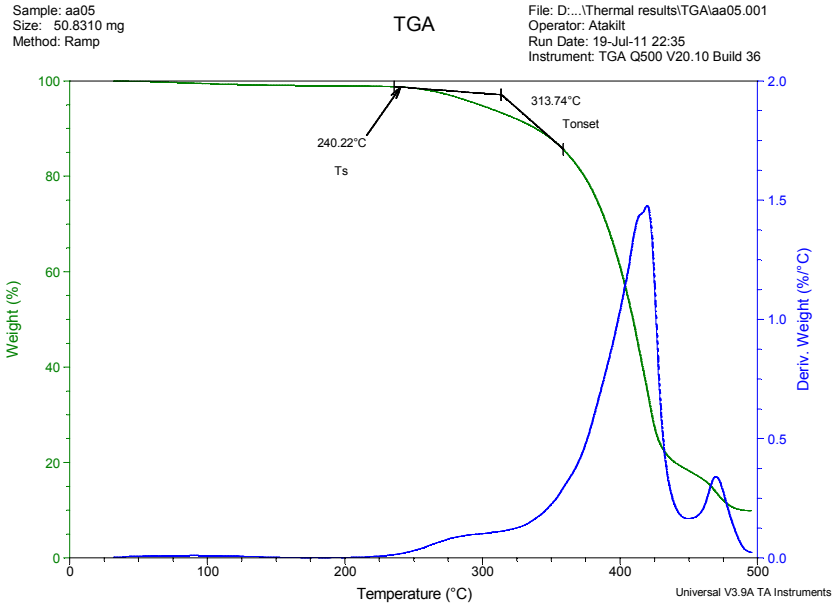

Characteristic decomposition curve of $[C_8Bipyr][NTf_2]$, determined by TGA, indicating the start and onset temperatures.

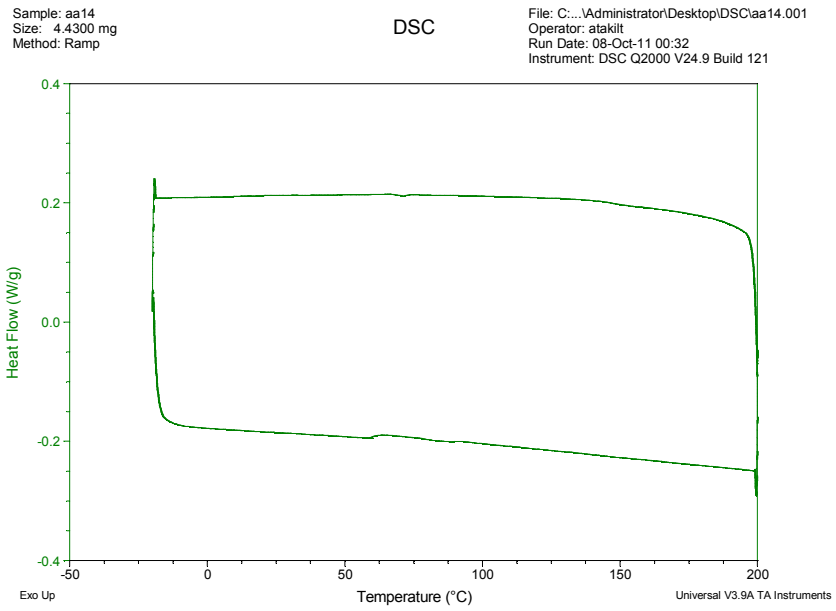

DSC of $[C_8Bipyr][NTf_2]$

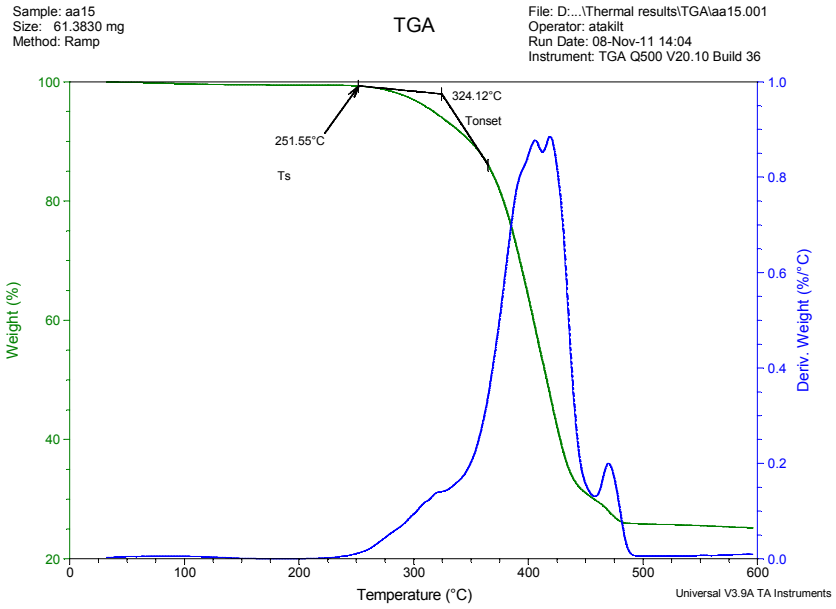

Characteristic decomposition curve of $[C_{10}Bipyr][NTf_2]$, determined by TGA, indicating the start and onset temperatures.

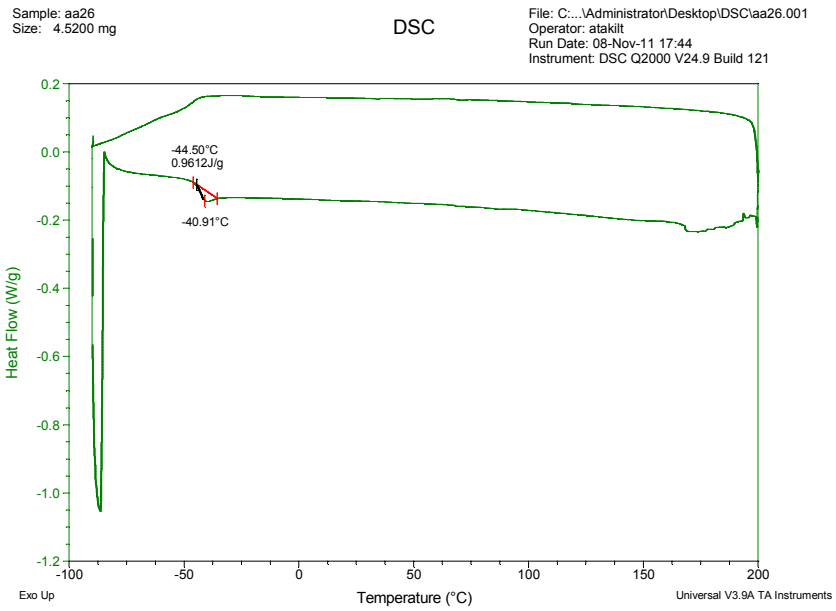

DSC of $[C_{10}Bipyr][NTf_2]$

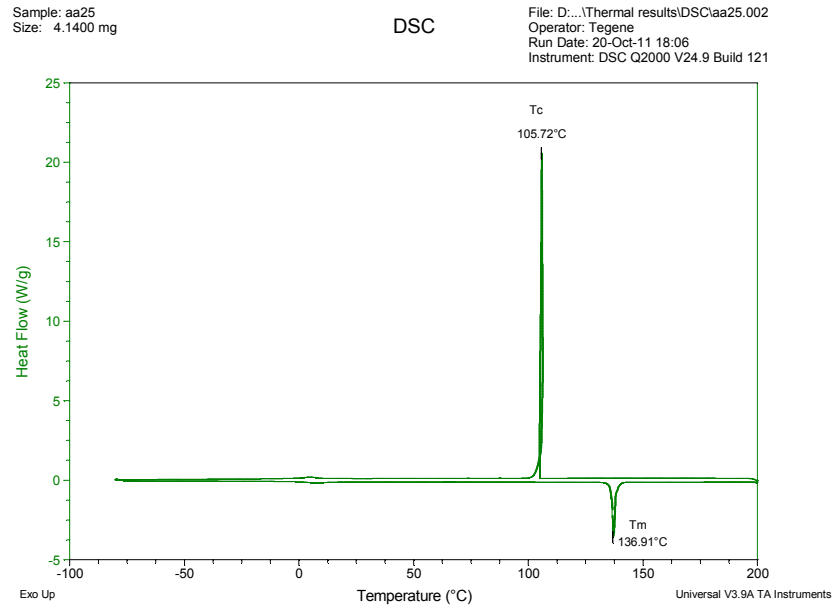

DSC of $[(C_2)_2Bipyr]\ [NTf_2]_{\ 2}$

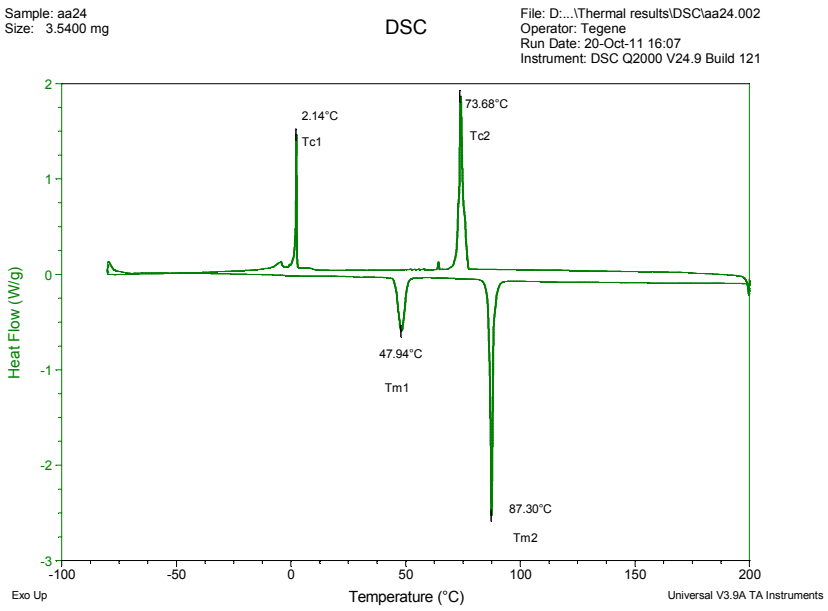

DSC of $[(C_4)_2Bipyr]\ [NTf_2]_2$

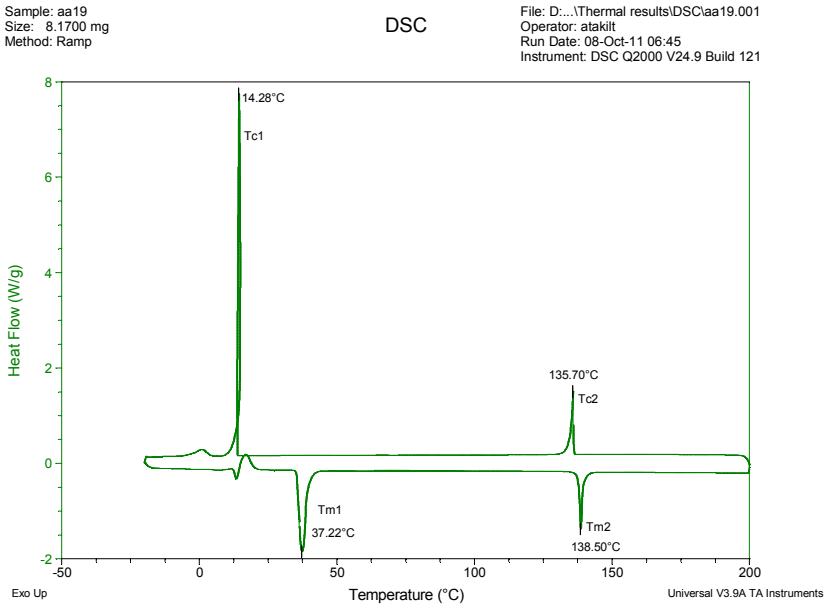

DSC of $[(C_8)_2Bipyr]\ [NTf_2]_2$

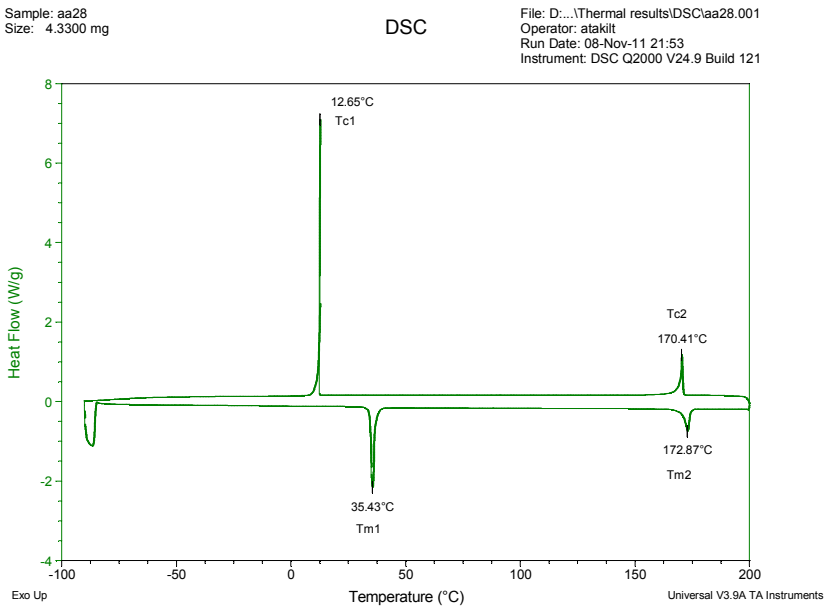

DSC of $[(C_{10})_2Bipyr]\ [NTf_2]_2$

Appendix 5

A5. XP spectra

5.1 XP spectra with component fittings of [C_1Phen]I for: (a) survey, (b) C 1s, (c) N 1s, (d) I 3d, (e) I 4d

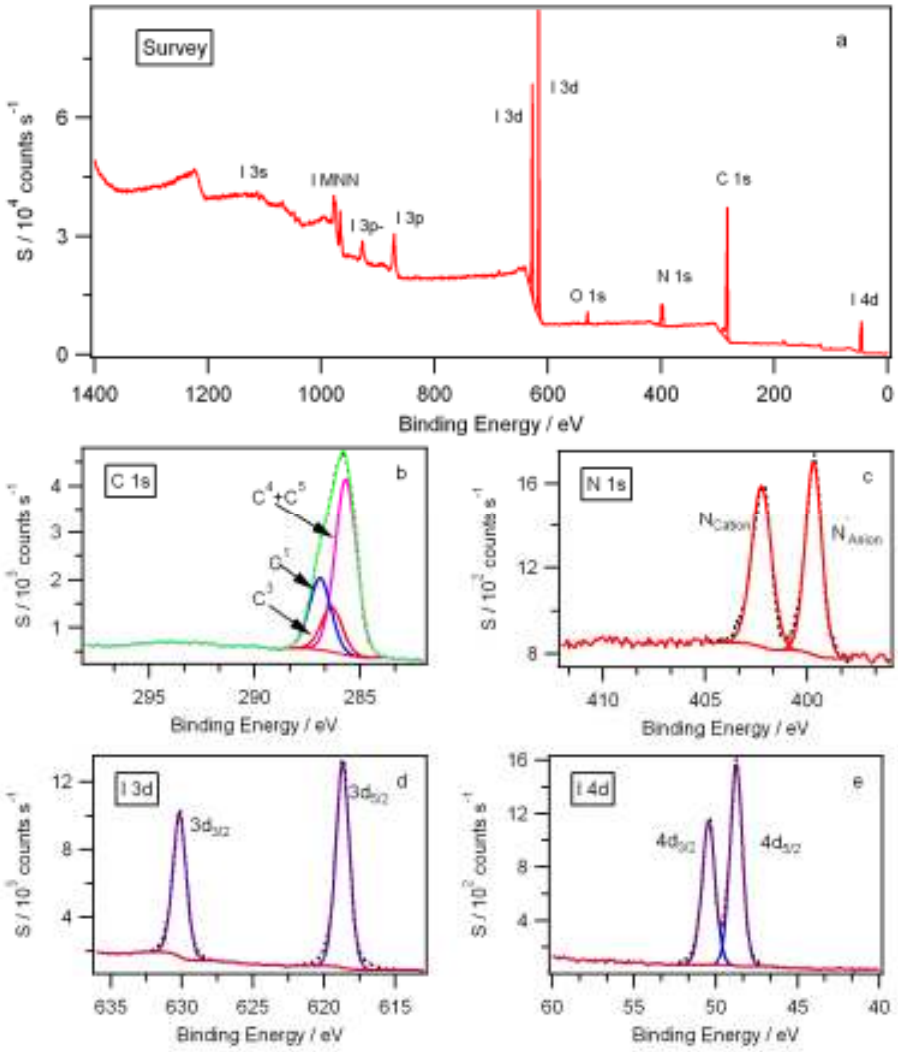

5.2 XP spectra with component fittings of [C_1Phen][PF_6] for: (a) survey, (b) C 1s, (c) N 1s, (d) F 1s, and (e) P 2p.

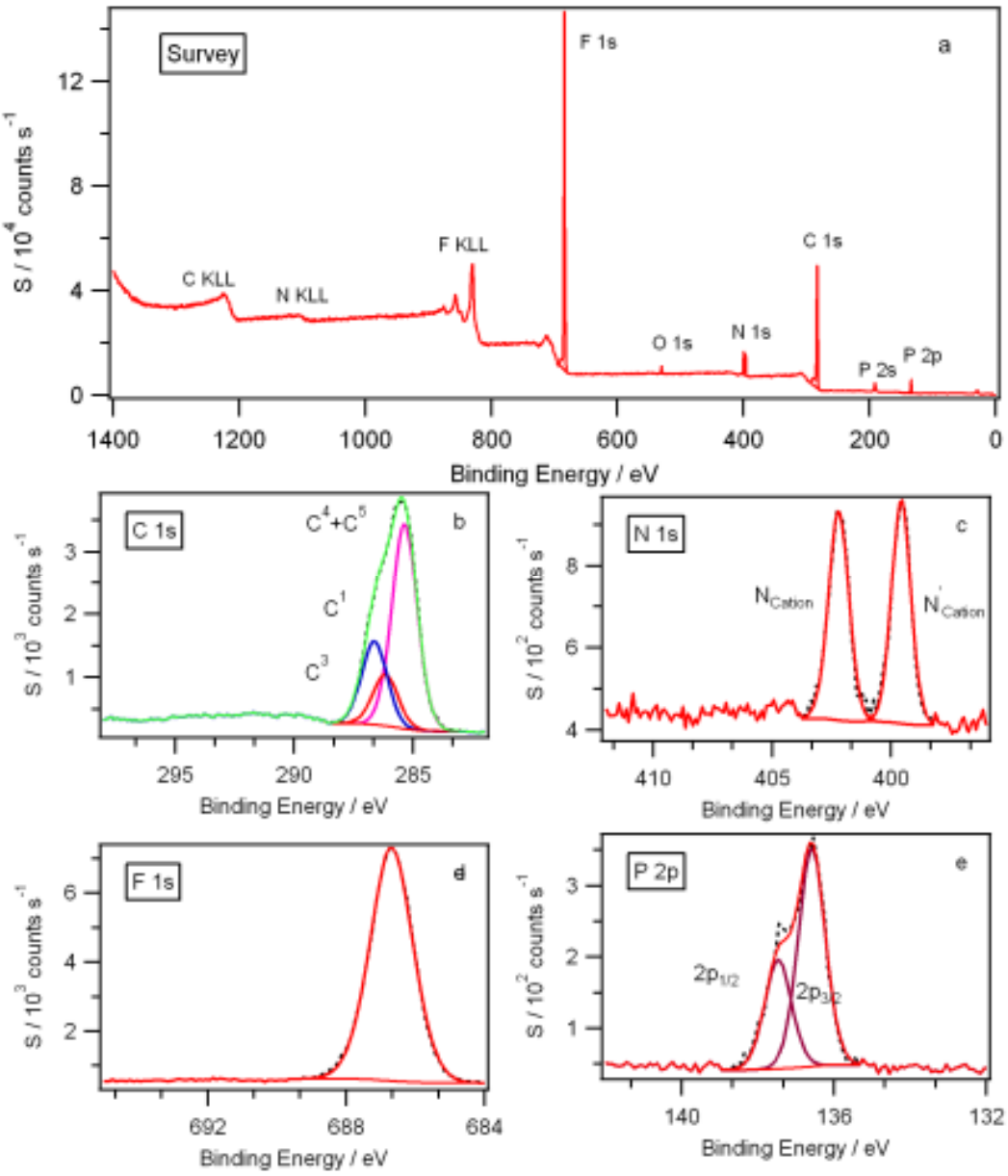

5.3 XP spectra with component fittings of [C_1Phen][NTf_2] for: (a) survey, (b) C 1s, (c) N 1s, (d) F 1s, (e) O 1s and (f) S 2p.

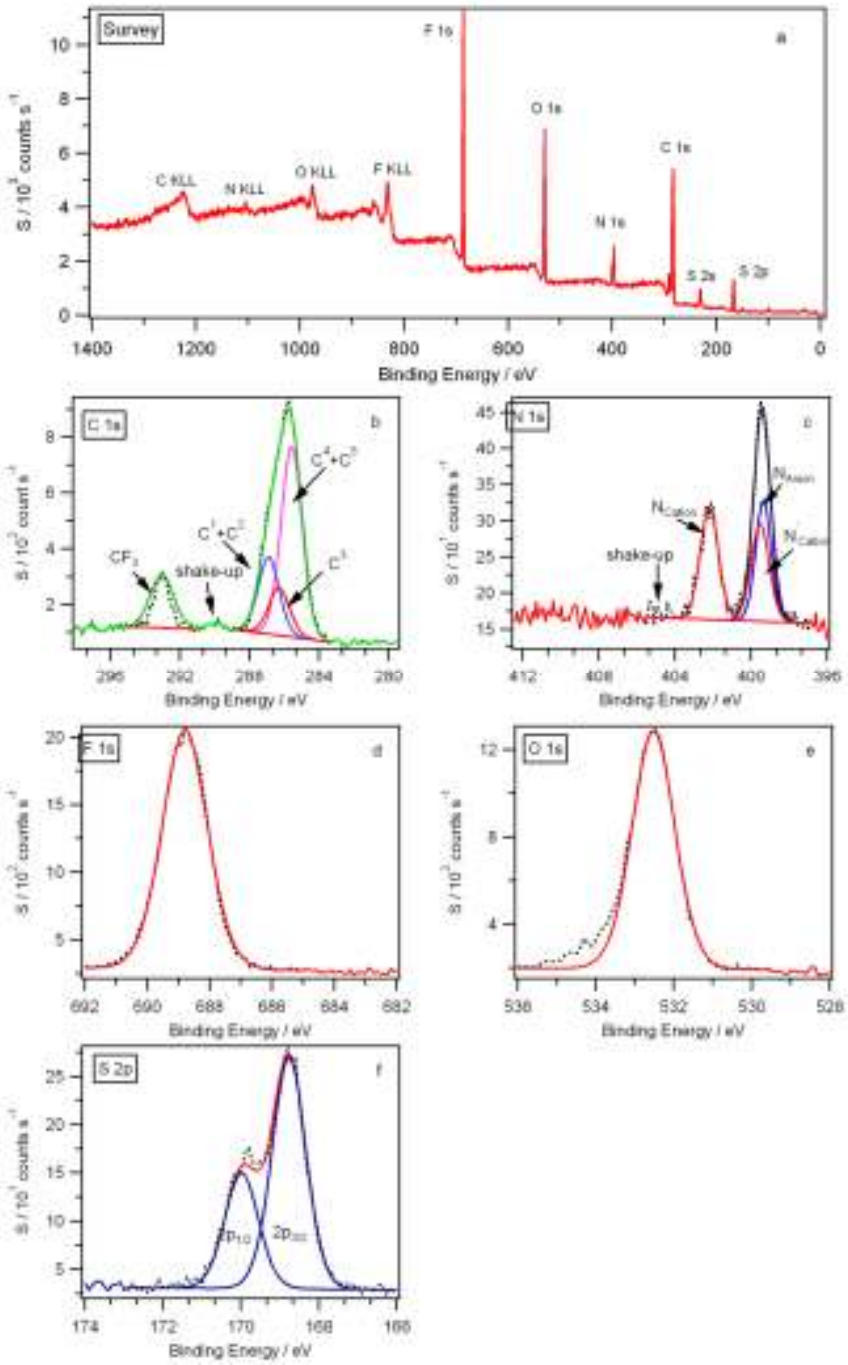

5.4 XP spectra with component fittings of [C_2Pyrr][NTf_2] for: (a) survey, (b) C 1s, (c) N 1s, (d) F 1s, (e) O 1s and (f) S 2p.

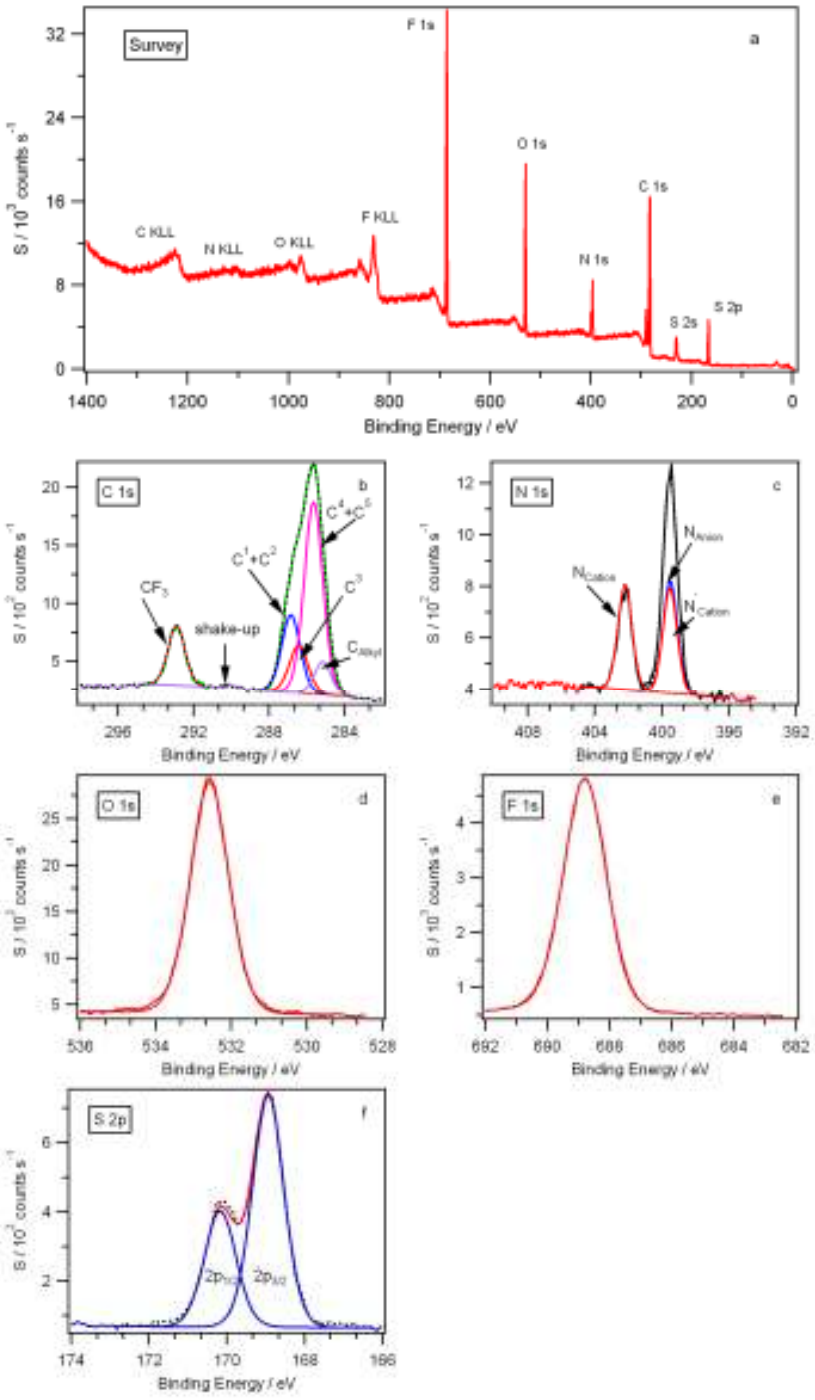

5.5 XP spectra with component fittings of [C_4Phen][NTf_2] for: (a) survey, (b) C 1s, (c) N 1s, (d) F 1s, (e) O 1s and (f) S 2p.

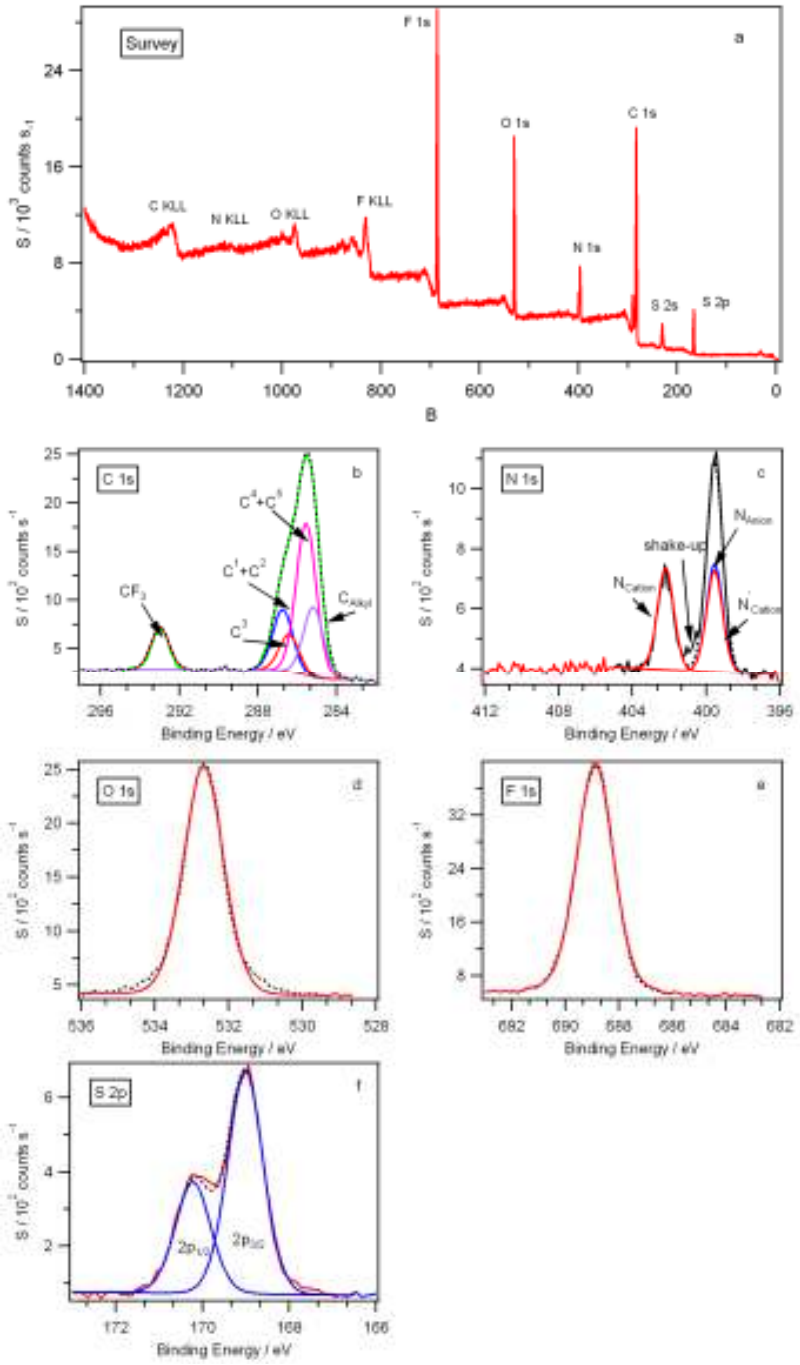

5.6 XP spectra with component fittings of [C_6Phen][NTf_2] for: (a) survey, (b) C 1s, (c) N 1s, (d) F 1s, (e) O 1s and (f) S 2p.

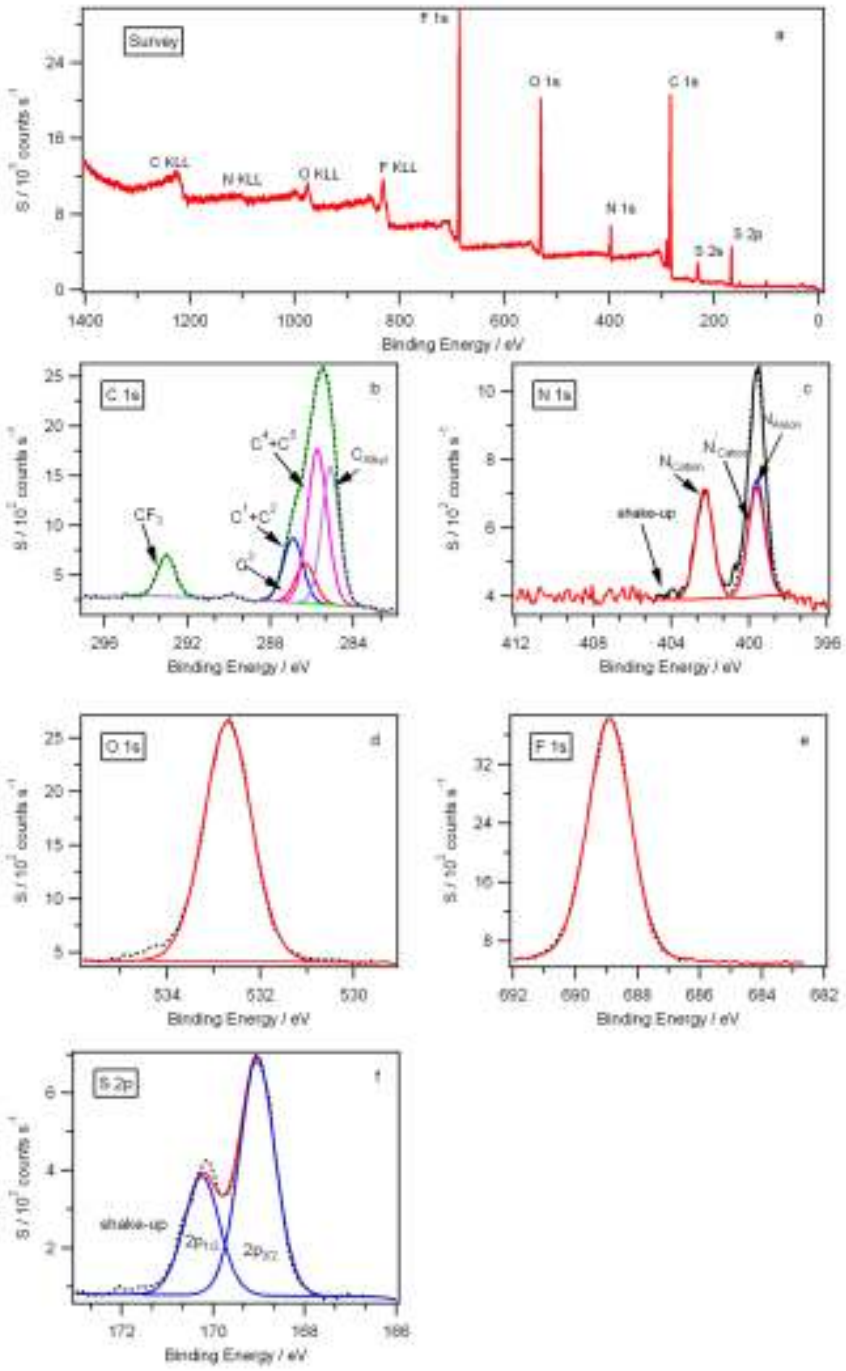

5.7 XP spectra with component fittings of $[C_6Phen][PF_6]$ for: (a) survey, (b) C 1s, (c) N 1s, (d) F 1s and (e) P 2p

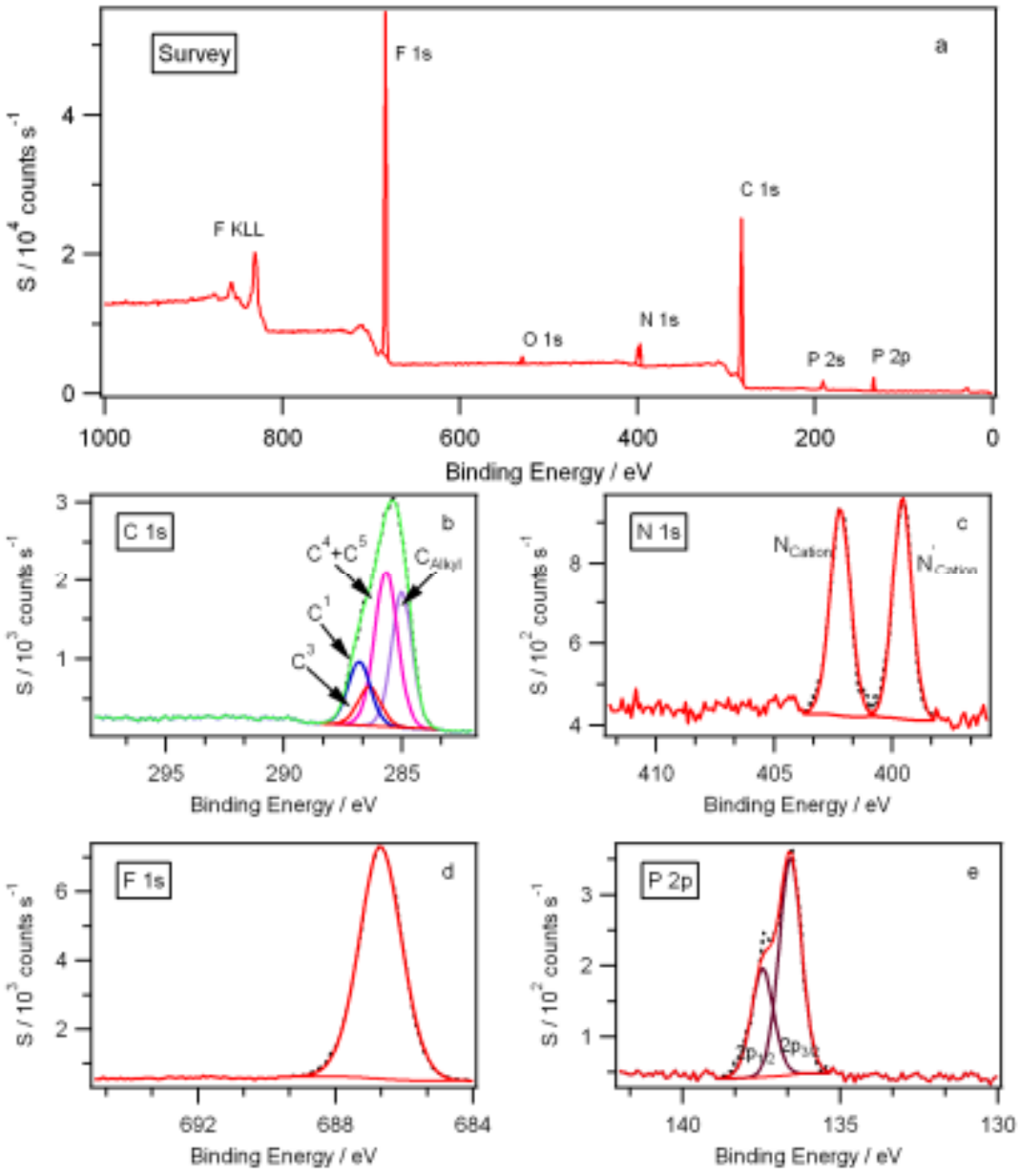

5.8 XP spectra with component fittings of [C_8Phen][NTf_2] for: (a) survey, (b) C 1s, (c) N 1s, (d) F 1s, (e) O 1s and (f) S 2p.

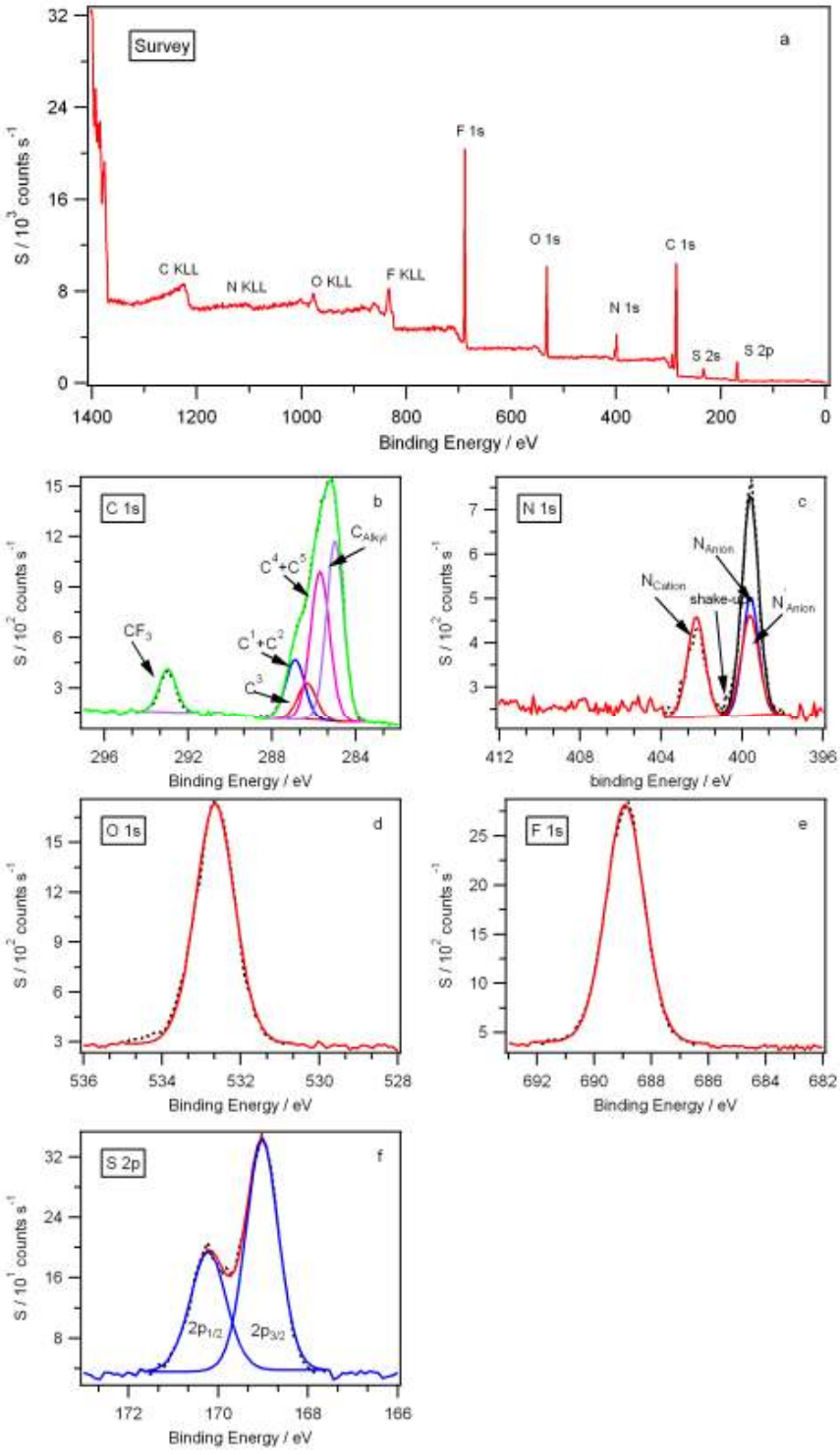

5.9 XP spectra with component fittings of [C_{10}Phen][NTf_2] for: (a) survey, (b) C 1s, (c) N 1s, (d) F 1s, (e) O 1s and (f) S 2p.

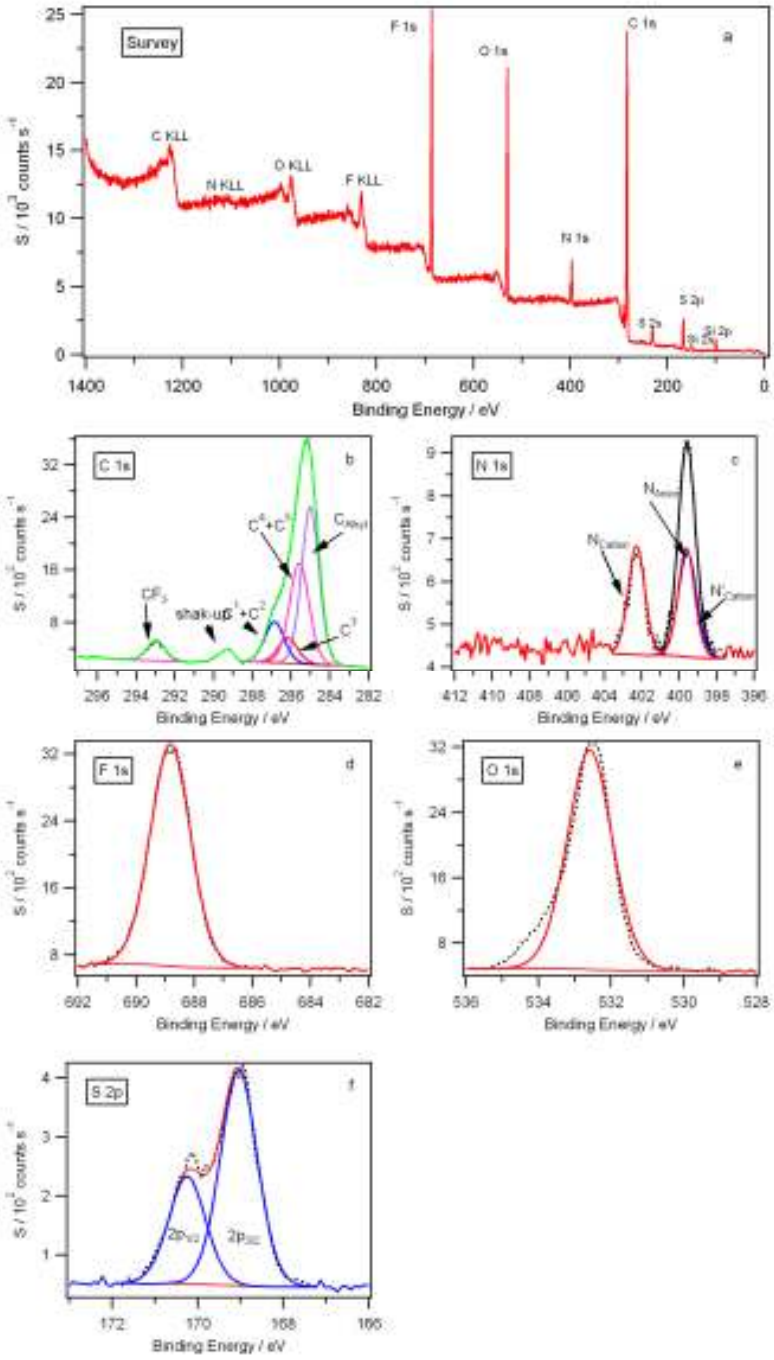

5.10 XP spectra with component fittings of [C_{12}Phen][NTf_2] for: (a) survey, (b) C 1s, (c) N 1s, (d) F 1s, (e) O 1s and (f) S 2p.

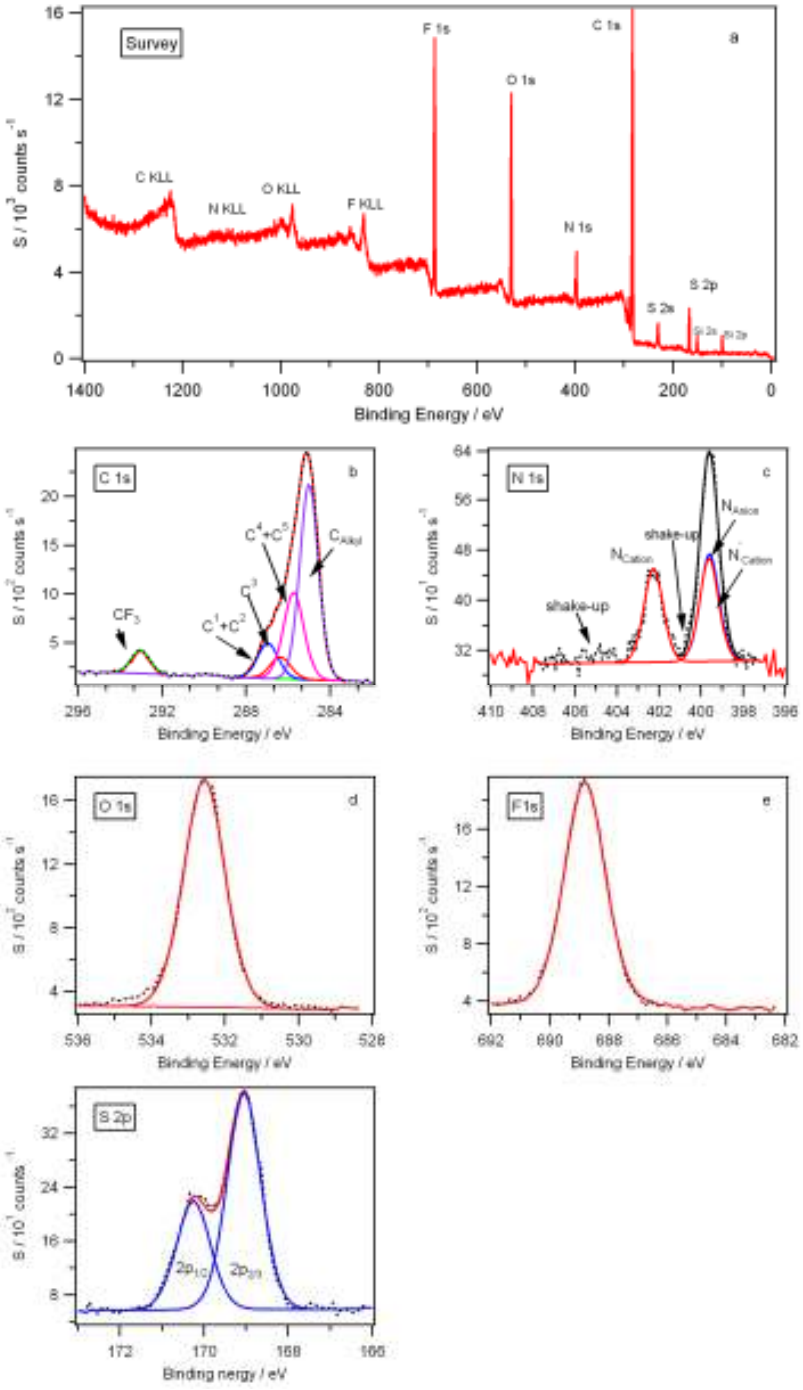

5.11 XP spectra with component fittings of [C_{14}Phen][NTf_2] for: (a) survey, (b) C 1s, (c) N 1s, (d) F 1s, (e) O 1s and (f) S 2p.

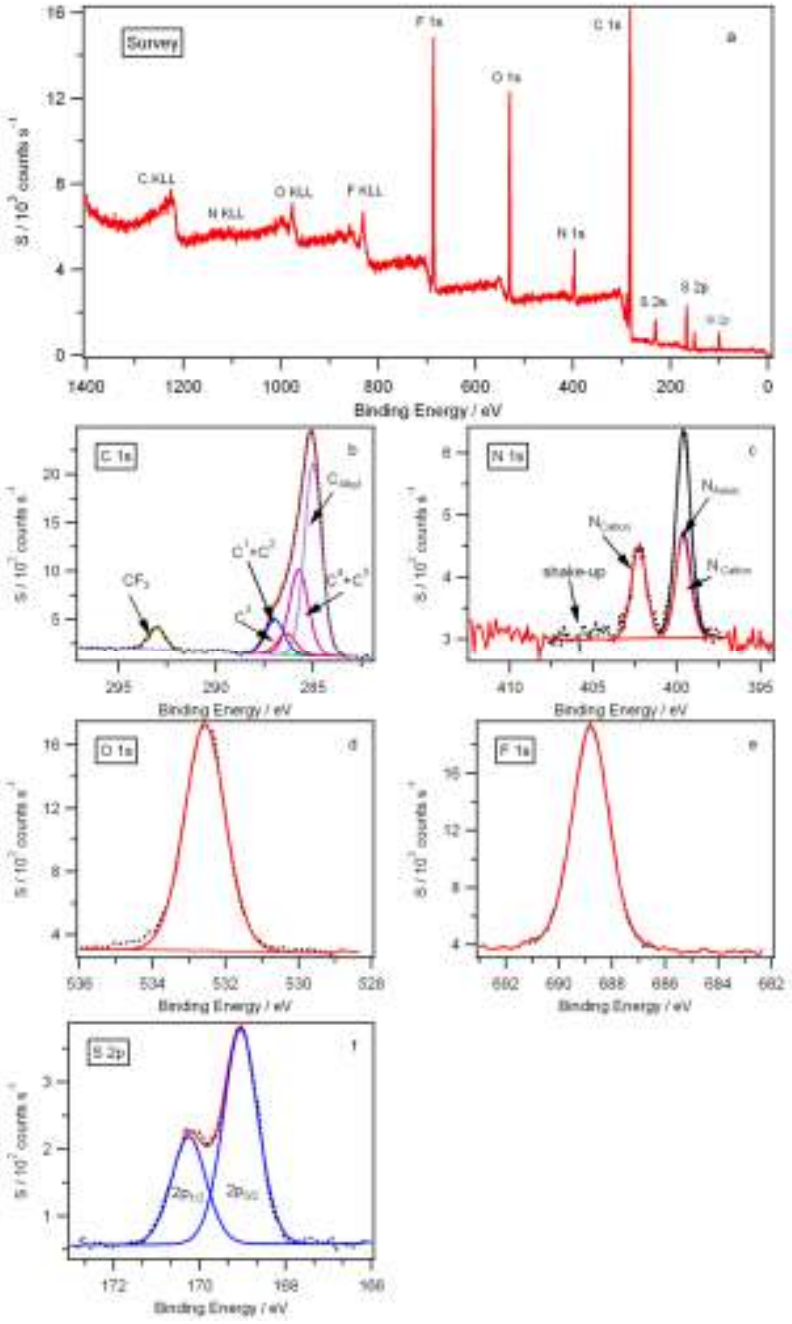

Appendix 6

A6. XP spectra

6.1 XP spectra with component fittings of [C_4Bipyr][NTf_2] for: (a) survey, (b) C 1s, (c) N 1s, (d) F 1s, (e) O 1s and (f) S 2p.

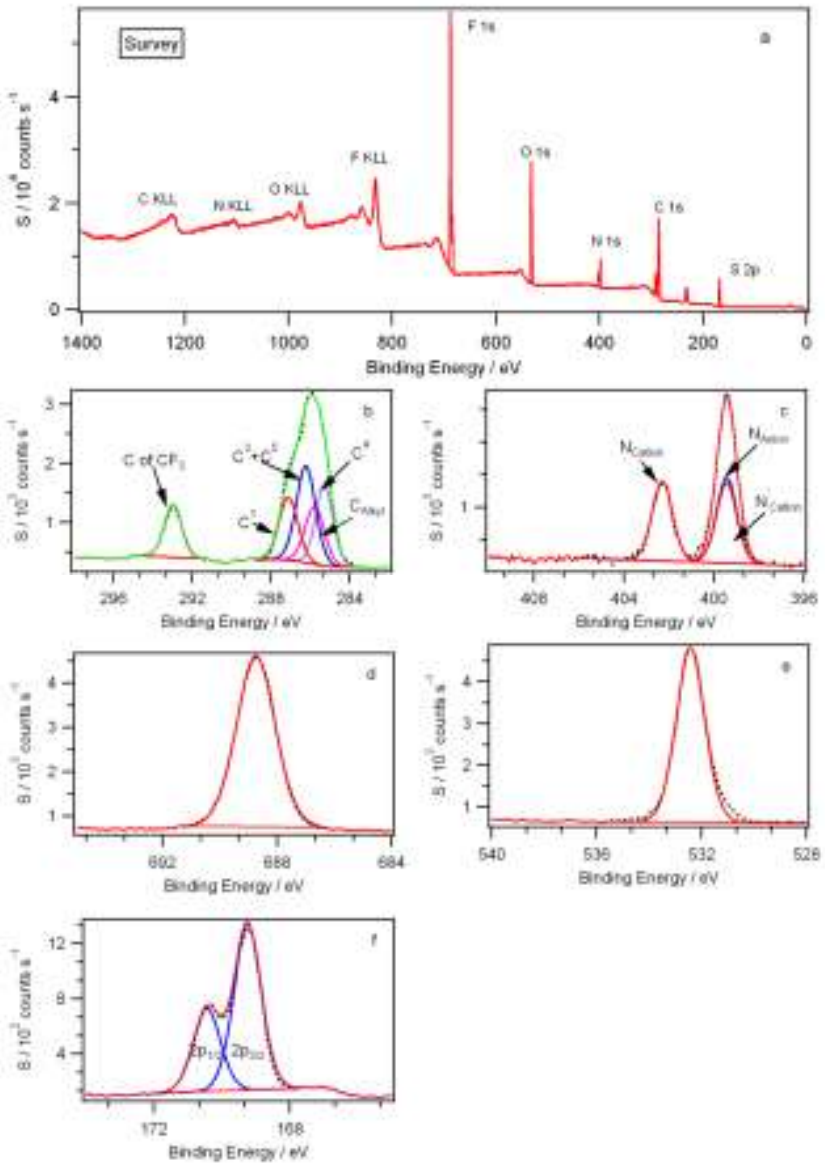

6.2 XP spectra with component fittings of [C_6Bipyr][NTf_2] for: (a) survey, (b) C 1s, (c) N 1s, (d) F 1s, (e) O 1s and (f) S 2p.

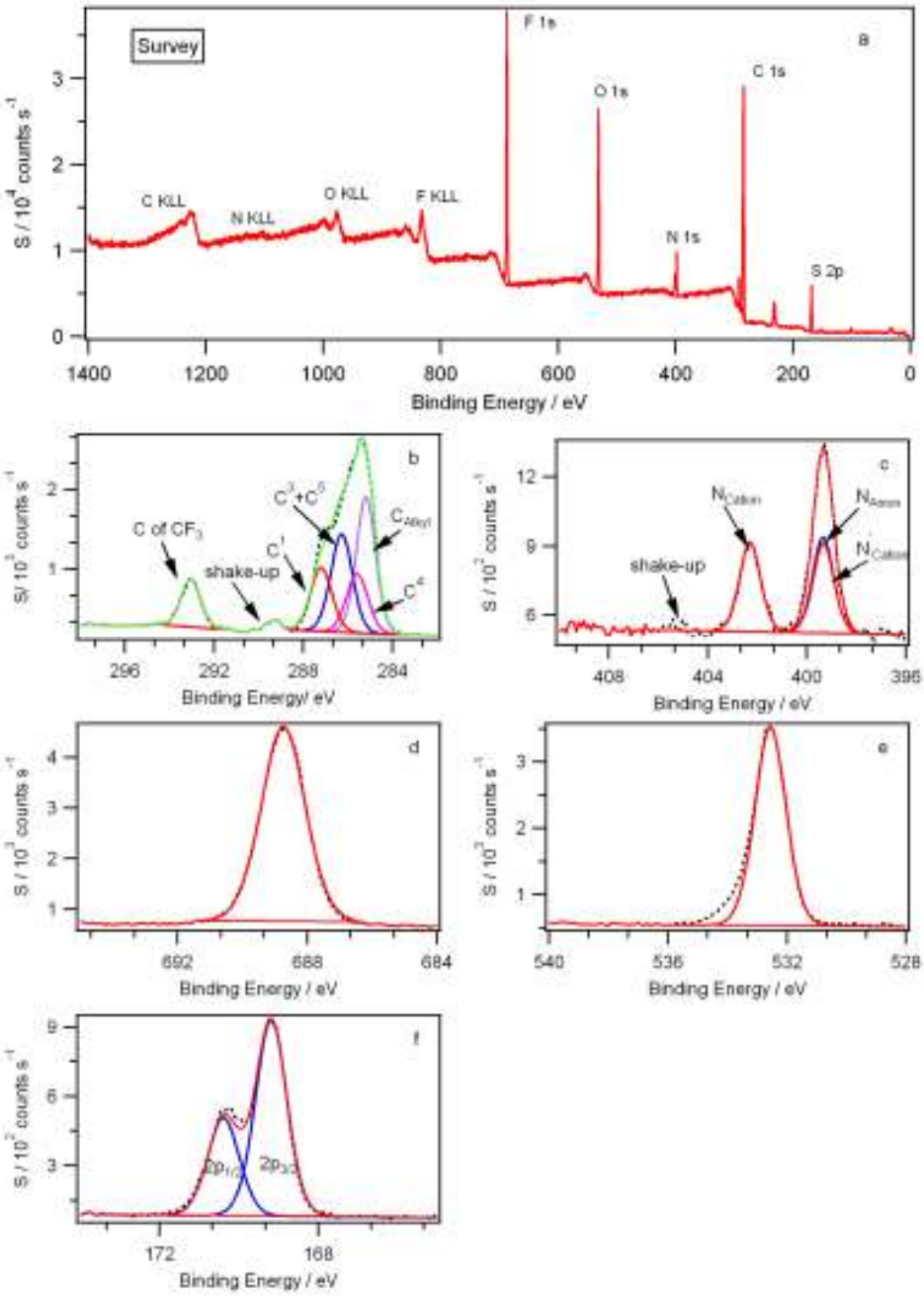

6.3 XP spectra with component fittings of [C_8Bipyr][NTf_2] for: (a) survey, (b) C 1s, (c) N 1s, (d) F 1s, (e) O 1s and (f) S 2p.